ROR1 and Rab27b – Novel biomarkers for chemoresistance in ovarian cancer

A thesis submitted to Middlesex University in partial fulfilment of the requirements for the degree of Doctor of Philosophy

Eamaan Syed Shafat
M00551383

Faculty of Science and Technology
Department of Natural Sciences
Middlesex University London
April 2021

Abstract

Ovarian cancer is one of the most lethal cancers of the female reproductive system. Most patients relapse with chemo-resistant form of the disease after chemotherapy. Preliminary research profiled drug resistant (IGROVCDDP) and sensitive (KB-5-5-11) cell line models using whole genome Affymetrix expression arrays which identified novel biomarkers; ROR1 and Rab27b. These were validated in publicly available microarray datasets and through PCR-based pilot study on ovarian cancer tissue blocks.

The aim of this project was to investigate ROR1 and Rab27b as biomarkers for chemoresistance in ovarian cancer. Ovarian cancer cell line panel was assembled comprising of; HEY, SKOV-3, OVCAR-3 and OAW42. The IC50 doses of four drugs; cisplatin, carboplatin, taxol and talazoparib for the cell lines were determined. qPCR was carried out to investigate gene expression levels of ROR1, Rab27b and EMT markers in response to drug treatments for each cell line. ELISA's and Immunocytochemistry were carried out to investigate protein expression and localization of the ROR1and Rab27b in response to drug treatments. An invasion assay was carried out to establish an invasion profile of the cell line panel. Knockdown of ROR1(and ROR2) in the resistant and sensitive cell lines was carried out to study the effects on chemo-resistance. Clinical tissue samples obtained from Westmead Hospital, Sydney, Australia were also stained and scored for ROR1(and vimentin). Kaplan-Meir survival analysis was carried out to investigate the impact of ROR1 (and vimentin) on patient outcomes.

HEY cells were found to be the most resistant ($p < 0.05$) and invasive ($p < 0.001$) while OVCAR-3 was the opposite ($p < 0.001$). Gene expression assays revealed ROR1 was highest in the resistant cell line. The protein assays revealed ROR1 expression was correlated with chemoresistance ($R^2 = 0.99$) and invasion ($R^2 = 0.82$). Knockdown studies in HEY and OVCAR-3 cells revealed a significant re-sensitisation to platinum-based drugs when undergoing simultaneous ROR1 and ROR2 silencing ($p < 0.05$). Tissues stained for ROR1 and Vimentin showed a poor overall survival in ovarian cancer patients with high ROR1 and vimentin scores. Rab27b gene and protein assays revealed varying expression patterns with drug treatment indicating the need for further studies to better understand its role in chemoresistance. Overall, ROR1 is a promising predictive biomarker for chemoresistance which will be invaluable in the field of personalized medicine for ovarian cancer.

Acknowledgements

Firstly, I would like to express my sincere gratitude to my supervisors Dr. Britta Stordal and Dr. Frank Hills for their continuous support of my PhD study. Their patience and compassion have made my time as a student at Middlesex University one of the most memorable periods in my academic career. Their guidance has helped me throughout the research and writing of this thesis. I am extremely fortunate and could not have imagined having better advisors and mentors for my PhD.

I would like to thank my peers; past and present for the stimulating discussions, the sleepless nights we were working together before deadlines, and for all the great memories we have had in the last five years. I would like to thank Anam Akhtar, Toby Landeryou, Cynthia Osemeke, Desiree Acha, Gabriel Rosa, Noor Hasan, Milan Vu, Ahlem Bennacer and Kaan Low. They have all been sources of inspiration at one point or another during the course of my PhD. I particularly want to thank Imeobong Antia for his relentless support and guidance as a fellow student and friend. I am grateful for the countless brainstorming sessions and more importantly all the life and career advice.

I want to extend my sincere thanks to the entire team at 8th Light; past and present. 8th Light has been my second home outside the lab and continually inspires me. I especially want to thank Jim, Amelia, Becca, Daisy, Himalee, Siobhan and Elle. You have all played a part in my tech journey and I will always be grateful. I also want to express my appreciation to Dan, Gabi, Makis and Katarina for all the advice and support during their time at 8th Light.

Finally, I would not have accomplished what I have without the love and unconditional support of my family. I want to thank my brother and sister for their encouragement and patience when I felt like giving up. My heartfelt gratitude to my parents who have sacrificed everything and continue to do so for my comfort and wellbeing. And to the most important person in my life; my grandmother (Teta) who I lost last year; I dedicate my PhD thesis to her (May her soul rest in peace).

TABLE OF CONTENT

Abbreviations

ABC family	ATP Binding Cassette family
ABCB1	ATP Binding Cassette Subfamily B Member 1
AKT	Protein Kinase B
ALL	Acute lymphocytic leukaemia
ANOVA	Analysis of variance
ATP	Adenosine triphosphate
BCIP	5-bromo-4-chloro-3-indolyl phosphate
BER	Base Excision Repair
BRAF	Serine/threonine-protein kinase B-Raf
BSA	Bovine Serum Albumin
CA-125	Cancer antigen 125
CCDC68	Coiled-Coil Domain Containing 68
CD154	Cluster of differentiation 154
cDNA	Complementary DNA
Chk2	Check Point Kinase 2
CLL	Chronic lymphocytic leukaemia
CO_2.	Carbon dioxide
CRD	Cysteine-rich domain
CRUK	Cancer Research United Kingdom
CT	Computerized tomography
Ct	Cycle threshold
CTR1	Copper transporter 1
CXCR4	C-X-C chemokine receptor type 4
DAB	3,3'-Diaminobenzidine
DAPI	4′,6-diamidino-2-phenylindole
DMSO	Dimethyl sulfoxide-d6
DNA	Deoxyribonucleic acid
dNTP	Deoxynucleoside triphosphate
DPX	Dibutylphthalate Polystyrene Xylene
ECL	Enhanced chemiluminescence
EDTA	Ethylenediaminetetraacetic acid
EGFR	Epidermal growth factor receptor
ELISA	Enzyme-linked immunosorbent assay
EMT	Epithelial–mesenchymal transition
EOC	Epithelial ovarian cancer
EphA2	Ephrin type-A receptor 2
ERBB2	Erb-B2 Receptor Tyrosine Kinase 2
ERCC1	Excision Repair Cross-Complementation Group 1
ERCC2	Excision repair cross-complementation group 2
ECM	Extracellular matrix
FBS	Fetal bovine serum

FIGO	International Federation of Gynecology and Obstetrics
FITC	Fluorescein isothiocyanate
FZ domain	Frizzled domain
GAPDH	Glyceraldehyde 3-phosphate dehydrogenase
GPCR	G protein-coupled receptors
GTPases	Guanosine triphosphatases
HCl	Hydrochloric acid
HGFR	Hepatocyte growth factor receptor
HGSC	High grade serous carcinoma
HRP	Horse-radish Peroxidase
HR	Homologous recombination
IC50	Half maximal inhibitory concentration
Ig	Immunoglobulin
IGF1R	Insulin-Like Growth Factor 1 receptor
ICC	Immunocytochemistry
IHC	Immunohistochemistry
IP	intraperitoneal
KD	Knockdown
KDa	Kilo Dalton
KR domain	Kringle domain
KRAS	Kirsten rat sarcoma viral oncogene
LGSC	Low grade serous carcinoma
MAD2	Mitotic Arrest Deficiency Protein 2
MAPK	mitogen-activated protein kinase
MET	Mesenchymal-epithelial tansition
mL	Milliliter
mM	Millimole
MRI	Magnetic resonance imaging
mRNA	Messenger ribonucleic acid
MRP2	Multidrug resistance-associated protein 2
MuSK	Muscle-Specific Kinase
MW	Molecular weight
NaOH	Sodium hyroxide
NBT	p-nitroblue tetrazolium chloride
NER	Nucleotide excision repair
NKX2-1	NK2 homeobox 1
nM	Nano Mole
NHL	non-Hodgkin lymphomas
NHEJ	Non-homologous end joining
NOTCH3	Neurogenic locus notch homolog protein 3
OC	Ovarian cancer
OS	Overall survival
P-gp	P-glycoprotein
PAR	Poly (ADP-ribose)
PARP	Poly (ADP-ribose) polymerase

PBS	Phosphate-buffered saline
PBMCs	Peripheral blood mononuclear cells
PFS	Progression free survival
pH	Potential of Hydrogen
PI3K	Phosphoinositide 3-kinases
PIK3	Phosphatidylinositol-4,5-bisphosphate 3-kinase
PRD	Proline-rich domain
PgD2	Prostaglandin D2
qPCR	Quantitative polymerase chain reaction
Rab27b	Ras related protein 27b
RGB	Red Green Blue
RGS16	Regulator of G Protein Signalling 16
RhoA	Ras homolog family member A
RIPA buffer	Radioimmunoprecipitation assay buffer
RMI	Risk of malignancy index
RNAi	RNA interference
ROR1	Receptor Tyrosine Kinase Like Orphan Receptor 1
RPMI-1640 media	Roswell Park Memorial Institute 1640 Medium
RTK	Receptor tyrosine kinase
SDF-1/	Stromal cell-derived factor 1
SDS	Sodium dodecyl sulfate
S/TRD1	Serine/threonine-rich domain
SFM	Serum-free media
siRNA	Small interfering RNA
SNAI1,	Snail Family Transcriptional Repressor 1
SNAI2	Snail Family Transcriptional Repressor 2
TGFβ	Transforming growth factor beta
TMA	Tissue microarrays
TMB substrate	3,3',5,5'-Tetramethylbenzidine
TP53	Tumour protein 53
TAE	Tris-acetate-EDTA
TIC	Tubal intraepithelial carcinoma
uL	Micro litre
UV	Ultraviolet
VEGF	Vascular endothelial growth factor
WNT	Wingless-related integration site
Wnt5a	Wnt Family Member 5A
RNA	Ribonucleic acid
XPA	Xeroderma pigmentosum complementation group A
ZEB	Zinc-finger E-box binding

LIST OF FIGURES

LIST OF TABLES

Chapter 1

Introduction

1.1 Background

Ovarian cancer (OC) is the cause of more deaths per year compared to other female reproductive system related cancers (Permuth-Wey and Sellers, 2009). Patients presenting with advanced stages of the disease have a poor prognosis and a 5-year survival rate of about 10-30% (Hennessy *et al*., 2009). This is mainly due to a majority of cases being detected and diagnosed at an advanced stage which is a result of lack of screening and recurrent development of chemoresistance (Song *et al*., 2014). Epithelial ovarian cancer (EOC), which makes up to 80% of the neoplasms is one of the most malignant forms of ovarian cancer (Morgan *et al*., 2011). EOC compared to other types of cancer is very sensitive to chemotherapy. However, it is associated with a 5-year survival of 50% (Helm and States, 2009).

Ovarian cancer is mostly sporadic but can occur due to hereditary deleterious mutations of the BRCA1 and BRCA2 genes. These are tumour suppressor genes that can develop mutations leading to increased risk of ovarian (and breast) cancer (King *et al*., 2003). Up to 10% of the women diagnosed with ovarian cancer carry a BRCA1 or BRCA2 germline mutation (Parkin *et al*., 2005). Somatic mutations (42.9% BRCA1 and 28.6% BRCA2) also contribute to the loss of BRCA function, increasing the number of ovarian cancer patients with deregulated homologous recombination (HR) (Hennessy *et al*., 2010). These mutations cause a defect in the homologous recombination DNA repair mechanism. Since BRCA1 and BRCA2 genes are essential in the HR pathway, any disruption can create a predisposition to different human cancers (Venkitaraman, 2002).

1.2 Epidemiology and Risk factors

According to 2016 incidence statistics carried out by Cancer research UK, ovarian cancer was found to be the sixth most common cancer among females in the UK (CRUK). The World Ovarian Cancer Coalition Atlas (2018) reported that ovarian cancer was the seventh most common cancer worldwide and the eighth most common cause of death in women. These mortalities are due to the fact that patients present with late stages of the disease and as such have minimal chances of survival.

Ovarian cancer occurrence has extensive geographic variation, with higher incidences in developed parts of the world which include North America and Europe (Reid *et al*., 2017). Incidence rates in this part of the world generally exceed 8 per 100,000 , in Africa and Asia it is the lowest (≤3 per 100,000) whereas in South America the rates are intermediate (5.8 per 100,000) (Herrinton *et al.*, 1994; Kliewer and Smith, 1995). It is worth noting that for women who migrate from low incidence countries (Asia) to high incidence countries (North America) a gradual increase in OC incidence has been observed(Holschneider and Berek, 2000).

According to Mavaddat *et al*. (2013), the lifetime risk of developing ovarian cancer in the UK is 1 in 60 with the median age of patients enrolled in randomised trials being 58 years. Interestingly, this is several years younger than the median age of diagnosis in the overall UK population which is 63 years. According to the above study, women are diagnosed roughly 10 years earlier than the median age of diagnosis if they carry a genetic disposition to ovarian cancer. Several epidemiological studies reported that a lack of ovulation can contribute to a lower risk of ovarian cancer. This includes pregnancy, use of oral contraception and tubal ligation-reduced reflux of menstrual products onto the ovary (Tsilidis *et al*., 2011).

Ovarian cancer is considered to be a disease of mostly perimenopausal and postmenopausal women with over 80% of the women being affected over the age of 40 and less than 1% affecting women under the age of 20 (Holschneider and Berek, 2000). A three to seven-fold increased risk has been observed in first degree relatives of probands (first genetically affected individual in the family) particularly if multiple relatives are affected and at an early age(Negri *et al*., 2003). Most hereditary ovarian cancers occur due to mutations in the BRCA genes and account for 10-15% of all cases (Malander *et al*., 2004; Van Der Looij *et al.*, 2000). Women carrying the BRCA1 mutation are 40% more likely to develop epithelial ovarian cancer whereas those carrying the BRCA2 mutation are 20% more likely to develop the same.

1.3 Pathogenesis of Epithelial Ovarian Cancer

To date, no widely accepted pathogenesis of ovarian cancer has been described. One of the biggest problems in uncovering the pathogenesis is the heterogeneous nature of ovarian cancer, comprising various histologic types with varying characteristics (Gross *et al*., 2010). According

to Prat (2012), 40% of ovarian tumours are of non-epithelial types however only 10% of ovarian *cancers* are non-epithelial. There have been different theories explaining the origin of ovarian cancers outlined in the following sections.

1.3.1 Incessant Ovulation Theory

Traditional theories described the origin of ovarian cancers from the epithelial surface of ovarian cells (Budiana *et al*., 2019). These surface epithelial cells experience physical trauma through ovulation and are then immediately repaired. Ovulation occurs repeatedly throughout the individual's life resulting in repetitive trauma to the epithelium and in turn causing cellular DNA damage. Having undergone DNA damage, the epithelial cells become very susceptible to change which enables invagination to the cortical stroma (Budiana *et al*., 2019). Cortical inclusion cysts are formed when these invaginations are trapped resulting in formation of a sphere of epithelial cells in the stroma. Epithelial cells, while inside the ovary, are exposed to hormones stimulating cell proliferation. These eventually transform them into cancer cells (Erickson *et al*., 2013; Kurman and Shih, 2010).

This theory aligns with the epidemiologic data where an association between the number of ovulatory cycles with the risk of ovarian cancer was observed (Peres *et al.*, 2017; Purdie *et al*., 2003; H. P. Yang *et al.*, 2016). However, this theory can be considered flawed as it is unable to explain the pathogenesis of ovarian cancer with varying histological types and prognostic differences (Koshiyama *et al.*, 2014). There are no histological similarities between the ovarian surface epithelium (mesothelium) and serous, endometrioid, mucinous, clear cells or transitional cells (Kurman and Shih, 2010). Polycystic ovary syndrome patients experience a decreased ovulation but are at a higher risk of developing ovarian cancer therefore making this theory contradictory (Erickson *et al*., 2013; Kurman and Shih, 2010)

1.3.2 Fallopian Tube Theory

Since it was initially accepted that ovarian cancer originated from the ovary itself, only few studies investigated other sites for ovarian cancer precursor lesions (Kurman and Shih, 2010). It was reported that patients with BRCA1/2 gene mutations undergoing prophylactic salpingo-

oophorectomy had epithelial dysplasia in the fallopian tubes at high incidences (50%). This dysplasia resembled high-grade serous ovarian carcinoma and was termed tubal intraepithelial carcinoma (TIC).

Histologically similar characteristics of ovarian and high-grade serous peritoneal cancer were found in other studies irrespective of BRCA status (Budiana *et al*., 2019). In some studies, when the contralateral ovary of patients with ovarian cancer were examined, it showed either normal histology or changes in morphology not indicative of high-grade serous neoplasm characteristics (Kurman and Shih, 2010). It can be concluded from these studies that the fallopian tube is the most likely location for ovarian cancer precursor lesions ultimately spreading to adjacent ovarian sites.

Mutation of the TP53 gene is also observed in TIC. Immunohistochemical examinations in the normal fallopian tubes show expression of TP53 in secretory cells(Budiana *et al*., 2019; Erickson *et al*., 2013; Gross *et al*., 2010). These were identical to mutations in TP53 gene in serous ovarian cancer. However, all TP53 mutations are not cancerous, and its expression is considered to be a response that demonstrates DNA damage in tubal epithelial cells as a result of being exposed to oxidants and cytokines. A significant percentage (50%) of TP53 mutations eventually become cancerous (Erickson *et al*., 2013; Gross *et al*., 2010).

About 70-90% of TICs are found in the distal part of the fallopian tube, the fimbria region. The fimbriae being located very close to the ovary are exposed to similar environmental stresses as the ovary. Additionally, this region is rich in blood vessels thereby facilitating metastasis to the ovary via the bloodstream (Kurman and Shih, 2010). Initially this theory was considered controversial but is now widely accepted (Budiana *et al*., 2019).

1.3.3 Two-Pathway Theory

Originally proposed in 2004 (Kurman and Shih, 2010), the two-pathway theory aimed to integrate both clinical histological and genetic findings of ovarian cancer. According to this theory, ovarian cancer is divided into type I and type II. Low-grade serous, mucinous, endometrioid, clear cell, and transitional histology types made up the type I ovarian cancer.

Type II ovarian cancer consists of high-grade serous, undifferentiated and carcinosarcoma histology types (Kurman and Shih, 2010).

In type I ovarian cancers, the precursor lesions are thought to originate in the ovary. Here, the cancer grows slowly and is considered to be benign and genetically stable (Koshiyama *et al*., 2014). Once the intermediate (borderline) phase is surpassed, a series of ongoing morphological changes occur in ovarian tumour eventually resulting in ovarian cancer. A traditional pathway of type I ovarian cancer pathogenesis involves ovarian surface epithelial inclusion cysts receiving proliferation stimulation from the environment. This then transforms them into cancerous cells. In type I ovarian cancers, KRAS and BRAF mutations are the most common genetic changes and are both involved in the activation of the oncogenic MAPK pathway (Erickson *et al.*, 2013; Kurman and Shih, 2010).

Unlike type I ovarian cancer, the precursor lesions of type II ovarian cancers are thought to originate from outside the ovary in type II ovarian cancer. One of regions of origin is believed to be from the fallopian tube (Labidi-Galy *et al*., 2017). In this category the cancer is fast growing, aggressive, genetically unstable and diagnosed at an advanced stage. Most type II ovarian cancers carry a TP53 gene mutation (50-80%), overexpression of HER2/neu (10-20%) and AKT (12-18%) genes (Budiana *et al.*, 2019). Interestingly, HER2 + ovarian cancer xenografts haver shown satisfactory response to a combination of trastuzumab (Herceptin) and pertuzumab in preclinical experimental studies (Faratian *et al*., 2011; Sims *et al*., 2012)
Type II ovarian cancers are also associated with BRCA gene defects which was reported up to 20-25% (Hennessy *et al*., 2010; Jonathan A. Ledermann *et al.*, 2016; Manchana *et al.*, 2019). Precursors for this type of cancer originate in the fallopian tube where TP53 mutations are prominent. In addition to this, inflammatory cytokines and reactive oxygen species trigger secretory epithelial cells present in the fallopian tubes to undergo neoplastic changes. Studies showed that there is no consistency in TP53 mutations and therefore ovulation is still categorized as a risk factor (Koshiyama *et al.*, 2014). Although this theory explains pathogenesis of ovarian cancer better than other theories it continues to lack an understanding of the development of the cancer in cells of non-ovarian origin (Koshiyama *et al*., 2014).

1.4 Histology

Ovarian cancer is classified into three main types depending on cell of origin: epithelial, germ cell and sex-cord stromal. The most common of these is the epithelial ovarian cancer making up to 90% of occurrences (Momenimovahed *et al.*, 2019) while the latter two make up 5-10% of all ovarian cancer cases (Stewart *et al.,* 2019). Histologically, there are four primary subtypes of epithelial ovarian cancer; serous, endometrioid, mucinous and clear cell (Jayson *et al*., 2014). The serous tumours are further classified into high-grade serous carcinomas (HGSC) or low-grade serous carcinomas (LGSC) (Jayson *et al.*, 2014). About 70-80% of all subtypes of epithelial ovarian cancer fall under HGSCs whereas less than 5% are categorized as LGSCs. The endometrioid, mucinous and clear cell subtype make up 10%, 3% and 10% respectively of ovarian cancer cases (Stewart *et al.*, 2019).

1.4.1 Epithelial Ovarian Cancer

More recently, Stewart *et al* (2019) have suggested that epithelial ovarian cancer has three point of origin sites; ovarian, tubal or other epithelial sites in the pelvis (Stewart *et al.*, 2019). Epithelial ovarian cancer is divided into two categories of tumours: Type I tumours and Type II tumours (Chien and Poole, 2017). The type I tumours are theorized to be caused from continuous ovulation cycles, inflammation and endometriosis. The risk of ovarian cancer is considered to be increased with the occurrence of endometriosis and is associated with 5 – 15 % of epithelial ovarian cancer (Jayson *et al*., 2014; Mallen *et al*., 2018). The majority of these cancers occur as low-stage disease presenting with a good prognosis that those not associated with endometriosis. However, type II tumours are usually linked with high mortality rates (Stewart *et al*., 2019) and often diagnosed at an advanced stage. Type II tumours are associated with mutation is the BRCA and TP53 gene which are known as tumour suppressor genes (Stewart *et al*., 2019).

1.4.1.1 LGSC and HGSC

As mentioned earlier, HGSC make up to 90% of the serous tumour types while LGSC make up to 10% (Bergamini *et al*., 2016). Both serous subtypes have different clinical presentations, molecular profiles and prognosis with LGSC presenting a significantly longer survival rate and

overall better prognosis compared to HGSC (Bergamini *et al.*, 2016; Stewart *et al*., 2019). Women with LGSC are diagnosed at a younger age (19 to79 years with a mean of 52 years) compared to women diagnosed with HGSC (38 to 90 years with a mean of 62 years) (Okoye *et al*., 2016). Originally, LGSC was believed to originate in a stepwise fashion from the ovaries (Kurman and Shih, 2010), however a more recent study suggests that LGSC may also have tubal origin although this is still controversial (Wang *et al*., 2019). In contrast, it is now widely accepted that HGSC originate in the fallopian tubes eventually spreading to the ovaries and peritoneum (McCluggage *et al.*, 2017; Paley *et al*., 2001).

1.4.2 Endometrioid and Clear Cell Carcinomas

Endometrioid carcinomas originate from endometriosis and usually diagnosed in early stages. This results in an improved prognostic outcome (Vargas, 2014). This subtype is considered treatable since it possesses a histology that is chemosensitive (Stewart *et al*., 2019). Similar to endometrioid carcinomas, clear cell carcinomas make up 10% of epithelial ovarian cancers and also have a comparable prognosis (Chan *et al*., 2008). However, if diagnosed at an advanced stage the prognosis is far worse than cases diagnosed with HGSC in the equivalent stage (Hoskins *et al*., 2012; Tammela *et al*., 1998). This difference in prognosis is primarily due to the chemoresistant nature of clear cell carcinoma (Shu *et al*., 2015).

1.4.3 Mucinous Carcinoma

Ovarian mucinous carcinomas are regarded as rare and make up less than 3% of all ovarian carcinomas (Seidman *et al*., 2004, 2003). They are classified as either benign, borderline or malignant as well as invasive or non-invasive (Ricci *et al*., 2018). Patients with mucinous ovarian carcinoma present with multicystic tumours. These contain large amounts of intracellular mucin (more than 50% of the cytoplasm) in about 90% of the tumour cells (Kelemen and Köbel, 2011). These tumours grow differently than those originating from the gastrointestinal tract and grow as cystic gland-forming neoplasm (Kelemen and Köbel, 2011). In contrast to other carcinoma histotypes, invasive mucinous ovarian carcinomas carry benign or atypical epithelium with tumour KRAS mutations that are similar to those in colorectal and pancreatic cancer (Howe and Conlon, 1997; Shibata *et al*., 1993). Although KRAS mutations

carry on in these malignant cancers, they are not found in high grade ovarian tumours (Pieretti *et al*., 2002).

Improved histological diagnosis has led to increasing evidence that different histotypes of ovarian cancer have different response patterns to platinum-based chemotherapy (Ricci *et al*., 2018). Most patients with mucinous ovarian carcinomas diagnosed at an early stage do not require adjuvant chemotherapy and can be treated with surgery. However, in patients with advanced mucinous ovarian carcinomas, adjuvant chemotherapy is necessary despite no effective therapeutic regimen being yet defined (Ricci *et al*., 2018). Taking the low incidence of mucinous ovarian carcinomas into account, the most challenging aspect of treatment is designing trials that involve strategies to identify and streamline effective treatment.

1.4.4 Germ cell and Sex- cord stromal ovarian tumours

Ovarian malignant germ cell tumours originate from the primitive germ cell of the embryonic gonad and histologically are heterogeneous (Shaaban *et al*., 2014). They make up 20% of ovarian neoplasms but only 5% of germ cell tumours are malignant and 95% are benign mature cystic teratomas (Shaaban *et al*., 2014). Ovarian malignant germ cell tumours makes up 2.6% of the (malignant) ovarian neoplasm (Quirk and Natarajan, 2005). Classic morphology makes diagnosis straightforward. However, variation in morphology leads to diagnostic issues since these tumours tend to have similar neoplasms as high-grade epithelial ovarian tumours. In addition to this, germ cell tumours tend to mimic their own subtypes (Rabban and Zaloudek, 2013). Clinically, there are many differences between ovarian malignant germ cell tumours and ovarian epithelial carcinomas. The former, at the time of diagnosis tend to be much larger and progress rapidly (Shaaban *et al*., 2014). Although this tumour can occur in various age groups it has the highest incidence among 15-19 year-olds (Smith *et al*., 2006). Although these tumours are rare, there has been some success in treating germ cell ovarian tumours. They are more sensitive to conventional chemotherapy developed in the 1960s and 70s. Additionally, most information with regards to its clinical management has been extrapolated from testicular cancer, which is considered to be very similar (Gershenson, 2012).

Similar to germ cell tumours, ovarian sex cord-stromal tumours are rare and make up about 7% of primary ovarian tumours (Haroon *et al*., 2013). They are heterogeneous and formed by cell types that are diverse in nature originating from the gonadal sex cords or stromal cells (Haroon *et al*., 2013; Shim *et al*., 2013). These tumours are associated with different hormone-mediated syndromes and present a range of different clinical features (Horta and Cunha, 2015). They also affect various age groups but commonly present in younger patients as a low-grade disease with a non-aggressive clinical progression. This makes them suitable for surgical treatment with a generally favourable prognosis (Horta and Cunha, 2015).

1.5 Management and Treatment

According to the International Federation of Gynaecologists and Obstetricians (FIGO) guidelines (Table 1.1), ovarian cancers that are diagnosed for the first time are managed clinically based on their initial surgical staging (Heintz *et al*., 2006). The FIGO stage of the tumour is a very important prognostic marker. Cytoreduction, a tumour debulking surgery, is part of the standard first line treatment and is an important step in prognosis following the determination of the tumour stage (Banerjee *et al*., 2011). For decades, the general protocol for management of ovarian cancers comprised of a combination of cytoreduction and chemotherapy (Cristea *et al*., 2010).

The importance and significance of surgical effort for the patient's survival is irrefutable. After debulking surgery, the volume of residual disease is still the best predictor of progression-free survival and overall survival (Elattar *et al*., 2011). Although primary debulking surgery is preferred, neoadjuvant chemotherapy followed by interval debulking surgery is an option for some patients, including the elderly, women with a significant disease burden, and those with multiple comorbidities (Rauh-Hain *et al*., 2017; Wright *et al*., 2016). Two trials released in the last ten years concluded that there was no distinction between primary and interval tumour debulking (Kehoe *et al*., 2015; Vergote *et al*., 2010). However, some oncologists express reservations about the findings' generalizability (Reuss *et al*., 2019). A phase III Japanese study published in 2020 failed to demonstrate that neoadjuvant chemotherapy is non-inferior to primary debulking surgery (Onda *et al*., 2020), and a phase III cooperative group trial assessing this issue in high-volume centres is being scheduled (Reuss *et al*., 2019). Multiple scoring

systems have been proposed to help define the most suitable patients for primary debulking (Fagotti *et al*., 2006; Suidan *et al*., 2017). As stated earlier, maximal debulking effort remains the standard of care, regardless of the procedure's timing, and research shows that patients are often willing to accept a slight increase in perioperative complications and mortality in exchange for a potential increase in overall survival (Havrilesky *et al*., 2019)

A significant percentage of women recently diagnosed with ovarian cancer either relapse or develop disease progression. A majority of women with epithelial ovarian cancer respond to chemotherapy treatment initially but develop resistance to the treatment over time (Kaye *et al*., 2011).

STAGE I: Tumour confined to ovaries	
FIGO Stage	**Stage description**
I	• Cancer only in the ovary (or ovaries) or fallopian tube(s) • Not spread to nearby lymph nodes or to distant sites
IA	• Cancer is in one ovary • Tumour is confined to inside of ovary or the cancer is in one fallopian tube and is only inside the fallopian tube. • No cancer on the outer surfaces of the ovary or fallopian tube. • No cancer cells are found in the fluid (ascites) or washings from the abdomen and pelvis
IB	• Cancer is in either ovaries (both) or fallopian tubes but not on their outer surfaces • No cancer cells are found in the fluid (ascites) or washings from the abdomen and pelvis • Not spread to nearby lymph nodes or to distant sites

IC Tumour limited to one or both ovaries	
IC1	• Surgical spill
IC2	• Capsule surrounding the tumour ruptured before surgery
IC3	• Cancer cells are found in the fluid (ascites) or washings from the abdomen and pelvis

STAGE II and III: Tumour involves 1 or both ovaries with pelvic extension (below the pelvic brim) or primary peritoneal cancer	
FIGO Stage	**Stage description**
II	• Cancer is in one or both ovaries or fallopian tubes and has spread to other organs (such as the uterus, bladder, the sigmoid colon, or the rectum) within the pelvis **or** there is primary peritoneal cancer
IIA	• Cancer spread to or has invaded (grown into) the uterus or the fallopian tubes, or the ovaries
IIB	• Cancer on the outer surface of or grown into other nearby pelvic organs such as the bladder, the sigmoid colon, or the rectum
IIIA1	• Cancer in one or both ovaries or fallopian tubes, **or** there is primary peritoneal cancer, and it may have spread or grown into nearby organs in the pelvis

IIIA2	• Cancer in one or both ovaries or fallopian tubes, **or** there is primary peritoneal cancer, and it has spread or grown into organs outside the pelvis. • During surgery, no cancer is visible in the abdomen, but tiny deposits of cancer are found in the lining of the abdomen when it is examined
IIIB	• Cancer in one or both ovaries or fallopian tubes, **or** there is primary peritoneal cancer, and it has spread or grown into organs outside the pelvis. • The deposits of cancer are large enough for the surgeon to see, but are no bigger than 2 cm (about 3/4 inch) across
IIIC	• Cancer in one or both ovaries or fallopian tubes, **or** there is primary peritoneal cancer, and it has spread or grown into organs outside the pelvis. • The deposits of cancer are larger than 2 cm (about 3/4 inch) across and may be on the outside (the capsule) of the liver or spleen
IVA	• Cancer cells found in the fluid around the lungs (called a malignant pleural effusion) with no other areas of cancer spread such as the liver, spleen, intestine, or lymph nodes outside the abdomen
IVB	• Cancer spread to the inside of the spleen or liver, to lymph nodes other than the retroperitoneal lymph nodes, and/or to other organs or tissues outside the peritoneal cavity such as the lungs and bones

Table1. 1 FIGO stages adapted from American Cancer Society last reviewed April 2018

1.5.1 Primary disease

Owing to the diverse symptoms of ovarian cancer in the late stages of the disease such as bloating, pelvic or abdominal pain, urinary urgency etc, it can present to different medical specialists before gynaecologists and general practitioners (Jayson *et al.*, 2014). Typically, when ovarian cancer is suspected serum CA 125 concentration is measured and an abdominal and transvaginal ultrasound are carried out (Kauff *et al.*, 2002).

CA 125 is a protein that can be found on the surface of ovarian cancer cells as well as in some healthy tissues. This protein is often found in high concentrations in the blood of women with ovarian cancer (Scholler and Urban, 2007). It was used as a biomarker when Bast *et al.* (1981) isolated the monoclonal antibody OC125 in cancerous ovarian tissue relative to healthy ovarian tissue in the early 1980s. Elevated serum CA 125 levels have been confirmed in ovarian epithelial carcinoma, and the serum CA 125 level is important for diagnosis, prognosis, disease monitoring, and treatment follow-up (van Dalen *et al.*, 2000). CA 125 circulating antigen identification has become an important tool in the diagnosis and monitoring of ovarian epithelial carcinoma, and it is the most studied tumour biomarker in epithelial ovarian cancer treatment (Guo and Peng, 2017). Although some researchers believe that serum CA 125 has no therapeutic benefit for monitoring recurrence in post-operative epithelial ovarian cancer patients, Guo and Peng (2017) reported follow-up monitoring that were promising (Guo and Peng, 2017). Their retrospective analysis found that post-operative epithelial ovarian carcinoma patients with CA125 value <35 U/ml had already displayed recurrent lesions in ecological and imaging examinations or in laparotomy exploration and biopsy, however when given timely treatment the prognosis was improved.

In the UK, CA 125 is used to generate a risk of malignancy index (RMI) to determine the probability that a mass (cystic/solid) is malignant and to prioritize its referral to specialists (Jacobs *et al.*, 1990). However, the RMI threshold to determine the direction of management continues to be explored (Jayson *et al.*, 2014). The non-specific presentation to non-gynaecological specialists can result in important steps such as a vaginal examination not being carried out that could confirm a pelvic mass possibly associated with abdominal swelling and

gross ascites (Jayson *et al*., 2014). A computerized tomography (CT) scan of the abdominopelvic region can help evaluate the degree of the tumour involvement. Further assessment of the pelvic tumour can also be carried out by a magnetic resonance imaging (MRI) scan. In some instances, the tumour originates in the peritoneum leading to the spread of low volume cancer and no discrete ovarian tumour. The tumour in this case is then referred to as primary peritoneal cancer and is primarily of the serous type (Jayson *et al*., 2014).

1.5.1.1 Surgery

Cytoreductive or debulking surgery plays a vital role in the management of high-grade serous ovarian cancer. Not only is this procedure necessary for diagnosing and staging (FIGO) the tumour but also an intervention for therapeutic purposes (Jelovac and Armstrong, 2011). The aim of this surgical procedure is to eliminate as much of the disease as possible with the residual disease being an independent prognostic factor of survival and absence of it indicating lower risk of recurrence (Gadducci *et al*., 2019). The use of neoadjuvant chemotherapy is now widely accepted where complete surgical debulking is not achievable (Jayson *et al*., 2014; May *et al*., 2017).

1.5.1.2 First line chemotherapy for early-stage disease

According to Trimbos *et al*. (2003), adjuvant chemotherapy in the early stages of epithelial ovarian cancer improves overall survival by 8 % where the hazard ratio (0.67) acquired is in favour of treatment. Based on data from two adjuvant trials, it was suggested that patients who had undergone complete debulking and staging surgery might not benefit from adjuvant chemotherapy (Trimbos *et al*., 2010). The completeness of surgical staging was found to be substantially associated with improved outcomes in patients with early ovarian cancer, and the advantage of adjuvant chemotherapy tended to be limited to patients with non-optimal surgical staging. However, data from the ICON1 trial which was a long term follow up of patients with stage I disease, suggested that patients with grade 3 or clear cell; grade 2/3, stage Ib; and grade 1–3 stage 1c disease. should be considered for treatment with cytotoxic chemotherapy (Swart, 2007).

1.5.1.3 First line chemotherapy for advanced disease

For the past 4 decades the standard regimen of care for treating ovarian cancer has been platinum-based chemotherapy (Pepa *et al*., 2015). However, in a 1996 study it was observed that survival improved with the addition of a taxane; paclitaxel to cisplatin (McGuire *et al*., 1996). In non-randomized trials there were concerns of efficacy of carboplatin and paclitaxel efficacy in patients with small volume, resected, stage III disease although this was a less toxic and highly active combination. However, Ozols *et al* (2003) confirmed that chemotherapy regimens comprised of carboplatin and paclitaxel is easier to administer and results in less toxicity in patients with advanced ovarian cancer. It was also established that this regimen is not inferior in comparison to cisplatin and paclitaxel combination. Another randomized phase III trial also showed similar effects of Docetaxel–carboplatin to paclitaxel–carboplatin on progression-free survival and response (Vasey *et al*., 2004). Thus, a combination of the less toxic carboplatin is now administered with paclitaxel or docetaxel as an alternative first-line chemotherapy regimen for patients with newly diagnosed ovarian cancer. (Ozols *et al*., 2003; Vasey *et al*., 2004). The addition of a third cytotoxic drug was tested for overall and progression free survival in patients with advanced-stage disease and primary peritoneal carcinoma. However, this addition did not prove to be beneficial and the standard of care has remained carboplatin and paclitaxel (Bookman *et al*., 2009).

Several subsequent trials have been carried out to further expand options for first-line treatment. Two such trials have used antiangiogenic anti-vascular endothelial growth factor (VEGF) antibody; bevacizumab concurrently with carboplatin and paclitaxel (R. A. Burger *et al*., 2011; Perren *et al*., 2011) and another trial incorporated a VEGF receptor tyrosine kinase inhibitor; pazopanib as a maintenance treatment (Du Bois *et al*., 2013). A Japanese study had a different approach in which paclitaxel fractionated into a dose-dense weekly routine was observed to improve progression-free survival and overall survival (Pujade-Lauraine *et al*., 2012; Rustin *et al*., 1996).

Another randomised trial that investigated efficacy of intraperitoneal chemotherapy raised interest and, to a certain extent, some debate (Armstrong *et al*., 2006). In this trial study, intravenous cisplatin with paclitaxel was compared to intraperitoneal and intravenous

chemotherapy with cisplatin and paclitaxel. Higher dose of cisplatin and dose-dense paclitaxel which was administered in the experimental group which showed significant improvement in survival rates. However, this treatment was only deliverable to 42% of patients due to neurological and gastrointestinal toxicities. Although this approach seemed promising with the potential to deliver greater concentrations of cytotoxic chemotherapy to the tumour compared to intravenous methods, the uptake has generally been poor. Currently more tolerable intraperitoneal regimens are being trialled (Jayson *et al*., 2014).

With its success, the Gynaecologic Oncology Group (GOG)/NRG Oncology portfolio has shaped the standard of care in ovarian cancer. Some examples of this include the approval of bevacizumab in front line therapy and also supporting its use in platinum sensitive recurrent disease. It has also helped manifest the role of intraperitoneal (IP) chemotherapy for advanced stage disease. The tables below summarise pertinent details of frontline intravenous (Table 1.2) and IP (Table 1.3) trials

Protocol	Stages	Debulking	Treatment	PFS (months)	RR/HR PFS	OS (months)	RR/HR OS	Conclusions
GOG 111	III/IV	Suboptimal (>2cm residual)	Cp/Cytoxan Cp/P	13 18	Reference 0.7 (95% CI 0.5-0.8)	24 38	Reference 0.6 (95% CI 0.5-0.8)	Addition of P improves outcome
GOG 132	III/IV	Suboptimal (>2cm residual)	Cp/P Cp P	14 16 11	Relative hazard for progression in P vs Cp = 1.41 (95% CI 1.15-1.73) Relative hazard for progression in Cp/P vs Cp = 1.06 (95% CI 0.929 -1.42)	25.9 30.2 26.3	Relative hazard for death in P vs Cp = 1.15 (95% CI 0.929-1.42) Relative hazard for death in Cp/P vs Cp = 0.99 (95% CI 0.795-1.23)	Cisplatin containing arms superior to paclitaxel alone establishes cisplatin/paclitaxel as standard
GOG 158	III	Optimal (>1cm residual)	P/Cp P/C	19 21	Reference 0.88 (95% CI 0.75 – 1.03)	48.7 57.4	Reference 0.84 (95% CI 0.70 – 1.02)	Non-inferiority study establishes P/C as standard
GOG 162	III/IV	Suboptimal	24 h P/Cp 96 h P/Cp	12.3 12.5	Reference 1.00 (95% CI 0.784 – 1.28)	2.49 2.54	Reference 1.12 (95% CI 0.860 – 1.45)	No benefit to prolonged P infusion
GOG 182-ICON	III/IV	Optimal and Suboptimal	P/C P/C/G P/C/PLD T/C- >P/C G/C- >T/C	16 16.3 16.4 15.4 15.4	Reference 1.028 (95% CI 0.984 1.066 1.037)	44.1 44.1 44.2 40.2 39.6	Reference 1.006 (95% CI 0.885 – 1.144) 0.952 (95% CI 0.836 – 1.085) 1.051 (95% CI 0.925 – 1.194) 1.114 (95% CI 0.982 – 1.264)	Addition of third chemotherapy agent did not yield clinical benefit
GOG 218	III/IV	Suboptimal and Optimal III/IV	P/C P/C/B P/C/B- >B	10.3 11.2 14.1	Reference 0.908 (95% CI 0.795 – 1.040) 0.717 (95% CI 0.625 – 0.824)	39.3 38.7 39.7	Reference 1.036 (95% CI 0.827 – 1.297) 0.915 (95% CI 0.727 – 1.152)	Result supports use of bevacizumab in front line therapy
GOG 262	III/IV	Optimal, Suboptimal and Neo-adjuvant	Q3wk P/C +/-B DD P/C +/- B	14 14.7	Reference 0.89 (95% CI 0.74 – 1.06)	39 40.2	Reference 0.94 (95% CI 0.72 – 1.23)	DD P did not improve survival outcomes Subset analysis suggests DD P of benefit in patients not receiving B

P=Paclitaxel, C=Carboplatin, CP=Cisplatin, G = Gemcitabine, T = Topotecan, PLD = Pegylated Liposomal Doxorubicin, B=Bevacizumab
DD = Dose Dense, PFS = progression-free survival, OS = overall survival wk. = week, yrs. = years, RR = Relative Risk,
HR = Hazard Ratio, CI = confidence interval, NR = Not Reported, hr = hour.

Table1. 2 Frontline intravenous trials for advanced stage of ovarian cancer adapted from DiSilvestro (2019)

Study	Stage	Debulking	Treatments	PFS (months)	HR PFS	OS (months)	HR OS	Conclusion
GOG104	III/IV	Optimal (<2cm residual)	C (IV)//Cyt (IV) C (IP)//Cyt (IV	N/A	N/A	41 49	Reference HR = 0.76 (95% CI 0.61–0.96	IP arm superior Lack of P impacts relevance
GOG 114	III	Optimal (<1cm residual)	P (IV)//C (IV) Ca (IV) x2 then P (IV)//C (IP)	22.2 27.9	Reference HR = 0.78 (95% CI 0.66–0.940)	52.2 63.2	Reference HR = 0.81 (95% CI 0.65–1.00)	Borderline OS improvement IP regimen not routinely adopted
GOG 172	III	Optimal (<1cm residual)	P (IV)//C (IV) P (IV)//C (IP)//P (IP)	18.3 23.8	Reference HR = 0.80 (95% CI 0.64–1.00)	49.7 65.6	Reference HR = 0.75 (95% CI 0.58–0.97)	Dramatic OS improvement tempered by toxicity concerns
GOG 252	III/IV	Optimal/ Suboptimal	DD P (IV)//Ca (IV)//B (IV) DD P (IV)//Ca (IP)/B(IV)) P (IV)//C (IP)//P (IP)//B (IV	24.9 27.4 26.2	Reference HR = 0.925 (95% CI 0.802–1.07) HR = 0.977 (95% CI 0.847–1.13)	Pending Final Manuscript	N/A	No benefit to IP therapy

C=Cisplatin, Cyt = Cytoxan, P=Paclitaxel, Ca = Carboplatin, B=Bevacizumab, IV = intravenous, IP = intraperitoneal, DD = dose dense weekly, HR = hazard ratio, PFS = progression free survival, OS = overall survival, mo = months, CI = confidence interval, cm = centimetres.

Table1. 3 Frontline intraperitoneal trials for advanced stage of ovarian cancer adapted from DiSilvestro, (2019)

While frontline treatment involving debulking followed by platinum and taxane based chemotherapy can be effective, less than 50% of the patients with advanced stage ovarian cancer survive for 5 years (Hope and Blank, 2010). Although second-line treatments are available, a recurrence due to drug resistance results in lower response rates. This has led to the rationale that following complete response to conventional treatment extended chemotherapy needs to be developed in order to delay and/or evade recurrence. An approach to this extended therapy is termed maintenance chemotherapy. This is based on the theory that inadequate exposure of slow dividing tumour cells to front-line cycle dependant cytotoxic treatment can potentially be removed over time by continual treatment (Ozols, 2003; Rowinsky and Donehower, 1995).

As mentioned earlier, bevacizumab was used as concurrently with front line therapy and approved in Europe and eventually in the United states (R. A. Burger *et al*., 2011; Perren *et al*., 2011). However, a majority of patients who had complete remission had a recurrence of the disease (Tsibulak *et al*., 2019). Several randomized trials were carried out exploring optimal front-line therapy however dose-densing, addition of a third chemotherapy agent or intraperitoneal administration did not improve overall survival (R. A. Burger *et al*., 2011; Perren *et al*., 2011). Recently PARP inhibitors showed promising results as a maintenance therapy in patients with BRCA 1/2 mutations. Due to its impressive survival benefits in recurrent epithelial ovarian cancer (Mirza *et al*., 2016), PARP inhibitors role in the front-line maintenance therapy has garnered interest. This has also led to the development of several trials namely: SOLO-1, PAOLA-1, GOG-3005 and PRIMA trials. The first trial; SOLO-1, showed patients who were newly diagnosed with advanced disease, carried BRCA1/2 mutation and responded to platinum-based chemotherapy seemed to benefit from maintenance therapy with olaparib (Moore *et al*., 2018). Although this study examined platinum sensitive patients who were BRCA1/2 mutation carriers it has raised interest in exploring the activity of PARP inhibitors in the front-line in BRCA wildtype patients.

1.5.2 Second line chemotherapy

Patients who develop recurrent disease usually receive second line chemotherapy; however only a subgroup are eligible for second surgery. The outcome of the DESKTOP I trial recommended scores that predicted the option of a complete cytoreduction in recurrent ovarian cancer. Assuming factors such as (1) complete resection at first surgery, (2) good performance status, and (3) absence of ascites was present, resection was considered (Harter *et al*., 2011, 2009, 2006).

In the 2011 (Harter *et al*.) study, the subgroups of patients harbouring distinct tumour masses for which maximal resection was possible, made up 51% of the patient cohort. Of these 76% had a complete resection thus validating the scores predicting complete resection. Promising results from this study led to prospective randomised trials of surgery in recurrent disease (ClinicalTrials.gov Identifier: NCT01166737 and NCT00565851)

In a study carried out by Rustin *et al*. (2010), patients who developed recurrent disease were randomised and received chemotherapy based on either recurrence or on clinical relapse. Recurrence typically ensues 3-4 months before clinical presentation and is detected by CA-125 concentration. Elevated levels of CA-125 which led to early intervention did not result in improved survival. However, this resulted in poor quality of life due to earlier treatment with chemotherapy during a period where patients could have otherwise been asymptomatic. For patients with recurrent ovarian cancer, the regimen of chemotherapy treatment is decided based on the interval between the last cycle of platinum-based chemotherapy to the start of progression the disease (Eisenhauer *et al*., 1997; Markman *et al*., 1991). According to these retrospective studies, platinum-resistant disease is the progression of the cancer within 6 months of the last platinum-based treatment and has a response rate of less than 15%. Patients with a 6-12-month platinum free interval are considered to have a partially platinum-sensitive disease and those with recurrence occurring after 12 months have increasing sensitivity to platinum-based regimens (Eisenhauer *et al*., 1997; Markman *et al*., 1991).

In ovarian cancer the median overall free survival is about 18 months (Shimokawa *et al*., 2018). Since first-line chemotherapy treatments last up to 5 months, a majority of recurrent disease is responsive and as such sensitive. Several trials have demonstrated the effectiveness of using combination of platinum containing drugs such as carboplatin with paclitaxel, gemcitabine (González-Martín *et al*., 2005; Parmar *et al*., 2003; Pfisterer *et al*., 2006) or pegylated liposomal doxorubicin (Pujade-Lauraine *et al*., 2010), in treating platinum-sensitive recurrent disease. The strategy of using platinum-based regimens on platinum-sensitive disease patients has more recently led to subsequent resistance to the treatment (Jayson *et al*., 2014). Patients with disease progression continues with platinum-based treatment or those with have developed a platinum resistance often have the worst prognosis (Jayson *et al*., 2014). In the past these patient's disease was managed with one drug (pegylated liposomal doxorubicin or topotecan) (Gordon *et al*., 2001) which has resulted in poor responses. Some patients, however, have been observed to respond to dose-dense regimens which are more potent than just one drug (Meyer *et al*., 2001; Sharma *et al*., 2009; van der Burg *et al*., 2002). These patients will benefit most by participating in trials of new agents and regimens. Establishing the drug sensitivity through chemo-sensitivity assays or genetic screening arrays have been studied and the recommendations so far have been within clinical trial settings (Burstein *et al*., 2011; Cree *et al*., 2007).

The GOG/NRG Oncology plays an important role in the recommendation of drugs for patients with recurrent disease. Previous GOG trials examined the role of cisplatin and paclitaxel as well as other chemotherapy agents, in a successive single agent trial (DiSilvestro, 2019). With over a hundred trials carried out for the treatment of recurrent ovarian cancer, the more recent developments include poly (ADP-ribose) polymerase (PARP) inhibitors, immunotherapy and angiogenesis inhibitors which have been studied within GOG/ NRG Oncology. Examples of these trials are detailed in the table 1.4 below.

Trial	Phase	Eligibility criteria	Regimens	PFS/RR	Conclusions
GOG 213	III	Platinum sensitive	P or G/C P or G/C with Bevacizumab	10.4 mo 13.8 mo HR = 0.628 (95% CI 0.534-0.739)	Addition of bevacizumab improves outcome. OS benefit 42.2 vs 37.3 mo. (HR = 0.823, 95% CI 0.680–0.996)
GOG 170D	II	Platinum sensitive/resistant	Bevacizumab	40.3% progression free at 6 months, 21.0% RR	Results support further development of bevacizumab in ovarian cancer
GOG 186G	II	Platinum sensitive/resistant	Bevacizumab Bevacizumab/Everolimus	4.5 mo 5.9 mo HR = 0.95 (95% CI 0.66–1.37)	Addition of everolimus does not improve outcome
GOG 186I	II	Platinum sensitive/resistant	Bevacizumab Bevacizumab/Fosbretabulin	4.8 mo 7.3 mo HR = 0.69 (95% CI 0.47–1.00)	Addition of fosbretabulin improves outcome
GOG 186F	II	Platinum sensitive/resistant	Docetaxel/Trabectedin	4.5 mo 30% response rate	Regimen active
NRG GY001	II	Recurrent Clear Cell Carcinoma	Cabozantinib	0% response rate	Cabozantinib not active in this unselected cohort
NRG GY003	II	Platinum sensitive/resistant	Nivolumab Nivolumab/Ipilimumab	2.0 mo 3.9 mo HR = 0.599 (95% CI 0.388–0.925	Improvement in outcome supports continued development of regimen
GOG 280	II	Platinum sensitive/resistant	Veliparib	31.4% RR in combination arm 8.2 mo 26% RR	Demonstrated activity of Veliparib in this selected population

P=Paclitaxel, G = Gemcitabine, C=Carboplatin, PFS = progression-free survival, RR = response rate, HR = hazard ratio, CI = confidence interval, mo = months

Table1. 4 Recurrent disease treatment trials for ovarian cancer with outcomes reported and other pertinent details. Table adapted from DiSilvestro, (2019) and trial details sourced from Markman (2011) and Wp *et al*. (2018).

1.5.3 Targeted therapies

In many studies the addition of bevacizumab in combination with chemotherapy as a first line therapy has proved to prolong progression free survival along with a tolerability profile that is considered acceptable and preserved quality of life (R. A. Burger *et al*., 2011; Perren *et al*., 2011; Aghajanian *et al*., 2015, 2012). Another class of targeted therapies that has recently been studied are PARP inhibitors. With the loss of function of BRCA genes, PARP proteins are recruited to aid in the repair of damaged DNA. Inhibition of the PARP molecule prevents the BRCA defective cancer cell from repairing chemotherapy induced DNA damage. This makes the cancer cell vulnerable to cytotoxic drugs through concept known as synthetic lethality further described in section 1.5.6; Figure 1.4 (Drew, 2015; Kaelin, 2005). An FDA approved PARP inhibitor; olaparib has shown to be associated with a significantly longer median progression free survival (8.4 months) when used as a monotherapy in patients with platinum-sensitive, relapsed, high-grade serous ovarian cancer (Ledermann *et al*., 2014, 2012; Jonathan A Ledermann *et al*., 2016). However, no significant difference was observed in overall survival between patients treated with and without olaparib. Analysis of the study data based on BRCA mutation status demonstrated that platinum-sensitive relapsed serous ovarian cancer patients harbouring a BRCA mutation benefitted most from olaparib treatment (Ledermann *et al*., 2014).

1.5.4 Platinum based chemotherapy:

1.5.4.1 Cisplatin

In 1965, Cisplatin, a platinum compound was first shown to have antibiotic activity (Rosenberg *et al*., 1965). Its anti-tumour activity was established in animal models and was subsequently introduced into clinical trials (Rosenberg *et al*., 1969). Cisplatin was eventually the chemotherapeutic drug of choice for targeting various malignancies(Dasari and Tchounwou, 2014). For over 15 years the standard of care for ovarian cancer has included the use of platinum-based drugs. Cisplatin is the prominent chemotherapy drug of choice followed by combinations of carboplatin-based treatments (Raja *et al*., 2012). This is due to its effective antitumor potency which is known to demonstrate clinical responses against a range of tumours (Siddik, 2003).
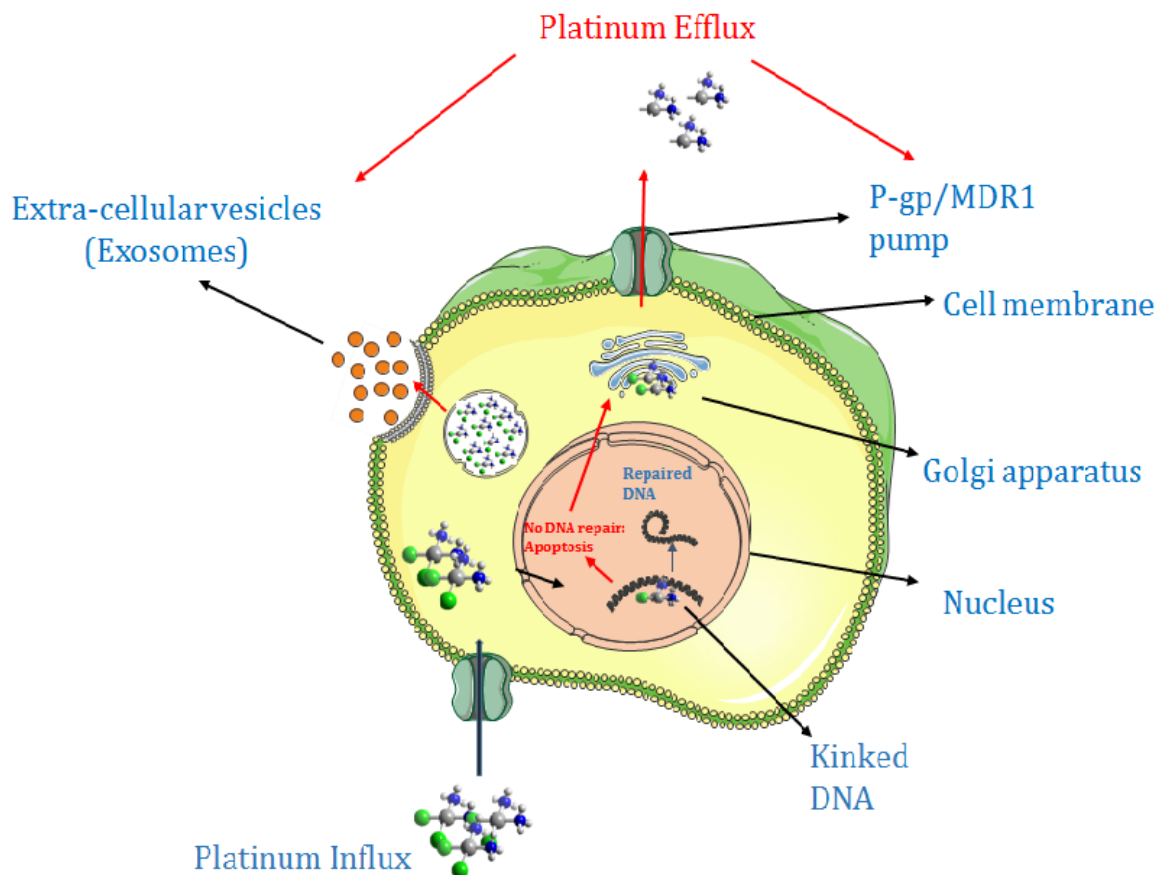
Figure1. 1 Mechanism of Action of Platinum based drugs adapted from Rocha et al., (2018). The Platinum drug enters the cell and into the nucleus. It binds to the DNA and forms adducts which results damage to the DNA leading to apoptosis/cell death. The drug can also be effluxed out the cell through the P-gp/MDR1 pump or as extra cellular vesicles such as exosomes.

Cisplatin's mode of action involves entering the nucleus (Figure 1.1) and interacting with the DNA to form adducts as shown in Figure 1.2. These in turn lead to the formation of intra- and inter- strand crosslinks which trigger several pathways to repair the lesions or to induce apoptosis (Galluzzi *et al*., 2012). Cisplatin is the perfect representation of how a minute change in its own chemical structure can significantly impact the target cells biological activity. It is composed of platinum ion that is doubly charged and surrounded by a total of four ligands. The amine ligands are bound on the left which form stronger bonds with the platinum ion. The chloride ligands bound on the right allow the platinum ion to bind with DNA bases through leaving groups that are formed (Figure1.2 A) (Goodsell, 2006). However, the molecular mechanisms of these crosslink formations are not properly understood and therefore could have an effect on survival (Dasari and Tchounwou, 2014)

Figure1. 2 Activation of cisplatin and induction of DNA damage. A) Cisplatin is activated by exchange of one or two of its chloride molecules for water molecules resulting in monoaquated and diaquated cisplatin, respectively. B) Cisplatin forms covalent bonds with DNA creating intra-strand DNA adducts, which make up a majority if the DNA lesions and inter-strand crosslinks (Browning *et al*., 2017).

In ovarian cancer patients, cisplatin is the most active chemotherapeutic drug used, with most patients initially responding well to the treatment. However, a more aggressive and chemo-resistant malignancy can develop, even after several treatment doses (Helm and States, 2009, Pink *et al*., 2015)

1.5.4.2 Carboplatin

Rosenberg's pioneering work with cisplatin led to several platinum-based metal complexes being studied in the treatment of cancers. Over a thousand platinum compounds have been tested since the 1970s, 185 of which were active (Sousa *et al*., 2014b). This initiated worldwide research leading to the synthesis of 3000 plus analogous compounds. Although some of the new compounds were considered to be less toxic than cisplatin only few were approved for commercialization. One of these was the compound Carboplatin (McWhinney *et al*., 2009; Wheate *et al*., 2010). A derivative of cisplatin, carboplatin has a similar mechanism of action.

What sets it apart from cisplatin is its structure and toxicity (Sousa *et al*., 2014a). Carboplatin (1,1-cyclobutyldicarboxylate) is one of the main anti-tumour drugs used for the treatment of ovarian, head, neck, testicular and small cell lung cancer (Fuertes *et al*., 2003). Like cisplatin its mechanism of action involves targeting the DNA and efficiently binding to it forming "adducts". This thereby leads to cell death by inhibiting replication and transcription (Brabec and Kasparkova, 2005). Depending on the nature of these adducts several transduction pathways are affected therefore inducing necrosis or apoptosis in the tumour cell. The kind of adducts formed can range from interchain diadducts to mono or intra adducts as shown in Figure 1.3 below (Hah *et al*., 2006).
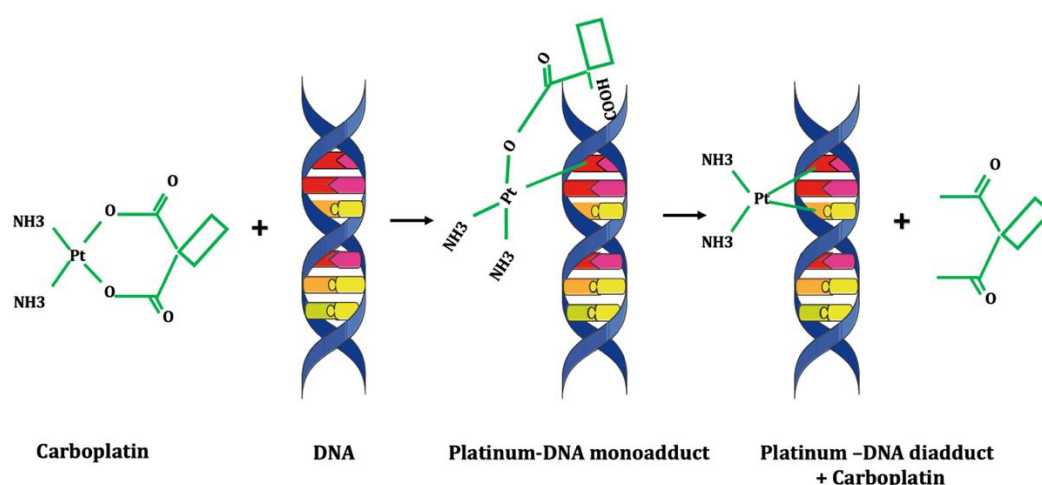
Figure1. 3 Carboplatin mechanism of action. Carboplatin activates when it enters cells forming intra- and inter-strand cross-linkage of DNA molecules known as adducts. Depending on the kind of adduct it can trigger apoptosis of tumour cells or affect several transduction pathways (Sousa *et al*., 2014a).

1.5.5 Taxol

Taxol, otherwise known as paclitaxel, was first isolated in 1962 from the Pacific yew tree *Taxus brevifolia* Nutt's bark (Liebmann *et al*., 1993; Manfredi and Horwitz, 1984; Walsh and Goodman, 2002). It was only entered into clinical trials after a 1981 National Cancer Institute screening programme (Renneberg, 2007). Following *in vivo* screens of tumour implanted mouse models, it was reported to possess broad spectrum anti-tumour activity(Renneberg, 2007). Further interest grew in the use of Paclitaxel with the discovery of its mechanism of action followed by its ability to cause regression of tumours in mammary tumour xenografts (Walsh and Goodman, 2002).

In cancer cells, paclitaxel targets microtubules by promoting stable microtubule assembly from β-tubulin heterodimers and inhibits their depolymerisation which results in cell cycle arrest in the G2/M phase (Shu *et al*., 1997). This prevents cell division and replication and ultimately leads to apoptosis (Rowinsky and Donehower, 1995; Schiff *et al*., 1979; Schiff and Horwitz, 1980; Zhang *et al*., 2014). In many solid tumours, paclitaxel has been used in combination with cisplatin as a treatment strategy. While cisplatin leads to inhibition of DNA replication by binding to the DNA strands, paclitaxel works by stabilising polymerised microtubules as a result of which leads to cytotoxicity (Rohena and Mooberry, 2014). Their differing mechanisms of action make them a preferred combination therapy in cancer.

1.5.6 PARP Inhibitors

Poly (ADP-ribose) polymerase (PARP) is vital in regulating cellular processes such as DNA repair. One of the early DNA damage responses is the activation of PARP among other molecules (Herceg and Wang, 2001). Tumour cells have an increased replication rate and therefore achieve genomic instability with high possibilities of DNA mutations. Single strand breaks and double strand breaks undergo repair through several DNA repair mechanisms. In single strand breaks, the Base Excision Repair (BER) mechanism eliminates the damaged bases using DNA glycosylase. PARP is essential in the BER pathway (Toss and Cortesi, 2013).

PARP was first described in the early 1960's and was later suggested to have an influence on alkylator chemotherapy (Chambon *et al*., 1963, Durkacz *et al*., 1980). The PARP family is made up of seventeen structurally similar proteins and possess enzymatic and scaffolding properties. They are also able to recruit the essential proteins for DNA repair (Toss and Cortesi, 2013). PARP 1 and PARP 2 are best characterized from the PARP family. They are necessary DNA repair proteins that are functional in the BER mechanism without which may lead to cell death. This characteristic makes the PARP proteins suitable targets for therapy and therefore PARP inhibitors have since been developed and followed upon as a therapeutic alternative to classical cytotoxic chemotherapy agents (Anwar *et al*., 2015).

Several PARPis have been approved for use in the treatment of ovarian cancer after years of development. Treatment of recurrent disease (the PARP inhibitor is used to shrink the tumour) and maintenance after platinum-based chemotherapy are the two approved roles of PARP inhibitors in ovarian cancer (Murthy and Muggia, 2019). The clinically relevant PARP inhibitor ovarian cancer trials are summarised in Table 1.5 below.

Trial	Phase	Eligibility	Arms	No. of Pts	PFS (mo)	OS (mo)
Study 19 NCT00753545 (Ledermann *et al.*, 2012)	2	Platinum-sensitive, high-grade serous ovarian cancer, received at least 2 platinum-based regimens	Maintenance olaparib 400 mg BID (capsule)	136	8.4	NSD
			Placebo	129	4.8	NSD
SOLO2/ENGOT-Ov21 NCT01874353 (Pujade-Lauraine *et al.*, 2017)	3	Platinum-sensitive, high-grade serous ovarian cancer or high-grade endometrioid cancer, received at least 2 lines of chemotherapy, with pathogenic *BRCA* mutations	Maintenance olaparib 300 mg BID	196	19.1	NM
			Placebo	99	5.5	NM
SOLO1 NCT01844986(Moore *et al.*, 2018)	3	Newly diagnosed, high-grade serous or high grade endometrioid ovarian cancer with pathogenic *BRCA* mutations	Maintenance olaparib 300 mg BID	260	Not yet reached (hazard ratio 0.30, *P* < 0.001)	NM
			Placebo	131	13.8	NM
Kaufman *et al.*, (2015)	2	Germline *BRCA* mutation and platinum-resistant ovarian cancer, breast cancer treated with three or more previous regimens, pancreatic cancer with previously administered gemcitabine, or prostate cancer previously treated with hormonal therapy and one systemic therapy	Treatment olaparib 400 mg BID (capsule)	298	Primary endpoint ORR: 26.2%; In pts with ovarian cancer, response rate 31.1%	Median OS in ovarian cancer pts: 16.6
ARIEL2, Part 1 NCT01891344 (Swisher *et al.*, 2017)	2	Recurrent, platinum-sensitive high-grade ovarian cancer, received at least 1 platinum-based regimen	Treatment rucaparib 600 mg BID	204	*BRCA* mutated: 12.8 LOH high: 5.7 LOH low: 5.2	NR
ARIEL3 NCT01968213 (Coleman *et al.*, 2017)	3	Platinum-sensitive, high-grade serous or endometrioid ovarian cancer, received at least 2 platinum-based regimens	Maintenance rucaparib 600 mg BID	375	10.8 (*BRCA*-mutated cohort PFS 16.6, HRD cohort PFS 13.6)	NM
			Placebo	189	5.4	NM
ENGOT-OV16/NOVA NCT01847274 (Mirza *et al.*, 2016)	3	Platinum-sensitive ovarian cancer, either germline *BRCA* mutation or high-grade serous histology, received at least 2 platinum-based regimens	Maintenance niraparib 300 mg daily	372	Germline *BRCA*-mutated cohort: PFS 21.0 *vs.* 5.5	NM
			Placebo	181	Non-germline *BRCA* mutated, HRD positive cohort: PFS 12.9 *vs.* 3.8 Overall non-germline BRCA mutated cohort: PFS 9.3 *vs.* 3.9	

Trial	Phase	Eligibility	Arms	No. of Pts	PFS (mo)	OS (mo)
NCT01116648 (Liu *et al*., 2014)	2	Platinum-sensitive ovarian cancer, either high-grade serous cancer or germline *BRCA* mutation	Olaparib 200 mg BID (capsule) + cediranib 30 mg daily	44	17.7	NR
			Olaparib 400 mg BID (capsule)	46	9.0	NR
NCT01081951 (Oza *et al*., 2015)	2	Platinum-sensitive, high-grade serous ovarian cancer, received up to 3 courses of platinum-based chemotherapy	Olaparib 200 mg BID (capsule) + paclitaxel 175 mg/(m^2) + carboplatin AUC 4, then maintenance olaparib 400 mg BID (capsule)	81	12.2	NR
			Paclitaxel 175 mg/(m^2) + carboplatin AUC 6	81	9.6	NR
TOPACIO (ovarian cancer cohort) NCT02657889 (Konstantinopoulos *et al*. 2018)	1/2	Recurrent, platinum-resistant/refractory ovarian cancer	Niraparib 200 mg daily + pembrolizumab 200 mg IV every 21 days	62	Primary endpoint ORR: 25%	NR

Table1. 5 Clinical studies of clinically relevant PARP inhibitors. High-grade serous ovarian cancer as described here includes fallopian tube and primary peritoneal cancer. Unless otherwise specified, the olaparib formulation is the tablet formulation. The maintenance designation implies maintenance after complete or partial response to platinum-based chemotherapy. The clinicaltrials.gov identifier is included where available. Progression-free survival data is statistically significant. AUC: area under the curve; BID: twice a day; HRD: homologous recombination deficient; NM: not mature; No.: number; NR: not reported; NSD: no statistically significant difference; ORR: objective response rate; OS: overall survival; PFS: progression-free survival; Pts: patients

PARP inhibitors function by inhibiting timely repair of single strand breaks that further results into double strand breaks when it encounters a replication fork (Arnaudeau *et al*., 2001). In patients with BRCA mutation-related cancers such as high grade serous ovarian cancer, the presence of a wild-type BRCA1 or 2 genes is lacking in the tumour cell. Normal cells maintain at least a single wild-type copy of the relevant BRCA gene making it is possible for the PARP inhibitors to specifically destroy the tumour cell without harming the normal cells (Kaye *et al*., 2011). The concept of synthetic lethality is thereby exploited by this approach. Synthetic lethality (Figure 1.4) is described as a condition in which two singularly individual defective pathways permit viability of cells but when combined becomes lethal (Toss and Cortesi, 2013).
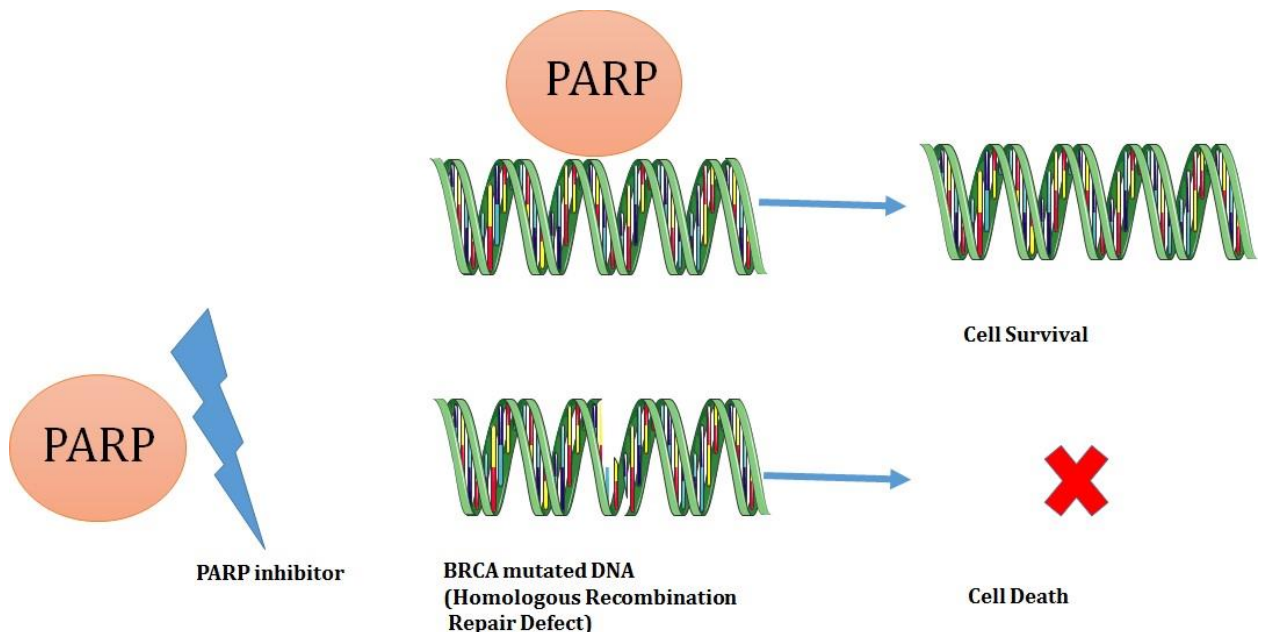
Figure1. 4 Mechanism of action of PARP inhibitors. PARP proteins are required to repair DNA strand breaks particularly in BRCA defective DNA. PARP inhibitors prevent the PARP proteins from binding to the damaged DNA thereby resulting in cell death. This phenomenon is known as synthetic lethality in which simultaneous loss of both the BRCA and PARP proteins leads to lethality (Helleday, 2011).

The impairment of the BER mechanism through PARP inhibition does not allow for the repair of single strand breaks that may be caused by alkylating agents. This leads to a double strand break and as such patients with a defective homologous recombination mechanism (BRCA mutation carrier) experience cancer cell death due to the PARP inhibitors aberrant activation of

Non-homologous end joining (NHEJ). The NHEJ repair pathway results in genomic instability of HR-deficient cells induced by PARP inhibitors. This makes the mechanism of NHEJ critical in the hypersensitivity of cells with a defective HR mechanism to PARP inhibitors and results in the lethality of PARP inhibitors to these cells.

Therefore, tumour cells that possess a defective HR mechanism are more sensitive to PARP inhibitors blocking BER (Kruse *et al*., 2014). Studies carried out in 2005 indicated that cells with BRCA mutations were more sensitive to PARP inhibitors compared to the wild type and heterozygous mutant cells. This further emphasised their promising role in BRCA mutated ovarian cancer patient treatment (Helen E Bryant *et al*., 2005; Farmer *et al*., 2005a). Up to 50% of high-grade ovarian cancers may have defects conferring sensitivity to PARP inhibition (Ashworth, 2008; Baldwin *et al*., 2000; Press *et al*., 2008) suggesting that PARP inhibition could be more widely applicable in the treatment of sporadic rather than BRCA mutated ovarian cancer.

1.6 Mechanism of Resistance

1.6.1 Platinum Drugs (Cisplatin and Carboplatin):

Despite cisplatin being considered one of the most effective chemotherapeutic treatments for various cancers, it has limitations; the most challenging being acquired resistance to the drug by target cells. When a cancer cell develops cisplatin resistance it essentially is failing to respond to the drug at clinically relevant concentrations and undergo apoptosis. Resistance may be caused due to chronic drug exposure or the cancer cells may be intrinsically resistant before they receive therapy (Siddik, 2003). Another mechanism that contributes to resistance is drug efflux mediated my extracellular vesicles (EV). The secretion of drugs into the cargo of EVs shed by cancer cells allows for drug efflux from those cells (Gong *et al*., 2013; Muralidharan-Chari *et al*., 2016; Sousa *et al*., 2015).

Indeed, it has been suggested that (a) cancer cells that secrete more EVs achieve the highest levels of resistance (Dorayappan *et al*., 2018; Muralidharan-Chari *et al*., 2016; Shedden *et al*., 2003) and (b) drug-resistant cells will export more drugs into their EVs than drug-sensitive cells

(Gong *et al*., 2013; Guerra *et al*., 2019; Khoo *et al*., 2019; Safaei *et al*., 2005). *In vitro* and *in vivo*, a massive increase in the release of EVs has been identified as one of cancer cells' responses to photodynamic treatment and chemotherapeutic drugs (Aubertin *et al*., 2016).
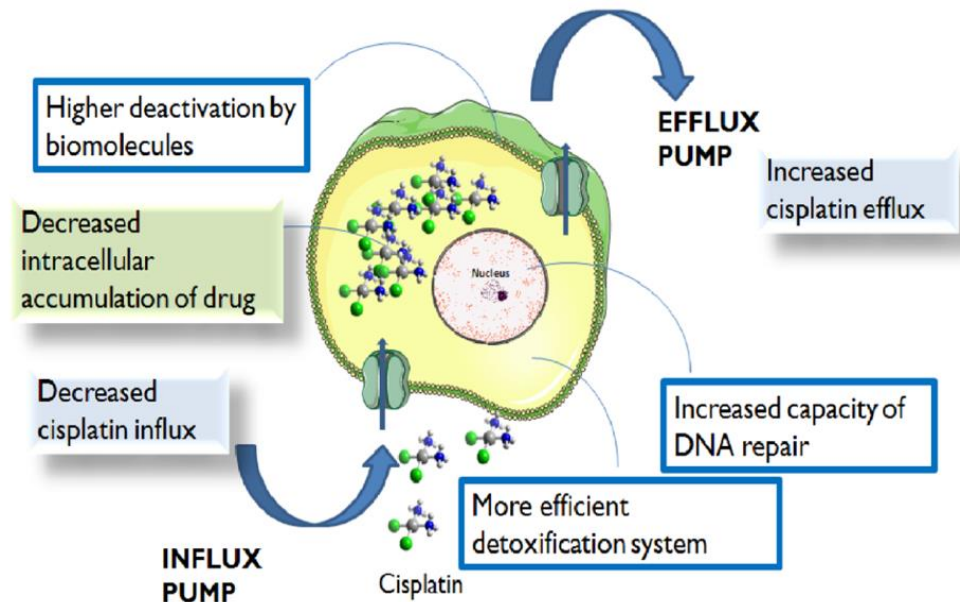
Figure1. 5 Mechanism of Cisplatin Resistance adapted from (Trudu et al., 2015). Cisplatin resistance is considered to be multifactorial and involves several mechanisms some of which include increased efflux of cisplatin or decreased influx of cisplatin which can lead to reduced intracellular accumulation of cisplatin and restoration of DNA through increased repair.

Tumour cell line studies established from clinically aggressive tumours showed that cisplatin resistance was markedly higher than previously acknowledged as they require a 50-100 fold increased dose of the cytotoxic drugs compared to that needed for tumour cells that were sensitive (Kelland *et al*., 1995)(Hagopian *et al*., 1999; Hills *et al*., 1989). This suggests that these cell lines may perhaps be intrinsically resistant and having slight or no response to treatment from the beginning. However, recent studies established clinically relevant drug-resistant cell lines by mirroring the patient's condition during chemotherapy. These cell line develop what is known as acquired resistance. A 2014 study showed that cell lines developed from patients before and after therapy demonstrated between two- and eight-fold resistance compared to their parental cell line (McDermott *et al*., 2014). A plethora of complex resistance

mechanisms have shown to be involved in platinum resistance (Figure 1.5). The mechanisms on deeper analysis, reveal the activation and involvement of pathways that intrinsically play major role during development or as defence against toxins (Shen *et al*., 2012).

Cisplatin-resistant cells which display numerous phenotypic changes are well documented (Brozovic, 2017; Galluzzi *et al*., 2012; Shen *et al*., 2012). These changes include cross resistance to either structurally related or unrelated chemotherapeutic drugs, decreased platinum accumulation and DNA adduct levels in cisplatin resistant cells, changes in the level of gene expression with regards to cell survival such as, DNA damage repair, apoptosis, transporters, transcription factors and oncogenes to name a few (Kasherman *et al*., 2009; Reed, 1998). By implementing a complex self-defence mechanism to evade extracellular cytotoxic compounds, cells develop cisplatin resistance as well as resistance to other chemotherapeutic drugs. In order to survive, the cells activate a defective or active/defensive phenotype by either silencing or activating gene expression on exposure to platinum compounds (Shen *et al*., 2012).

A number of anticancer drugs are associated with multidrug resistance, a phenomenon whereby there is an increased efflux of the drug through non-selective members of the ATP binding cassette (ABC) family of ATPases (Wang *et al*., 2010). The ATP-binding cassette sub-family C 2 also known as MRP2 is an export protein found to play a major role in drug efflux; specifically cisplatin (Kool *et al*., 1997; Wang and Lippard, 2005) However, the reduced uptake of cisplatin is most often due to limited intracellular accumulation (Baekelandt *et al*., 2000). Other cisplatin-resistant cells (for example the 4lMcisR6 cell line and its parental cell lines) have consistently shown a decrease in accumulation of cisplatin regardless of the underlying mechanisms of cisplatin resistance (Loh *et al*., 1992).

The transmembrane protein, copper transporter 1 (CTR1) was discovered to play a vital role in cisplatin uptake (Ishida *et al*., 2002; Kilari *et al*., 2016; More *et al*., 2010). CTR1 protein is localized in the plasma membrane as well as in the intracellular vesicles. Several studies reflected that cells do not experience cisplatin cytotoxicity if pre-treated with copper however copper chelators lead to higher accumulation of cisplatin resistance and aggravate cytotoxicity (Ishida *et al*., 2010; More *et al*., 2010). Treatment with clinically relevant concentrations of

cisplatin downregulates CTR1 by internalizing and degrading it (proteasome-mediated). Multiple instances of acquired cisplatin resistance is therefore in part a result of this mechanism (Holzer *et al*., 2006; Holzer and Howell, 2006).

Another important mechanism responsible for cisplatin resistance is in DNA damage and repair. Several DNA repair pathways which operate as a result of DNA damage have been identified to recruit specific proteins to form complexes and repair the damage in order for the cells to survive. However, some of these repair pathways are defective due to the dysfunction, reduction or lack of repair proteins (Weil and Chen, 2011). Cancer cells take advantage of these mechanisms and upregulate DNA repair and enhance resistance to chemotherapy (Ghosal and Chen, 2013). Cisplatin anti-tumour activity works primarily by interacting and targeting chromosomal DNA. The sensitivity of cancer cells to cisplatin is therefore linked to the impairment in the DNA-cisplatin interaction mechanism (Basu and Krishnamurthy, 2010).

Cisplatin-induced DNA damage is considered to be a major lesion caused by intra-strand cross links which in turn are repaired through the nucleotide excision repair pathway (NER)(Basu and Krishnamurthy, 2010). DNA repair proteins such as the ERCC2 and XPA have been shown to be overexpressed during NER pathway activation such that it is correlated with the cisplatin resistance. Cancer cells therefore seem to adjust their sensitivity to cisplatin in order to tolerate cisplatin-mediated damage by increasing DNA repair (Basu and Krishnamurthy, 2010). The NER mechanism used in cisplatin-induced DNA repair is multilayered, involving epigenetic, transcriptional, and posttranslational regulation (Basu and Krishnamurthy, 2010). Base excision repair (BER) however, does not impact cisplatin intrastrand adduct processing but in fact modulates cisplatin intrastrand cross-links (ICL) DNA repair (Kothandapani *et al*., 2011). It has been reported that the BER-deficient/inhibited cells' resistance to cisplatin is not due to general intrastrand or ICL DNA damage, but rather to cisplatin-specific DNA damage (Kothandapani *et al*., 2011).

Although carboplatin is considered to have less side effects than cisplatin due to its pharmacodynamics, it is less potent in some cases due to the differential adduct formation rates with DNA. The difference in the toxicity levels is caused by Carboplatin's low reactivity rate with nucleophiles in the cell it enters (Hah *et al*., 2006; McWhinney *et al*., 2009). As mentioned

earlier the development of resistance to platinum-based chemotherapy such as cisplatin is a major challenge faced in the clinic. Carboplatin is no exception to this problem since the response of the tumour cell which confers carboplatin resistance is not very well understood (Shahzad *et al*., 2009; Wernyj and Morin, 2004). Studies show that the intracellular mechanisms through which the cells develop resistance to carboplatin are similar to cisplatin resistance. These mechanisms include increase in the detoxification of the drug (by thiol groups and glutathione), improved tolerance to nuclear damage and DNA repair which in turn leads to decrease in intracellular accumulation of carboplatin and resulting in reduced apoptosis (Stewart, 2007; Wang and Lippard, 2005). Therefore, triggering greater DNA damage, undermining DNA repair mechanism and inducing or preventing apoptosis could result in reduced survival rate of tumour cells and perhaps overcome resistance (Burger *et al*., 2011; Shahzad *et al*., 2009).

1.6.2 Taxol Resistance

Further research into the mechanisms of microtubule formation revealed that cells have the ability to enable cells to evade cytotoxicity. This evasion tactic leads to failed chemotherapy and eventually chemoresistance (Ganguly *et al*., 2010). Signalling pathways have a major role to play in the development of paclitaxel resistance. Their effects include the inhibition of apoptosis, activation of mitogen-activated protein kinase, intracellular signalling pathway PIK3 (phosphatidylinositol-4,5-bisphosphate 3-kinase) and others (Ferlini *et al*., 2009; Gottesman *et al*., 2009; Orr *et al*., 2003; Wang *et al*., 2006). The upregulation of the P-glycoprotein (P-gp), mutation in the β-tubulin gene are also considered mechanisms by which cancer cells develop resistance (Johnatty *et al*., 2013; Lagas *et al*., 2012; Mechetner *et al*., 1998).

P-gp, which is a cell membrane transport protein and encoded by multi-drug resistance gene ABCB1, has a pivotal role in exporting taxanes and other cytotoxic molecules outside the cell (Pauli-Magnus and Kroetz, 2004). Therefore, its increased expression has been associated with poor response to chemotherapeutic drugs (Baekelandt *et al*., 2000; Ng *et al*., 2000) whereas tissues containing a low presence of functional P-gp were more sensitive to chemotherapeutics (Allen *et al*., 2000). Additionally, elevated expression of P-gp has also been linked to a multidrug-resistant phenotype (Glazer and Rohlff, 1994; Jekerle *et al*., 2006). It is worth

mentioning that the over-expression of P-gp in cancer model of acquired cisplatin resistance is rare as it does not transport cisplatin and perhaps can be upregulated as a general stress response to long term treatment with cisplatin(Stordal *et al*., 2012a)

Overall, paclitaxel resistance mechanisms are complex and involve multiple genes and steps which have not been fully understood yet. In order to improve the chemotherapy response of patients with late stages of ovarian cancer, fully understanding these resistance mechanisms will aide in developing more targeted therapies (Duan *et al*., 2005; Kampan *et al*., 2015).

1.6.3 PARP inhibitor resistance

Like platinum therapies, cancer cells also develop resistance to PARP inhibitors. Several mechanisms have been identified to be involved in PARP inhibitor resistance such as increased Homologous Recombination (HR) capacity, altered Non-Homologous End Joining (NHEJ) capacity, decreased levels or activity of PARP-1 and decreased availability of PARP inhibitor intracellularly (Montoni *et al*., 2013). HR defects already existing in the cell serve as an initial abrasion allowing PARP inhibitor to terminate tumours deficient of HR (Ashworth, 2008). However, there are conditions which are able to restore HR functionality leading to PARP inhibitor resistance (Ashworth, 2008; Barber *et al*., 2013). These include the reversion of the mutation on the BRCA gene (Ashworth, 2008; Sakai *et al*., 2008; Swisher *et al*., 2008; Wang and Figg, 2008). The loss of BRCA gene function leads to genomic instability which is considered to be a cause of the reversion of the BRCA mutation (Aly and Ganesan, 2011). The BRCA reversion mutation, which restores the wild-type BRCA2 reading frame, was first identified as a secondary mutation that could be a significant clinical mediator of acquired resistance to platinum-based chemotherapy and PARP inhibitors (Edwards *et al*., 2008; Sakai *et al*., 2008). The following are the definitions of BRCA reversion mutations (Lin *et al*., 2019): (1) a base shift that converts a nonsense mutation to a missense mutation, and (2) an insertion or deletion that restores the open reading frame.

The upregulation of the NHEJ pathway is said to be one of the causes of synthetic lethality of PARP inhibitor in cells deficient of HR (Montoni *et al*., 2013). The NHEJ pathway is usually inhibited by PARP-1 and therefore a reduction in its activity in these cells potentially leads to

an increased resistance to PARP inhibitor (Patel *et al*., 2011). Alternatively, normal NHEJ functioning and genomic instability associated with it has been suggested to be a cause for the reversion of the BRCA mutations. This is also accompanied by the partial restoration of HR functionality and thus leads to the progression towards PARP inhibitor resistance (Chiarugi, 2012). Depending on the context, the increase or decrease of NHEJ capacity can result in PARP inhibitor resistance. Preceding studies have described the role of PARP1 and HR in the maintenance of genomic stability. However, the alternate double strand break repair modality; NHEJ directly links the DNA broken ends disregarding the strands sequence homology (Weterings and Chen, 2008). Patel *et al* (2011) demonstrated the role of NHEJ in stimulating hypersensitivity of HR deficient cells to PARP inhibitors. The study showed that in HR deficient cells, PARP inhibition promotes the error prone NHEJ activity. The genomic instability caused by PARP inhibitors can be reversed by disabling NHEJ thus preventing HR deficient cells from lethality caused by PARP inhibition or PARP1 silencing. This highlights the critical balance between NHEJ and HR but implicates NHEJ as a key player in cytotoxicity of PARP inhibitor treated HR deficient cells (Patel *et al*., 2011).

In order for the PARP inhibitor to be effective in anti-cancer therapy its target PARP-1 must be available for inhibition. This is because PARP-1 still binds to strands of broken DNA in PARP inhibitor treated cells but does not convert to PAR or enable DNA repair. Hence reduced PARP-1 levels can lead to PARP inhibitor resistance (Liu *et al*., 2009; Montoni *et al*., 2013). The catalytic activity of PARP-1 also affects the PARP inhibitor activity. Therefore, any decrease in PARP-1 activity can have an effect on PARP inhibitor efficacy (Oplustilova *et al*., 2012). Also, recent studies have shown that breast cancer cells that efficiently flush out PARP inhibitor through multidrug efflux pumps; including P-gp, from the cell tend to become resistant to PARP inhibitor therapy (Oplustilova *et al*., 2012).

As mentioned earlier, increased P-gp expression has been implicated in elevated efflux of chemotherapeutic substances (Grimm *et al*., 2010; Sedukhina *et al*., 2015). Resistance to PARP inhibitor; Olaparib, was shown to be correlated with increased expression of P-gp. Several studies suggested that these PARP inhibitors were a substrate of P-gp (Borst, 2012; Durmus *et al*., 2015; Lawlor *et al*., 2014; Rottenberg *et al*., 2008), however this could be overcome by

applying a P-gp inhibitor combined with another PARP inhibitor (AZD2281) . PARP inhibitors that were non- Pgp substrates such as Veliparib and CEO-8983 were more promising in delivering effective treatment (Lawlor *et al*., 2014).

Multiple preclinical studies have been carried out to target P-gp in order to overcome resistance. However, the clinical impact of inhibitors of P-gp has been hindered with lack of specificity and toxicity (Bitler *et al*., 2017). Seeing as P-gp is upregulated in resistant tumours the focus has shifted towards understanding the mechanisms upstream of those regulating P-gp that could be better targets and tolerated (Callaghan *et al*., 2014). Thus, in the context of PARP inhibitor resistance, targeting P-gp activity could be a more effective approach however further research is required (Bitler *et al*., 2017).

1.7 Epithelial to Mesenchymal Transition and chemo resistance

Epithelial to mesenchymal transition (EMT) is the process of cell phenotypes changing from an epithelial to mesenchymal morphology. This is regarded as an important stage in the invasion and metastasis of cancer (Takai *et al*., 2014). The role EMT plays in pathogenesis of cancer and other diseases has been recognized in recent years (Baum *et al*., 2008; Hugo *et al*., 2007; Yang and Weinberg, 2008). The gradual redistribution or downregulation of E-cadherin and cytokeratin, which are apical and basolateral epithelial cell specific tight and adherens junction proteins, have been shown to be associated with EMT. In addition to this, the expression of mesenchymal marker proteins vimentin and N-cadherin was also observed (Grünert *et al*., 2003; Huber *et al*., 2005).

The process of EMT is regulated by transcription factors such as SNAIL, zinc-finger E-box binding (ZEB) and basic helix-loop-helix transcription factors. In response to external cues, these key transcription factors are controlled by signalling pathways such as the TGFβ and WNT pathways (Lamouille *et al*., 2014; Thiery and Sleeman, 2006; K. Yang *et al*., 2016). The role of EMT as an important element in cancer metastasis is widely accepted (Wang *et al*., 2016). Several studies have postulated that at the primary site, non-motile epithelial cancer cells develop mesenchymal characteristics making them migratory in nature. When seeded at the secondary site they undergo mesenchymal-to-epithelial transition (MET) (Kalluri and

Weinberg, 2009; Polyak and Weinberg, 2009; Thiery and Sleeman, 2006). At the secondary site where the metastatic tumour forms, it displays the same phenotype (epithelial) as the cancer cells at the primary site leaving almost no trace of its transient mesenchymal state. Several *in vitro* studies have suggested that the early stage of metastasis is induced by EMT. This is also supported by mouse models of metastatic human cancers however there is limited clinical evidence supporting the incidence of EMT in tumour cases (Wang *et al*., 2016).

Recent studies have displayed an unexpected role of EMT in cancer drug resistance (Fischer *et al*., 2015; Zheng *et al*., 2015). The link between EMT and chemo resistance, caused by an enhancement of cancer cell survival, cell fate transition, and/or up-regulation of drug resistance-related genes, has been supported by data reported in these studies. However, these findings also challenge the vitality of the role of EMT in cancer metastasis. Being a complex cellular process regulated by several transcription factors and signalling molecules, the exact mechanism fundamental to EMT are still unclear. As such, the tumour models used in the Fischer *et al* (2015) and Zheng *et al* (2015) studies must be accounted for before dismissing the role of EMT in cancer metastasis and tumour invasion. In 2014, *et al* carried out a study which demonstrated that the EMT status functioned as independent predictors in ovarian cancer patients. The EMT status observed in this study was represented by decreased E-cadherin expression and appeared to stimulate dissemination of cells from the tumour (Thiery *et al*., 2009). These cells not only became invasive but also developed resistance to drug treatment (Iwatsuki *et al*., 2010; Yang *et al*., 2006). As such EMT has the ability to promote multidrug resistance thereby allowing for accelerated tumour progression.

1.8 Biomarkers for chemoresistance in ovarian cancer

Despite the recent advancement in chemotherapeutics and extensive research into mechanisms of resistance, ovarian cancer is a complicated disease to treat and manage. Over the years, several studies have comprehensively elucidated the role of several tissue-based tumour biomarkers. These have been labelled as potential predictors of chemo resistance in subtypes of epithelial ovarian cancer (Deo *et al*., 2020). Several biomarkers have been explored and their prognostic values examined in epithelial ovarian cancer. These include receptor tyrosine kinases (EGFR, IGF1R), angiogenic factors (VEGF, EphA2), apoptotic proteins (p53, cell-cycle

kinases), immune mediators (Immunoglobulins, B7-H3) (Huang *et al.*, 2010) Examples of promising biomarkers identified for the prediction of chemo resistance include Check Point Kinase 2 (Chk2) protein, Prostaglandin D2 (PgD2) and NOTCH3 (Alkema *et al.*, 2016; Alves *et al.*, 2019; Bell *et al.*, 2011; Brown *et al.*, 2015; J.-G. Jung *et al.*, 2016). However, other biomarkers that have been identified such as MAD2 (Mitotic Arrest Deficiency Protein 2), IGF1R (Insulin-Like Growth Factor 1 receptor) and ERCC1 require a larger cohort size and suitable endpoints to further validate their promise as valid predictors of chemo resistance in high grade serous ovarian cancer (Deo *et al.*, 2020).

1.8.1 Novel Biomarkers for chemoresistance

Previous studies have used ovarian cancer cell line IGROVCDDP and cervical cell line KB-8-5-11 and their respective parental cell lines IGROV-1 and KB-3-1 to examine cisplatin resistance and the mechanisms involved (Stordal *et al.*, 2012b)(O'Shannessy *et al.*, 2013). IGROVCDDP is cisplatin-resistant compared to its parent cell line while KB-8-5-11 is collaterally sensitive to cisplatin due to its developed resistance to colchicine (Figure 1.6 (a)). These cell lines were then profiled in order to view genes that would be significantly and differentially expressed in the cisplatin resistant and sensitive cell line models. These are shown in Figure 1.6 (b)

The IGROVCDDP cisplatin-resistant ovarian cell line is considered an unusual model since it is also resistant to paclitaxel, a taxane, which has been shown to be mediated by P-gp (Stordal *et al.*, 2012b). This cell line models resistance phenotypes of ovarian cancer patients that are typically non-responsive to standard platinum/taxane chemotherapy combinations (Lawlor *et al.*, 2014). The KB-8-5-11 cells are paclitaxel resistant models of cervical cancer cell lines which also overexpress ABCBI (P-gp). However, these cells are sensitive to cisplatin that is not an ABCB1 substrate making them an ideal model for cisplatin sensitivity biomarker discovery (Doherty *et al.*, 2014) .

Based on an Affymetrix array experiment (Table 1.6) (unpublished), a large panel of differentially expressed genes were identified from these cell lines. It was then hypothesised

that genes expressed in opposite directions in these cell lines would be linked to platinum response. These were then shortlisted to clinically relevant genes using a web-based platform called OvMark which associates the gene of interest with the survival outcome producing Kaplan Meier curves for patients with ovarian cancer (Madden *et al*., 2014). The genes identified with significant expression between the resistant and sensitive cell line models were ROR1, Rab27b, CCDC68 and RGS16 as shown in Table 1.6.
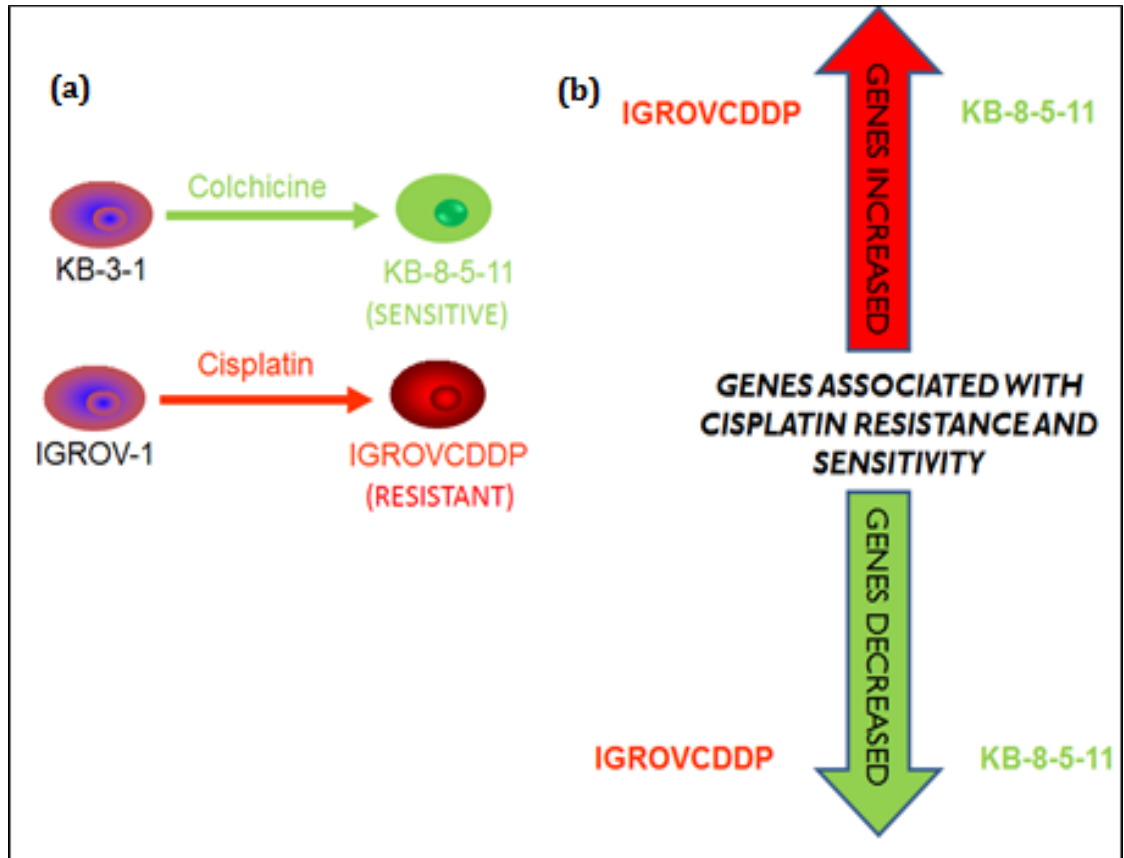
Figure1. 6 Workflow of Biomarker discovery (a) KB-8-5-11 was developed from KB-3-1 cells treated with colchicine making them collaterally sensitive to cisplatin. Collateral sensitivity occurs when the acquisition of resistance to colchicine produces increased sensitivity to cisplatin . IGROVCDDP was developed from IGROV-1 cells and is cisplatin resistant (b) Whole genome Affymetrix expression array was used to profile IGROVCDDP and KB-8-5-11. Genes expressed in opposite directions were selected as the candidate biomarkers**.**

Gene	Full Name	Probe ID	IGROV-1 vs IGROVCDDP Platinum Resistant			KB-3-1 vs KB-8-5-11 Platinum Sensitive		
				Fold Change	FDR		Fold Change	FDR
RGS16	regulator of G-protein signalling 16	7922717	↑	4.20	8.38×10^{-5}	↓	-2.49	2.40×10^{-4}
ROR1	receptor tyrosine kinase-like orphan receptor 1	7901969	↑	3.75	2.07×10^{-5}	↓	-3.06	6.27×10^{-3}
CCDC68	coiled-coil domain containing 68	8023401	↓	-4.84	8.42×10^{-5}	↑	2.89	3.68×10^{-3}
RAB27B	member RAS oncogene family	8021301	↓	-2.54	1.41×10^{-4}	↑	2.02	1.65×10^{-3}
↑- Increased Expression ↓- Decreased Expression								

Table1. 6 Results from Affymetrix Array for four genes identified: IGROVCDDP vs KB-8-5-11. This shows increased expression of the biomarkers RGS16 and ROR1 in the resistant model (IGROVCCDP) and its decreased expression in the sensitive model (KB-8-5-11). CCDC68 and RAB27B showed expression in the opposite direction with decreased expression in IGROVCDDP and increased expression in KB-8-5-11.

Affymetrix Significant Difference in Pt Resistant IGROVCDDP		Ovmark Pt treated PFS (n=554)			Ovmark Pt treated OS (n=561)			Taqman IGROVCDDP (n =4)		Taqman KB-8-5-11 (n =4)	
		Hazard Ratio	p-value	Change in Expression Associated with Poor Prognosis	Hazard Ratio	p-Value	Change in Expression Associated with Poor Prognosis	Fold change IGROVCDDP	p-value	Fold change KB-8-5-11	p-value
RGS16	↑ ☐	1.298 (1.071 - 1.574)	p=0.007	↑	1.146 (0.9007 - 1.459)	p=0.2666	-	23.30	3.58×10^{-3}	-4.47	0.013
ROR1	↑	1.216 (1.004 -1.473)	p=0.045	↑	1.155 (0.9064 - 1.472)	p=0.2437	-	12.68	1.49×10^{-3}	-7.75	4.52×10^{-5}
CCDC68	↓	0.8135 (0.6699-0.9879)	p=0.036	↓	0.8472 (0.663 - 1.083)	p=0.1847	↓	-5.85	8.16×10^{-3}	3.92	0.016
RAB27B	↓	0.7236 (0.5969 - 0.8771)	p=0.0009	↓	0.7772 (0.61 - 0.9902)	p=0.04083	↓	ND		2.53	0.039

Table1. 7 Biomarkers identified from OvMark Screen shows association of the biomarkers with survival outcome of ovarian cancer patients.
This table shows the qPCR data from IGROVCDDP and KB-8-5-11 cell lines aligns with a survival data of biomarkers in publicly available datasets.
The p values in bold are statistically significant.

Table 1.7 shows the expression of biomarkers in agreement with data obtained in the Affymetrix assay. These results were further validated through qPCR experiment (Taqman). Based on preliminary research (unpublished data) that has been conducted by Dr. Stordal, four novel gene expression biomarkers were identified which potentially predict platinum resistance: ROR1 and RGS16 or sensitivity RAB27B and CCDC68 in ovarian cancer. In Figure 1.7 Kaplan Meier curves were produced to show the combination of increased and decreased expression of (a) RAB27B/ CCDC68 and ROR1; and (b) RAB27B/ CCDC68 and RGS16 respectively. These presented to be promising signatures with progression free survival (PFS) and overall survival (OS) as significant outcomes. The low hazard ratios (0.47) and p-values (p<0.00007) of this study showed considerable separation of the survival curves. It is also worth noting that when gene expression was combined, the PFS and OS values presented significantly low hazard ratios which showed better survival in that patient group.
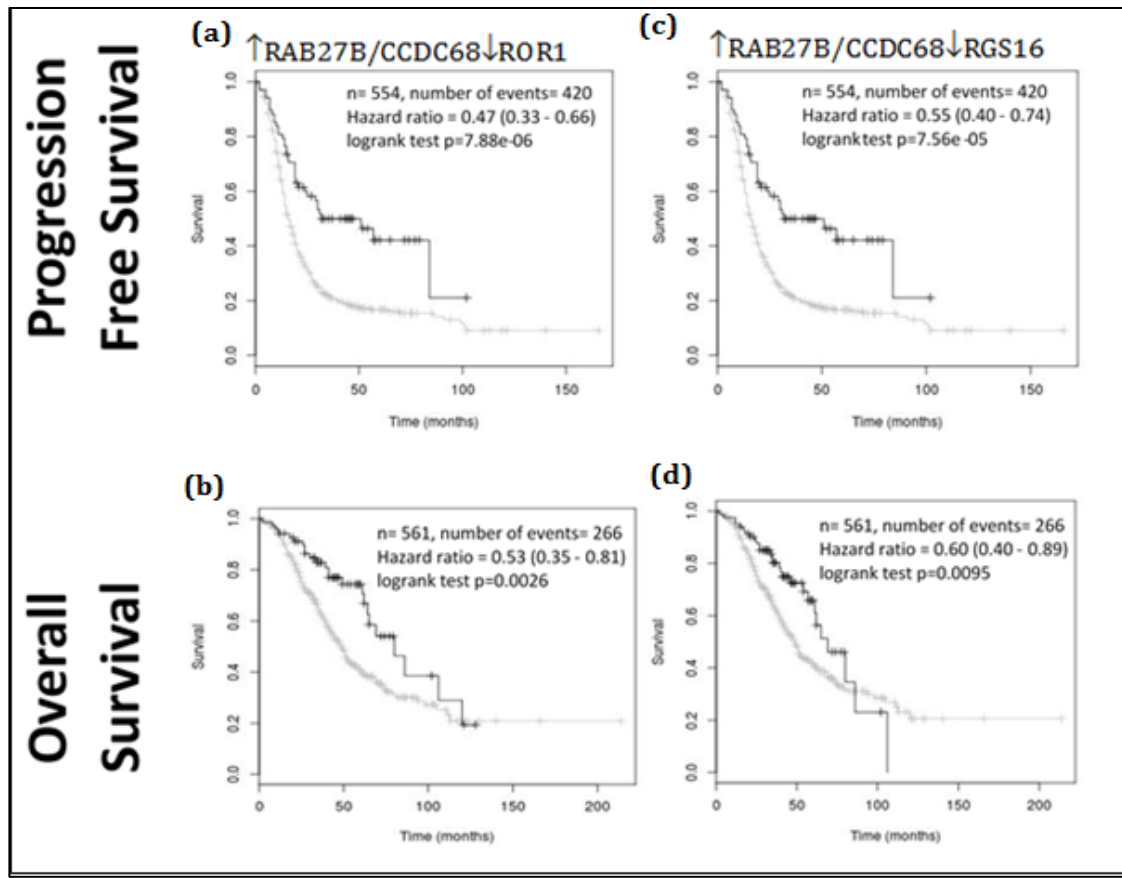
Figure1. 7 Combination of novel biomarker gene expression in publicly available microarray dataset for ovarian cancer. Patients are divided into high and low expressers on the median. ↑Rab27b/CCDC68↓ROR1 depicts (a) Progression Free Survival or (b) Overall survival and similarly ↑Rab27b/CCDC68↓RGS16 depicts (c) Progression Free Survival or (d) Overall survival. The black specifies the combination of novel gene expression whereas the grey line indicates the remaining patients in the data set.

Earlier biomarker studies have generally focused on gene expression and its association with survival in ovarian cancer but not to chemoresponse (Bosquet *et al*., 2014; Spentzos *et al*., 2004). The involvement of the biomarkers of interest in chemoresistance can be established through their association with different pathways. For example, ROR1 acts as a receptor in the Wnt signalling pathway and its overexpression in ovarian cancer cells has resulted in poor clinical outcome (Claire Henry *et al*., 2015). Therefore, its higher expression indicates the likelihood of resistance to treatments (Ford *et al*., 2014a; H. Zhang *et al*., 2014a). Similarly, members of the RGS16 family are part of molecular mechanisms leading to resistance by cancer cells. Some studies suggest that activation of receptors from the RGS16 family results in the activation of survival pathways (mediated by the AKT pathway) (Hooks *et al*., 2010). RAB27B plays a vital

role in exosome biogenesis and secretion which has a significant role in intercellular communication impacting drug resistance. Since CCDC68 is localized on the same chromosome as RAB27B (chromosome 18 q21.2), it could potentially have a part to play in resistance mechanisms. Although there are no published studies linking it to chemoresistance in ovarian cancer its expression has been reported in a number of other malignancies such as pancreatic ductal adenocarcinoma and colorectal cancer (N Radulovich *et al*., 2015; Sheffer *et al*., 2009).

It is clear from the literature that these four biomarkers are involved in various pathways that effectively impact the cells response to chemotherapeutic drugs. Currently, there are no clinically relevant biomarkers that aid personalised chemotherapy treatments in ovarian cancer patients. As a result, it is impossible to predict the patient's response to treatment in order to deliver an optimal regimen. Therefore, the need for reliable biomarkers is essential in order to assess chemoresponse and accordingly tailor chemotherapy to each patient. Using these biomarkers in combination has the potential to create an effective predictive model for response to chemotherapy in these patients. In short, it may be possible to use these biomarkers to predict which patient with ovarian cancer will be responsive or resistant to platinum drugs and PARP inhibitors. However, for this project focus will be placed on ROR1 and Rab27b solely due to substantial published work in other cancers that can inform the role of these biomarkers in the context of ovarian cancer. This constraint to only two biomarkers is also due to limitation on resources.

1.8.1.1. Receptor Tyrosine Kinase Orphan Receptors (ROR)

RORs are transmembrane proteins that belong to the receptor tyrosine kinase (RTK) family (Zheng *et al*., 2016) and as such are known as receptor tyrosine kinase orphan receptors. As shown in figure 1.8, structurally ROR consist of an extracellular Immunoglobulin (Ig)-like domain which is followed by cysteine rich domain known as the Frizzled (FZ) domain. This is further followed by a Kringle (KR) domain which stretches into the transmembrane domain(Borcherding *et al*., 2014; Hojjat-Farsangi *et al*., 2014; Yamaguchi *et al*., 2012). Several studies indicate that the FZ domain plays a role in the receptor-ligand interactions(Forrester *et al*., 2004; Roszmusz *et al*., 2001).

ROR consists of two sister receptors; ROR1 and ROR2 that are structurally very similar. Their expression was first identified in neuroblastoma cell lines (Reddy *et al*., 1997). They are located on chromosome 1 and 9 respectively (Reddy *et al*., 1997). Initially they were named orphan receptors since their endogenous ligands were unknown. ROR belongs to the noncanonical wingless-related integration site (Wnt) signalling pathway. ROR1 and ROR2 play an integral role in this pathway as type I single pass transmembrane glycoproteins(Karvonen *et al*., 2017). They also happen to be closely related to the MuSK (muscle-specific kinase) and Trk (tropomyosin) family receptors (Forrester *et al*., 2004; Karvonen *et al*., 2017; Masiakowski and Carroll, 1992).

As mentioned earlier, RORs are made up of three extracellular domains, a transmembrane domain and an intracellular domain. Through comparative genomic studies it was found that the three extracellular and one intracellular domain were conserved in drosophila, Caenorhabditis elegans, mice and humans (Katoh and Katoh, 2005). Two splice variants for ROR1 have been identified; one known as truncated-ROR1 (t-ROR1) as it lacks all the extracellular domain and the other lacking both the transmembrane and intracellular domain (Reddy *et al*., 1996). Almost all studies so far have concentrated on ROR1 in its full-length form. According to reports by Gentile *et al*. (2011), it has been suggested that the intracellular kinase domain of ROR1 does not exhibit biological activity. However, others have claimed its importance in signal transduction to proteins downstream (Mikels *et al*., 2009).

Interestingly, additional cytosolic domains seem to have been acquired by vertebrate ROR proteins. These are known to be vital in downstream signalling. Vertebrate RORs (Figure 1.8) also contain a serine/threonine-rich domain (S/TRD1), a proline-rich domain (PRD), and another serine/threonine-rich domain (S/TRD2) (Minami *et al*., 2010). Since the cysteine-rich domain (CRD) (in the Frizzle domain) has been shown to bind Wnt ligands for many cell receptors it has been the main focus in many studies (Rehn *et al*., 1988). By comparing levels of expression and loss of function phenotypes between homologs of ROR2 and Wnt5a, Wnt5a was found to be a ligand for ROR2 in drosophila and mouse studies (Green *et al*., 2007; Oishi *et al*., 2003). However, ligands that definitively bind to ROR1 are still unclear. In addition to this, the Kringle extracellular domain and the immunoglobulin domain have yet to be well

characterized resulting in limited understanding of the functions of ROR proteins (Rebagay *et al*., 2012). It should be mentioned that even though *in vitro* studies showed binding of Wnt5a to ROR1 (Fukuda *et al*., 2008), ROR1 has been associated with numerous non-Wnt responses (Sanchez-Solana *et al*., 2012). It is also generally presumed that ROR1 is a pseudokinase. This means that it lacks key properties necessary for kinase activity thereby making it "inactive" (Raju and Shaw, 2015). This inactivity occurs either due to its tyrosine phosphorylation being undetectable (Bicocca *et al*., 2012) or due to trans phosphorylation by other kinases (Gentile *et al*., 2011).
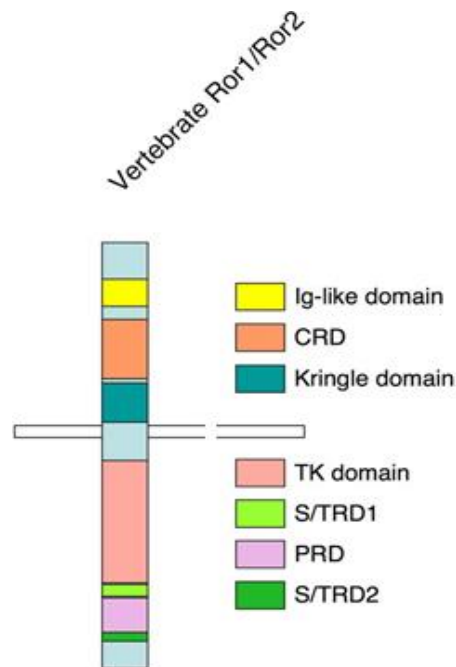
Figure1. 8 ROR structure in different species. Ig- Immunoglobulin, CRD- Cysteine rich domain, TK domain- Tyrosine Kinase domain, S/TRD-Ser/Thr rich domains, PRD- Proline rich domain (Green *et al*., 2008; Minami *et al*., 2010).

The mammalian ROR proteins were initially characterized based on their expression patterns in neural tissues (Oishi *et al*., 1999). In mouse models both ROR1 and ROR2 were found to play a role in the maintenance of the neural progenitor cell fate in mouse brain that was still developing (Endo *et al*., 2012). The expression patterns of ROR1 and ROR2 during the mouse embryonic development were some-what overlapping in a wide range of tissues (Matsuda *et al*., 2001). Interestingly, ROR2 expression decreases before birth while RNA levels of ROR1 was

detectable in same postnatal tissues although its expression also drops in adult tissues (Oishi *et al*., 1999). In humans ROR2 mutations were found to be associated with syndromes resulting in limb malformations such as brachydactyly type B and recessive Robinow syndrome Afzal *et al*., 2000; Afzal and Jeffery, 2003; Oldridge *et al*., 2000).

1.8.1.1.1 ROR and Cancer

Although ROR1 and ROR2 possess similar expression patterns in face and heart development they exhibit different embryonic brain and limb expression patterns(C. E. Henry *et al*., 2017). In normal embryonic and fetal development ROR1 plays a pivotal role, however it is absent in mature tissues (Hojjat-Farsangi *et al*., 2014). ROR1 has been implicated in the oncogenic functions of cancerous cells. ROR1's importance in cell survival was demonstrated in siRNA mediated knockdown experiments that triggered apoptosis in Hela cells (MacKeigan *et al*., 2005). Elevated expression levels of ROR1 were observed in several haemato- and non-haematological malignancies (Barna *et al*., 2011; Gentile *et al*., 2011; S. Zhang *et al*., 2012a). Detection of high levels of ROR2 in several cancers were also reported. However, the decrease in their expression resulted in reduced cell invasion as well as remodelling of the cell's extracellular matrix (Morioka *et al*., 2009; O'Connell *et al*., 2013; Wright *et al*., 2009). Studies have shown ROR2's role in cell survival and proliferation making it, along with ROR1, a potential therapeutic target for different cancers. It should be noted that based on the cellular context RORs may either have tumour progression or inhibiting roles (Green *et al*., 2014).

1.8.1.1.2 ROR: Haematological malignancies

Expression of ROR1 was first identified in B-Cell chronic lymphocytic leukaemia (CLL). High levels of ROR1 expression, but not ROR2, were observed in primary CLL cells (Baskar *et al*., 2008). Another study (Fukuda *et al*., 2008) identified ROR1 in CLL post *ex vivo* transduction of CD40 ligand (CD154) and infusion of autologous transduced cells into patients with advanced stages of CLL. This resulted in the reversal of immunosuppression which is characteristic of CLL and in the generation of anti-ROR1 antibodies. These anti-ROR1 antibodies specifically bound to CLL cells from CLL patients but did not bind peripheral blood

mononuclear cells (PBMCs). As CLL progresses, it was found that ROR1 expression also increases making it a prognostic indicator for CLL as well as a biomarker (Daneshmanesh *et al.*, 2013).

The increased expression of ROR1 in various haematological malignancies such as non-Hodgkin lymphomas (NHL), acute lymphocytic leukaemia (ALL) and myeloid malignancies has been described since its discovery in CLL (Barna *et al.*, 2011; Daneshmanesh *et al.*, 2013; DaneshManesh *et al.*, 2008). When compared to PBMCs, the ROR1 mRNA and/or protein levels are increased in all or subsets of NHLs (Barna *et al.*, 2011; Daneshmanesh *et al.*, 2013). Similar elevated expressions were also observed in acute lymphoblastic leukaemia (ALL) patients particularly those with translocation at t (1;19) (q23; p13). The importance of ROR1 in the survival of ALL cells carrying t (1;19) (q23; p13) translocations was further validated in a Bicocca *et al.* (2012) study. Here, a siRNA library was screened to identify critical tyrosine kinases within the tyrosine kinome responsible for pathogenesis of ALL.

1.8.1.1.3 ROR: Solid malignancies

ROR expression, particularly ROR1, has been observed in several solid malignancies. Tissue microarray analysis of primary samples in lung, pancreatic and colon cancer showed more than 30% strong staining for ROR1(Zhang *et al.*, 2012b). In a majority of lymphoma, ovarian, prostate, skin, uterine, testicular and adrenal cancers moderate staining for ROR1 was observed (S. Zhang *et al.*, 2012b).

ROR1's pivotal role in regulating apoptosis was identified through an RNAi-based screening in cervical cancer (HeLA) cells (MacKeigan *et al.*, 2005). In lung adenocarcinoma, its expression is driven by NKX2-1 (TITF1, a proto-oncogene implicated in lung cancer (Boggaram, 2009; Yamaguchi *et al.*, 2012a). ROR1 expression was subsequently elevated leading to increase of EGF ligand-induced EGFR signalling and c-Src activation and phosphorylation (Yamaguchi *et al.*, 2012a). In an earlier mentioned study (Masiakowski and Carroll, 1992; Oishi *et al.*, 1999), moderate autophosphorylation of ROR1 was observed. However, this characteristic was not prevalent in immunoprecipitated ectopic ROR1 present in COS-7 cells which led to the

conclusion that ROR1 is a pseudokinase. Phosphorylated ROR1 was identified in several cell lines in the same study which was MET (HGFR) mediated, but not EGFR or ERBB2 mediated.

ROR1 gene silencing mouse models with transplanted non-small lung carcinoma cells (NCIH1993), was associated with increased anoikis (anchorage-dependant cell death) and decreased tumour growth (Gentile *et al*., 2011). This indicated that ROR1 may in fact behave as a pathway activator. In human neoplastic breast cancer cells, ROR1 is expressed whereas in stromal cells it appears to be absent (Zhang *et al*., 2012a). In addition to this high expression levels were noted to be linked to higher grade and more aggressive form of the disease. It was also reported that increased levels of ROR1 in both cell lines and patients was associated with EMT related genes; vimentin and ZEB-1(Cui *et al*., 2013). In triple-negative- breast cancer cell lines, EMT genes namely, SNAI1, SNAI2, ZEB1, and vimentin were downregulated when ROR1 was silenced. Furthermore, the knockdown of ROR1 in a triple negative breast cancer cell line; MDA-MB-231reduced the cell migration in xenografts (Cui *et al*., 2013).

In a study carried out by Rabbani *et al.* (2010), low to non-detectable protein levels of ROR1 was observed in the kidneys of healthy individuals. However, ROR1 mRNA was detected in 81.3% of tissues and 94% of PBMCs of renal cancer patients. These findings suggested that ROR1 is an important indicator of renal cancer.

In the context of ovarian cancer, RORs have been found to play a role in driving pathways that are thought to be involved in chemoresistance (C E Henry *et al*., 2016). One such pathway is known as the Wnt signalling pathway. These are responsible for epithelial to mesenchymal transition (EMT) regulation in cells (Ford *et al*., 2014b). Through *in vivo* studies EMT was found to be associated with more aggressive and invasive subtypes of ovarian cancer as well as chemoresistance (Ford *et al*., 2014b; Haslehurst *et al*., 2012; Miow *et al*., 2015). Patients exhibiting the mesenchymal phenotype had shorter disease specific survival and increased Wnt signalling (Tothill *et al*., 2008). The EMT profile can therefore help predict patient responses to chemotherapy based on the fact that if the mesenchymal-type cells are more aggressive they are likely to be more resistant to chemotherapy (Miow *et al*., 2015). Recent studies have suggested that ROR1 and ROR2 are both Wnt receptors (Claire Henry *et al*., 2015).

They also correlate with poor patient prognosis and in many tumours drive EMT (Cui *et al*., 2013; C E Henry *et al*., 2016). Therefore, this study investigating the expression of these RORs will help understand their role in pathways that are directly or by association implicated in chemoresistance.

Although there have been several studies investigating the characteristics and roles of ROR1 and ROR2, their biochemical activities are still not well defined. As a result, there is a gap in the knowledge of our understanding of how RORs control cellular process and mechanisms in normal as well as cancer cells. The dysregulation of RTKs show characteristics pivotal to maintaining tumours in several cancers (Gschwind *et al*., 2004; Lemmon and Schlessinger, 2010). Furthermore, their interaction with certain ligands and kinase activities makes them prime targets for therapeutic approaches.

1.8.1.1.4 ROR: EMT and Wnt Signalling

A crucial pathway that has also been identified is the Wnt signalling pathway. Like EMT, it has been linked to development and more recently has garnered interest as a potential target for cancer therapy (Chien *et al*., 2009; Horvath *et al*., 2007). As mentioned earlier, Wnt signalling is involved in developmental pathways which involve the differentiation, polarity, migration, invasion, adhesion and survival of cells (Chien *et al*., 2009). It is these same processes that also form the fundamental mechanisms involved in tumorigenesis and metastasis. Aberrant Wnt signalling pathway has been associated with several cancers typically with high prevalence and/or poor outcomes such as breast, ovarian, colorectal and prostate cancer(Ying and Tao, 2009). For many years Wnt signalling has shown to affect cancer cell migration and adhesion and a study by Ford *et al.* (2013) presented evidence that this may be guided through EMT suggesting a link between the two pathways.

There are several studies that have implicated ROR in EMT (Cui *et al*., 2013; C E Henry *et al*., 2016) as well as in Wnt signalling (Claire Henry *et al*., 2015). Attempts to target Wnt signalling in cancer have largely focused on downstream targets in the pathway and these have proved unsuccessful (Clevers and Nusse, 2012). However, new approaches have been leaning towards targeting upstream components of the pathway which play a key role in oncogenesis (Kawano

and Kypta, 2003; Shi *et al*., 2007). Since ROR is an upstream component of the Wnt signalling pathway, this makes it a relevant target. Additionally, being the common denominator between EMT and Wnt signalling, this underlines the importance of ROR being considered as a biomarker.

In terms of ovarian cancer, the Wnt signalling pathways have been studied and found to be inherently important (Barbolina *et al*., 2011). It has shown to promote the progression of the cancer through gene mutations and changes in expression of extracellular inhibitors and intranuclear transcription cofactors (Yoshioka *et al*., 2012). Furthermore, ROR1 and ROR2 have been investigated in ovarian cancer and have shown to play a role in EMT (C E Henry *et al*., 2016; Takai *et al*., 2014) and also act as receptors in Wnt signalling (Claire Henry *et al*., 2015). This link between ROR, EMT and Wnt signalling discussed above seems to hold for ovarian cancer and therefore is of great interest.

1.8.2 Ras-Related Protein (Rab-27B)

Rab27b is a member of the Rat Sarcoma (Ras) -associated Binding (Rab) oncogene family (Bao *et al*., 2014). These secretory small guanosine-5′-triphosphate-binding enzyme (GTPases) are known to control endocytosis and exocytosis vesicle-trafficking (Ren *et al*., 2016) and makes up the largest family of small GTPases (Fukuda, 2008). The Rab GTPases act as molecular switches that rotate between an active GTP-bound and inactive guanosine diphosphate-bound conformational position (Grosshans *et al*., 2006; S. R. Pfeffer, 2005). The Rab proteins play a role transporting cargo and formation of vesicles. This allows the exchange of different macromolecules and proteins across different compartments and endomembrane system (Paul *et al*., 2014). These proteins are also involved in docking and fusion of vesicles to their target destination (S. Pfeffer, 2005). There have been several studies that demonstrate the role that vesicle trafficking and exocytosis have on tumorigenesis. Rab27 consists of two isoforms, Rab27a and Rab27b(Barr and Lambright, 2010; Yasuda *et al*., 2012). Normally, Rab27b is expressed largely in secretory cells and regulates common Rab27 effectors which in turn regulate secretory pathways(Johnson *et al*., 2010). A 2010 study revealed that Rab27b controls the release of growth regulators and vesicle exocytosis which leads to invasive tumour growth and metastasis in breast cancer (Hendrix *et al*., 2010a; J.-X. Zhang *et al*., 2012). This suggests

that Rab27b has tumorigenic functions and contributes to development of cancer. Since ovarian cancer and breast cancer harbour similar genetic mutations it can be hypothesized that the effects of Rab27b expression may be similar in ovarian cancer.

Several studies have examined the effect of Rab27b on different cancers, however so far there is only one study that associated the overexpression of Rab27b with ovarian cancer (Ren *et al*., 2016). This study revealed that Rab27b was upregulated, and its overexpression was associated with progression of the tumour and poor clinical outcome. As this study suggested, additional investigations need to be undertaken to understand the underlying mechanisms by which Rab27b functions in ovarian cancer progression. The aim of this project is to explore this along with its possible links to chemoresistance.

1.8.3 Regulator of G protein signalling (RGS16)

RGS16 is a 202 amino acid protein that belongs to the RGS protein signalling family. These play a role in the increase of GTPase activity of the Gα subunit to attenuate G-protein coupled receptor (GPCR) signalling pathways (X. Li *et al*., 2013; Wu *et al*., 2013). This results in the RGS proteins binding to the activated Gα protein subunit and enhancing termination of the G protein activity through GTP hydrolysis (Miyoshi *et al*., 2009). The RGS family consists of 22 protein families that have a role to play in different cell types and signalling pathways in one way or another (Hu *et al*., 2008; Ross and Wilkie, 2000).

While RGS proteins have been recognized to effectively modulate G protein signalling, their roles in pathological and physiological conditions have not been fully investigated. Since RGS proteins have been reported to control proliferation and migration by inducing G protein it is likely that they may play a role in the progression of cancers. Hurst and Hooks (2009) demonstrated that RGS proteins displayed varying levels of expression between normal and cancerous tissues. However other studies have shown that RGS proteins have differential expression levels within the tumour microenvironment itself (Silini *et al*., 2012).

In the case of RGS16 specifically, it was associated with negatively regulating the MAPK, AKT/PI3K, RhoA, and SDF-1/CXCR4 oncogene pathways in both normal and cancer cell lines (Carper *et al*., 2014). These pathways are known to be involved in the progression of cancers through proliferation, migration, invasion, survival, chemoresistance and metastasis in several cancers(Osaki *et al*., 2004; Teicher and Fricker, 2010). Studies have also shown evidence of RGS16 playing a role in cancer signalling. In a study carried out by Wiechec *et al*. (2008), about 50% of the RGS16 locus in primary breast cancers that were analysed were found to be of high genomic instability (Liang *et al*., 2009). The overexpression of RGS16 in breast cancer cells inhibited proliferation and EGF-induced Akt phosphorylation. However, the low expression induced cell growth and resistance to drug treatment (Liang *et al*., 2009). Another microarray analysis reported decreased expression of RGS16 in lymph node metastasized pancreatic cancer compared to the non-metastasized cancer. This decreased expressed was found to be associated with low patient survival (Kim *et al*., 2010).

RGS16 has therefore been considered a prognostic marker in a number of cancers (Kim *et al*., 2010; Liang *et al*., 2009; Miyoshi *et al*., 2009). By extension it would be useful to investigate its expression pattern in ovarian cancers in relation to chemoresistance as there is still not much known about RGS16.

1.8.4 CCDC68

Coiled-coil domain containing 68 (CCDC68) is a putative tumour suppressor gene located on the 18q chromosome. Although it is considered a tumour suppressor its role in cancer progression is still not clear (Radulovich *et al*., 2015). In pancreatic ductal adenocarcinoma CCDC68 was documented to possess allelic losses. It was also revealed that downregulation of CCDC68 occurred in colorectal cancers (Sheffer *et al*., 2009). Although further validation is required, there is preliminary evidence to suggest that the loss of function of CCDC68 is associated with several malignancies (N. Radulovich *et al*., 2015; Sheffer *et al*., 2009).

Recently, CCDC68 was found to be a novel centriole subdistal appendage (SDA). The SDAs are important structures required for the anchorage of microtubules during the interphase stage

of cell cycle (Huang *et al*., 2017). However, the composition and mechanism of assembly of SDAs are not fully understood. CCDC68 was found to be essential in the hierarchical SDA assembly in human cells along with CCDC120. In addition to being considered a tumour suppressor gene it also plays a role in centrosome microtubule anchoring (Huang *et al*., 2017). There is little published work regarding chemoresistance mechanisms of CCDC68 in cancer which makes it an interesting choice in the biomarker panel.

1.9 Ovarian cancer cell line models

Cancer cell lines have been used as standard *in vitro* models to study mechanisms underlying resistance (Kreuzinger *et al*., 2015). The establishment of human cancer lines over the years has had an extraordinary impact on cancer research. It has enabled researchers to develop treatments that differentially benefit patients. A well-established and long-term approach for studying cytotoxicity and resistance mechanisms has been the development of drug resistant cell lines (McDermott *et al*., 2014). In the age of personalized medicine, it is imperative that cell line models are properly annotated for the different cancer subtypes and their molecular profile. This is especially important in a clinical setting when determining the best therapy option for patients or understanding resistance patterns. Once the molecular profile of the patient is determined the cell line model with the most similar profile can be selected for further studies (Domcke *et al*., 2013). Ovarian cancer has a distinct molecular background (Shih and Kurman, 2004) with high-grade serous ovarian cancer (HGSOC) subtype making it the most occurring form. Most of what is known about ovarian cancer is largely based on cell line models which were not appropriately characterized at a molecular level nor were they properly defined (Kreuzinger *et al*., 2015).

Heterogeneity of solid tumours pose a complication in the analysis of resistance mechanisms in addition to being a factor in its development (Gillet *et al*., 2011). Epithelial Ovarian Cancer is a highly complex heterogeneous cancer and as such is difficult to reproduce for *in vitro* studies. This results in the ineffective elucidation of the events involved in the initiation of the tumour, metastasis of the disease (Hasan *et al*., 2015) and subsequently chemoresistance. Previous studies have shown that samples obtained from primary tumour and metastatic sites possess significant genomic alterations owing to high intra-tumour heterogeneity (Bashashati *et al*., 2013; Hoogstraat *et al*., 2014). The different subtypes present varying sensitivities to platinum-

based therapies. Based on the expression profiles, HGSOC are further classified into the following expression subtypes; differentiated', 'immunoreactive', 'mesenchymal' and 'proliferative' (Bell *et al*., 2011; Tothill *et al*., 2008). These subtypes are relevant in examining prognostic significance. The mesenchymal signature presented the poorest outcomes in patients. It should be noted however that multiple signatures can be identified in a single tumour making this classification non-exclusive (Verhaak *et al*., 2013). In addition to molecular characterisation and expression profiles of subtypes, the morphological and growth characteristics are also important. Three *in vitro* morphological subtypes have been identified; epithelial, round and spindle (Beaufort *et al*., 2014). Along with the upregulation of mesenchymal markers the spindle morphology is a typical indicator of Epithelial to Mesenchymal transition (EMT) (Hollestelle *et al*., 2013; Zheng *et al*., 2013). Such morphological phenotypes are detected in multiple tumour type derived cell lines and appear to be linked to known traits of clinical relevance. This underlines the importance of translating the phenotypes *in vitro* to a clinical one.

This phase of the study focuses on selecting cell lines to create a panel that encompasses all these attributes in order to properly represent the genotype and phenotype profiles of chemotherapy resistant (and sensitive) models. Taking into account how the different phenotypes play a role in EMT, acquiring cell lines which model such variation will broaden the scope of understanding their roles in relation to the novel chemotherapy resistance biomarker. In line with this perspective Barretina *et al*. (2012) also suggests that investigating larger panels of cell lines in fact will aide in the identification of novel biomarkers for response to a more targeted approach. For this purpose, four ovarian cancer cell line models were selected and are described in chapter 2 section 2.1.1 (Table 2.1).

1.10 Aims:

The overall hypothesis of this project is that chemoresistance is directly or indirectly associated with ROR1and/or Rab27b expression which in turn impacts survival in ovarian cancer patients. The aim of the project is to:

To understand how the novel biomarkers ROR1 and Rab27b contribute to and mediate platinum and PARP inhibitor resistance in ovarian cancer.

1.11 Objectives:

The main objectives are:

1. Establishing a correlation between the transcript/protein expression profile of the biomarkers and chemoresistance to platinum based therapeutic drugs and PARP inhibitors.
2. To investigate whether knockdown of the biomarker affects chemoresistance.
3. To investigate the impact of biomarker expression on patient survival in clinical samples.

Chapter 2

General Methodology

2.1 Cell Culture

2.1.1 Selection of cell lines

To assess the suitability of the cell lines chosen to represent a range of resistant profiles, a set of fundamental criteria was defined. Although this list is not exhaustive it acts as a practical guide for selecting cell line models for this study.

1) The half-maximal inhibitory concentration (IC50) dose range is varied: This was to ensure that the cell lines are of varying resistance profiles to drugs treatments.

2) BRCA gene mutation status: In order to tailor the cell line models to resemble tumour samples the cell lines were chosen should possess a wildtype BRCA status. This is to account for High Grade Serous Ovarian Cancer (HGSOC) cases with non BRCA mutation related HR deficiency. This aids a broader understanding of the possible mechanisms involved in PARPi resistance.

3) Ability to grow well and reach the desired confluence.

Cell lines picked for this study are shown in Table 2.1 follows and were a gift from Prof. Bryan Hennessey, Royal College of Surgeons in Dublin.

Cell Line	BRCA1 mutation status	Methylation Status	Phenotype	Tumour Histology	Source
HEY	Wild type[a]	No[a]	Mesenchymal[b]	Serous[d]	Peritoneal deposit and xenograft[d]
SKOV-3	Wild type[a]	No[a]	Intermediate Mesenchymal[c]	Adenocarcinoma[e]	Ascites[e]
OVCAR-3	Wild type[a]	No[a]	Epithelial[c]	Serous[f]	Ascites[f]
OAW42	Wild type[a]	No[a]	Intermediate Epithelial[c]	Serous[g]	Ascites[g]
(a) Stordal *et al*., 2013 (b) Prislei *et al*., 2015 (c) Yi *et al*., 2015 (d) Buick *et al*., 1985 (e) Khosravi- Maharlooei *et al*., 2015 (f) Hamilton *et al*., 1983 (g) Hills *et al*., 1989					

Table2. 1 Clinical Properties of Ovarian cancer cell lines selected. Cell lines following the set criteria were selected in order to be clinically representative and as a risk reduction strategy to be able to study the selected biomarker

2.1.2 Maintenance of ovarian cancer cell lines

The human ovarian cancer cell lines (HEY, SKOV-3, OVCAR-3 and OAW42) were cultured under standard culture conditions in RPMI-1640 medium (Sigma Aldrich, UK) with 10 % fetal bovine serum (FBS) (Thermofisher Scientific, UK) at 37^0C and 5% CO_2 in T-75 flasks (Sarstedt AG & Co). Once cells reached 80-90% confluency they were washed with phosphate buffer saline (PBS) (Oxoid, UK) and then trypsinised with 0.25% Trypsin (Gibco), 0.02% EDTA in PBS for five minutes. The trypsin was then deactivated with equal volume of complete media (described above) forming a cell suspension. All cell lines were routinely tested for mycoplasma as described in section 2.1.4 and were found to be mycoplasma free.

2.1.3 Cell Counting

Cell counts for all cell lines were consistently carried out using a haemocytometer (Superior Marienfeld, Germany) after the deactivation of trypsin and formation of the cell suspension. Flasks were gently swirled so that cells were evenly distributed before pipetting out 1mL of cell suspension into a 1.5 mL Eppendorf tube. In a new Eppendorf tube 50 µL of the cell suspension was transferred, to which 50 µL of 0.4% trypan blue (Gibco) was added and gently mixed making up a total volume of 100 µL.

Using a pipette, the above cell suspension treated with Trypan blue was applied to the haemocytometer gently filling both the chambers under the coverslip. The haemocytometer was then observed under the microscope with a 10X objective lens. Live unstained cells were counted in the central grid of both chambers of the haemocytometer. The average cell counts from each chamber were taken and multiplied by 10,000 (10^4). This was then further multiplied by 2 to correct for the 1 in 2 dilution from the addition of trypan blue resulting in the number of viable cells/mL in the original cell suspension.

2.1.4 Maintenance of sterility of cell culture

Media from cell lines being cultured (HEY, SKOV-3, OAW42 and OVCAR-3) were collected from their respective confluent flasks and tested routinely for mycoplasma contamination. This was imperative as cells were being cultured in antibiotic-free media and as such were at higher risk of contamination. The protocol for this was adapted from Young L *et al* (2010) and described below. A PCR master mix of 24µl was prepared for each sample (Table2.2) to which 1µl of the respective conditioned media was added. For the positive control a confirmed positive mycoplasma sample was used whereas DNAase free water was used as the negative control. These were run in the PCR machine (Thermocycler Techne TC-3000G) under the conditions described in Table 2.3.

Mycoplasma PCR MasterMix	Volume
Green 2x Sigma Ready Mix	12.5µl
Forward primer 10µM *5'-GGGAGCAAACAGGATTAGATACCCT-3'*	0.5µl
Reverse primer 10µM *5'-TGCACCATCTGTCACTCTGTTAACCTC-3'*	0.5µl
DNAase free water	10.5µl
Total volume	24 µl

Table2. 2 Mycoplasma PCR Reagents

No. Cycles	Temperature (°C)	Time (minutes)
1	95	5
	94	0.5
40	55	0.5
	72	1
1	72	10
1	4	Hold

Table2. 3 Mycoplasma PCR Program

An agarose gel (2%) was prepared (Table 2.4) by adding 1X Tris-acetate-EDTA (TAE)(Sigma) to the agarose (ThermoFisher) and then heating it in the microwave. This was dissolved before 1.5µl of SYBR green nucleic gel stain (Sigma) was added to the solution. Once the agarose was

fully dissolved the gel was poured into an agarose gel mould and a comb was positioned into the gel to set. After casting and setting of the gel it was submerged in 1x TAE and 12µl of each sample and ladder (Sigma) was pipetted into the gel wells. The loaded samples were made up of 10µl of PCR product and 2µl of DNA loading buffer (Sigma). The PCR ladder was made up by mixing 5µl of PCR ladder (Sigma), 5µl sterile water and 2µl loading buffer. Samples were run at 100 Volts for one hour. An image of the gel was taken using a Licor Odyssey Infrared Imaging System at 600 nm for 30 seconds and analysed using the installed instrument software. The expected PCR product size was 270 bp and was best viewed with green background setting in the instrument software.

2% Agarose Gel	mL/g
Agarose	3g
1X TAE solution	150µl
SYBR Green nucleic gel stain	1.5µl

Table2. 4 Preparation of Agarose gel

The cell lines selected for this project were routinely tested using the protocol described. The image below in Figure 2.1 is a gel sample of one of several routine tests of the selected cell lines; HEY, SKOV-3, OVCAR-3 and OAW42 (found to be mycoplasma free). The mycoplasma positive cell line used as a positive control was JEG-3.
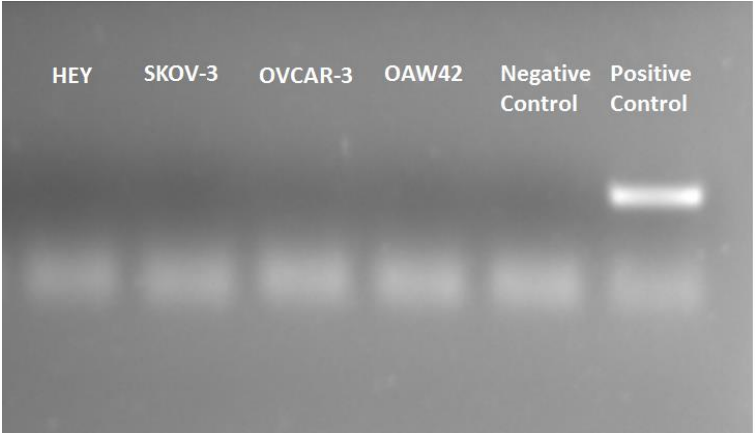
Figure2. 1 Gel image of cell lines tested for mycoplasma. Mycoplasma PCR gel image taken on the Licor Odyssey Infrared Imaging System at 600 nm for 30 seconds.

2.1.5 Growth assays of cell lines

The growth rate of each cell line was determined by plating 1×10^4 cells in 2mL of media in 6 well plates. The cells were plated in duplicate wells and trypsinised as described in section 2.1.2 after which they were counted (refer section 2.1.3) every 24 hours for four days. Biological replicates (n=3) were set up and the time cells reached double its amount (2×10^4 cells) was determined using Graphpad Prism. A line was drawn across the graph and the values in days was interpolated to determine the doubling time.

2.1.6 Cytotoxicity Assay

Cells from each cell line suspension were counted using a haematocytometer (as described in section 2.1.3) and 2×10^4 cells in 100µL were seeded in a 96-well plate (Sarstedt AG & Co) in triplicate as indicated in the Figure 2.2 below. The outer well of the plate were plated with 200µL of sterile deionised water to prevent dehydration of the plate (indicated in blue in the Figure 2.2 below). The plate was then incubated overnight at 37^0C and 5% CO_2 to allow attachment of the cells before adding drug doses. Different drugs were used on each cell line and a minimum of three biological replicates (n=3) were set up for each drug. The platinum-based drugs; Cisplatin and Carboplatin (Sigma), taxane drug; Taxol (Sigma) and PARP inhibitor; Talazoparib (SelleckChem, UK) were used in this assay.

Cell Line	Drug	Starting dose (Highest)	Dilution
HEY	Cisplatin	6.8 µg/mL	1:2
	Carboplatin	36.2µg/mL	
	Taxol	14.85ng/mL	
	Talazoparib	0.745µg/mL	
SKOV-3	Cisplatin	1.88µg/mL	1:2
	Carboplatin	15.6µg/mL	
	Taxol	2.16ng/mL	
	Talazoparib	0.1µg/mL	
OVCAR-3	Cisplatin	1µg/mL	1:2
	Carboplatin	2.2µg/mL	
	Taxol	1.44ng/mL	
	Talazoparib	2×10^{-3} µg/mL	
OAW42	Cisplatin	1µg/mL	1:2
	Carboplatin	7.68µg/mL	
	Taxol	3.27ng/mL	
	Talazoparib	0.235µg/mL	

Table2. 5 Drug doses and dilution for toxicity assay of cell lines

The IC50 doses for the selected cell lines were determined using IC50 doses established in previous research (Stordal *et al*, 2013), the highest dose of each drug was set a few doses higher than these pre-determined IC50 values (Table 2.5). A 2-fold serial dilution of the drug was then carried out in RPMI-1640 media. 100 µL of each dose was added across the plate starting with the lowest and finishing with the highest drug concentration. This was done in triplicate. Drug-free media was also plated (100µL) as a control. The plate was then incubated for a further five days at 37^{0}C and 5% CO_2.
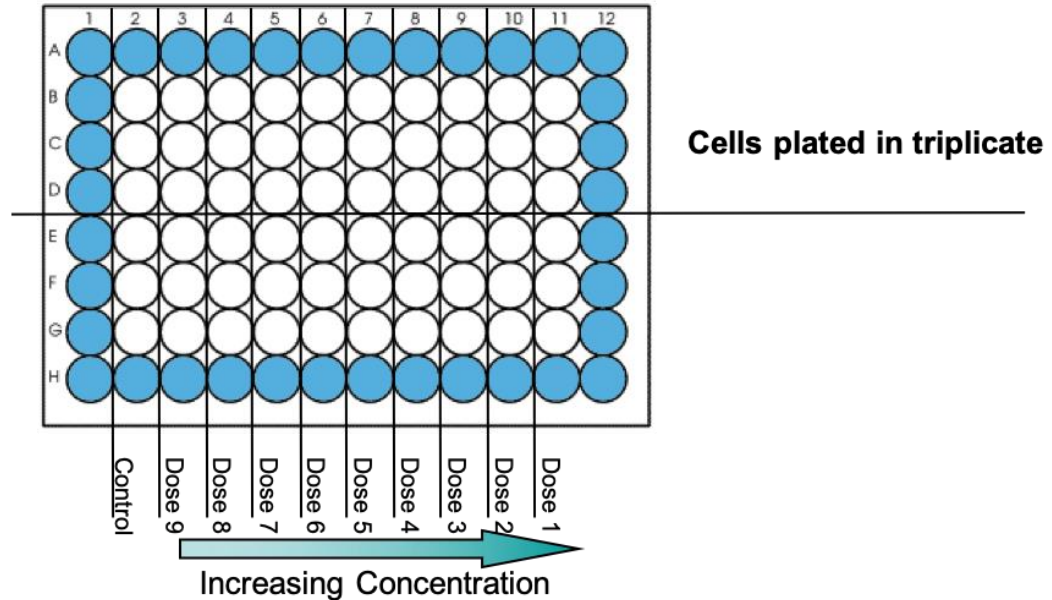
Figure2. 2 Cytotoxicity Assay in 96 well plate; drug doses serially diluted with concentration increasing from left to right of the plate. The blue wells contained deionised water to reduce dehydration.

On the day five of the treatment the drug waste from the plate was discarded and the plate was washed with PBS twice. Prior to this, 2.63g of fresh Phosphatase Substrate (Sigma Aldrich, UK) per 1mL of Sodium Acetate Buffer (0.1M Sodium Acetate pH 5.5, 0.1% Triton X-100) was prepared. Once the plate was washed, 100µL of the above acid phosphatase substrate solution was added to each well. The plate was once again incubated at 37°C but for about 1 hour. Incubation time was adjusted depending on the metabolism rate of the cells. The reaction in the wells was then stopped by adding 50 µL of 1 M Sodium Hydroxide (NaOH). The absorbance was then measured at 405nm on the plate reader (Omega FLUOStar, BMG Labtech) (Stordal *et al.*, 2012b). Using the complimentary Omega data analysis software (BMG Labtech) data was collected and exported onto Microsoft Excel. This was followed by calculating the mean and standard deviation of the absorbance for each drug dose. Using GraphPad Prism the data was normalised to absorbance values of control wells containing no cells as 0% and wells with no drug treatment as 100 % cell viability. Further analysis using a nonlinear regression fit (four parameter) was then carried out to determine the IC50 doses for each drug treatment.

2.1.7 Optimisation of Drug doses for Cell pellet preparation of the four cell lines

Doses for each drug determined from the cytotoxicity assay were optimised for each cell line to produce cell pellets for further experimental methods. Control (untreated) and drug treated cell pellets (minimum n=4) were produced for each cell line. Cells were grown in RPMI-1640 plus 10% FBS and subsequently seeded into T-75 flasks at a density of 6.25 x10^5 cells in 10mls of media. These were allowed to attach overnight before drugging the cells with IC50 doses of drugs determined from the cytotoxicity assays. On day four of drug treatment the cells were trypsinised and counted. This was followed by spinning the cells down and re-suspending the cell pellet in PBS two times. The cells are transferred and spun down a final time in an Eppendorf tube where the supernatant was discarded leaving a dry pellet.

The above steps were repeated for flasks seeded with a cell density of 2.58 x 10^5 cells. This was to replicate the conditions set up in the cytotoxicity assay into a T-75 flask. The harvested cell pellets were optimised to consist of cell counts within a range of 40-60% of the cell counts relative to their respective control cell pellets. This ensured that each sample was treated within the appropriately established IC50 dose for each drug.

In cases where the IC50 doses determined from the cytotoxicity assay did not have the desired effect, the doses were optimised by setting up five T-75 flasks seeded with the same cell density as above in each flask. The flasks were dosed with the IC50 dose as well as doses 2 and 4 times lower and higher than the determined IC50 dose. Cell pellet preparation was the same as described above. Cell counts for each dose were plotted and the final optimised dose was determined using Graph Pad Prism. Cell pellets were stored at -20 °C prior use in further experiments.

2.1.8 Invasion Assay

Cell lines growing in T-75 flasks were primed by removing serum containing media (Sigma) from cultures followed by thorough and gentle rinsing with serum-free media (SFM) (RPMI1640, Gibco). The cell lines were serum starved in the incubator for 5 hours by replacing culture medium with 10mL of SFM. Once the cells were starved, they were labelled by adding 10µL of DilC12 dye (10mg/mL in DMSO) and then incubated further for 2 hours. DilC12 dye is a weakly fluorescent dye until incorporated into cells whereupon it becomes strongly fluorescent.

A 96-well insert with an 8.0 µm pore size polyester membrane (Sigma) was coated with an extracellular matrix (ECM). This was prepared by mixing a solution A consisting of Collagen IV (Sigma), Fibronectin (Sigma), Laminin (Sigma), SFM with a solution B consisting of Collagen I (ThermoFisher), NaOH (Sigma), PBS (Fisher), Sterile water, Collagen IV, Fibronectin and Laminin detailed in table 2.6. All components of solution B were mixed by vortexing except Collagen I. This was added and mixed by pipetting up and down. 150µL of solution B was then added and mixed in solution A by pipetting once again. The inserts were then coated with 25µL of the above ECM mixture (solution A + solution B) and incubated at 37°C for 6 hours. After gelation 100µL of SFM media was added followed by removal of 80µL of the same SFM. A number of inserts were setup without coating with ECM so as to differentiate cell invasion from chemotaxis and as such act as a control to calculate total invasion. The set was as shown in figure 2.3 below
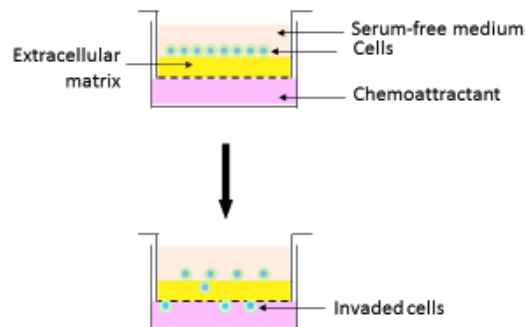
Figure2. 3 Representation of transwell chambers setup for invasion assay.

Component	Volume	Concentration
Solution A		
Fibronectin	11.97µl	(11.4µg/ml)
Laminin	11.97µl	(11.4µg/ml)
Collagen IV	105µl	(100µg/ml)
Serum free media	921.06µl	
Total	1050µl	
Solution B		
Collagen I	106.7µl	(0.8µg/ml)
1m NaOH	2.67µl	
PBS	35µl	
Sterile water	206.51µl	
Collagen IV	105µl	(100µg/ml)
Fibronectin	4.56µl	(11.4µg/ml)
Laminin	4.56µl	(11.4µg/ml)
Total	465µl	

Table2. 6 Components of collagen based extracellular matrix used to coat transwell inserts for invasion assay.

The pre-labelled cells were then harvested using dissociation solution TrypLE (Gibco) followed by addition of SFM. The cells were spun to remove cell dissociation solution and resuspended in SFM. A cell suspension was diluted to a seeding concentration of 400,000 cells/mL with SFM. To each insert well 50µL of diluted cell suspension was added (20,000 cells/well). At least one well was not seeded with any cells and was used as a blank. 170µL of complete media which functioned as the chemoattractant was then added to the receiver wells which were at the bottom of the transwell 96 well support (Sigma). The plate was incubated in 5% CO_2 at 37°C for 48 hours. The plate inserts were then removed followed by carefully swabbing the ECM with a cotton swab. The inserts were then placed back into the receiver plate and the fluorescence of invaded cell was measured at 549/565 nm in the plate reader (Omega FLUOStar, BMG Labtech).

2.2 Molecular Biology Techniques

2.2.1 Purification of RNA

The cell pellets harvested for each cell line from previous optimisation experiments (control and drug treated) underwent RNA extraction using the PureLink RNA Mini Kit (Ambion) as per manufacturer's protocol described in this section.

The frozen cell pellets prepared in section 2.1.7 were homogenised by re-suspending the cell pellets in 300µL of Lysis Buffer containing 1% 2-mercaptoethanol and then a 21-gauge syringe needle was used to break up the cell pellet followed by an additional step of vortexing at high speed until the cell pellet was completely dispersed and appeared to be fully lysed. Equal volume of 70% ethanol (molecular grade) was added to the cell homogenate and vortexed to ensure thorough mixing. The sample was then transferred to the spin cartridge with its collection tube and centrifuged at 12,000 x g for 15 seconds at room temperature. The flow through was discarded and the sample underwent on column DNase treatment. This involved adding 350 µL Wash Buffer I to the spin cartridge followed by spinning it at 12,000 x g for 15 seconds at room temperature. The spin cartridge was then inserted into a new collection tube and 80 µL of the PureLink DNase mixture (prepared as described in table 2.7) was added directly onto the Spin cartridge membrane and incubated for 15 minutes at room temperature. 350 µL of Wash Buffer I was again added to the Spin Cartridge followed by the same centrifugation step mentioned above. The spin cartridge was again inserted into new collection tube before adding 500 µL of Wash Buffer II. This was again centrifuged twice as described above and then centrifuged for the third time but for 1 minute in order to allow the membrane to dry with bound RNA. The spin cartridge was transferred into a recovery tube to which 100 µL of RNase free water was added to the centre of the spin cartridge and incubated for 1 minute at room temperature. The spin cartridge and recovery tube were centrifuged at 12,000 x g for 1 minute at room temperature. The purified RNA eluted into the recovery tube. The total RNA in each sample was quantified using the Nanodrop 2000 UV-Vis Spectrophotometer (Thermo Scientific). Prior to use for further experiments the extracted RNA was stored at -80 °C.

Component	Volume
10X DNase I Reaction Buffer	8µL
Resuspended DNase (~3U/µL)	10 µL
RNAase free water	0.5µL
Total volume	80 µl

Table2. 7 PureLink DNase Treatment Mixture

2.2.2 Quantitative Polymerase Chain Reaction

Quantitative polymerase chain reaction (qPCR) was carried out to assess the expression levels of the genes (Table 2.8) in samples that underwent cDNA conversion. The cDNA samples were made up with nuclease free water and 9 µL of which was added to each well of an opaque 96 well plate. A reaction mixture containing the Taqman master mix and Taqman assay primers (Life Technologies) were added to each well in the same plate. This is described in detail in table 2.9. Non-template controls of nuclease free water were also added to the plate. All samples were plated in triplicate. The plate was sealed and then loaded into the Roche LightCycler 96 PCR machine and run-on program conditions tabulated in table 2.10.

Primer	Assay ID
ROR1	Hs00938677_m1
ROR2	Hs00896176_m1
Rab27b	Hs01072206_m1
Vimentin	Hs00185584_m1
E-cadherin	Hs01023894_m1
N-cadherin	Hs00362037_m1
GAPDH	Hs02786624_g1

Table2. 8 Taqman Primers used in qPCR

Primer mix	For one reaction
20X Taqman Primer Assay	1 µL
2X Taqman Master Mix	10 µL
Total volume	11 µL
cDNA mix	**For one reaction**
cDNA sample	1 µL
Nuclease free water	8 µL
Total volume	9 µL

Table2. 9 qPCR Taqman Reaction Mix

Experiment parameters	Cycle conditions		
	Stage	**Temperature (°C)**	**Time (min)**
Reaction volume:20 µL **Ramp rate: 4.4**	Hold	50	02:00
	Hold	95	10:00
	Cycle	95	00:15
		60	01:00

Table2. 10 qPCR Program

The comparative cycle threshold (Ct) method was used to analyse relative gene expression of the biomarker genes to their respective controls (Livak and Schmittgen, 2001). The Ct values were corrected using Ct of the housekeeping gene GAPDH. Fold change in expression levels of genes and statistical significance was determined using GraphPad Prism.

2.3 Immunocytochemistry (ICC)

Cells (4 x 10^4 cells/mL) were plated at a volume of 400µL in each well of an 8-well chamber slide. The cells were allowed to grow till they reached about 60-80% confluency. Confluency was reached in 48 hours for all cell lines except OVCAR-3 which was reached at 120 hours. The media was then discarded and fresh media containing IC50 doses (Table 3.5) of the drugs

was added into each well. On day four of drug treatment the cells were washed three times with PBS and then fixed with 4 % paraformaldehyde in PBS for 8 minutes at room temperature. All washes were carried out with PBS and all incubations were at room temperature. The cells were then permeabilised with 0.1% Triton (Sigma) in PBS for 7 minutes. This was followed by a wash step after which the cells were blocked with 50% horse serum in PBS for 8 minutes. Optimal dilutions for primary antibodies (diluted in PBS) (Table 2.11) were added to each well(100µL) for 2 hours. The cells were then washed three times and a Goat anti rabbit IgG FITC labelled secondary antibody (Abcam) was added (50 µL) at a 1:100 dilution to each well. Where the primary antibody was raised in mouse, the secondary antibody (Table 2.12) used was a Goat anti Mouse IgG FITC labelled antibody (Abcam). The slide was incubated for 90 minutes and then washed three times before removing the gasket separating each chamber well. A coverslip was then placed on the slide covering each well spot using mounting media containing DAPI (Vectorshield) which is a fluorescent stain binding to DNA in the fixed cells. The slides were covered and allowed to dry in the dark for at least 1 hour before examining under the confocal microscope (Leica Microsystems, Wetzlar, Germany). Four fields per sample chamber well were chosen at random and photographed. The emission maximum of DAPI is 461 nm which falls within the blue colour spectrum. The DAPI and FITC stained portions of the fixed cells were viewed separately, and also as merged images shown in chapter 3 section 3.3.4.3. This was done using confocal microscopy on the Leica Microsystems microscope's imaging software.

Antibody	Source/Clonality	Dilution
ROR1(Proteintech)	Rabbit Polyclonal	1:100
ROR2(QED Bioscience)	Mouse Monoclonal	1:50
RAB27B (Proteintech)	Rabbit Polyclonal	1:100
VIMENTIN(Dako)	Mouse Monoclonal	1:100

Table2. 11 Primary Antibodies used in ICC

Antibody	Dilution
Goat Anti-Mouse IgG H&L(FITC)	1:100
Goat Anti-Rabbit IgG H&L(FITC)	1:100

Table2. 12 Secondary Antibodies used in ICC

The cells in the captured images were counted using the ImageJ software and then averaged. These images were first converted from RGB to 16-bit grayscale images. To distinguish the cells from the background the threshold feature was used. This suppressed certain pixels in the background by removing intensities within a certain threshold. A binary image is created which shows only the cell pixels. Using the 'analyse particles' feature in ImageJ the number of cells is automatically counted.

To count the cells and quantify intensity levels of biomarker expression for each cell, the images were first converted from RGB to 16-bit grayscale images. To distinguish the cells from the background the threshold feature was used. This suppressed certain pixels in the background by removing intensities within a certain threshold. A binary image is created which shows only the cell pixels. For cells that seem to have merged the 'watershed' feature in ImageJ is used to accurately cut them apart using a 1pixel thick line. This then followed by 'analyse particles' feature in ImageJ where the number of cells is automatically counted along with the intensity measurement of the biomarker expression. The intensity (expression) is normalized to the cell number for each drug treated cell to the untreated control for in each cell line.

2.4 Statistical analysis

Statistical analysis was carried out using Minitab17, GraphPad Prism and R statistical packages. The software's and tests used to carry out for each analysis are detailed in each chapter. For all tests, $p < 0.05$ was considered as statistically significant.

Chapter 3

Investigation of ROR1 as a novel biomarker

3.1 Introduction

As mentioned in chapter 1 Section 1.8.1.1.1 ROR1 has been previously implicated in several other malignancies and therefore makes it a reliable candidate gene to investigate for this study. A recent study by Fultang *et al*. (2020) discussed the role of ROR1 in regulation of chemoresistance in breast cancer. The ABC family of ATP-dependent drug transporters, specifically ABCB1/MDR-1 were identified to have a major underlying role in chemoresistance in breast cancer (Ji *et al*., 2019; Sui *et al*., 2012). Inhibitors of these transporters did not show much promise clinically to overcome multidrug resistance. The Fultang *et al*. (2020) study attempted to identify upstream regulators of the ABCB.1 and chemoresistance in breast cancer. ROR1 which has been described as an onco-foetal receptor (Fultang *et al*., 2019; S. Zhang *et al*., 2012a, 2012b) was identified as a key upstream regulator of ABCB1 (Fultang *et al*., 2020).

The results from this study (Fultang *et al*., 2020) showed an increased effect of platinum based and anthracycline chemotherapy drugs when ROR1 knockdown or inhibition (by small molecule inhibitors) were carried out. Other studies have also shown ROR1 functioning as a prognostic marker for tumour relapse and poor survival outcomes (Chien *et al*., 2016; C. Henry *et al*., 2017; E.-H. Jung *et al*., 2016; Wu *et al*., 2019; S. Zhang *et al*., 2012a). Gene expression data of breast cancer patients from NCBI's Gene Expression Omnibus (GEO) suggested that patients with poor chemotherapy response had an increased level of ROR1. Similar associations between ROR1 and response in ovarian cancer patients was observed (H. Zhang *et al*., 2014b). Since high grade serous ovarian cancer shares molecular and genomic similarities with certain types of breast cancer (Begg *et al*., 2017) it seems relevant to investigate ROR1 as a biomarker.

Mechanisms underlying chemoresistance in ovarian cancer is complex and therefore emphasises the need for effective biomarkers. Several studies have documented individual biomarkers for platinum-based chemotherapy resistance (Guo *et al*., 2020; Pokhriyal *et al*., 2019). Interestingly, ROR1 was not included in these biomarker lists. However, there are limited studies that have investigated ROR1 in ovarian cancers (Henry *et al*., 2015; Yin *et al*., 2017; Zhang *et al*., 2014). These studies have described a link between ROR1, EMT and the Wnt signalling pathway which has been described in chapter 1 section 1.8.1.1.4.

3.2 Methods

3.2.1 Knock-down of gene expression using small interfering RNA (siRNA)

3.2.1.1 Optimisation of siRNA reverse transfection using GAPDH

In order to assess the effectiveness of reverse transfection, certain optimisation steps were carried out. The cell density used was the same as in the cytotoxicity assay (section 2.1.6). Cells cultured in T-75 flasks were trypsinised and counted of which 2 x 10^4 cells/mL were seeded into a 96 well plate at 100 µL and T-25 flask at 5mL. Lipofectamine mix was then prepared with lipofectamine (ThermoFisher Scientific) and OptiMEM Reduced Serum Media (Life Technologies) and incubated for 5 minutes at room temperature. The Scramble (Ambion) and GAPDH siRNA (Ambion) were diluted to a final concentration of 30nM in OptiMEM media. 25µl of the diluted siRNAs were plated in triplicates in a 96-well plate and 500µl in a T-25 flask. This was followed by adding 25µl/500 µl of the lipofectamine mix into each well and flask respectively containing the diluted siRNA mix. The plate and flasks were shaken gently and incubated at room temperature for 15 minutes. Once the complexes were formed after incubation, 100 µl and 5mLs of cell suspensions obtained from the T-75 flasks were added to each well and flask respectively. The remaining empty wells in the 96 well plates were filled with 200 µl of sterile deionized water so as to prevent the contents of the plate from evaporating. The plate and flasks were incubated overnight at 37°C with 5% CO_2 to allow cells to attach. The cells were observed under the microscope up to 72 and 120 hours in order to assess cell viability following reverse transfection.

The house keeping gene GAPDH (Ambion) was used in the optimisation experiment to trial different siRNA conditions. The scramble (Ambion) was chosen as the negative control and non-transfected cells were used as the positive control. Details of these are shown in table 3.1 below

siRNA (Ambion)	Catalog No.
Scramble Select Negative Control no.1 siRNA	4390843
Silencer GAPDH siRNA	AM4605

Table3. 1 siRNA used in optimisation of GAPDH knockdown

3.2.1.1.1 Reverse Transfection of siRNA in 96 well plate andT-25 flask

The siRNA GAPDH knockdown was carried out on HEY and OVCAR-3 cell lines. The rationale was to select cell lines on either side of the resistance profile: most resistant and most sensitive. On day 1 of the knockdown experiment, these cells were trypsinised, counted and then re-suspended in fresh media to make up the required cell density (2×10^4). The optimisation process was carried out over two time points; 72 hours and 120 hours for each cell line in order to establish most effective duration of the knockdown. As described in section 3.2.1.1 the Scramble siRNA (Silencer® Select Negative Control No. 1 siRNA (Ambion) and GAPDH siRNA were diluted in OptiMEM to a final well/flask concentration of 30nM followed by addition of the lipofectamine mix. The plates and flasks were incubated at room temperature to form complexes for 15 minutes before adding 100 µl of cell suspensions to each well and 500 µl to each flask. The cells were incubated at 37°C and 5% CO_2 and allowed to attach overnight. The following day, each well and flask was replaced with fresh 10% FCS and RPMI media.

3.2.1.1.2 Take down of siRNA plates and flask

At 72 and 120 hours the plates for HEY and OVCAR-3 cells were washed with PBS following removal of the media and trypsinised. Media was added to wells to deactivate the trypsin. The contents of the triplicate wells were pooled into one tube and spun down for 5 minutes at 1000 rpm. The supernatant was discarded, and the cells were washed with 1 mL cold PBS and then

transferred to 1.5 ml Eppendorf tubes. There were once again spun down at maximum speed for one minute after which the supernatant was discarded.

Cells in the T-25 flask were harvested according to the protocol described in chapter 2 section 2.1.7. Cells harvested from the 96 well plates and T-25 flasks at 72 and 120 hours were counted and then underwent RNA extraction followed by a cDNA conversion step (as described in later section; 3.2.1.2.5). A qPCR experiment was then set up as described in chapter 2 section 2.2.2 to determine the optimal time point and siRNA concentration for most effective knockdown.

3.2.1.2 Optimisation of ROR1 and ROR2 knockdown

On day 1 of the ROR1/2 siRNA knockdown, HEY and OVCAR-3 cells were trypsinised and counted to establish cell suspension volumes of 2 x 10^4 cell/ml for both 96 well plates and T-25 flasks to be set up for take down at 72 and 120 hours. Lipofectamine mix and siRNA of varying concentrations was prepared as described in section 3.2.1.1. Scramble (Ambion) as well as ROR1 and ROR2 siRNAs (Table 3.2) were diluted in Optimem reduced serum media (ThermoFisher Scientific) to varying concentrations (10nM, 30nM and 50nM) appropriate for a 96 and T-25 flask volume. Reverse Transfection was carried out as described in section 3.2.1.1.1. Plates were rocked gently and incubated for 15 minutes at room temperature to allow complexes to form. Cell suspensions of 2 x 10^4 cells/mL were then added to each well and flask; 100μl was added to wells in 96-well plate and 5mLs of cell suspension was added to each T-25 flask. 200μl of distilled water was pipetted into the empty wells of the 96-well plates to avoid dehydration of the plate. Plates and flasks were incubated at 37°c with 5% CO2 to allow cells to attach overnight. Similar to the above optimisation experiment, each well and flask was replaced with fresh 10% FCS and RPMI media.

siRNA	Catalog No.	ID	Sense (5'-3')	Antisense (5'-3')
ROR1	AM51331	613	GGCUCUCCUUUCGGUC CACTT	GUGGACCGAAAGGAG AGCCTC
ROR2	AM51331	541	GGUGAAGUGGAGGUU CUGGTT	CCAGAACCUCCACUU CACCTG

Table3. 2 siRNA used in Knockdown experiment

3.2.1.2.1 Take down of plates and flasks

The plates were taken town at 72 and 120 hours as described in section 3.2.1.1.2. The absorbance was then measured at 405nm on the plate reader as described above in section to determine effects of varying siRNA concentrations on cell viability. Cells harvested (as described in chapter 2 section 2.1.7) from the flasks at 72 and 120 hours underwent RNA extraction and cDNA conversion (as in chapter 2 section 2.2.1 and chapter 3 section 3.2.1.2.5). Optimal knockdown conditions were then determined through data obtained from subsequent qPCR experiment.

3.2.1.2.2 Knockdown of ROR1 and ROR2 with optimised RNA concentration

Following on the above knock down optimisation experiments, the optimal siRNA dose concentration of ROR1 and ROR2 and time points were selected for HEY and OVCAR-3 cells. Knockdown experiments were set up similar to the above in a 96 well plate and T-25 flask for both cell lines. In addition to setting up ROR1 and ROR2 knockdown, a double knockdown of both ROR1 and ROR 2 in the same well/flask was also added. This consisted of the optimal siRNA concentration for ROR1 and ROR2 determined from the optimisation experiments above. Day 1 of the knockdown protocol was same as described above (as in section 3.2.1.1).

3.2.1.2.3 Drug treatment of knockdown cells

Media in the 96 wells plates was changed and replaced with fresh media containing different doses of cisplatin. Three doses of the drug were used for treatment in the knockdown experiment. The doses used were the IC50 dose determined as described in later section 3.3.2 (Table 3.5) and variations of the IC50 dose; double the dose and half the dose. Each dose was added in triplicate to ROR1, ROR2 and ROR1/2 knock down cells as well as the Scramble. However, additional siRNA transfected cells were also included in the plates and were not treated with cisplatin in order to act as a comparative control. The 96-well plates were then incubated at 37°C with 5% CO_2.The media in the T-25 flasks was replaced with fresh 10% FCS and RPMI media with the appropriate drug dose and were incubated till take down.

3.2.1.2.4 Take down of plate and flask

The 96-well plates were taken down as described in earlier section 3.2.1.1.2 and absorbance's read in the plate reader (Omega FLUOStar, BMG Labtech). Cells were harvested from the T-25 also as described earlier following cell counts.

3.2.1.2.5 cDNA conversion and qPCR

Total RNA was extracted using the PureLink RNA Mini Kit (Ambion) as described in chapter 2 section 2.2.1 and cDNA conversion was completed as described in chapter 2 section 2.2.2. The 96-well plate was analysed by acid phosphatase assay (section 2.1.6). The qPCR experiment was carried out using the TaqMan Gene Expression Assay (Applied Biosystems) protocol in which the expression of ROR1 and ROR2 was investigated. GAPDH gene was used as the housekeeping gene (Table 3.3). Samples were loaded and sealed into the Roche Light Cycler 96 RT-PCR machine and run on the program shown in chapter 2 section 2.2.2 Table 2.10. Results were analysed using Roche LightCycler 96 software.

Primer	Assay ID
ROR1	Hs00938677_m1
ROR2	Hs00896176_m1
GAPDH	Hs02786624_g1

Table3. 3 Taqman Primers used in qPCR of knocked down cells

3.2.2 Protein Chemistry Techniques

3.2.2.1 Harvesting Ovarian Cancer Cells

Cells were harvested by trypsinization as described in chapter 2 section 2.1.2 and 2.1.7. The cells were spun down twice and washed ice-cold PBS each time. The cell pellet was resuspended in RIPA buffer (Sigma) and 1 x Protease inhibitor (ThermoFisher). The cells were lysed by mechanical shearing using a syringe tip (21-gauge needle). The cells were kept on ice during the homogenisation process and then centrifuged at 13,000 rpm for 15 minutes. The supernatant was retained, and protein concentration was determined as described in section 3.2.2.2 below. Cell lysates were stored at -80°C until required.

3.2.2.2 Determining Protein Concentration of Cell lysates

A Bradford assay was carried out to determine the protein concentration of the cell lysates. A seven-point standard curve was produced using known concentrations of protein standards made up of Bovine Serum Albumin (BSA) (Sigma) in of Bio-Rad Protein Reagent (Bio-Rad Laboratories) which was diluted (1:4) with a starting concentration of 1 µg/µL. 4µL of the cell lysates were added to 16µL of deionized water to make a 1:5 dilution. This diluted standards and lysates were then added to wells in a 96-well plate containing 250µL of Bradford reagent. This was done in triplicates. The plate was read using the microplate reader (Omega FLUOStar, BMG Labtech) at 595nm. The absorbances of the standards were used to plot the standard curve from which the protein concentration of the lysates was interpolated.

3.2.2.3 Protein Electrophoresis

Proteins were separated based on their molecular size using a pre-cast 10-12% polyacrylamide gel (Biorad Laboratories). The cell lysate samples were prepared by mixing 2X Laemmli buffer (25% v/v glycerol, 2% w/v SDS, 0.01% w/v bromophenol blue and 65mM Tris (pH 6.8)) (Biorad Laboratories) along with 5% ß-mercaptoethanol. The samples were heated on a heat block at 90°C for 5 minutes. The samples were then loaded onto the gels (20µL per lane) along with the protein weight marker (5µL) and run at 150 Volts for 45 minutes.

3.2.2.4 Visualization of Proteins on Nitrocellulose membrane

The gel was detached from the cast slides and sandwiched between a pre-soaked transfer pack (Biorad Laboratories) consisting of nitrocellulose membrane and filter paper. The semi-wet transfer was then carried out using the Trans-Blot Turbo Transfer system (Biorad Laboratories). The setting was set to transfer for 7 min rapid transfer at 25 Volts and 2.5 Amp of current. The protein transfer was visualised using a Ponceau S stain (Sigma) by pouring it over the blot for about 20 seconds and then discarding the stain solution. The blot was then washed with deionised water to remove the stain in order to visualise the total protein transferred.

3.2.3 Immunological Techniques

3.2.3.1 Western blotting

Following the transfer, proteins on the nitrocellulose membrane was incubated with the antibody in order to detect and visualise the target protein (details of antibodies detailed in table 3.4). Before this, the membrane was blocked in 10 mL of 5% Skimmed Milk (Biorad Labortories) in 0.1% PBS-Tween (Sigma) for 1 hour. This was done to prevent non-specific binding of antibodies. The membrane was then incubated with the primary antibody solution specific to the protein of interest. This was a 1:1000 dilution of antibody made up in 3% Skimmed Milk in 0.1% PBS-Tween. The membrane was allowed to incubate with primary antibody overnight on a plate rocker at 4°C. The membrane was then washed with a wash buffer (0.3% PBS-Tween) three times for 10 minutes each. This was followed by a second incubation with a secondary antibody conjugated with Horse-radish Peroxidase (HRP) diluted to 1:1000 in 3% Skimmed Milk in 0.1% PBS-Tween for 1 hour. The membrane was then washed 3 times with wash buffer as above. An enhanced chemiluminescence (ECL) detection reagent (GE Healthcare) was added onto to membrane, enough to cover it, for 1 minute. The ECL reagent was then poured out and the membrane was visualized using the Licor Odyssey Infrared Imaging System at different wavelengths.

1° Antibody	Source/Clonality	Dilution
ROR1(Proteintech)	Rabbit Polyclonal	1:1000
ROR2 (QED Bioscience)	Mouse Monoclonal	1:1000
ß-Actin (Sigma)	Mouse Monoclonal	1:10,000
ß-Actin (Sigma)	Goat Polyclonal	1:10,000
2° Antibody	Source/Clonality	Dilution
Goat Anti-Rabbit IgG-HRP (Biorad)	Rabbit Polyclonal	1:1000
Goat Anti-Mouse IgG-AP (Biorad)	Mouse Monoclonal	1:1000

Table3. 4 Primary and secondary antibodies used for incubation of nitrocellulose membrane

The membrane was then washed with the wash buffer before incubating it with β-Actin primary antibody (1:10,000) (Sigma) in 3% Skimmed Milk (Biorad) in 0.3% PBS-Tween for 1 hour. This was followed by washing the membrane as described previously and then once again incubating the membrane with a secondary antibody (1:1000) conjugated with Alkaline Phosphatase in 3% Skimmed Milk in 0.3% PBS-Tween for another hour. The membrane was washed one final time as above before adding a solution of Sigma fast BCIP NBT tablets to the membrane. This reacted with the Alkaline phosphatase tagged to the secondary antibody to develop the β-Actin protein on the membrane, which served as the loading control.

The bands on the membranes were analysed using Image J software and the knockdown percentages were quantified. The relative amounts of each protein of interest were quantified as ratios relative to loading control. Each bands intensity was measured along with the background. These intensities were inverted, and the net intensities was measured by subtracting inverted intensities of the protein of interest and the background. The same was done for the loading control. The ratio of net protein and loading control was calculated and graphed into percentages. This method was adapted from Davarinejad H (2017).

3.2.3.2 Enzyme-linked immunosorbent assay: ROR1

The cell pellets as prepared in section 2.1.7 were also used to measure the levels of the biomarker protein (ROR1) in both control and drug treated cells for each cell line using a sandwich ELISA kit (DuoSet IC R&D systems). A 96-well plate was coated with 100 µL of the Total ROR1 capture antibody (rat anti-human ROR1 antibody, DuoSet IC R&D systems)) at a working concentration of 10ug/mL and incubated overnight at room temperature. This was followed by three washes using wash buffer (0.05% Tween20 in PBS, pH 7.2-7.4) and then a blocking step using Block buffer (1% BSA, 0.05% NaN3 in PBS, pH 7.2-7.4) for 2 hours. The plate was again washed as earlier and then plated with 100 µL of the Total ROR1 standards (recombinant human ROR1) as well as the sample. A six-point standard curve was set up using 2-fold dilutions of the standard starting with the highest concentration of 2ng/mL. The plate was again incubated for 2 hours at room temperature followed by the wash step. The Total ROR1 detection antibody (biotinylated goat anti-human ROR1 antibody, DuoSet IC R&D systems)) was pipetted (100uL) in to each well at a working concentration of 2ug/mL and incubated for 2 hours at room

temperature. The plate was washed and 100µL of Streptavidin conjugated to Horseradish peroxidase (1:200) (DuoSet IC R&D systems) was added to each well. Following a 20-minute incubation at room temperature the plate was washed and 100 µL of a substrate solution (1:1 mixture of Color Reagent A (H_2O_2) and Color Reagent B (Tetramethylbenzidine)) was added. The plate was incubated for the final time at room temperature for 20 minutes before adding 50 µL of stop solution (2N H_2SO_4). Using the Omega FLUOStar (BMG Labtech) plate reader, the optical density of each well was determined. The wavelength was set to 450nm with a correction set to 570nm.

3.2.4 Statistical Analysis

In Minitab, a one-way ANOVA was used to test for significance in a) the growth rate of the cell lines, b) to compare the dose responses for each drug between the cell lines., c) compare the invasiveness of cell lines in the panel. Tukeys test was used for post-hoc analysis. A one sample t-test was used to a) check for percentage of cell viability of drug treated cells for cell pellet preparation, b) to account for statistical significance of mRNA expression from qPCR.

GraphPad Prism was used to interpolate values of ROR1 in drug treated and untreated cells in ELISA. One-way ANOVA test was used to account for statistical significance in the expression levels of the biomarkers in the cell lines (with each drug treatment. The correlation between resistance and ROR1 expression was determined by the Pearson's correlation coefficient. Data produced from qPCR of knockdown experiments was analysed using the one-sample t-test, two-sample t-test and one-way ANOVA.

3.3 Results

3.3.1 Growth Curves of Cell Lines

The doubling time for each of the cell lines (n=3) was determined using the exponential growth equation in GraphPad Prism (Figure 3.1). These curves define the growth characteristics for each cell line; they allow determination of the appropriate time range for assessing the cytotoxic effects of the drug treatments used. The doubling times estimated here validate the effectiveness of carrying out a 5-day combination cytotoxicity-proliferation assay as it allows the cells to be exposed to the drug for sufficient time for it to have an effect on the cells.
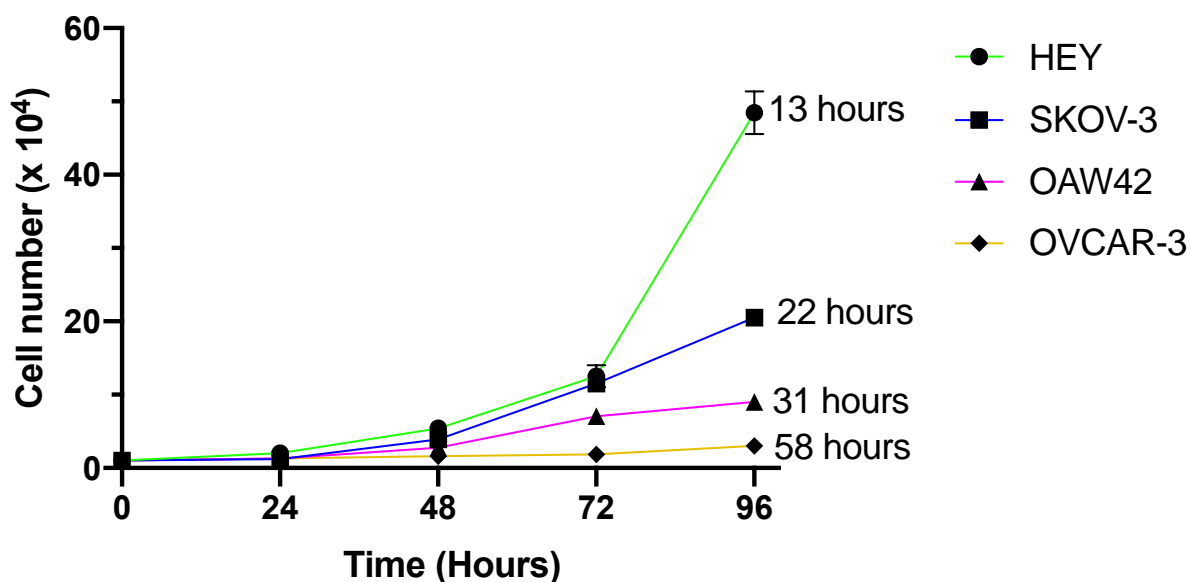
Figure3. 1 Growth curves of the four selected cell line HEY, SKOV-3, OAW42 and OVCAR-3. The cells were grown in 6 well plates for 96 hours and counted every 24 hours as described in section 2.1.5. Experiment repeats of n=3 was carried out and the mean cell counts for each cell line is represented by each coloured curve line. The doubling time for each cell line is depicted in hours and indicated next to each line in the graph. The HEY cell line has the shortest doubling time of 13 hours and OVCAR-3 cell line has the longest doubling time of 58 hours.

Figure 3.2 below demonstrates the cell numbers of all four cell lines over the 96-hour period. The growth rate of HEY was significantly higher than other OC cell lines and OVCAR-3 showed the lowest rate of growth. These differences were statistically significant from 24h onwards. At the 48 hours mark, these cell numbers were statistically significant ($p<0.001$) compared to the rest of the cell line panel.
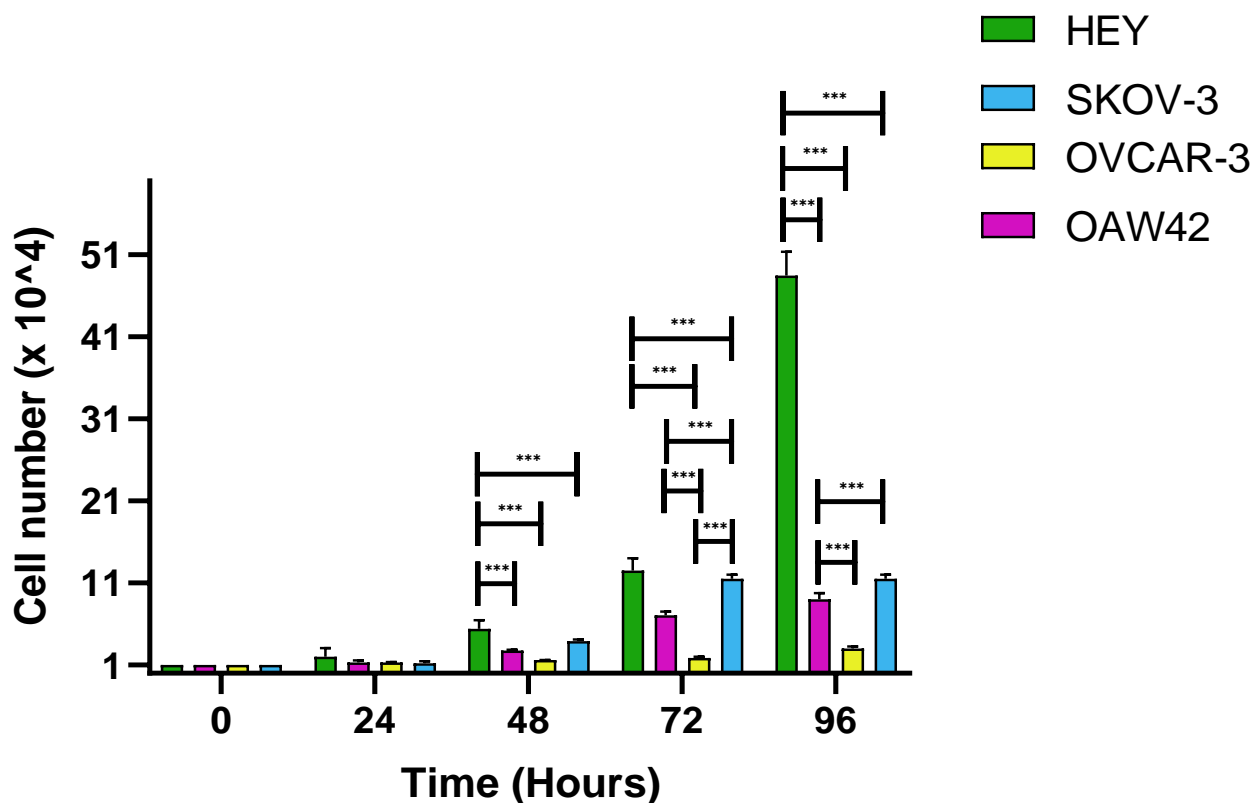
Figure3. 2 Cell number (x 10^4) of each cell line from the growth assay experiment. The number of cells per cell line counted every 24 hours over a 96-hour period. Experiment repeats of n=3 was carried out. A one-way ANOVA was carried out with '***' denoting significance of $p<0.001$. A post hoc analysis using Tukey's test was carried out.

3.3.2 Cytotoxicity assay and IC50 dose range

The results show that HEY cell line required the highest dose for each drug treatment making it the most resistant model in the cell line panel. The absorbance for each dose from the 96-well plate was averaged and normalized to the control. These values were then plotted as the concentration of the drug versus the percentage of cell viability. The IC50 was determined at the 50% mark on the y-axis versus the drug concentration on the x-axis. All steps were carried out using Graph pad Prism Version 5. The cytotoxicity assays revealed that the cell lines exhibited different resistance profiles to the four drugs. Figure3.3 shows the resistance profiles of all the cell lines to each drug. A significant difference ($p<0.05$) between cisplatin IC50 in HEY versus OVCAR-3 and OAWA42 cells was observed. The same applies to SKOV-3 cell versus OVCAR-3 and OAW42 cell lines.

However, there was no significant difference in the IC50 cisplatin dosage between HEY and SKOV-3 cells. The same trend follows with carboplatin treatment. The HEY cells also required a higher dose of the PARP inhibitor Talazoparib to reach IC50 dosage and showed a significant difference in the dosage requirements compared to SKOV-3 ($p < 0.05$), OVCAR-3 ($p < 0.01$) and OAW42 ($p < 0.01$) cell lines. OVCAR-3 required the lowest dosage concentration whereas there was no significant difference between the dosages required for SKOV-3 and OAW42. The HEY cells once again required the highest dose of Taxol compared to the other three cell lines($p < 0.001$). SKOV-3, however, showed higher sensitivity to taxol compared to OVCAR-3 and OAW42 ($p < 0.05$).
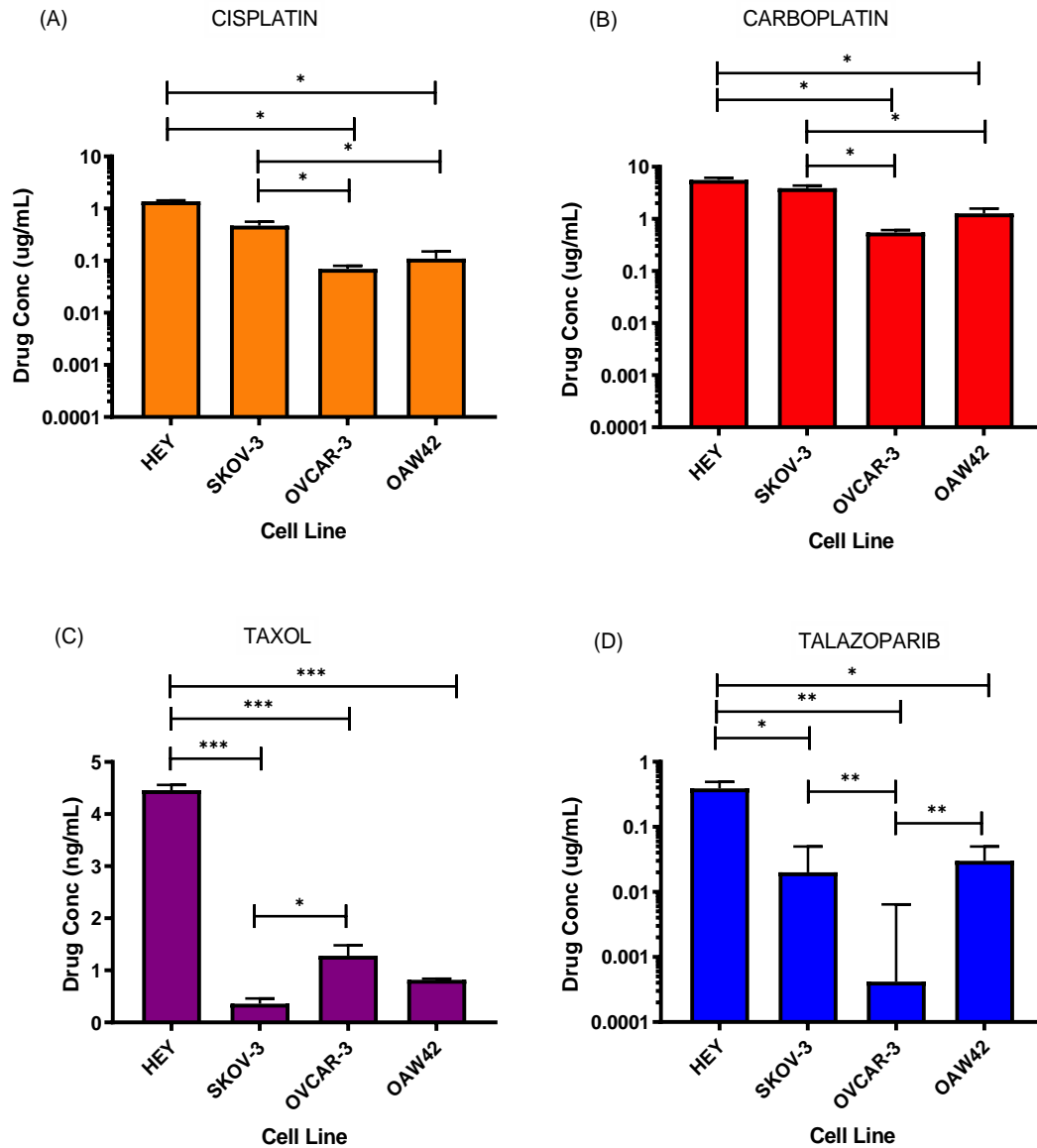
Figure3. 3 Bar graph of resistance profile of four cell lines to drug treatments (A)Cisplatin, (B)Carboplatin, (C) Taxol and (D) Talazoparib. The cell lines were treated with varying doses of drugs to determine IC50 doses as described in chapter 2 section 2.1.6. Experimental repeats of n=5 was carried out and the error bars represent standard deviation. The IC50 dose of each drug was compared across the cell line panel and analysed using a one-way ANOVA test. '*', '**' and '***' denotes the statistical significance of $p<0.05$, $p<0.001$ and $p<0.0001$ respectively. A post hoc analysis using Tukey's test was carried out

Although some drug doses required further optimisation in HEY, SKOV-3 and OVCAR-3 cell lines when upscaling to T-75 flasks, table 3.5 below shows the finalised IC50 doses of the four drugs for the cell lines which were determined through the cytotoxicity assay in 96-well plates.

Cell lines	Cisplatin(ug/mL)	Carboplatin (ug/mL)	Taxol(ng/mL)	Talazoparib (ug/mL)
	IC50 dose	IC50 dose	IC50 dose	IC50 dose
HEY	1.38±0.05	8.41±0.20	2.97±0.04	0.149±0.5
SKOV-3	0.47±0.09	3.90±0.46	0.72±0.005	0.02±0.03
OVCAR-3	0.07±0.01	0.55±0.06	1.28±0.20	4.2×10^{-4}±0.006
OAW42	0.11±0.04	1.28±0.30	0.8175±0.02	0.047±0.02

Table3. 5 Optimised IC50 doses from cytotoxicity assay and T-75 flasks (n=5). IC50 doses from cytotoxicity assay (as described in chapter 2 section 2.1.6) and optimised doses from five T-75 flask experiment of cisplatin, carboplatin, taxol and talazoparib treatment for the four cell lines as described in chapter 2 section 2.1.7**.** (Doses underlined were optimised in T-75 flasks)

3.3.3 Preparation of Cell Pellet

The control and drug-treated cell pellets for each cell line were harvested for downstream experiments to investigate biomarker expression. The cell counts for each drug-treated sample ranged from 40 to 60% relative to their respective control samples, and all were statistically significant (Figure 3.4).
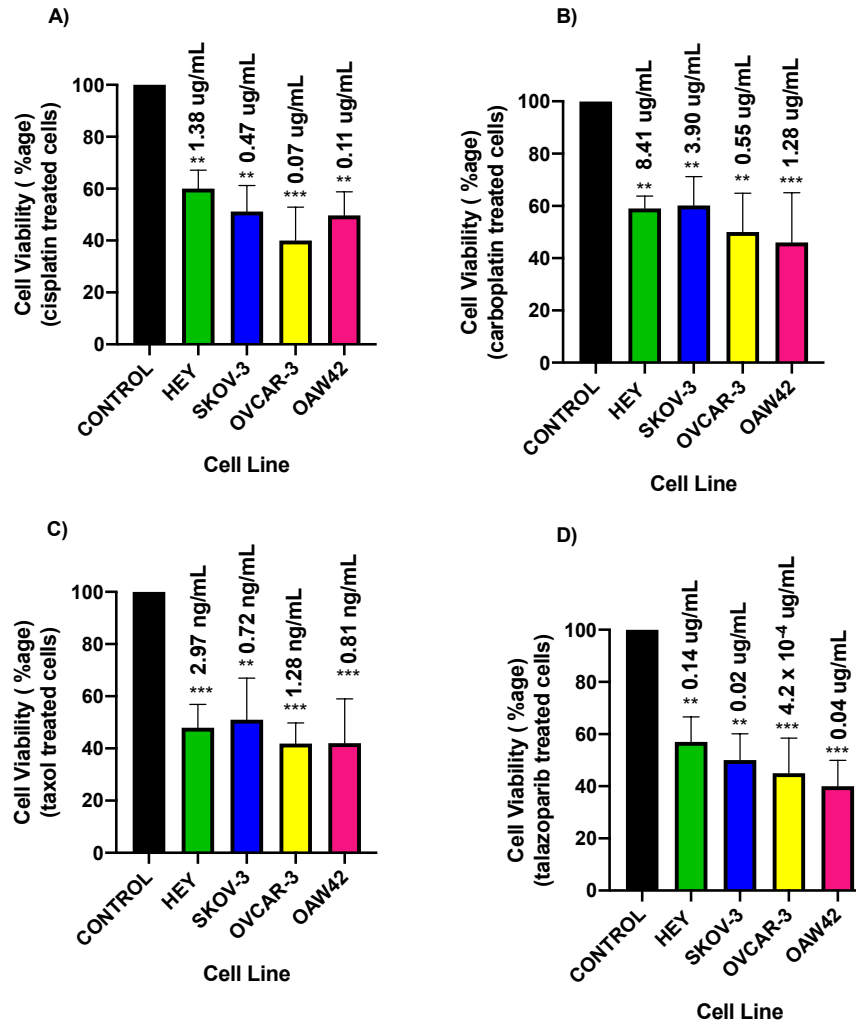
Figure3. 4 Cell viability percentage of the four cell lines when treated with IC50 doses of drug treatment. Cell pellets were harvested as described in chapter 2 section 2.1.7 with experimental repeats of n = 5. Cell viability of A) cisplatin, B) carboplatin, C) taxol and D) talazoparib were normalized to the respective untreated controls. Percentage of cell viability ranged between 40-60% upon drug treatment. A one-sample t-test was carried out comparing the viability of drug-treated cells back to untreated control cells (100% viability) with '**' and '***' denoting the significance of $p<0.001$ and $p<0.0001$ respectively.

3.3.4 Expression of ROR in cell line panel

3.3.4.1 mRNA expression levels of ROR1 and ROR2 in the cell line panel

The expression of ROR1 and ROR2 was examined at mRNA level in the qPCR assay for each cell line. There were significant changes in ROR1 and ROR2 expression between the different cell lines and following drug treatment. Due to inaccessibility to ROR1/2 positive control cells, the expression of ROR1 and ROR2 in the cell line panel were compared to HEY cells. The bar graphs below (Figure 3.5) show varying levels of expression relative to the HEY cell line as it was determined to be the most resistant in the cytotoxicity assays described above in section 3.3.Relative to the HEY cells, ROR1 levels were significantly decreased with a -3 ($\pm$ 0.1 SD) fold change in OVCAR-3 cells ($p<0.001$). A significant decrease ($p<0.05$) in ROR1 expression was also observed in OAW42 cells showing a downregulation of -2 ($\pm$ 0.3 SD) fold change compared to the HEY cells.

However, ROR2 levels were significantly higher ($p<0.0001$) with a 2.7($\pm$ 0.29 SD) fold increase in OAW42 cells and lower ($p<0.0001$) with a -22 ($\pm$ 0.612 SD) and -9 ($\pm$ 0.19 SD) fold decrease in SKOV-3 and OVCAR-3 cells respectively.
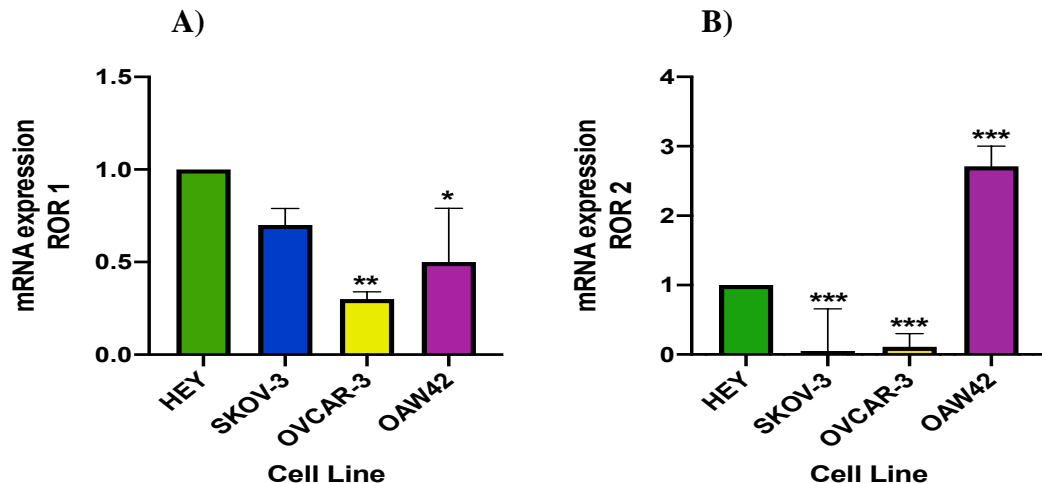
Figure3. 5 qPCR of all four cells demonstrating ROR1 and ROR2 expression. Relative mRNA expression of A) ROR1and B) ROR2. All cells are untreated and reflect the expression profile relative to the most resistant. cell line; HEY. Experiment repeats of n=3 was carried out. Significant fold change is observed in both directions. HEY cell line set to a constant of 1.0 on the Y-axis. A one sample t-test was carried out with '*', '**' and '***' denoting significance of $p<0.05$, $p<0.001$ and $p<0.0001$ respectively.

The ROR1 and ROR2 mRNA levels were also compared in drug treated and control (untreated) cells for each cell line. The expression levels were normalized to that from their respective controls. Figure 3.6 below shows the significant downregulation of ROR1 ($p < 0.05$) expression in HEY cells treated with drugs; cisplatin (-1.25-fold), carboplatin (-2.5-fold), taxol (-10-fold) and talazoparib (-5-fold), relative to the control. ROR2 expression also exhibited a -2 to 10-fold decrease with drug treatment when compared to the control, however taxol treated cells presented the opposite effect. Here, there was a significant increase ($p < 0.001$) of almost 2-fold in ROR2 expression compared to the control (Figure 3.6 (B))

A)

B)
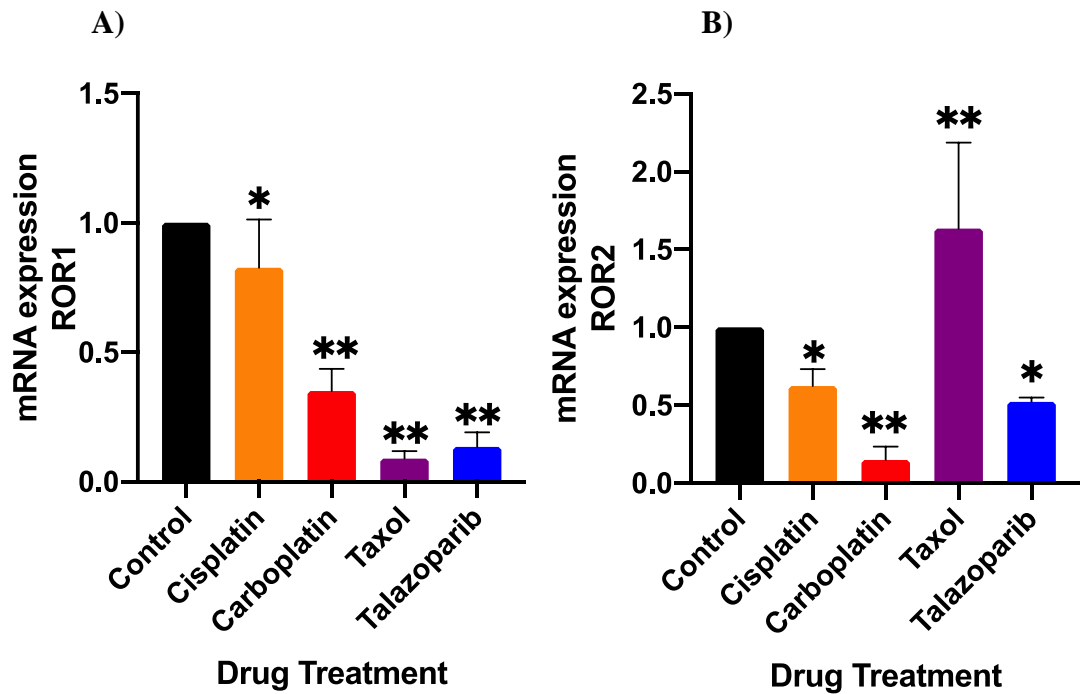
Figure 3. 6 qPCR of HEY cells. Relative mRNA expression of A) ROR1 and B) ROR2 in HEY cell line treated with IC50 doses of four drugs: cisplatin, carboplatin, taxol and talazoparib. Experiment repeats of n=3 was carried out. Cells treated with drugs are compared to their respective control (non-drug treated) to determine the fold change. Control cells set to a constant of 1.0 on the Y-axis. A one sample t-test was carried out with '*' and '**' denoting significance of $p < 0.05$ and $p < 0.001$ respectively.

ROR1 expression was substantially increased by almost 11 -fold in SKOV-3 cells treated with cisplatin but not with other drug treatments (Figure 3.7 (A)). ROR-2 expression was significantly increased in SKOV-3 cells treated with cisplatin ($p<0.001$), carboplatin ($p<0.05$) and taxol ($p<0.05$) by 2 to 3.5 -fold, but not with talazoparib (Figure 3.7(B)) when compared to the control.

A)

B)
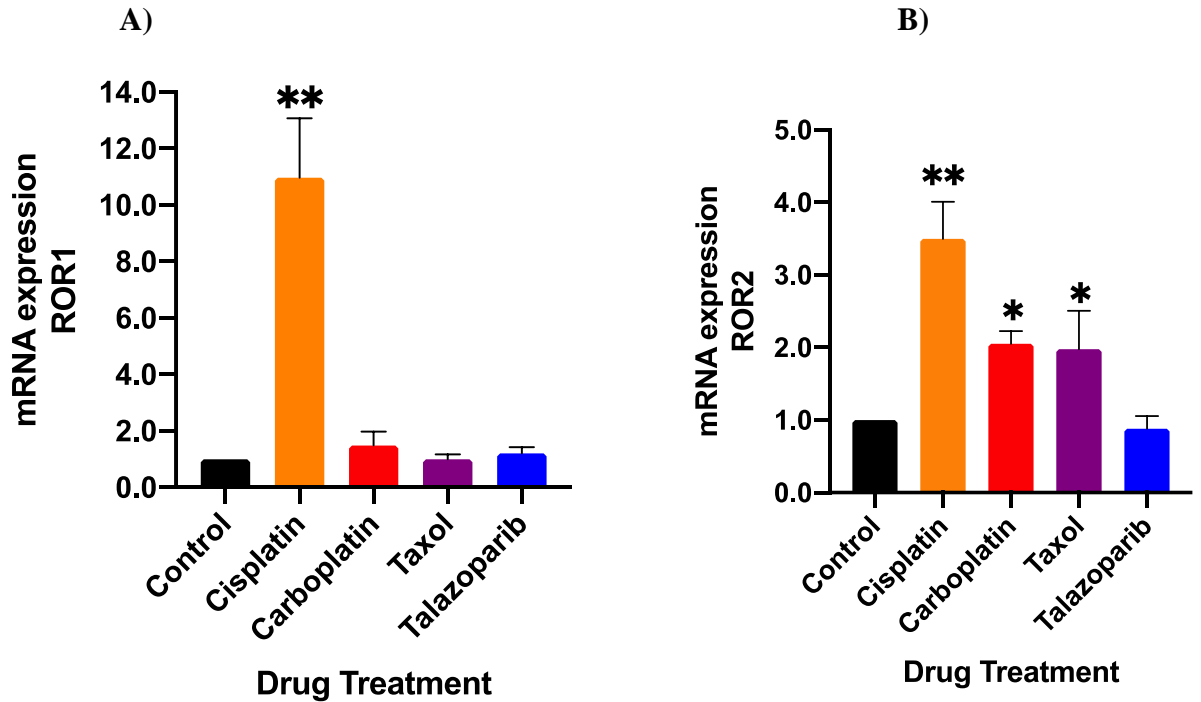
Figure3. 7 qPCR of SKOV-3 cells. Relative mRNA expression of A) ROR1and B) ROR2 in SKOV-3 cell line treated with with IC50 doses of four drugs; cisplatin, carboplatin, taxol and talazoparib. Experiment repeats of n =3 was carried out. Cells treated with drugs are compared to their respective control (non-drug treated) to determine the fold change. Control cells set to a constant of 1.0 on the Y-axis. A one sample t-test was carried out with '*' and '**' denoting significance of $p<0.05$ and $p<0.001$ respectively.

In contrast, drug treated OVCAR-3 cells showed a significant -2.5 to 4-fold downregulation of ROR1 ($p < 0.001$) and -10 to 12-fold downregulation of ROR2 ($p < 0.001$) expression when compared to their respective non-drug treated control as shown in the figure 3.8 below.

A)   **B)**
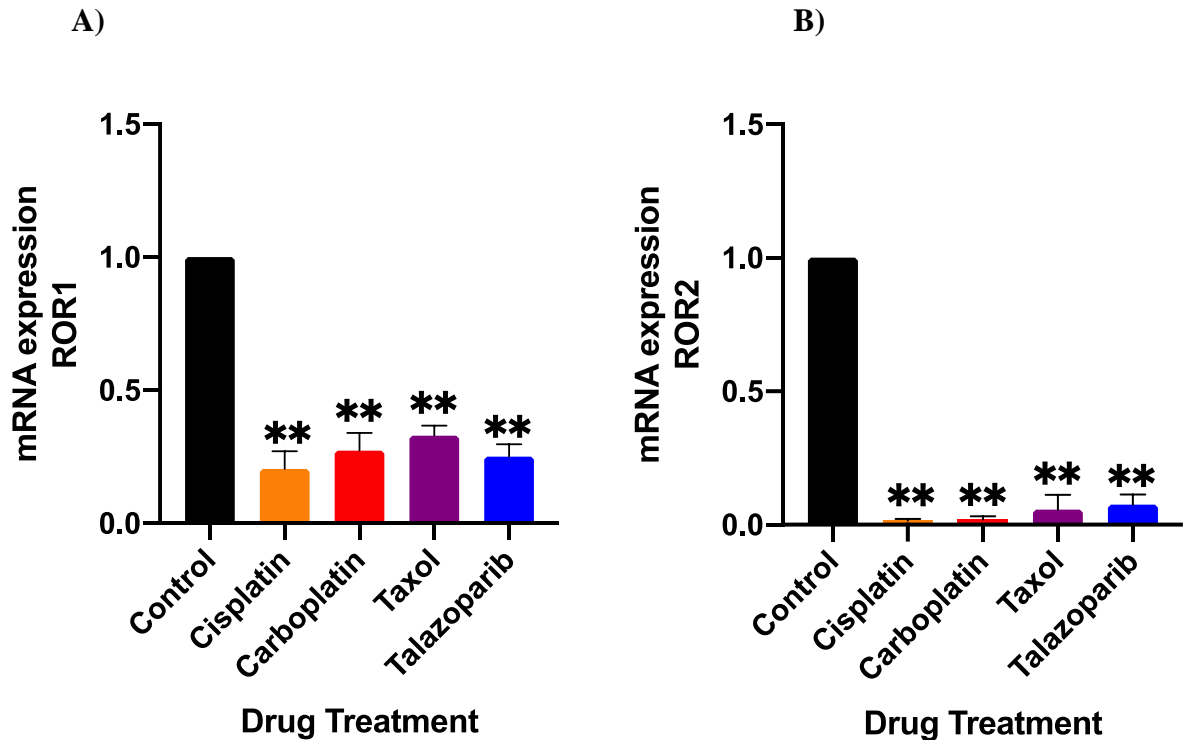
Figure3. 8 qPCR of OVCAR-3 cells. Relative mRNA expression of A) ROR1and B) ROR2 in OVCAR-3 cell line treated with IC50 doses of four drugs: cisplatin, carboplatin, taxol and talazoparib. Experiment repeats of n=3 was carried out. Cells treated with drugs are compared to their respective control (non-drug treated) to determine the fold change. Control cells set to a constant of 1.0 on the Y-axis. A one sample t-test was carried out with '*' and '**' denoting significance of $p < 0.05$ and $p < 0.001$ respectively.

In cisplatin and carboplatin treated OAW42 cells a significant 2.5 and 2-fold upregulation of at least a fold change ($p < 0.05$) of ROR1 was observed respectively. Taxol and talazoparib treated cells did not demonstrate any significant change in ROR1 expression relative to the control cells. ROR2 expression was significantly upregulated ($p < 0.05$) by 1.5 to 2-fold in cisplatin, carboplatin and talazoparib treated cells compared to its respective control. Taxol treated cells showed no significant change in ROR2 expression (Figure 3.9).

A)

B)
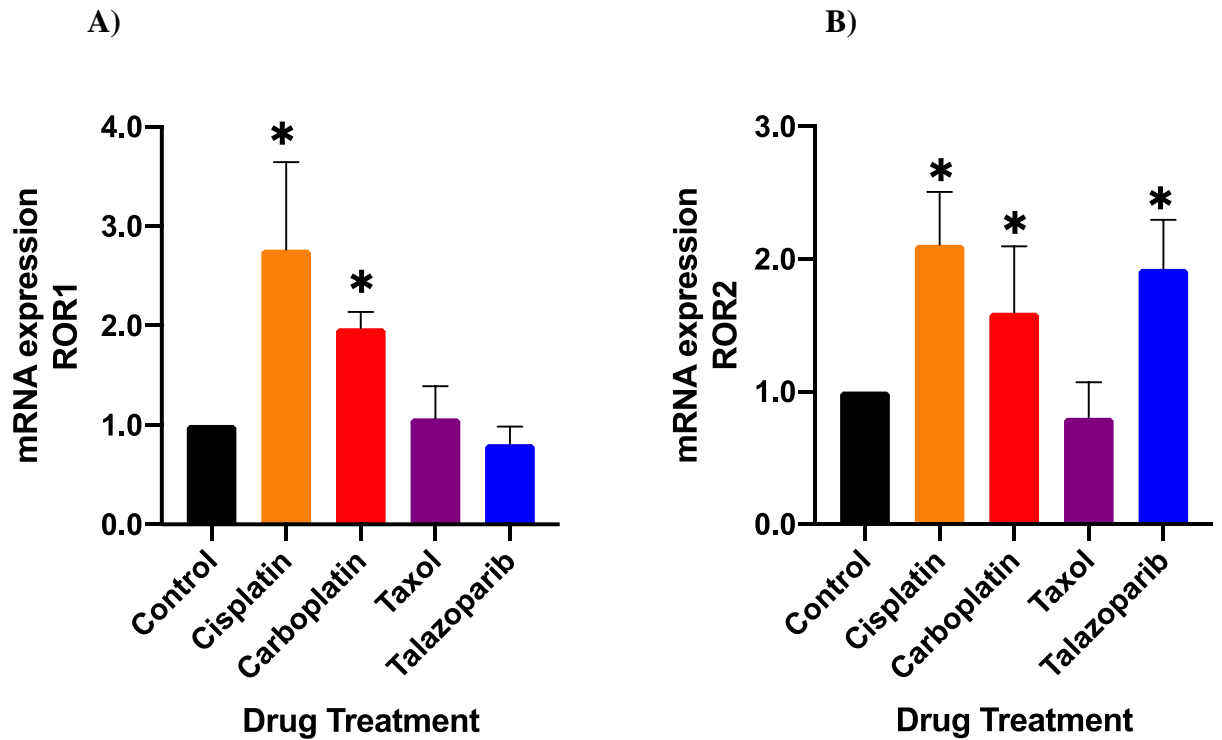
Figure3. 9 qPCR of OAW42 cells. Relative mRNA expression of A) ROR1and B) ROR2 in OAW42 cell line treated with IC50 doses of four drugs; cisplatin, carboplatin, taxol and talazoparib. Experiment repeats of n=3 was carried out. Cells treated with drugs are compared to their respective control (non-drug treated) to determine the fold change. Control cells set to a constant of 1.0 on the Y-axis relative to the control. A one sample t-test was carried out with '*' and '**' denoting significance of $p < 0.05$ and $p < 0.001$ respectively.

3.3.4.2 Analysis of Enzyme Linked Immunosorbent Assay (ELISA): ROR1

A six-point standard curve was plotted shown in the figure 3.10 following the protocol described in section 3.2.3.2.
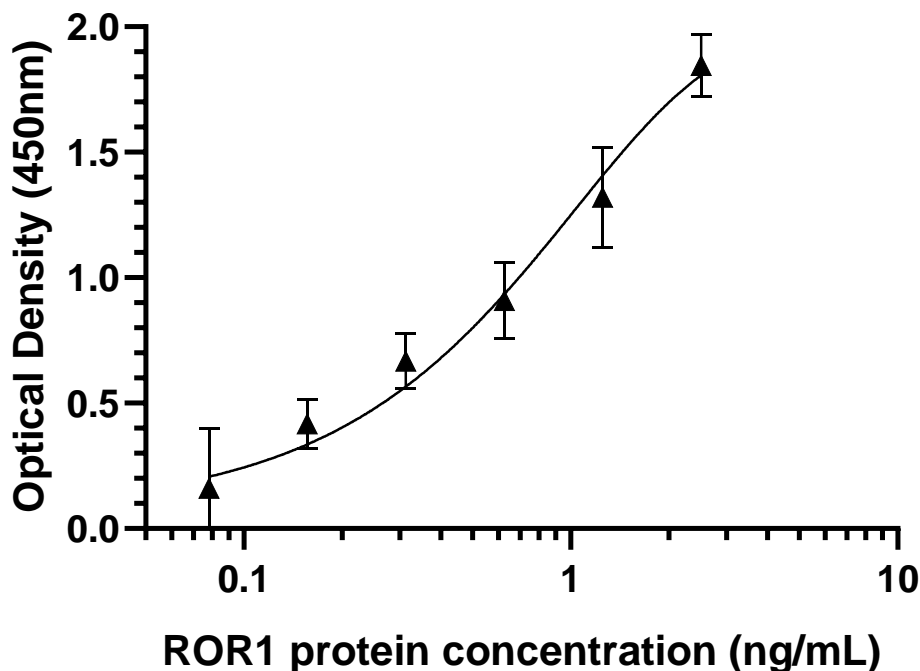
Figure3. 10 Standard curve plotted of ROR1 standards in sandwich ELISA. A six-point standard curve plotted to interpolate ROR1 protein concentration in the four cell lines (n=3) as described in section 3.2.3.2. The error bars represent the standard deviation of the means of each data point.

ROR1 protein expression in control and drug treated samples of the four cell lines (HEY, SKOV-3, OVCAR-3 and OAW42) was quantified by sandwich ELISA (Figure 3.11). The protein concentrations were interpolated from the standard curve. The protein expression was highest in HEY cells, followed by SKOV-3, OAW42 and OVCAR-3 respectively. This expression pattern was consistent with mRNA results in section 3.3.4.1 above. In HEY cells, the expression of ROR1 reduced with the different drug treatments however only a significant reduction by -1.5 (±0.0065) fold change was observed between the control and talazoparib treated HEY cells (p<0.05). There was also a decrease in ROR1 protein expression across the SKOV-3 cells. The drug treated cells appeared to show lower levels of ROR1 compared to the control however only the taxol treated cells had a significant decrease with a -1.5 (±0.00210)

fold change (p<0.05). In OVCAR-3 cells the levels of ROR1 protein expression also decreased with drug treatment. However only cisplatin treated cells showed a significant -1.5-fold decrease of ROR1 protein levels compared to the control (p<0.05). The OAW42 cells showed no significant difference in the levels of ROR1 protein expression in drug treated cells compared to the control cells. Talazoparib treated cells exhibited a significant 1.5 (±0.00120) fold change increase compared to the cisplatin treated cells (p<0.05).
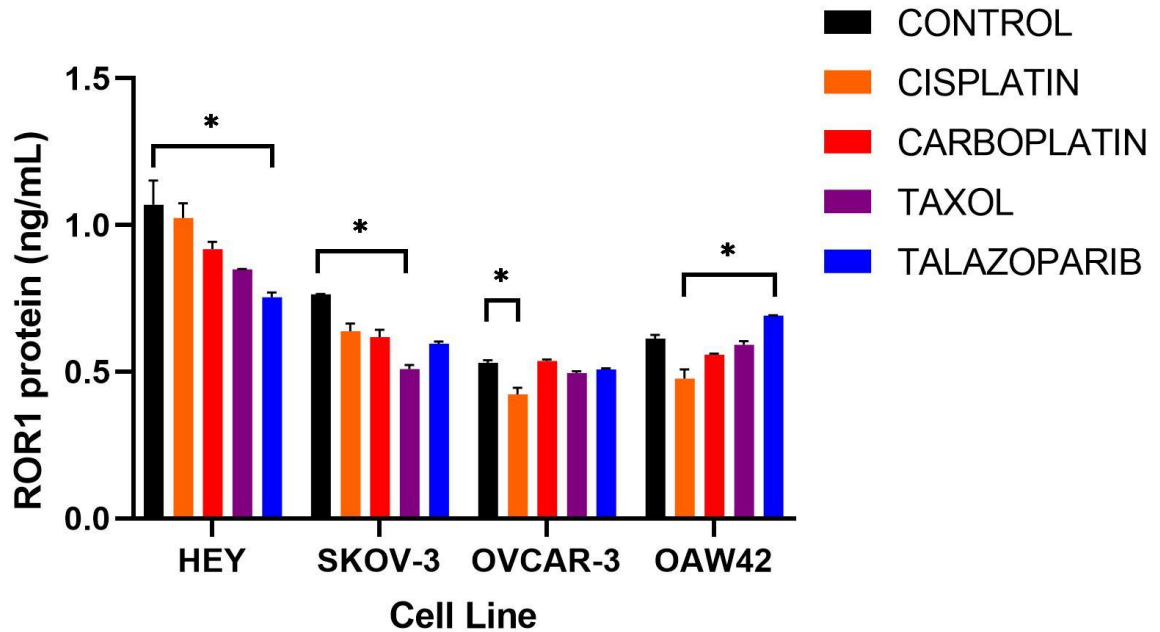
Figure3. 11 Protein levels of ROR1 in each cell line with different drug treatments was determined using a sandwich ELISA (n=3). Each cell line showed varying levels of ROR1 protein level upon drug treatment. A one-way ANOVA comparing ROR1 levels in drug treated and untreated cells for each cell line was carried out. '*' denotes statistical significance of p<0.05.

Overall, the ROR1 protein concentration levels were elevated in the HEY cell line compared to the other cell lines. As the HEY cell line is the most resistant in the cell line panel and demonstrates highest expression of ROR1 protein, this suggests a possible link between chemoresistance and ROR-1 expression. To confirm if ROR1 is associated with resistance to chemotherapy a correlation graph was plotted.
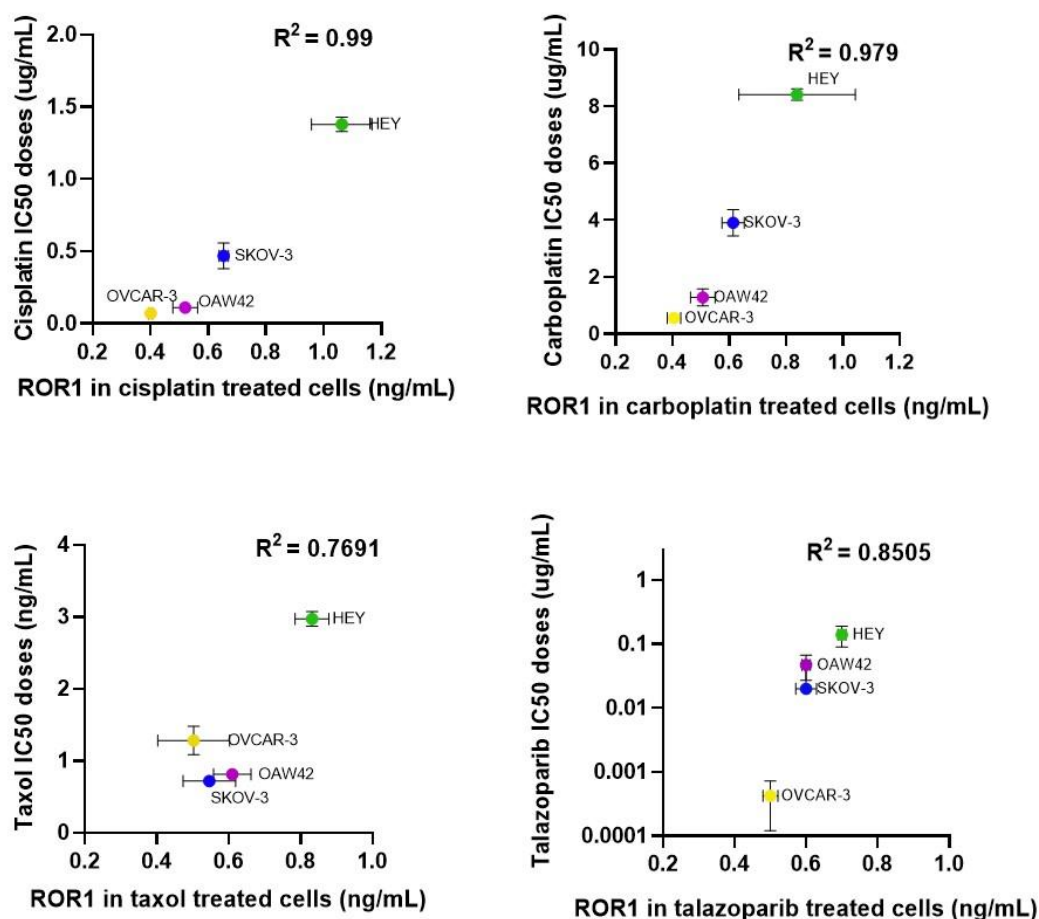
Figure3. 12 Correlation between the expression of ROR1 and the IC50 doses of all drug treatments in the cell line panel. There is a strong correlation between ROR1 and chemoresistance in A) cisplatin, B) carboplatin, C) taxol and D) talazoparib treated cells. The x-axis represents the ROR1 protein levels interpolated from the ELISA described in section 3.2.3.2. The y axis represents the IC50 doses of each drug determined through cytotoxicity assay as described in chapter 2 section 2.1.6. The Pearson coefficient is displayed on top right corner of each correlation graph.

The above figure 3.12 shows a positive strong direct correlation between ROR1 expression and chemoresistance in cisplatin ($R^2 = 0.99$) and carboplatin ($R^2 = 0.979$) treated cells. A positive correlation was also observed between ROR1 expression and chemoresistance in taxol ($R^2 = 0.7691$) and talazoparib ($R^2 = 0.8505$) treated cells. The HEY cells being the most resistant to all drug treatments in the cell line panel expressed the highest levels of ROR1 protein whereas OVCAR-3 cells being the most sensitive in the cell line panel expressed the lowest levels of ROR1. This was carried out using ROR1 expression from ELISA since this method was more quantitative than qPCR.

3.3.4.3 Confocal microscopy of cells after Immunocytochemistry (ROR1)

Confocal images captured at a magnification of 10X below (Figure 3.13) show the ROR1 expression in HEY control and drug treated cell line. The FITC label (green) indicates the ROR1 expression decreases upon drug treatment compared to the control.
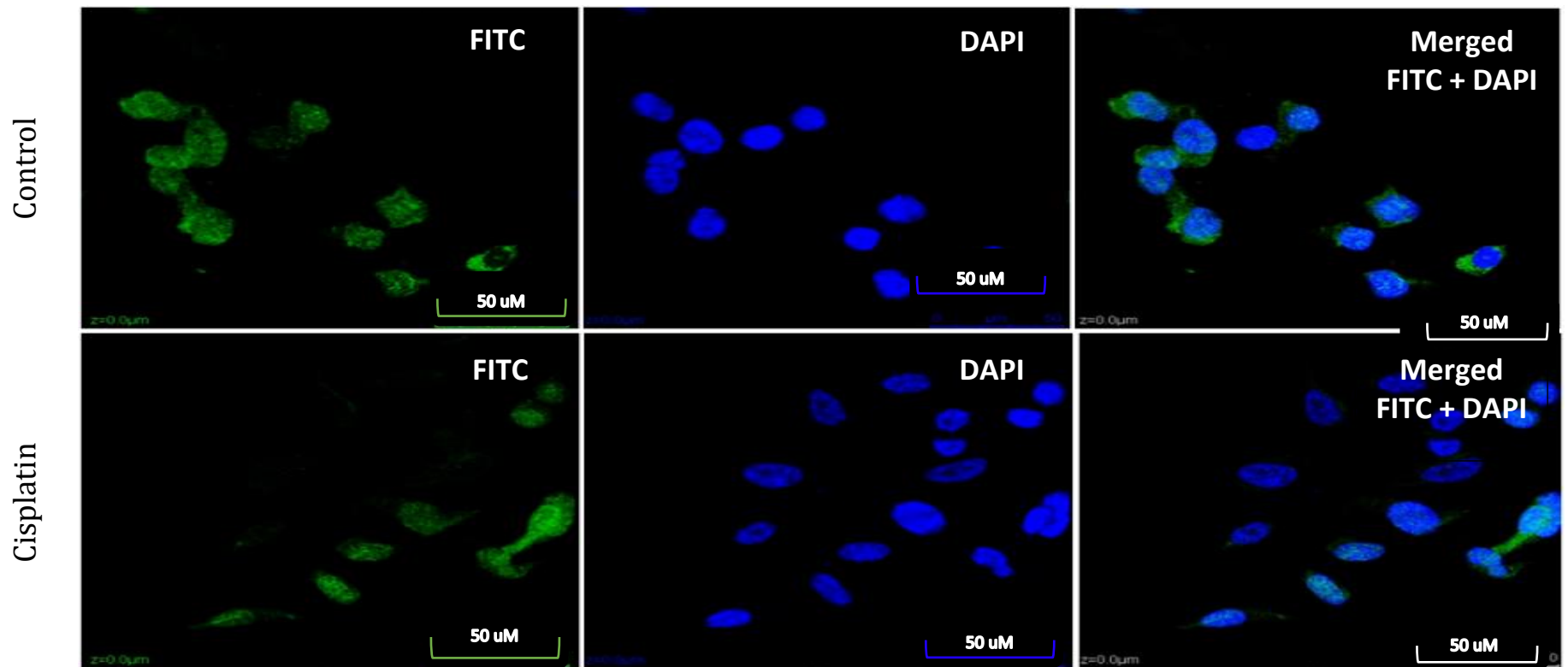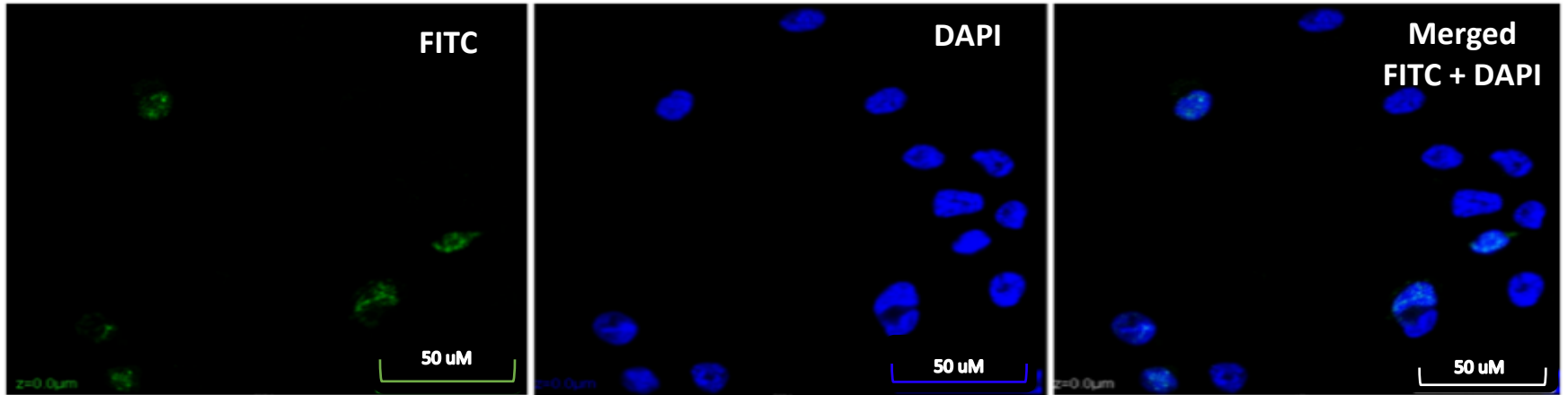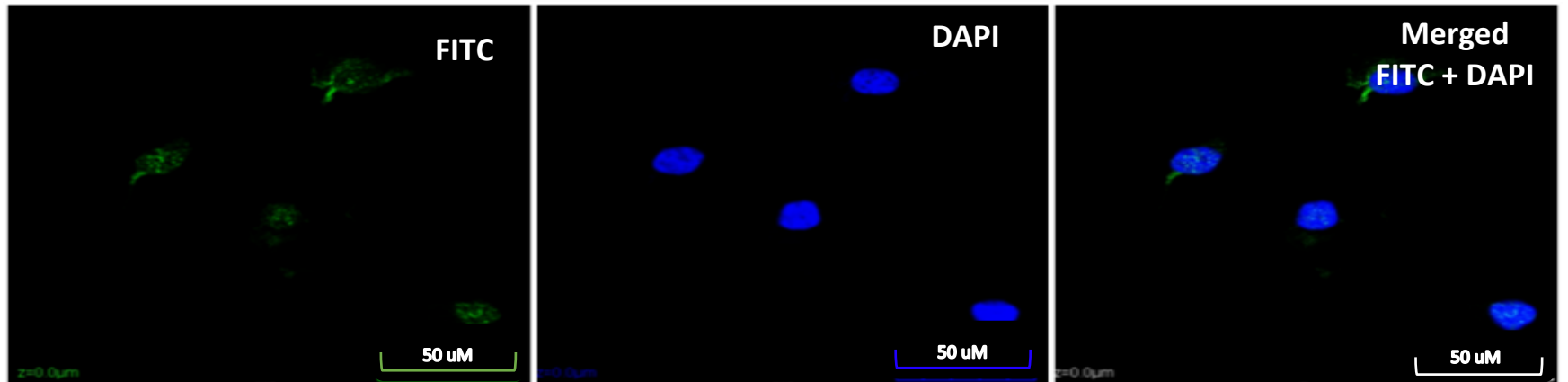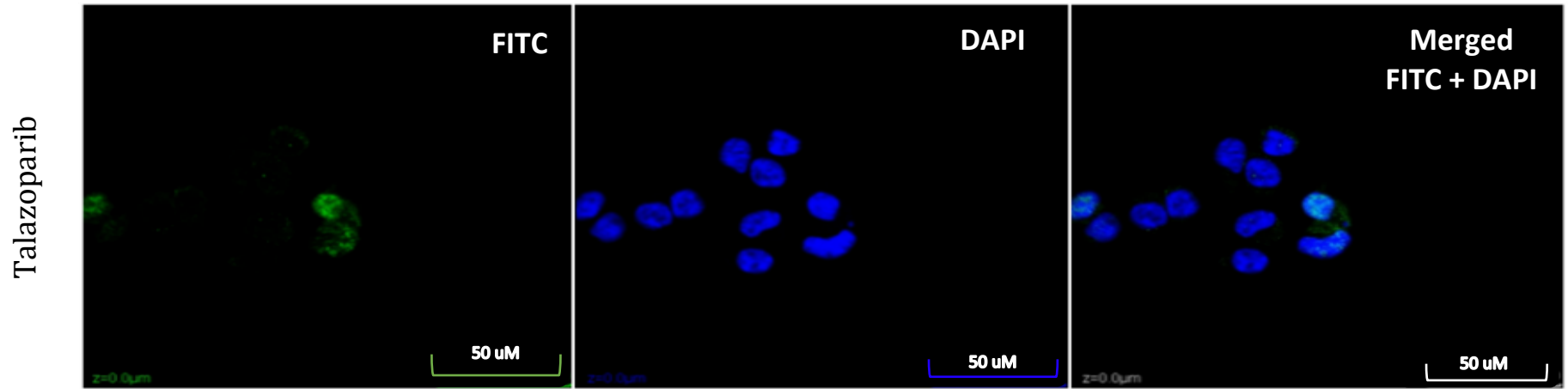
Figure3. 13 Confocal microscopic images of ROR1 expression stained with FITC (green) in HEY cell lines with drug treatments. Cells were counterstained with DAPI to show the localization of the nucleus. Images were captured at 10X magnification.

ROR1 expression was normalized to cell number in drug treated cells and all showed a decrease in expression relative to control untreated cells. Except for taxol treated cells, other drug treatments revealed a significant -2 to 5-fold decrease in ROR1 expression (Figure 3.14).
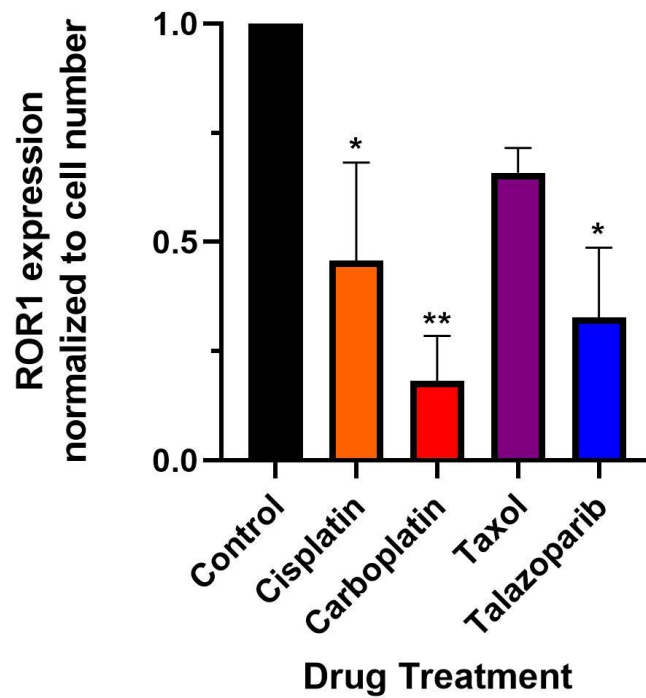
Figure3. 14 Measurement of ROR1 expression of drug treated HEY cells from confocal microscopy images. Intensity of ROR1 in drug treated cells measured relative to control untreated cells and normalized to cell number. A one sample t-test was carried out with '*' and '**' denotes statistical significance of $p < 0.05$ and $p < 0.01$ respectively.

Confocal images captured at a magnification of 10X below (Figure 3.15) show the ROR1 expression in SKOV-3 control and drug treated cell line. The FITC label (green) indicates the ROR1 expression decreases upon drug treatment compared to the control.

Carboplatin (left, rows): FITC | DAPI | Merged FITC + DAPI — 50 uM

Taxol (left, rows): FITC | DAPI | Merged FITC + DAPI — 50 uM
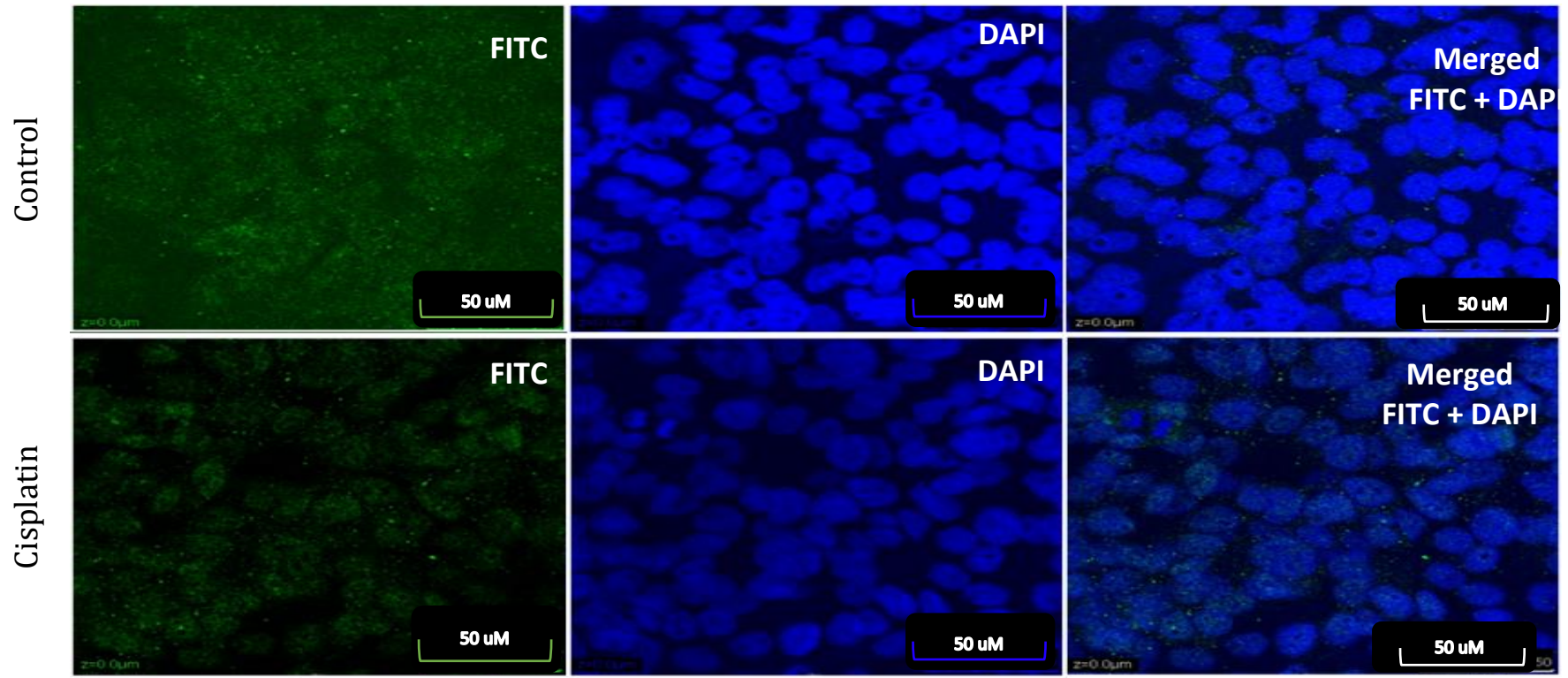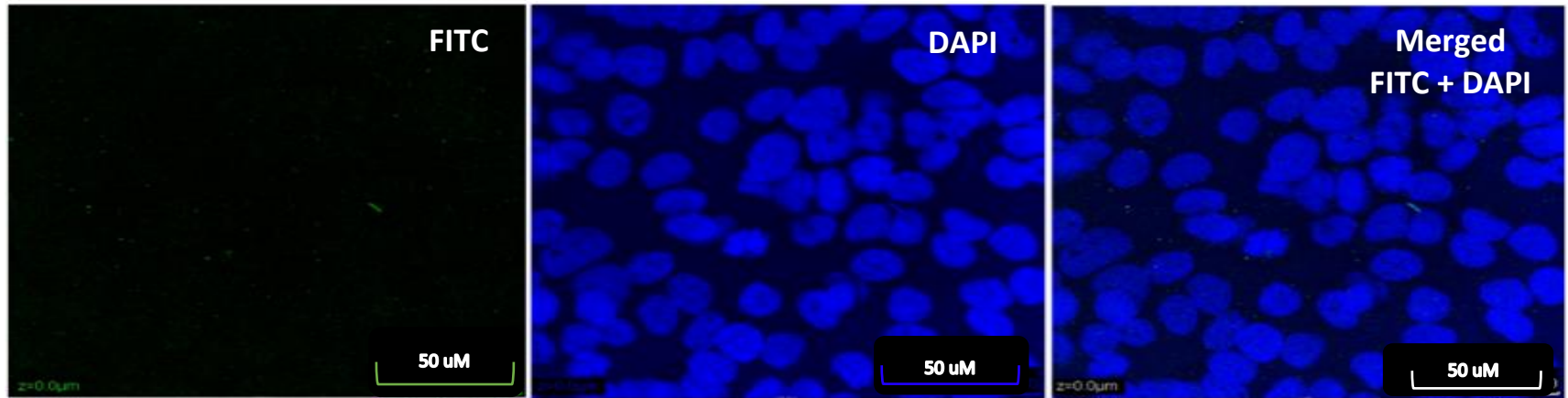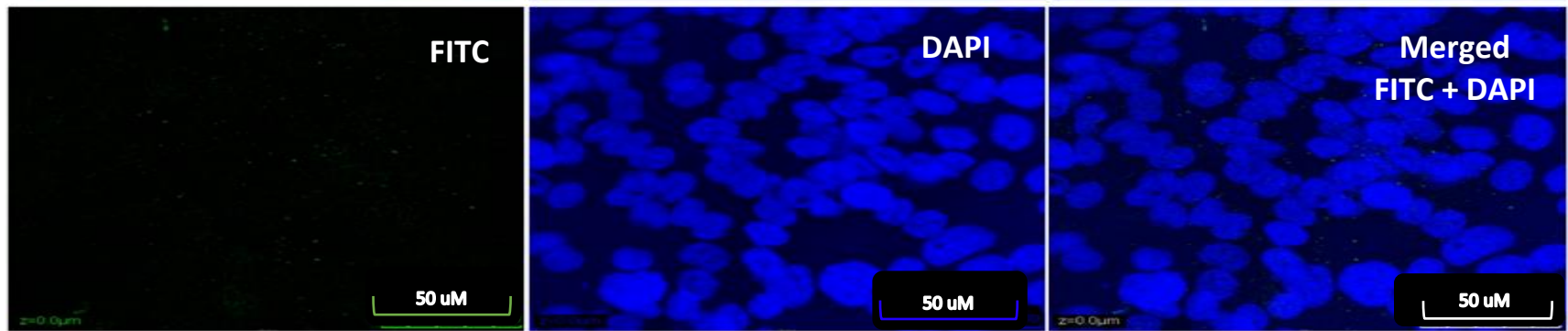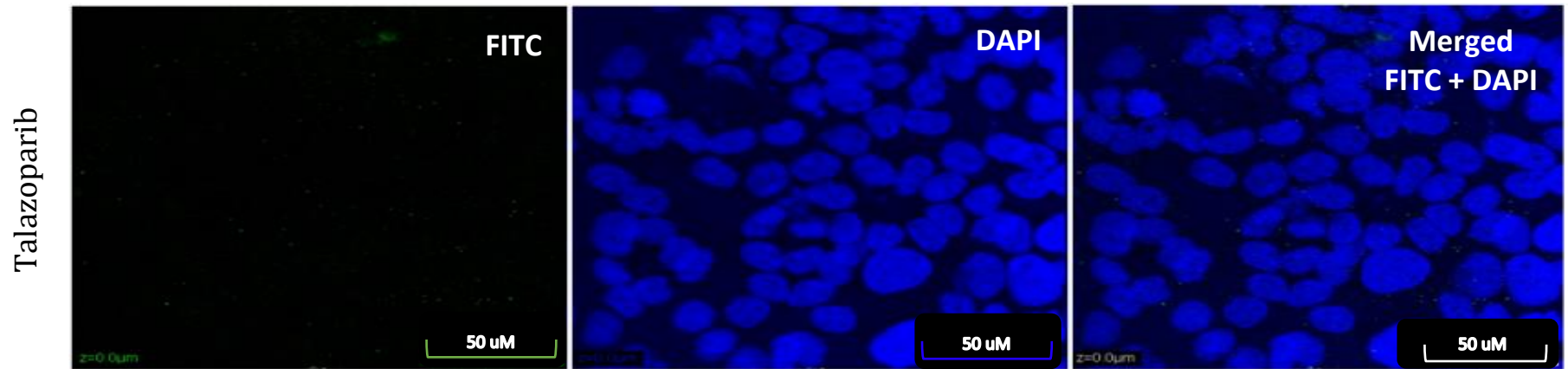
Figure3. 15 Confocal microscopic images of ROR1 expression stained with FITC (green) in SKOV-3 cell lines with drug treatments. Cells were counterstained with DAPI (blue) to show the localization of the nucleus. Images were captured at 10X magnification.

ROR1 expression was normalized to cell number in drug treated cells and all but cisplatin treated cells showed an increase in expression relative to control (untreated) cells. However, this was not a significant increase. Carboplatin treated cells showed a significant -2-fold decrease in ROR expression ($p < 0.05$) whereas taxol and talazoparib treated cells showed a significant ($p < 0.01$) -4 and -5-fold decrease respectively (Figure 3.16).
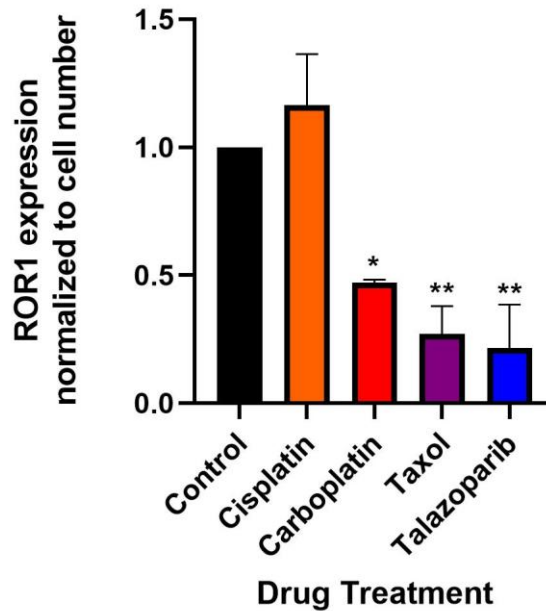
Figure3. 16 Measurement of ROR1 expression of drug treated SKOV-3 cells from confocal microscopy images. Intensity of ROR1 in drug treated cells measured relative to control untreated cells and normalized to cell number. A one sample t-test was carried out with '*' and '**' denotes statistical significance of $p < 0.05$ and $p < 0.01$ respectively.

Confocal images captured at a magnification of 10X below (Figure 3.17) show the ROR1 expression in OVCAR-3 control and drug treated cell line. The FITC label (green) indicates the ROR1 expression decreases upon drug treatment compared to the control.

Carboplatin | FITC | DAPI | Merged FITC + DAPI

Taxol | FITC | DAPI | Merged FITC + DAPI

50 uM
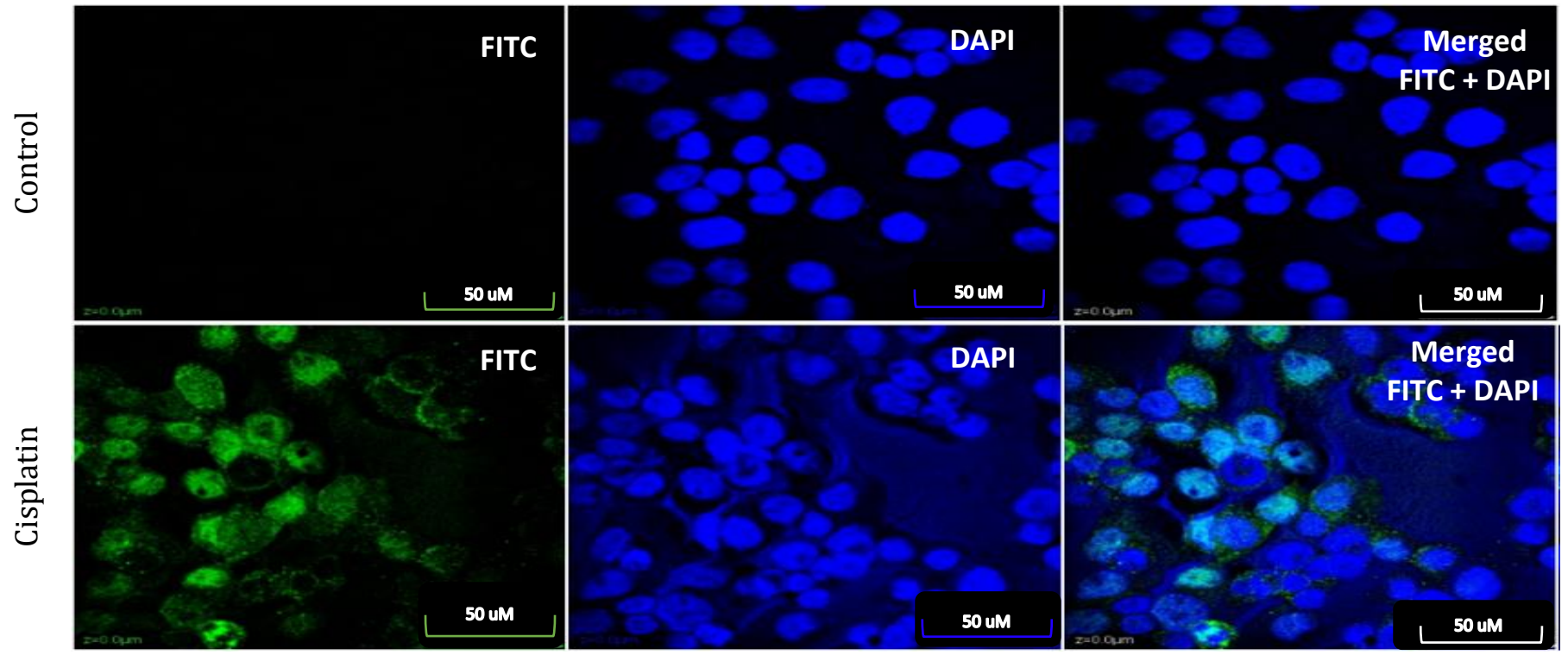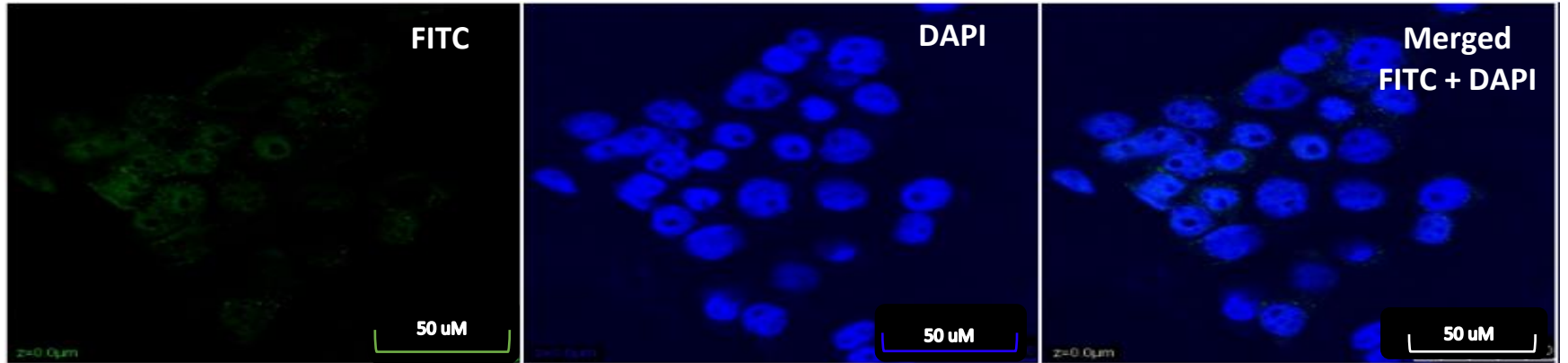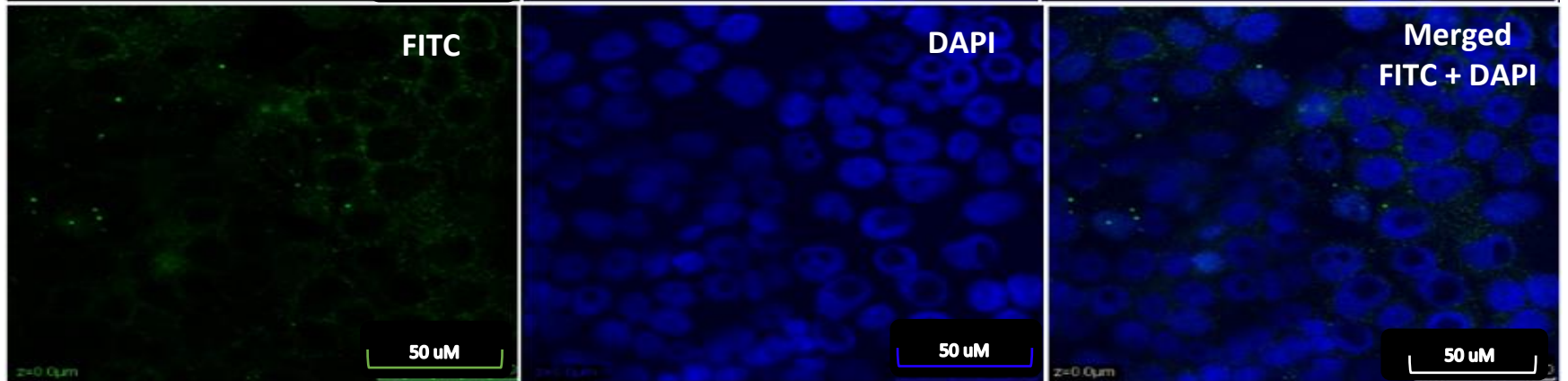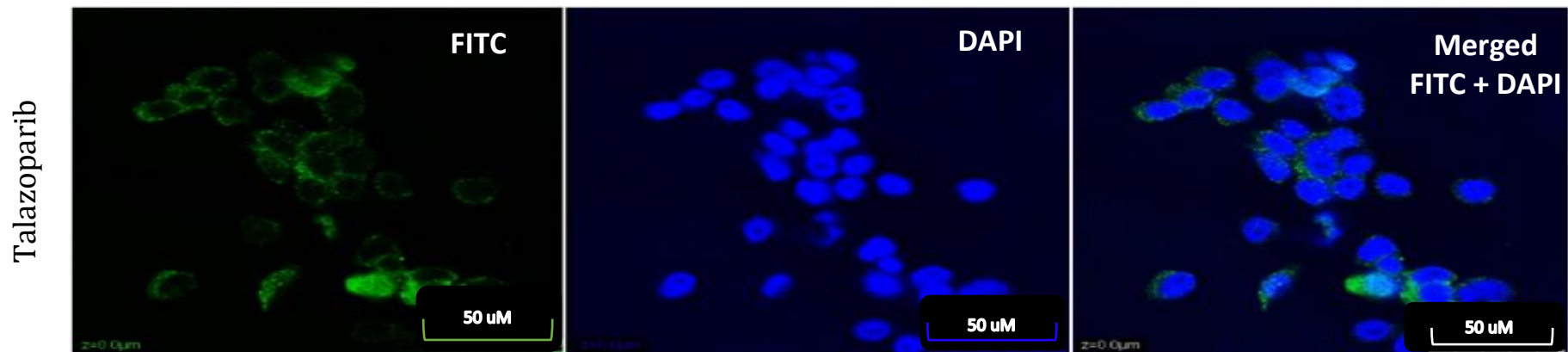
Figure3. 17 Confocal microscopic images of ROR1 expression stained with FITC (green) in OVCAR-3 cell lines with drug treatments. Cells were counterstained with DAPI (blue) to show the localization of the nucleus. Images were captured at 10X magnification.

ROR1 expression was normalized to cell number in drug treated cells. Cisplatin treated cells did not show any significant fold change in ROR1 expression compared to the control cells. All other drug treated cells showed a visible decrease however carboplatin and taxol treated cells showed a significant (p<0.01) -3-fold decrease in ROR1 expression. (Figure 3.18).
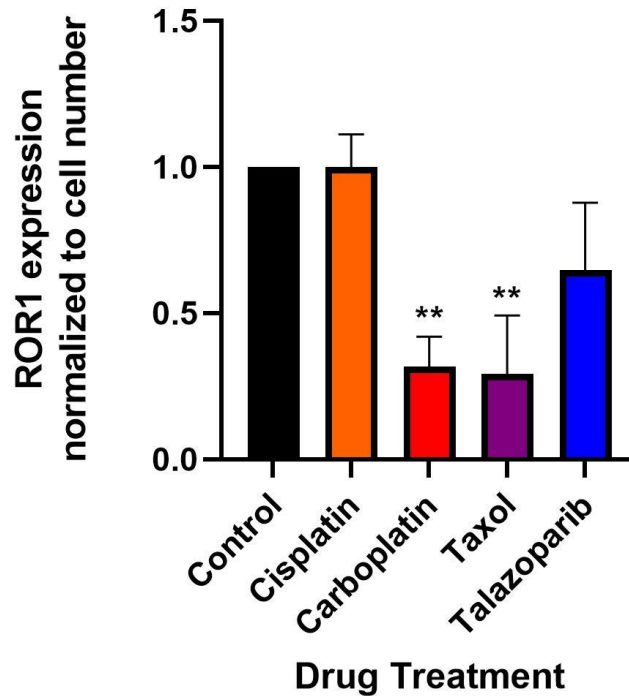
Figure3. 18 Measurement of ROR1 expression of drug treated OVCAR-3 cells from confocal microscopy images. Intensity of ROR1 in drug treated cells measured relative to control untreated cells and normalized to cell number. A one-sample t-test was carried out with '**' denotes statistical significance of p<0.01.

Confocal images captured at a magnification of 10X below (Figure 3.19) show the ROR1 expression in OAW42 control and drug treated cell line. The FITC label (green) indicates the ROR1 expression decreases upon drug treatment compared to the control.

Carboplatin

FITC · DAPI · Merged FITC + DAPI · 50 uM

Taxol

FITC · DAPI · Merged FITC + DAPI · 50 uM
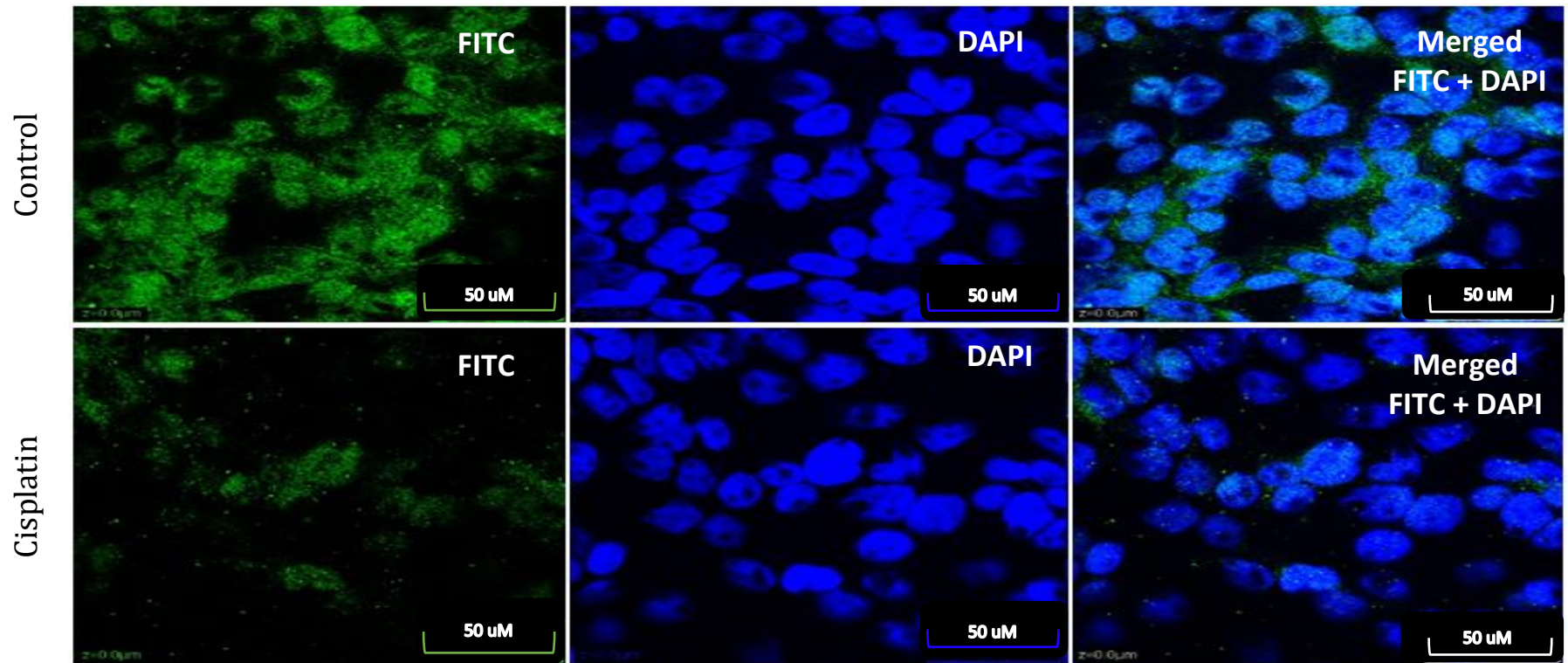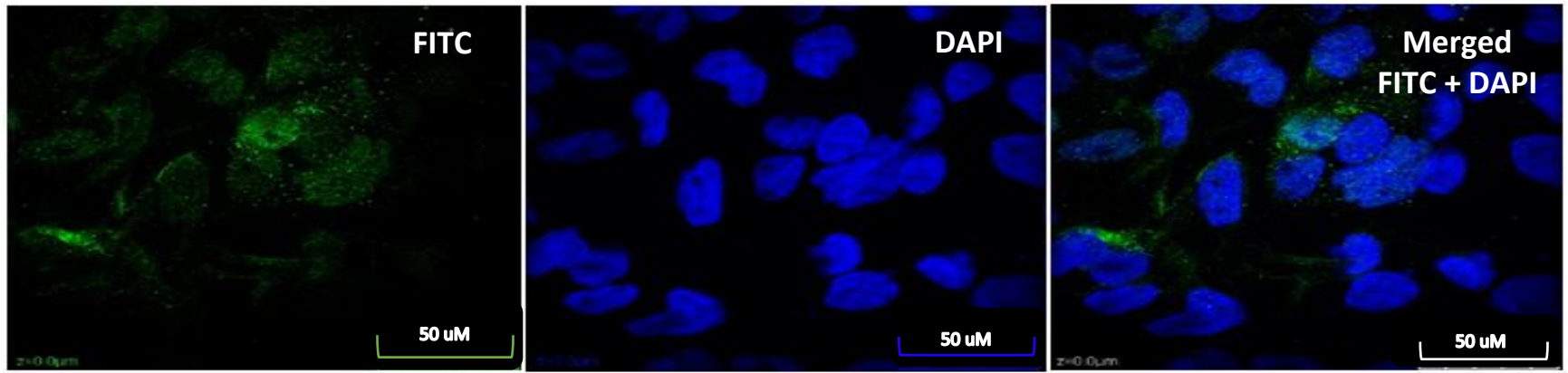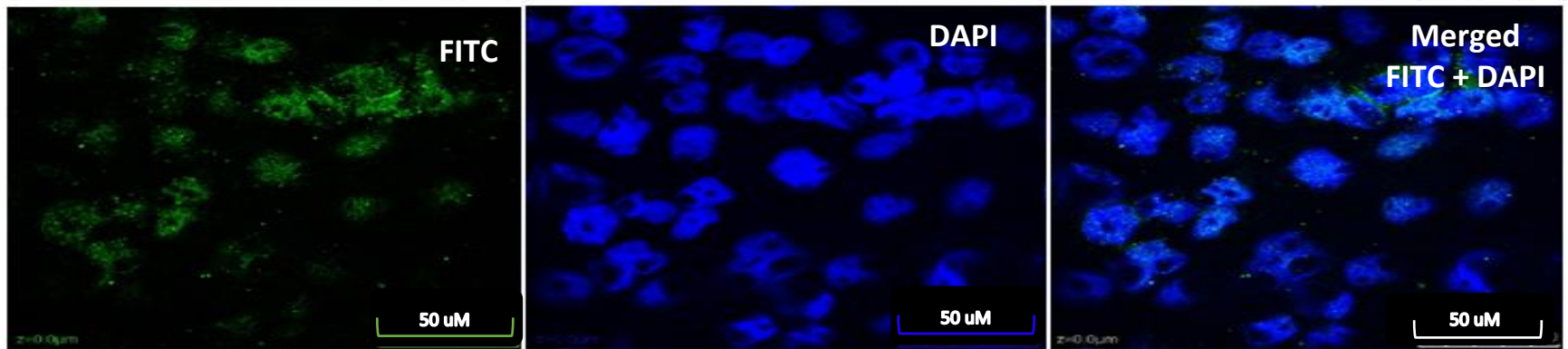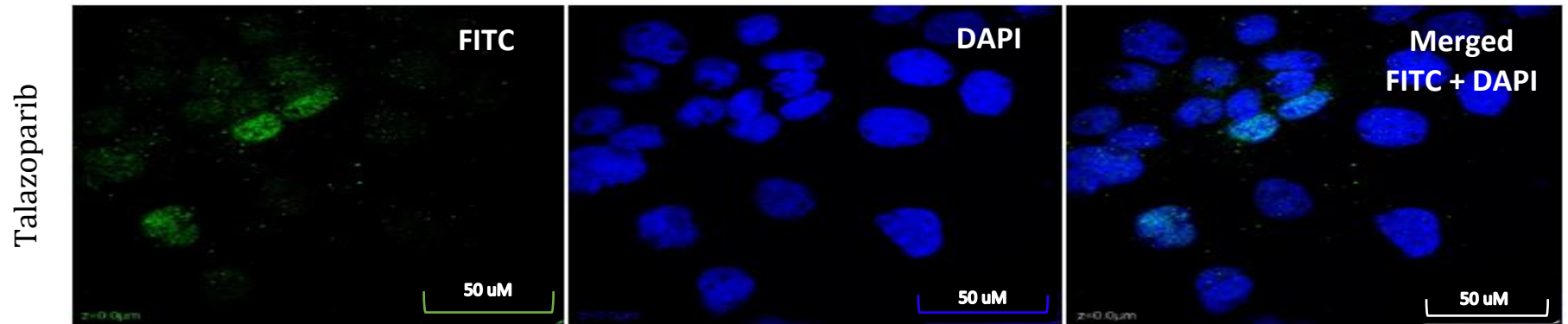
Figure3. 19 Confocal microscopic images of ROR1 expression stained with FITC (green) in OAW42 cell lines with drug treatments. Cells were counterstained with DAPI (blue) to show the localization of the nucleus. Images were captured at 10X magnification

ROR1 expression was normalized to cell number in drug treated cells. All drug treated cells expressed lower levels of ROR1 relative to the control untreated cells. Cells treated with cisplatin, taxol and talazoparib demonstrated a significant -3-fold decrease in ROR1 expression compered to control untreated cells (p<0.01). Although carboplatin treated cells showed a decrease (two-fold) in ROR1 expression it was not significant (Figure 3.20).
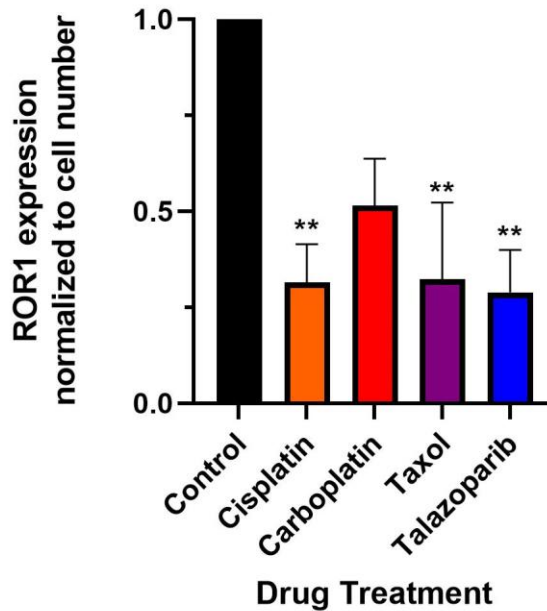
Figure3. 20 Measurement of ROR1 expression of drug treated OAW42 cells from confocal microscopy images. Intensity of ROR1 in drug treated cells measured relative to control untreated cells and normalized to cell number. A one sample t-test was carried out with '**' denotes statistical significance of p<0.01.

Confocal microscopy images of cells stained for ROR2 were not included as no fluorescence signal was detected. There are several factors that may have contributed to this however, further optimisations required to address this were not carried out due to constraints on time and resources (ROR2 antibody).

3.3.5 mRNA expression levels of EMT markers in the cell line panel

Results from the qPCR were as expected, cells lines with mesenchymal phenotype expressed higher levels of vimentin and N-cadherin while cell lines with epithelial phenotype expressed higher levels of E-cadherin. In figure 3.21 below the expression levels of the EMT markers Vimentin and N-Cadherin are represented relative to HEY cells which are of the mesenchymal phenotype (Prislei *et al*., 2015). The mRNA levels of EMT marker E-Cadherin is represented in the cell lines relative to OVCAR-3 which is of the epithelial phenotype (Yi *et al*., 2015). The results in the figure below demonstrate that expression of mesenchymal markers vimentin and N-cadherin is higher in SKOV-3 cells whereas there is a significant decrease in OVCAR-3 ($p<0.001$) and OAW42 ($p<0.05$) cells exhibiting a -3 and -2-fold decrease respectively. The epithelial marker E-cadherin was represented in the cell lines relative to OVCAR-3 as it possesses the epithelial phenotype as described in chapter 2 table 2.1 (Yi *et al*., 2015). Both HEY and SKOV-3 showed a significant decrease ($p<0.05$) in E-cadherin levels compared to OVCAR-3 cells with fold changes of -2 and -1.92 respectively.
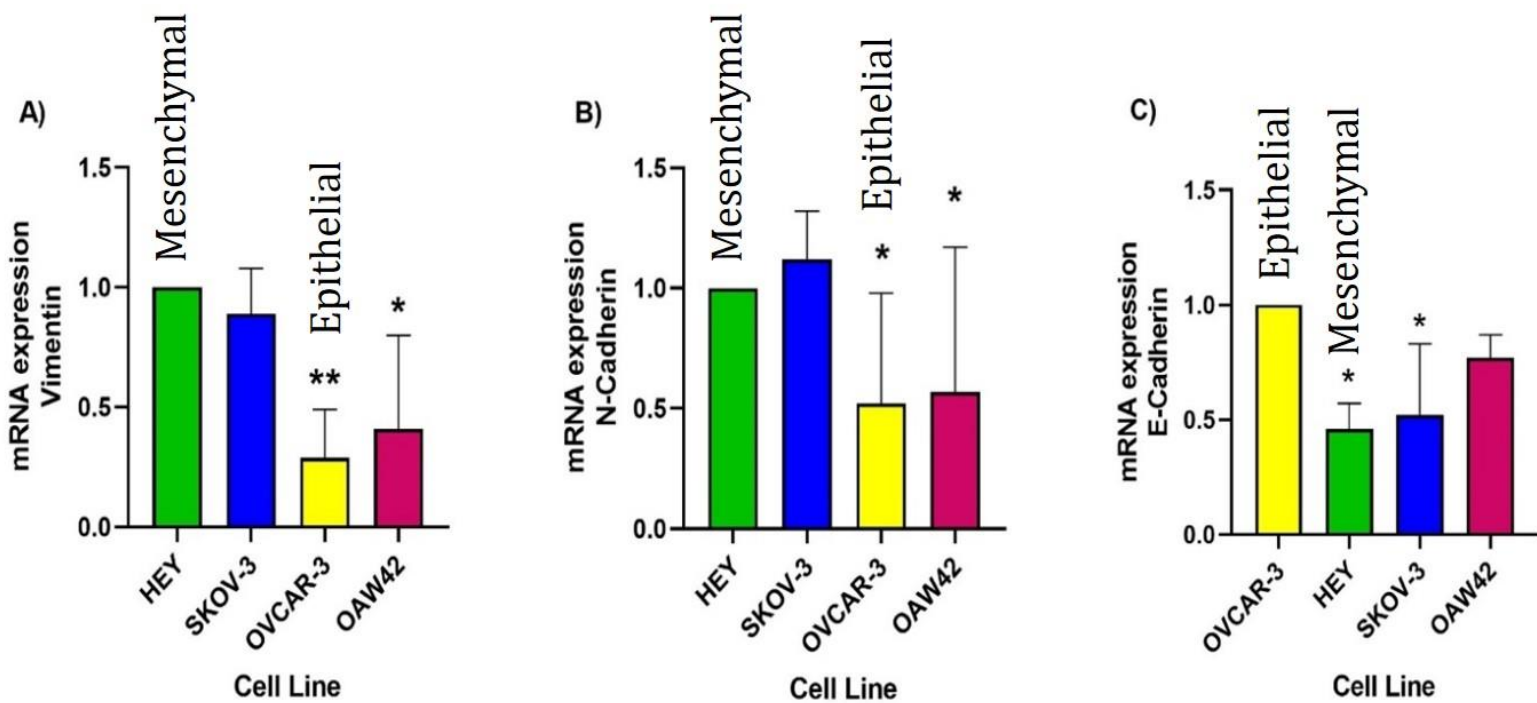
Figure3. 21 qPCR of EMT markers relative to resistant and sensitive cell line models. mRNA expression of (A) Vimentin, (B) N-Cadherin and (C) E-Cadherin in all the cell lines are represented relative to the mesenchymal model cells HEY (A and B) and epithelial model OVCAR-3 (C). Experiment repeats of n=3 was carried out and a one sample t-test was used with '*' and '**' denoting significance of $p<0.05$ and $p<0.001$ respectively.

The expression of each marker in drug treated cells is shown relative to the control (non-drug treated) cells in the figures below. The fold change through the drug treated cells vary across each marker gene. In the HEY cell line (figure 3.22) expression of the mesenchymal marker vimentin had a two-fold increase ($p<0.05$) with cisplatin treatment relative to the control. However, carboplatin, taxol and talazoparib treated cells showed no significant change in Vimentin expression. The mesenchymal marker N-Cadherin showed significantly ($p<0.05$) downregulated levels of -2 to 12-fold while the epithelial marker E-Cadherin showed significant downregulation ($p<0.001$) from -10 to 12-fold with drug treatment when compared to non-drug treated control.
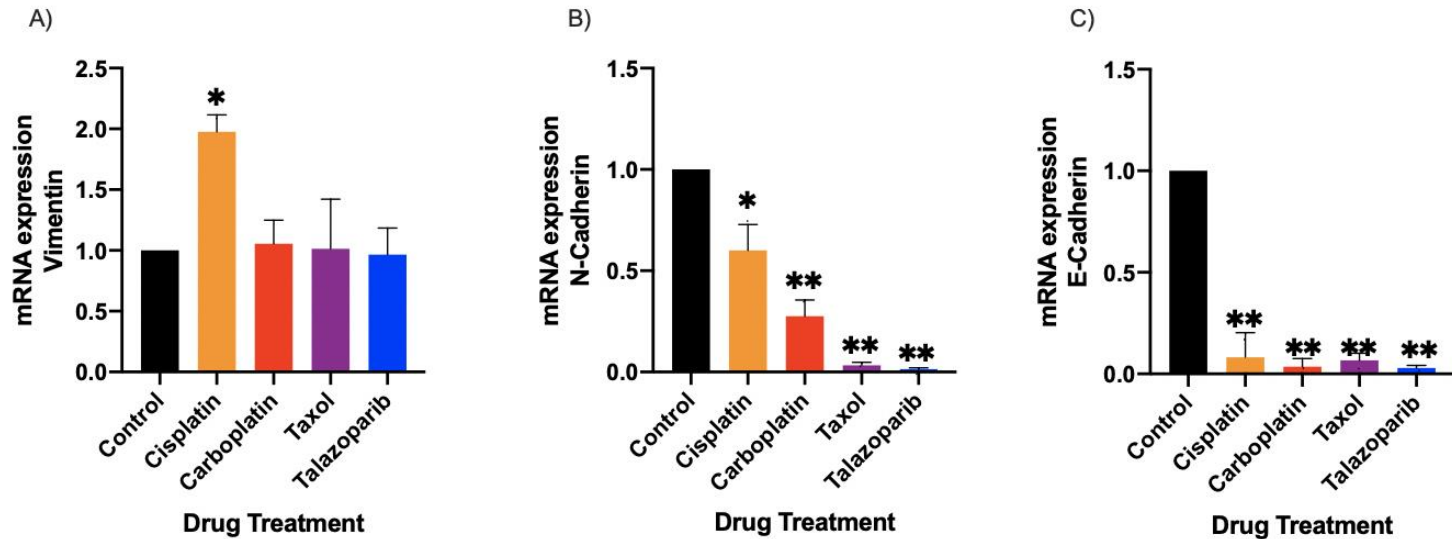
Figure3. 22 qPCR of EMT markers in HEY cells. Relative mRNA expression of A) Vimentin, B) N-Cadherin and C) E-Cadherin in HEY cell line treated with four drugs: cisplatin, carboplatin, taxol and talazoparib. Experiment repeats of n=3 was carried out. Cells treated with drugs are compared to their respective control (non-drug treated) to determine the fold change. Control cells set to a constant of 1.0 on the Y-axis relative to the control. A one sample t-test was used with '*' and '**' denoting significance of $p<0.05$ and $p<0.001$ respectively.

In the SKOV-3 cell line (figure 3.23) expression of the mesenchymal marker vimentin, although not significant had a -1 to -2-fold decrease with taxol and talazoparib treatment relative to the control. The cisplatin treated SKOV-3 cells however, had a significant increase (nearly two-fold) of Vimentin expression ($p < 0.05$) in comparison to its control whereas the carboplatin treated cells were consistent with the control cells. The mesenchymal marker N-Cadherin as well as epithelial marker E-Cadherin showed a significant decrease ($p < 0.05$) with drug treatment with fold changes ranging from -2 to -5-fold.
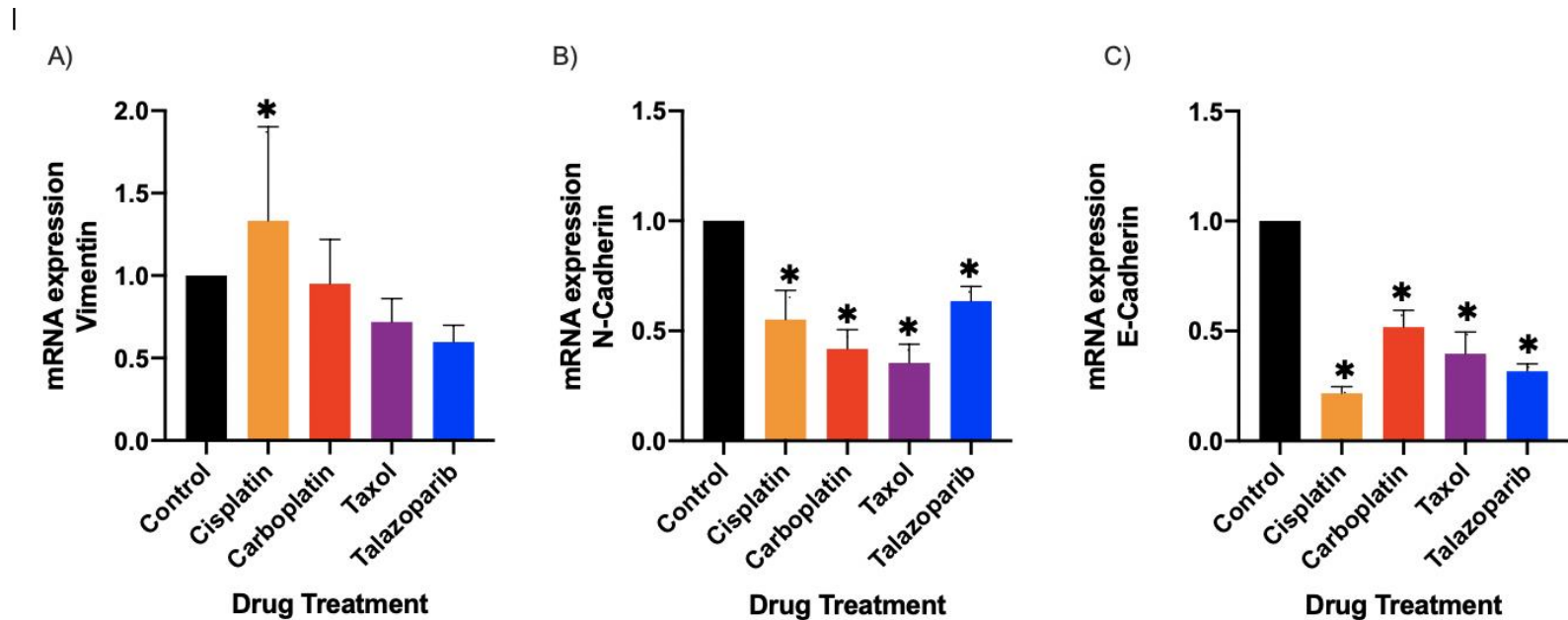
Figure3. 23 qPCR of EMT markers in SKOV-3 cells. Relative mRNA expression of A) Vimentin, B) N-Cadherin and C) E-Cadherin in SKOV-3 cell line treated with four drugs: cisplatin, carboplatin, taxol and talazoparib. Experiment repeats of n=3 was carried out. Cells treated with drugs are compared to their respective control (non-drug treated) to determine the fold change. Control cells set to a constant of 1.0 on the Y-axis relative to the control. A one sample t-test was used with '*' denoting significance of $p < 0.05$.

In the OVCAR-3 cell line (figure 3.24) expression of the mesenchymal marker vimentin significantly decreased ($p<0.05$) by -2 to -3-fold with drug treatment relative to the control. The mesenchymal marker N-Cadherin similarly decreased significantly ($p<0.05$) with drug treatment by -2 to -5-fold except in cisplatin treated cells. Interestingly, the epithelial marker E-Cadherin did not exhibit significant fold change in the drug treated cells compared to the control.
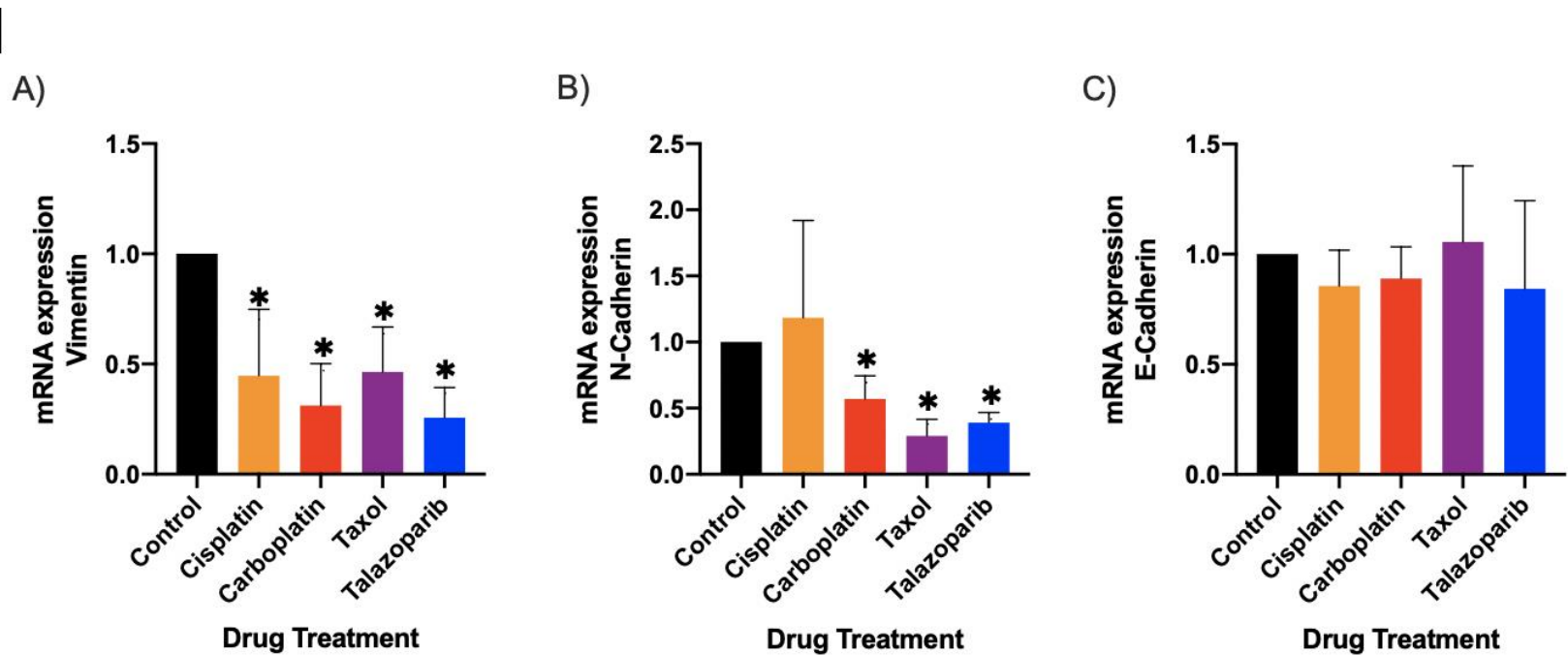
Figure3. 24 qPCR of EMT markers in OVCAR-3 cells. Relative mRNA expression of A) Vimentin, B) N-Cadherin and C) E-Cadherin in OVCAR-3 cell line treated with four drugs; cisplatin, carboplatin, taxol and talazoparib . Experiment repeats of n=3 was carried out. Cells treated with drugs are compared to their respective control (non-drug treated) to determine the fold change. Control cells set to a constant of 1.0 on the Y-axis relative to the control. A one sample t-test was used with '*' denoting significance of $p<0.05$.

In the OAW42 cell line (figure 3.25) expression of the mesenchymal markers; Vimentin and N-Cadherin as well as the epithelial marker E-cadherin was significantly decreased ($p < 0.05$, $p < 0.001$) with drug treatment relative to the respective control. The decrease ranged from -2 to -10-fold change in expression relative to the control.
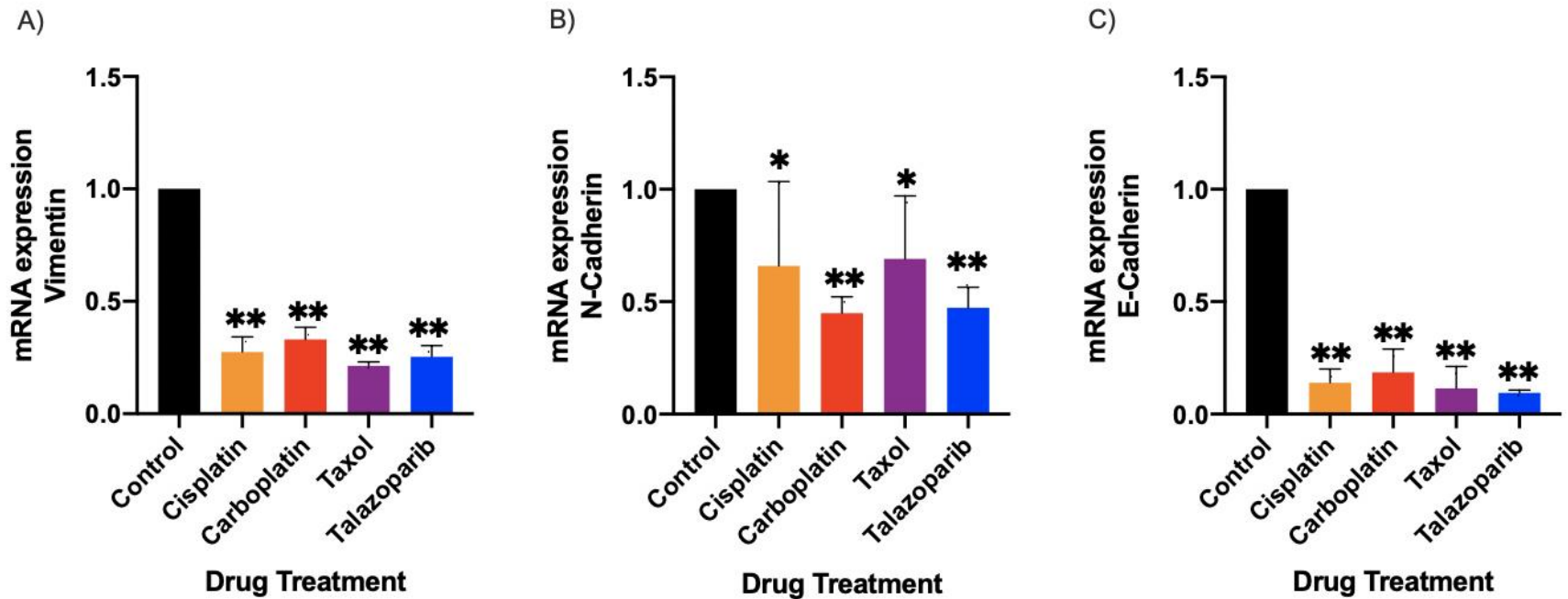
Figure3. 25 qPCR of EMT markers in OAW42 cells. Relative mRNA expression of A) Vimentin, B) N-Cadherin and C) E-Cadherin in OAW42 cell line treated with four drugs: cisplatin, carboplatin, taxol and talazoparib. Experiment repeats of n=3 was carried out. Cells treated with drugs are compared to their respective control (non-drug treated) to determine the fold change. Control cells set to a constant of 1.0 on the Y-axis relative to the control. A one sample t-test was used with '*' denoting significance of $p < 0.05$.

.

3.3.6 Cell invasion using collagen invasion assay

Invasion assays were carried out on the four cell lines to determine their invasiveness through an extracellular matrix (ECM). The bar graph below in figure 3.26 shows the percentage of invasion of each cells line. These percentages were determined by subtracting the reading of the blank wells (containing no cells) from each sample and then normalizing it to the control wells (containing no extracellular matrix).
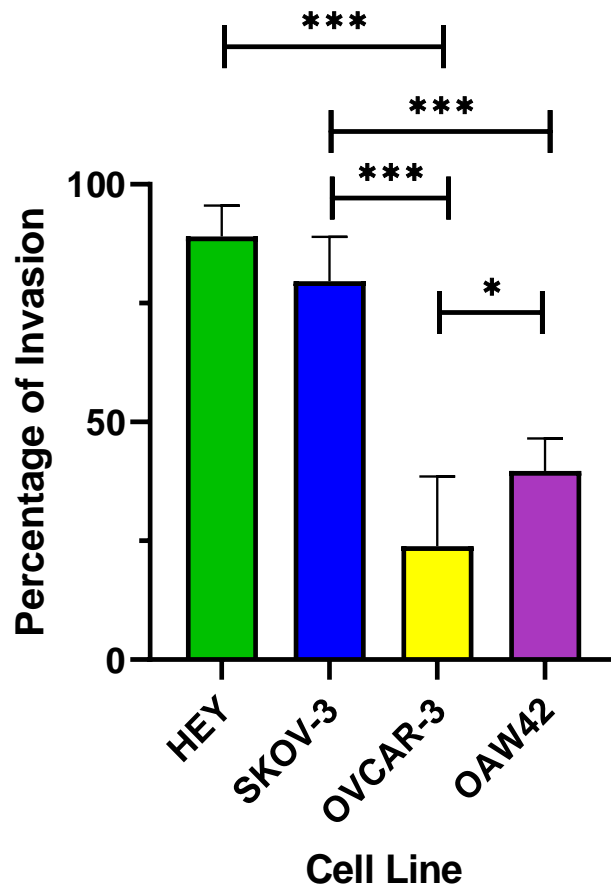
Figure3. 26 Invasion Assay of the four cell lines (n=3) show the varying degrees of invasiveness. The invasiveness of each cell line through an extracellular matrix was determined as described in chapter 2 section 2.1.8. The HEY cell line exhibits the highest percentage (89%) of invasion while OVCAR-3 shows the lowest (23%). A one-way ANOVA test comparing each cell line was carried out where '*' and '***' denotes statistical significance of $p < 0.05$ and $p < 0.001$ respectively. A post hoc analysis using Tukey's test was carried out.

The HEY cells demonstrated the highest percentage of invasion (89% ± 6.47 SD) in comparison to the other cell lines. SKOV-3 cells were a close second with a 79 % invasion. This was followed by the OAW42 cells and finally the OVCAR-3 cells with 40 and 24 percent invasion respectively. These results demonstrate that resistant cell lines are more invasive.

Interestingly, cell lines with increasing invasiveness also demonstrated a strong correlation with ROR1 expression. As shown in the figure 3.27 below, the resistant cell line HEY which has the highest concentration of ROR1 protein was the most invasive followed by SKOV-3 and OAW42, making OVCAR3 cell line which is the least resistant and with the lowest ROR1 protein concentration, the least invasive.
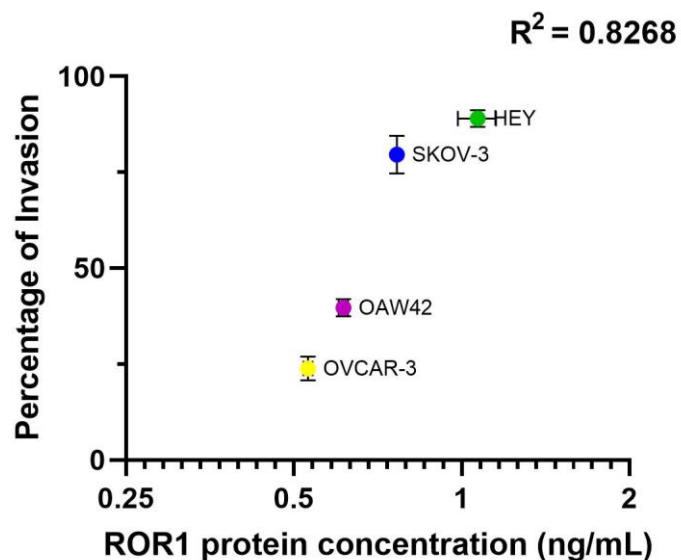
Figure3. 27 Correlation between cell invasiveness and ROR1 expression in the cell lines. A strong postitive association (R^2 = 0.8268) was observed between the invasion profile and ROR1 protein expression of the four cells lines. The x axis is in a log 10 scale and represents the protein concentration of ROR1 obtained from an ELISA (described in section 3.3.4.2). The y axis represents the percentage of invasion obtained from the invasion assay (described in section 3.3.6) The resistant cell line HEY with the highest ROR1 expression was the most invasive while the sensitive cell line OVCAR-3 with the lowest ROR1 expression was the least invasive.

3.3.7 siRNA Knockdown

Prior to investigating the effect of ROR1 knockdown on chemotherapy drug induced viability, the knockdown method was first optimised using the housekeeping gene GAPDH.

3.3.7.1 Optimisation of siRNA reverse transfection using GAPDH

The siRNA reverse transfection protocol was optimised using siRNA of the housekeeping gene GPADH. Based on a previously optimised experiment (unpublished) a concentration of 30nM siRNA was used to knockdown the GAPDH gene. Two time points were also observed for the most efficient knockdown: 72 hours and 120 hours.

Figure 3.28 below shows significant knockdown of GAPDH at the mRNA level using qPCR in the drug resistant cell line HEY (A) and in drug sensitive cell line OVCAR-3 (B). In the qPCR assay the Scramble and GAPDH knockdown cells were normalised to the non-transfected (NT) control. GAPDH is significantly ($p<0.001$) knocked down (97 % and 90% respectively) at both time points for both cell lines. However, in the OVCAR-3 cell line at 120 hours there was a significant increase ($p<0.05$) in GAPDH in the scramble compared to the non-transfected control.
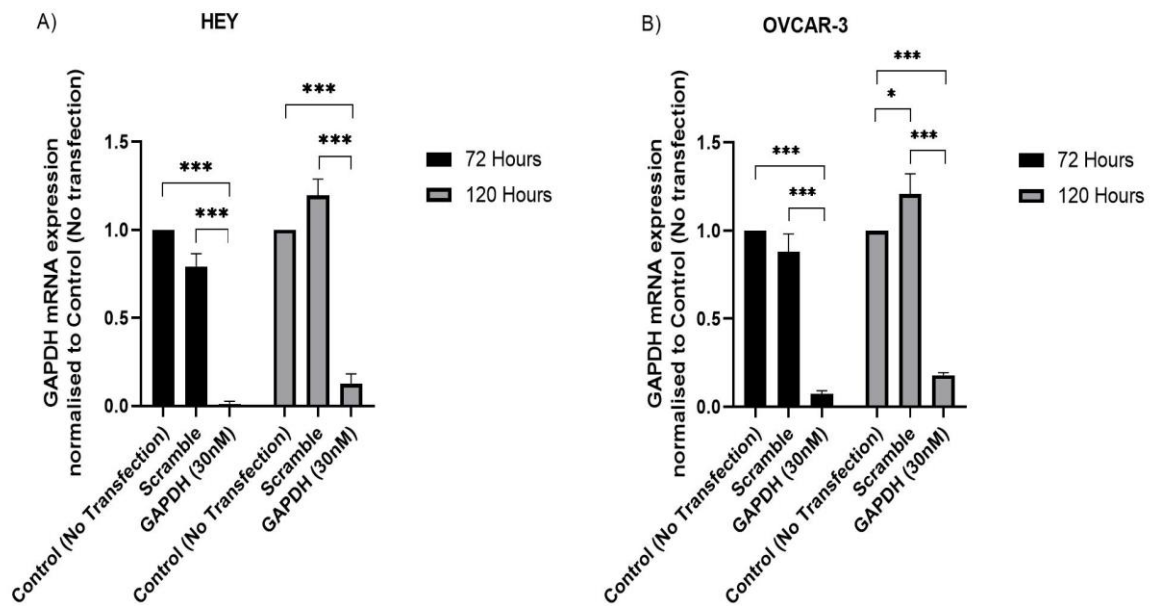
Figure3. 28 qPCR assay showing siRNA knockdown of GAPDH. The graph above shows siRNA dose of 30nM transfected into HEY cells (A) and OVCAR-3 (B) at two different time points as detailed in section 3.2.1.1. Experiment replicates of n=3 was carried out for reproducibility. A qPCR experiment was then carried out to assess mRNA expression at 72- and 120-hours. A two-sample t-test comparing the GAPDH expression to its non-transfected and scramble control at the respective time points was carried out where '*' and '***'denotes statistical significance of $p < 0.001$.

The figure 3.29 below shows western blots carried out to validate knockdown of GAPDH at the protein level. In the HEY cells (A), knockdown (75%) appeared to be effective at 72 hours. In the OVCAR-3 cell line (B) a similar knockdown (82%) effect was observed at 72 hours compared to knockdown at 120 hours.
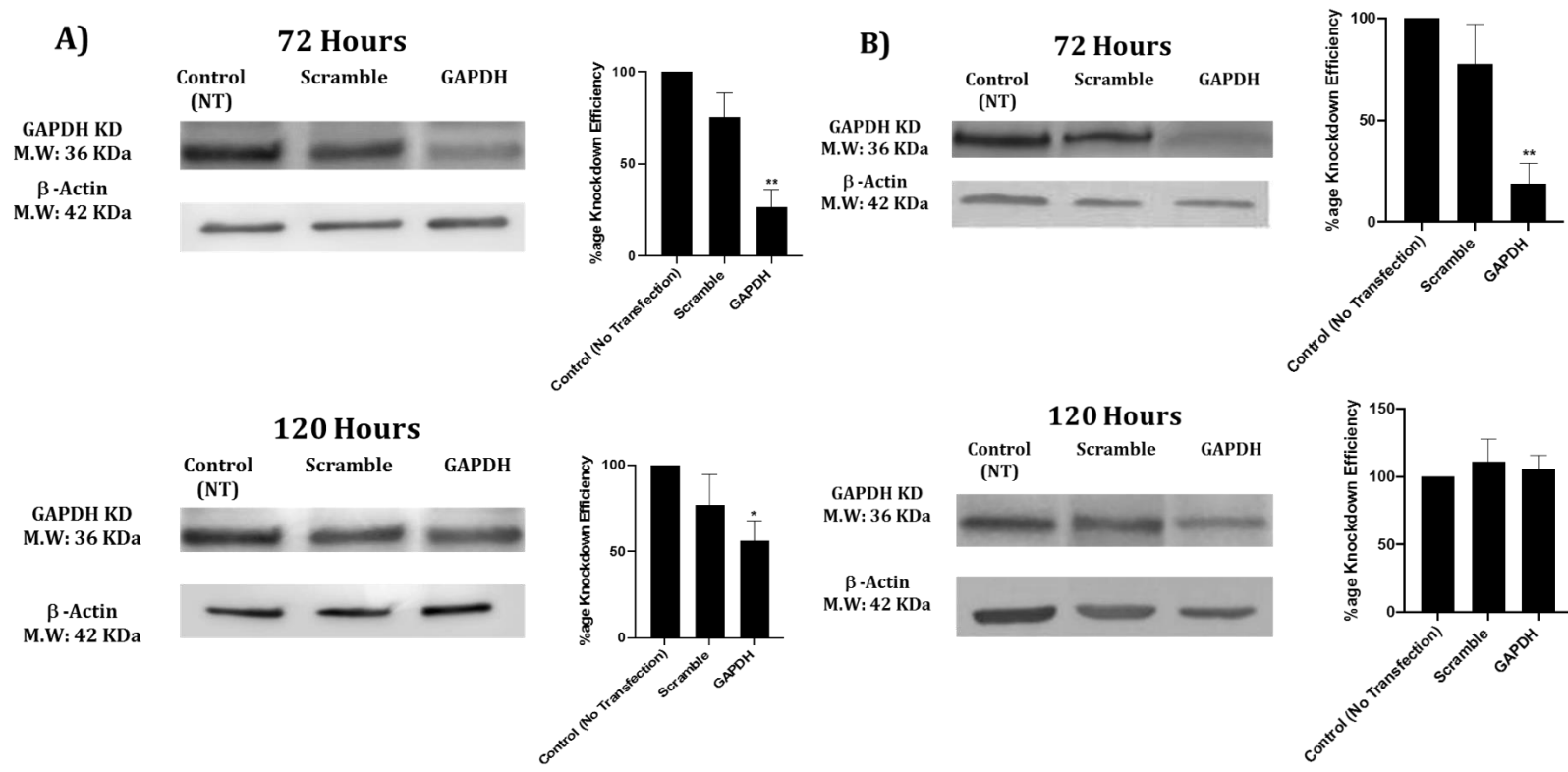
Figure3. 29 Western blots showing siRNA knockdown of GAPDH (n =1). The blots are representative of three individual experiments. The blots above show knockdown of GAPDH in (A) HEY cells and (B) OVCAR-3 at two different time points as detailed in section 3.2.1.1. Western blot was carried out to assess protein expression at 72 and 120-hours. The western blot experiments show effective knockdown at 72 hours. The housekeeping gene beta-Actin was used as a loading control. Percentage knockdown represented as graph on right side of each blot. A one sample t-test comparing the GAPDH knockdown to the respective no transfection control was carried out where '*' and '**'denotes statistical significance of $p<0.05$ and $p<0.01$ respectively.

.

3.3.7.1.1 Effect of GAPDH knock down on cell growth

3.3.7.1.1.1 HEY cell line

Cell counts were carried out at 72 and 120 hours to determine if transfection affected viability of the cells. This is to ensure that the knockdown effects observed was not due to loss of cells upon siRNA transfection but in fact a successful knockdown. Replicate counts were recorded, averaged and plotted in the graph shown in the figure 3.30. At 72 hours no significant difference in cell number was found between the non-transfected control, scramble and GAPDH knockdown cells. However, at 120 hours, a significant decrease of almost 20% in cell number was observed in the GAPDH knockdown cells when compared to its respective scramble ($p < 0.05$) and non-transfected control cells ($p < 0.01$).
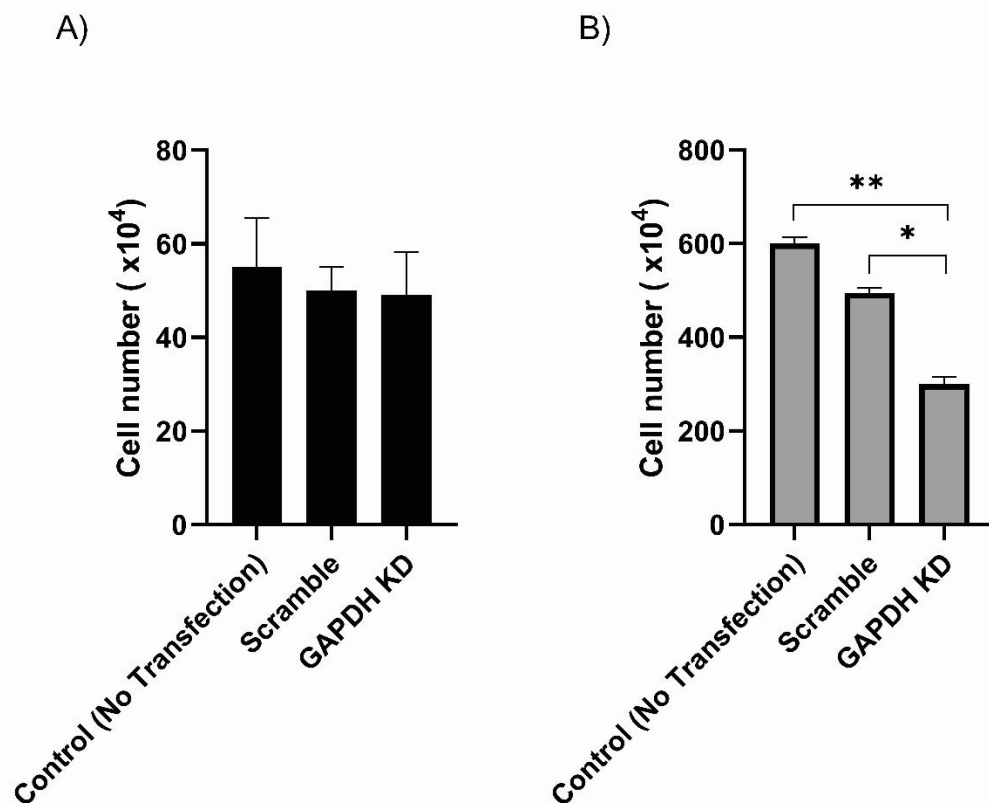
Figure3. 30 HEY cell counts post transfection at different time points. The graphs show cell counts of HEY cell line post siRNA at (A) 72 hours and (B) 120 hours. Cells were counted as described in chapter 2 section 2.1.3. Experiment replicates of n=3 was carried out for reproducibility. A two-sample t-test-test comparing cell counts between each group was carried out where '*' and '**'denotes statistical significance of $p < 0.05$ and $p < 0.01$ respectively.

KD: Knockdown

3.3.7.1.1.2 OVCAR-3 cell line

The cell number in OVCAR-3 cells (Figure 3.30) at 72 hours did not show any significant change. At 120 hours there was a significant 45% decrease (p<0.05) in GAPDH knockdown cells when compared to the non-transfected control.
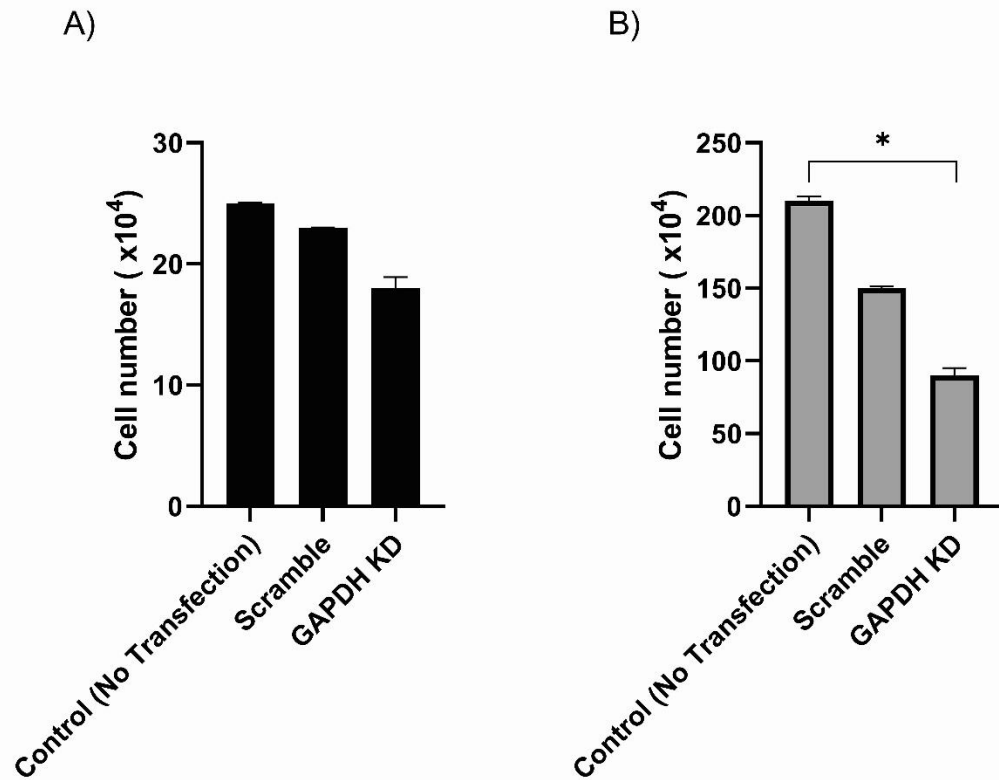
Figure3. 31 OVCAR-3 cell counts post transfection at different time points. The graphs show cell counts of OVCAR-3 cell line post siRNA at (A) 72 hours and (B) 120 hours. Cells were counted as described in chapter 2 section 2.1.3. Experiment replicates of n=3 was carried out for reproducibility. A two-sample t-test-test comparing cell counts between each group was carried out where '*'denotes statistical significance of p<0.05.

KD: Knockdown

The optimisation experiments reveal that knockdown of GAPDH using 30nM is effective at both time points when observed at the mRNA level. However, western blot experiments suggest knockdown is most effective at 72 hours in both the HEY and OVCR-3 cell lines. It is also worth noting that at 120 hours the change in cell number suggests that transfection may affect cell viability which has been taken into account while optimising knockdown in the following section for ROR1 and ROR2 where varying siRNA concentrations are used.

3.3.7.2 ROR1 and ROR2 knockdown using siRNA reverse transfection

3.3.7.2.1 Optimisation of knock down time points: HEY cell line

In the cisplatin-resistant cell line, HEY, knockdown experiments were carried out by transfecting varying siRNA concentrations (10nM, 30nM and 50nM) and Lipofectamine complex into the cells grown in T-25 flasks. Since GAPDH knockdown was optimised using 30nM of siRNA, a lower (10nM) and higher (50nM) concentration limit was selected to establish a more optimised siRNA concentration. Knockdown effects were then detected using qPCR to measure the relative expression levels of ROR1 and ROR2 to their respective scramble controls. Knockdown of ROR1 was observed to be most effective with a -17-fold decrease (p<0.001) when transfected with 50nM of siRNA at 72 hours. The knockdown of ROR2 was best observed at 72 hours with an siRNA concentration of 10nM for a maximal knockdown effect resulting in a -5-fold decrease (Figure.3.32).

The effect of knockdown at 72 hours was marginally higher than 120 hours for all siRNA concentrations. Although effects were statistically significant at 120 hours, the desired effect was achieved at shortest time point of 72 hours. Therefore 72 hours was considered the optimal time point.

A)
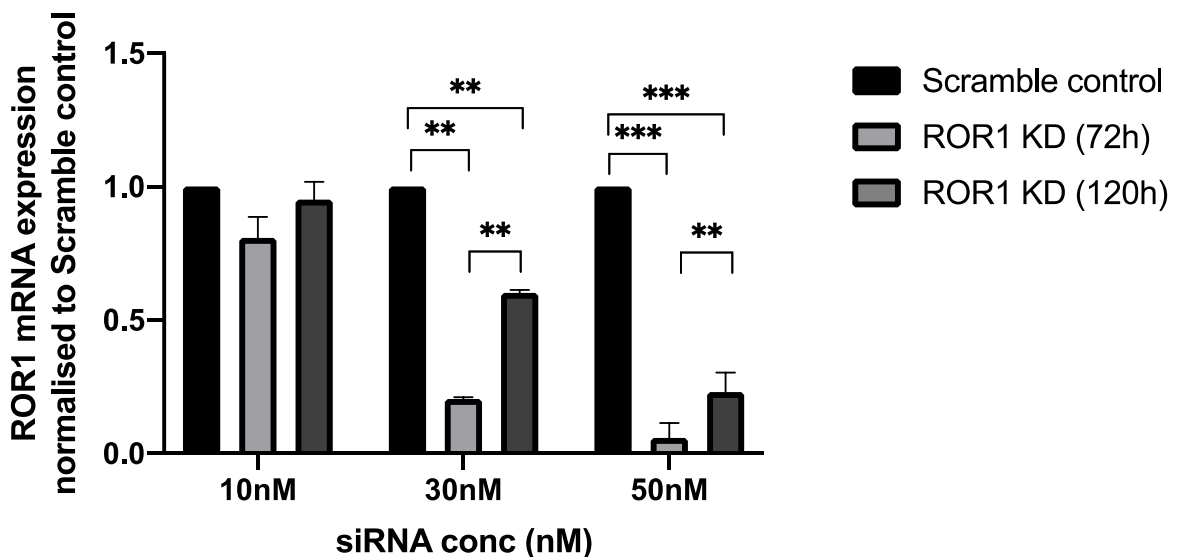
B)
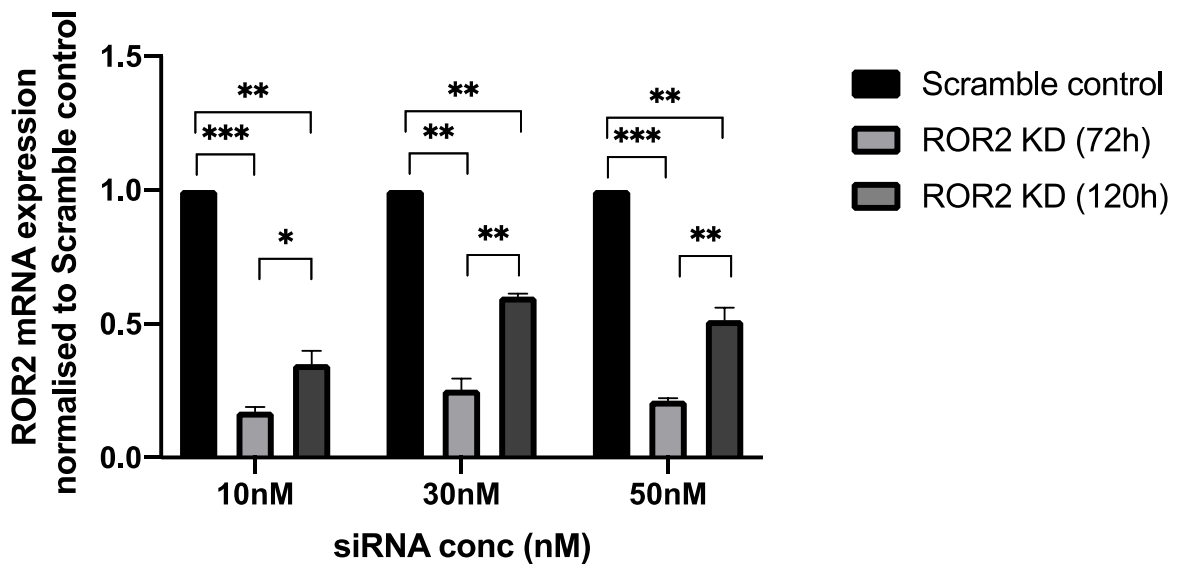
Figure3. 32 siRNA knockdown of ROR1 and ROR2 at different concentrations in HEY cells.
The graph above shows siRNA dose ranges transfected into HEY cells at two different time points
as detailed in section 3.2.1.2. Experiment replicates of n=3 was carried out for reproducibility. A
qPCR experiment (Section 3.2.1.2.5) was then carried out to assess mRNA expression in single A)
Knockdown of ROR1 at varying (10nM, 30nM and 50nM) siRNA concentration at 72- and 120-
hours B) Knockdown of ROR2 at varying (10nM, 30nM and 50nM) siRNA concentration at 72- and
120-hours. A two-sample t-test comparing the siRNA doses to their respective scramble control was
carried out where '*', '**' and '***'denotes statistical significance of $p<0.05$, $p<0.01$ and $p<0.001$
respectively. KD: Knockdown

The knockdowns were further confirmed by protein expression from western blots shown in
the below figure 3.33. Knockdown effects at protein level were consistent with mRNA
expression levels. ROR1 and ROR2 knockdown in HEY cell lines were observed using
Western blots. Optimal knockdown effect was detected at 72 hours with 50nM (80%) and
10nM (70%) siRNA concentration respectively
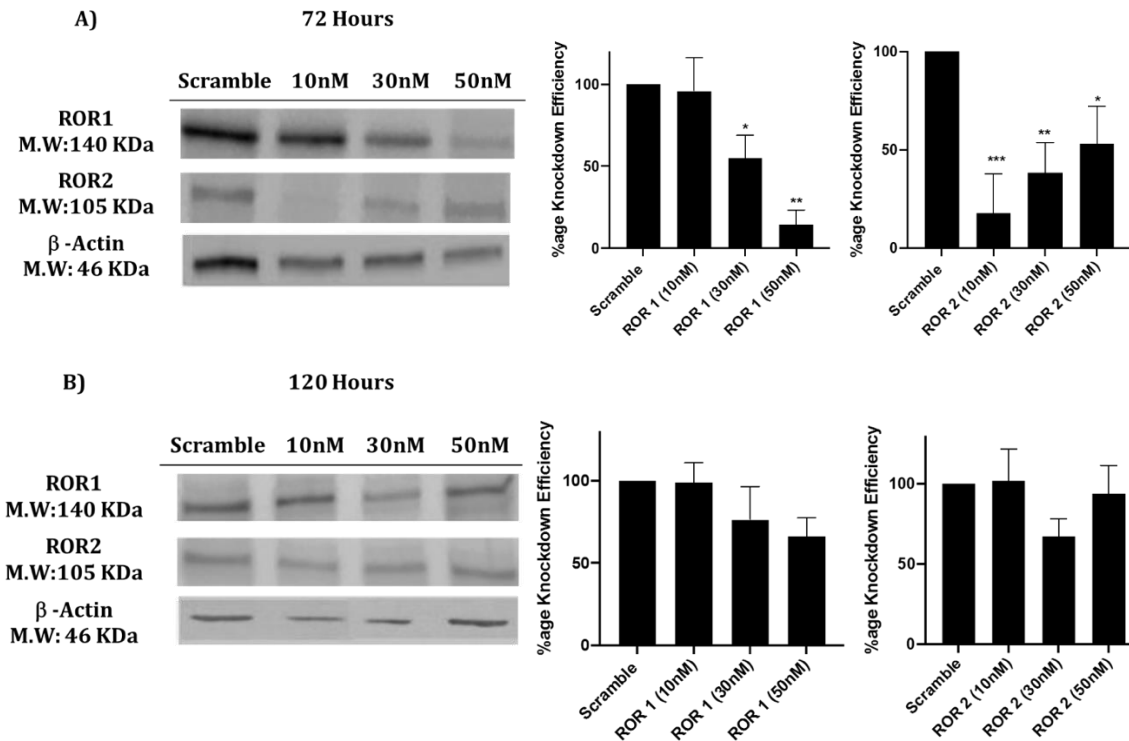
Figure3. 33 siRNA knockdown of ROR1 and ROR2 at different concentrations in HEY cells (n=1). The blots are representative of three individual experiments Blots reflect protein expression of ROR1 and ROR2 knockdown in siRNA transfected HEY cells. Left panel: A) ROR1 and ROR2 knockdown at 72 hours. Right panel: B) ROR1 and ROR2 knockdown at 120 hours. In each panel, top row ROR1 knockdown, middle row ROR2 knockdown, bottom row beta-actin (loading control). At the right of each blot is the graph showing percentage knockdown of each siRNA concentration relative to the scramble. A one sample t-test comparing the siRNA doses to their respective scramble control was carried out where '*' and '**'denotes statistical significance of $p < 0.05$ and $p < 0.01$ respectively.

Upon determining the optimal siRNA concentration for ROR1 and ROR2 knockdown, a double knockdown with these siRNA concentrations was also carried out as shown figure 3.34 below. A -12-fold and -5-fold decrease in ROR1 and ROR2 respectively was observed showing double knockdown was most effective compared to singular knockdown of ROR1 and ROR2.
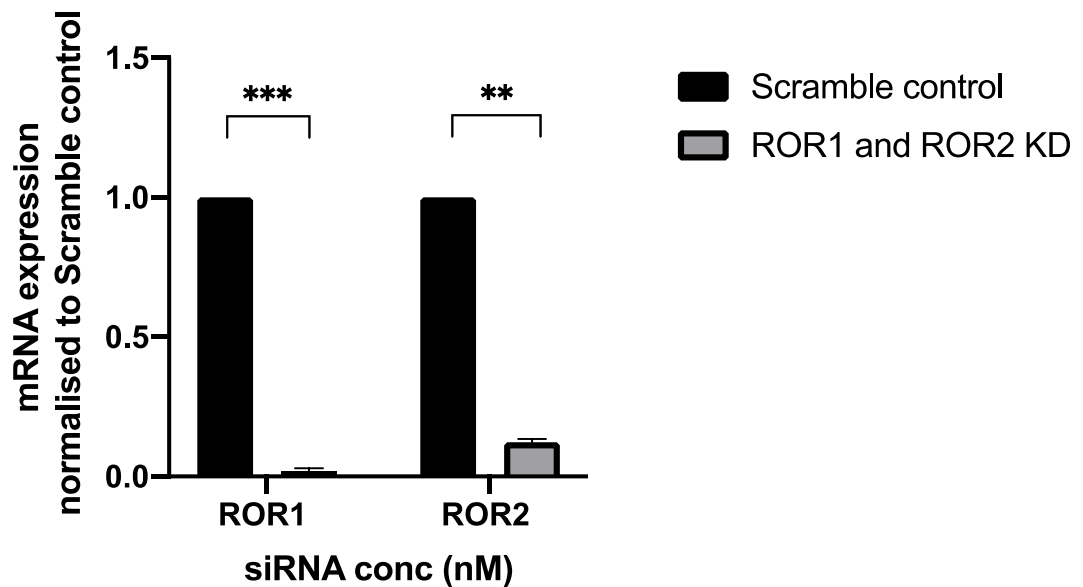
Figure3. 34 Double siRNA knockdown of ROR1 and ROR2 in HEY cells. Knockdown was carried out at optimal siRNA concentrations of ROR1 and ROR2 at optimal time point simultaneously as determined above. Optimal siRNA concentration of 50nM for ROR1 and 10nM for ROR2 was used to carry out the double knockdown experiment at 72 hours. Experiment replicates of n=3 was carried out for reproducibility. A one sample t-test comparing ROR1 and ROR2 knockdown to their respective scramble control was carried out where '**' and '***'denotes statistical significance of $p<0.01$ and $p<0.001$ respectively.

KD: Knockdown

Using western blots, double knockdown effect of ROR1 and ROR2 was observed as shown in the figure 3.35 below. Percentage knockdown of ROR1 and ROR2 compared to the control was 97% and 90% respectively.
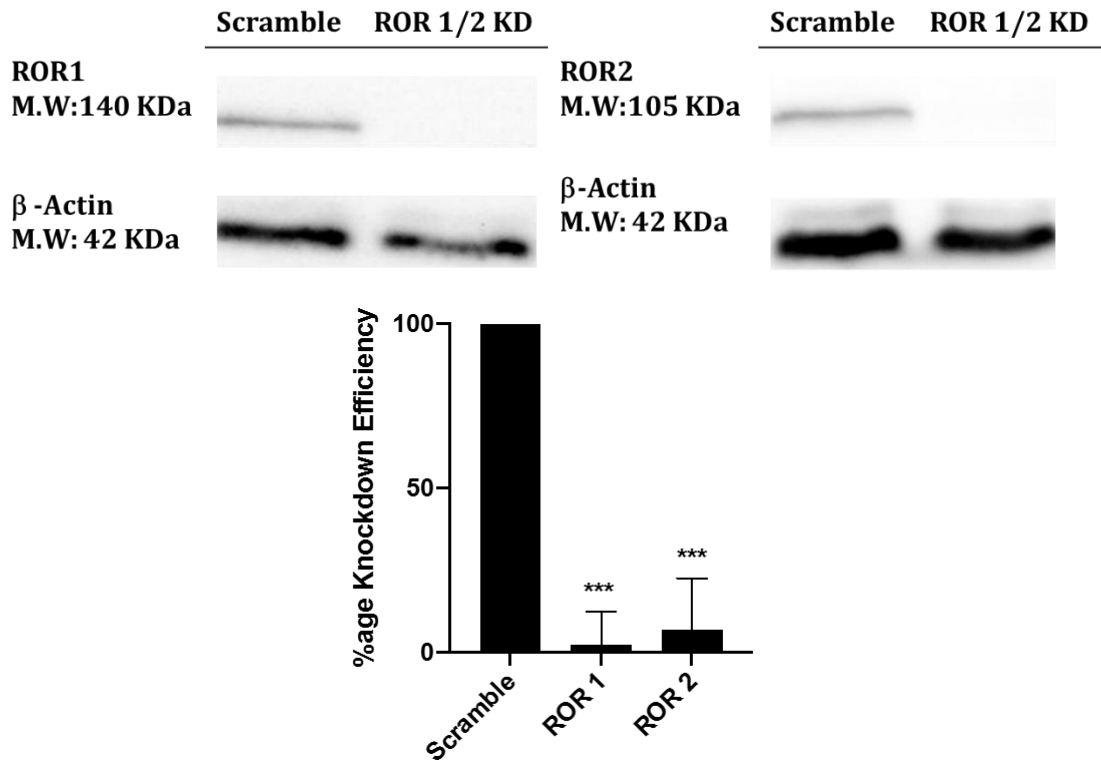
Figure3. 35 Double siRNA knockdown of ROR1 and ROR2 in HEY cells (n=1). The blots are representative of three individual experiments. Simultaneous knockdown was carried out using optimal siRNA concentration of 50nM for ROR1 and 10nM for ROR2 at 72 hours as described in section 3.2.1.2.2. The percentage of knockdown efficiency was graphed as shown at the bottom of both blots. A one sample t-test comparing ROR1 and ROR2 knockdown to their respective scramble control was carried out where '**' and '***'denotes statistical significance of $p<0.01$ and $p<0.001$ respectively.

KD: Knockdown

3.3.7.2.2 Optimisation of knock down time points: OVCAR- 3 cell line

Knockdown experiments were also carried out in the cisplatin sensitive cell line OVCAR-3 in T-25 flasks. Similar to the transfection protocol carried out with the HEY cell line, varying concentrations of siRNA (10nM, 30nM and 50nM) in a Lipofectamine complex were transfected to determine the dose producing significant ROR1 and ROR2 knockdown. Using qPCR, the relative expression of ROR1 and ROR2 to their respective scramble siRNA was analysed (Figure 3.36). Interestingly, the optimal dose for ROR1 knockdown in OVCAR-3 cells was the same as that observed in the HEY cell line (50nM of siRNA, $p<0.001$). However, effective ROR2 knockdown (-10-fold decrease compared to the scramble) required a lower concentration of siRNA; 10nM ($p<0.001$). The time point with the maximal knockdown effect was at 72 hours for both cases.

A)
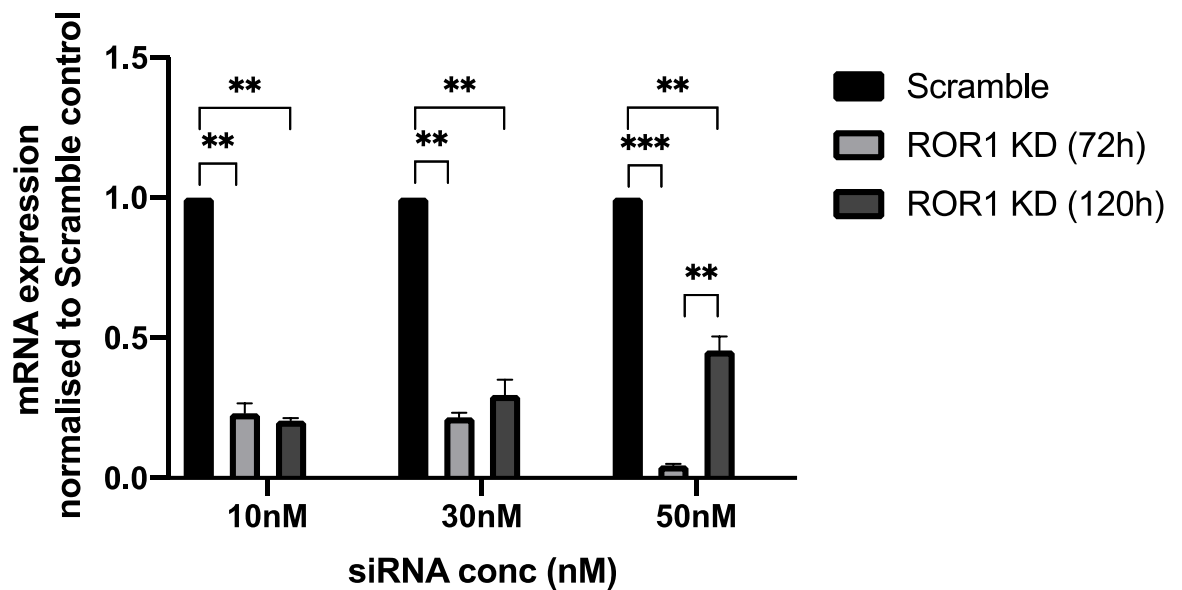
B)
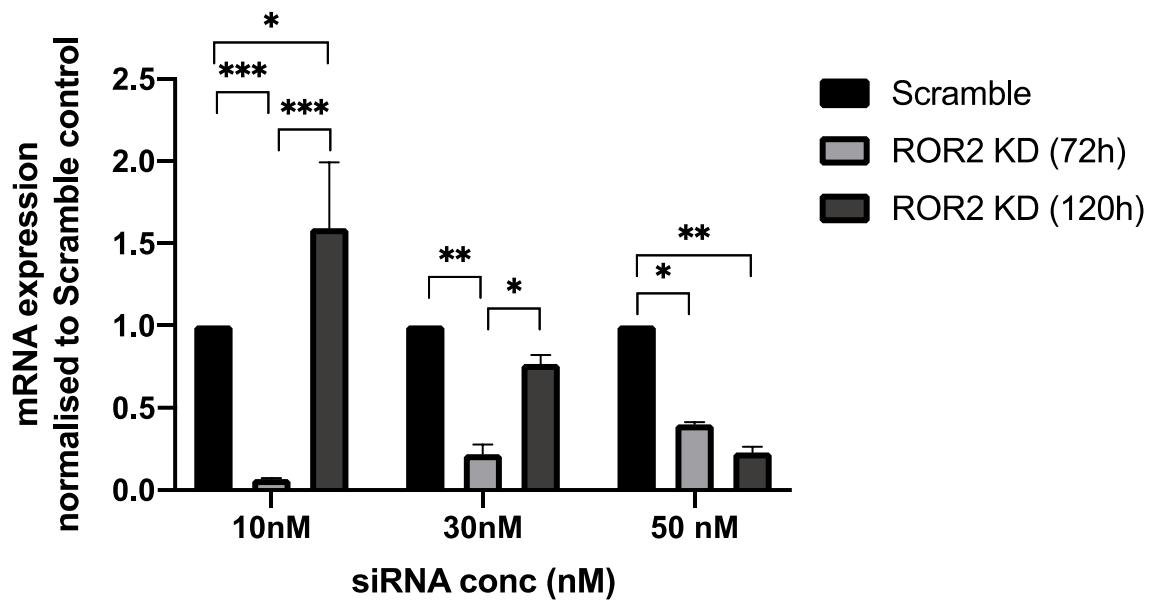
Figure3. 36 siRNA knockdown of ROR1 and ROR2 at different concentrations in OVCAR-3 cells. The graph below shows siRNA dose ranges transfected into OVCAR-3 cells at two different time points as described in section 3.2.1.2.2. Experiment replicates of n=3 was carried out for reproducibility. A qPCR experiment was carried out to assess mRNA expression in single and double knockdown of ROR1 and ROR2 A) Knockdown of ROR1 is most effective when transfected with 50nM of siRNA at 72h B) ROR2 knockdown is most effective at 72h when transfected with 10nM of siRNA. A two-sample t-test comparing the siRNA doses to their respective scramble control was carried out where '*', '**' and '***'denotes statistical significance of $p<0.05$, $p<0.01$ and $p<0.001$ respectively.

KD: Knockdown

The knockdowns were further confirmed on western blots shown in the figure 3.37 below. Knockdown effects at protein level were consistent with mRNA expression levels. ROR1 and ROR2 knockdown in OVCAR-3 cell lines were observed using Western blots. Similar to the HEY cells, optimal knockdown effect in the OVCAR-3 cell line was detected at 72 hours with 50nM (70% knockdown) and 10nM (80% knockdown) siRNA concentration respectively.
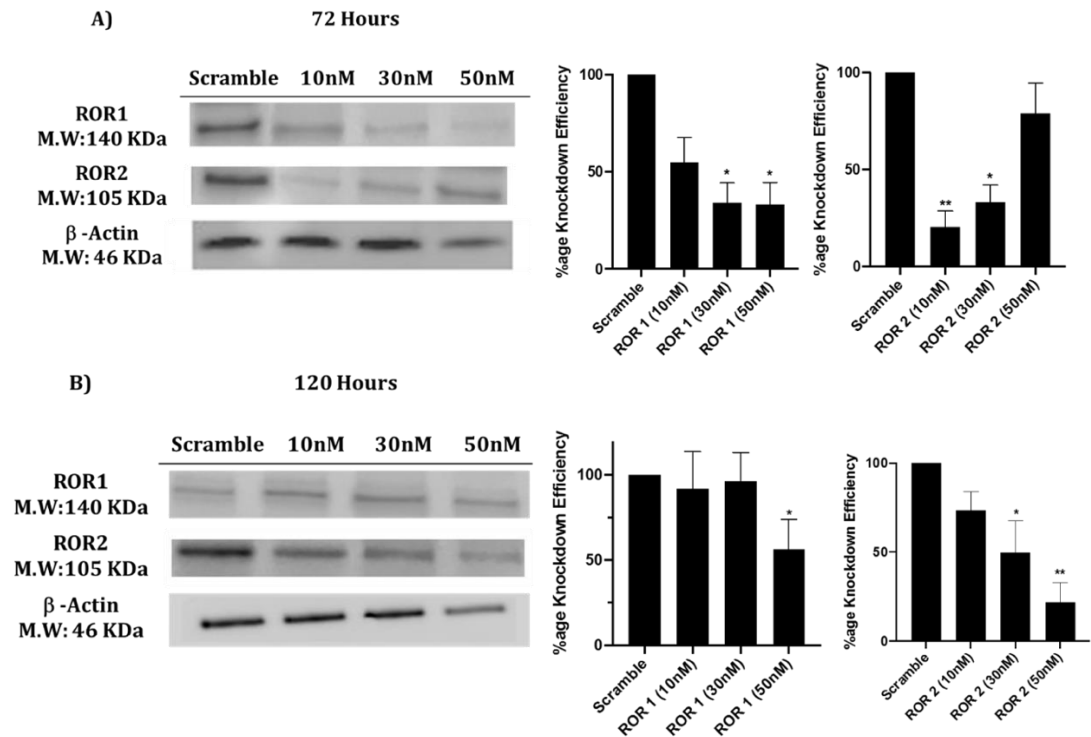
Figure3. 37 siRNA knockdown of ROR1 and ROR2 at different concentrations in OVCAR-3 cells (n=1). The blots are representative of three individual experiments. Representative Western blots reflect protein expression of ROR1 and ROR2 knockdown in siRNA transfected HEY cells. Left panel: A) ROR1 and ROR2 knockdown at 72 hours. Right panel: B) ROR1 and ROR2 knockdown at 120 hours. In each panel, top row ROR1 knockdown, middle row ROR2 knockdown, bottom row beta-actin (loading control). At the right of each blot is the graph showing percentage knockdown of each siRNA concentration relative to the scramble. A one sample t-test comparing the siRNA doses to their respective scramble control was carried out where '*' and '**'denotes statistical significance of $p<0.05$ and $p<0.01$ respectively.

Following on the singular knock down of ROR1 and ROR2, a double knockdown with the above optimised doses was also carried out as shown in Figure 3.38 below. ROR1 decreased significantly decreased by -5-fold (p<0.001) while ROR2 decreased by ten-fold.
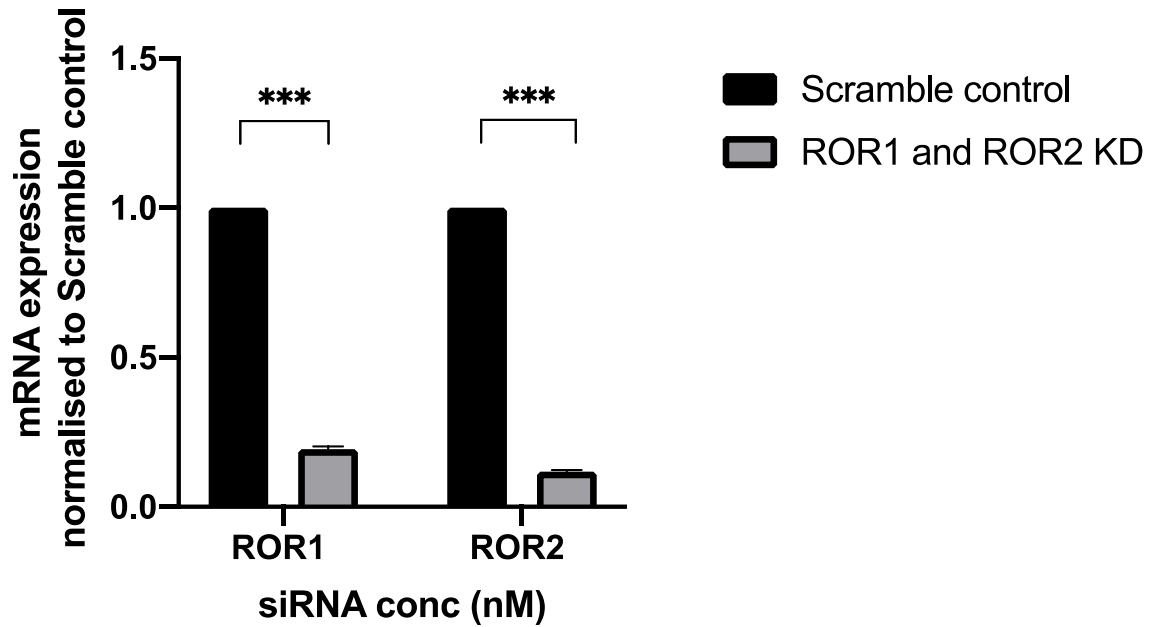
Figure3. 38 Double siRNA knockdown of ROR1 and ROR2 in OVCAR-3 cells. Knockdown was carried out at optimal siRNA concentrations of ROR1 and ROR2 siRNA at optimal time point simultaneously as determined above. Optimal siRNA concentration of 50nM for ROR1 and 10nM for ROR2 was used to carry out the double knockdown experiment at 72 hours. Double knockdown was most effective compared to singular knockdown of ROR1 and ROR2. Experiment replicates of n=3 was carried out for reproducibility. A one-sample t-test comparing the siRNA doses to their respective scramble control was carried out where '***'denotes statistical significance of p<0.001. KD: Knockdown

Similar to the HEY cells double knockdown effect of ROR1 and ROR2 was observed by western blots as shown in the figure 3.39 below. A 70% knockdown of ROR1 and 80% knockdown of ROR2was observed both of which had a significance of p<0.001.
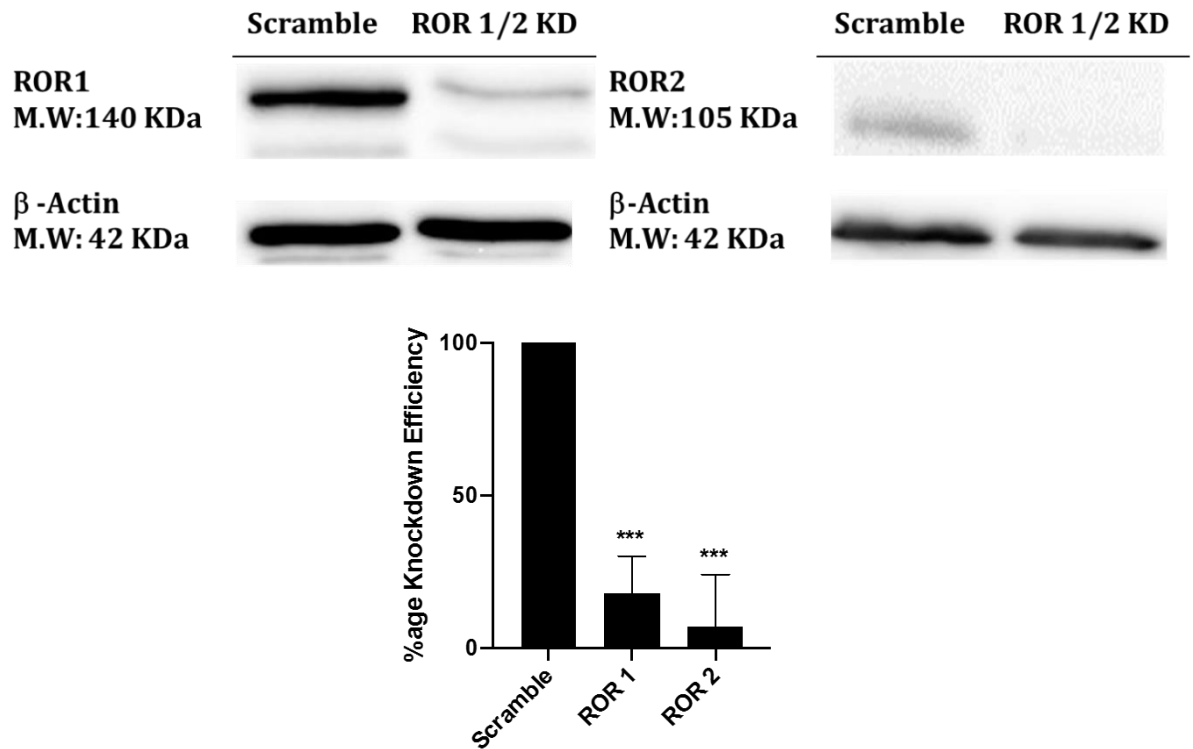
Figure3. 39 Double siRNA knockdown of ROR1 and ROR2 in OVCAR-3 cells (n=1). The blots are representative of three individual experiments. Simultaneous knockdown was carried out using optimal siRNA concentration of 50nM for ROR1 and 10nM for ROR2 at 72 hours as described in section 3.2.1.2.2. The percentage of knockdown efficiency was graphed as shown at the bottom of both blots. A one sample t-test comparing ROR1 and ROR2 knockdown to their respective scramble control was carried out where '***'denotes statistical significance of p<0.001.

KD: Knockdown

3.3.7.2.3 Effect of knockdown on cell growth: HEY cell line

The HEY cells grown in the T-25 flasks were incubated at 72 hours and 120 hours post transfection. Each flask was transfected with an siRNA concentration of 10nM, 30nM and 50nM individually along with a Scramble transfected flask and non-transfection control flask.

Cell counts of each flask were recorded. At 72 hours (Figure 3.40) cells transfected with 10nM and 30nM of siRNA showed significant differences in their cell number relative to their scramble flasks. Cells that were transfected with 50nM of siRNA for ROR1 showed a significant 20% decrease in their cell count when compared to the non-transfected control. It is important to note that there is a significant difference in cell number between the non-transfected control and the Scramble for cell transfected with 10nM and 30nM of siRNA. This indicates that transfection may have an effect on cell growth and therefore must be taken into account.
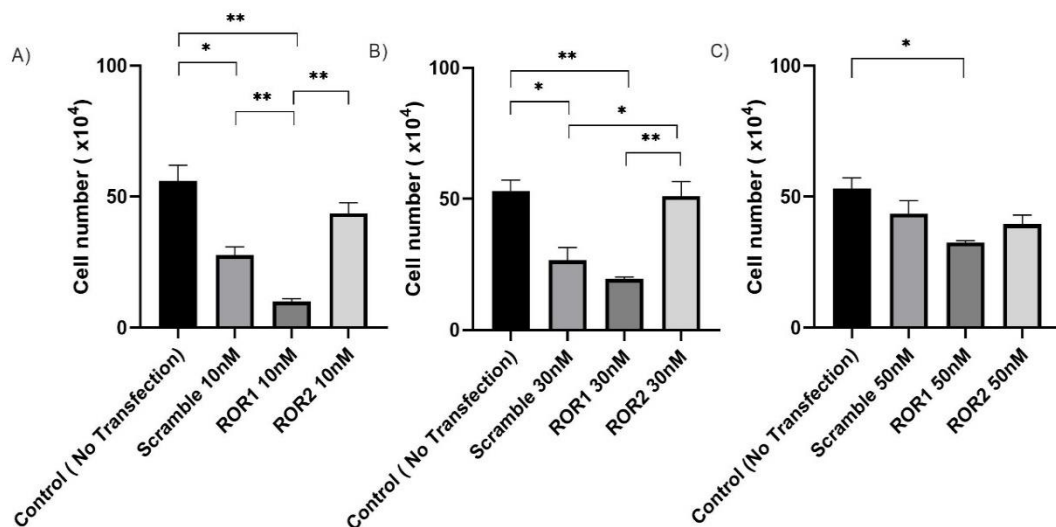
Figure3. 40 HEY cell counts post transfection at 72 hours. The graphs show cell counts of HEY cell line post siRNA transfection (10nM, 30nM and 50nM) at 72 hours. Cells were counted as described in chapter 2 section 2.1.3. A) Cells were transfected with 10nM of ROR1 and ROR2 siRNA. B) Cells were transfected with 30nM of ROR1 and ROR2 siRNA. C) Cells were transfected with 50nM of ROR1 and ROR2 siRNA. Experiment replicates of n=3 was carried out for reproducibility. A one-way ANOVA test comparing cell counts between each group was carried out where '*' and '**'denotes statistical significance of $p<0.05$ and $p<0.01$ respectively. A post hoc analysis using Tukey's test was carried out.

At 120 hours (Figure 3.41) there was a more modest effect of knockdown in cell counts across the panel of the transfected cells. It is also worth mentioning that the cell number far exceeds those at 72 hours. However, based on the mRNA expression data, it suggests that this increased cell number (compared to cells at 72 hours) and minimal differences in cell counts (between control, scramble and ROR1/2 knockdowns at different siRNA concentrations) could be attributed to the reversal of the knockdowns.
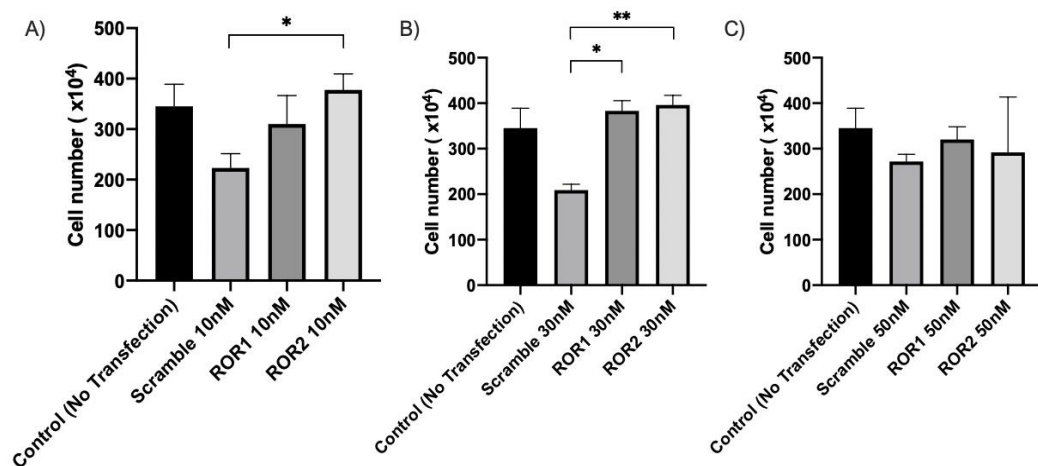
Figure3. 41 HEY cell counts post transfection at 120 hours. The graphs show cell counts of HEY cell line post siRNA transfection (10nM, 30nM and 50nM) at 120 hours. Cells were counted as described in chapter 2 section 2.1.3. A) Cells were transfected with 10nM of ROR1 and ROR2 siRNA. B) Cells were transfected with 30nM of ROR1 and ROR2 siRNA. C) Cells were transfected with 50nM of ROR1 and ROR2 siRNA. Experiment replicates of n=3 was carried out for reproducibility. A one-way ANOVA test comparing cell counts between each group was carried out where '*' and '**'denotes statistical significance of $p < 0.05$ and $p < 0.01$ respectively. A post hoc analysis using Tukey's test was carried out.

The graphs in figures above further confirm selecting a concentration of 50nM and 10nM for knocking down ROR1 and ROR2 respectively and the optimal time point of 72 hours for observing said effect.

3.3.7.2.4 Effect of knockdown on cell growth: OVCAR-3 cell line

Similar to HEY cells, the OVCAR-3 cells displayed significantly different cell counts when transfected with the varying concentrations of siRNA. Transfection with 10nM, 30nM and 50nM of ROR1 siRNA showed no significant difference at 72 hours when compared to the respective scrambles (figure 3.42 below). However, in all cases there was significant difference between the non-transfected control and scramble. Cells transfected with 10nM of ROR2 siRNA did not show a significant change in cell counts when compared to it respective scramble. There was however a significant 20% and 10% increase respectively in cell counts following transfection with 30nM and 50nM of ROR2 siRNA compared to the scramble (p<0.05).
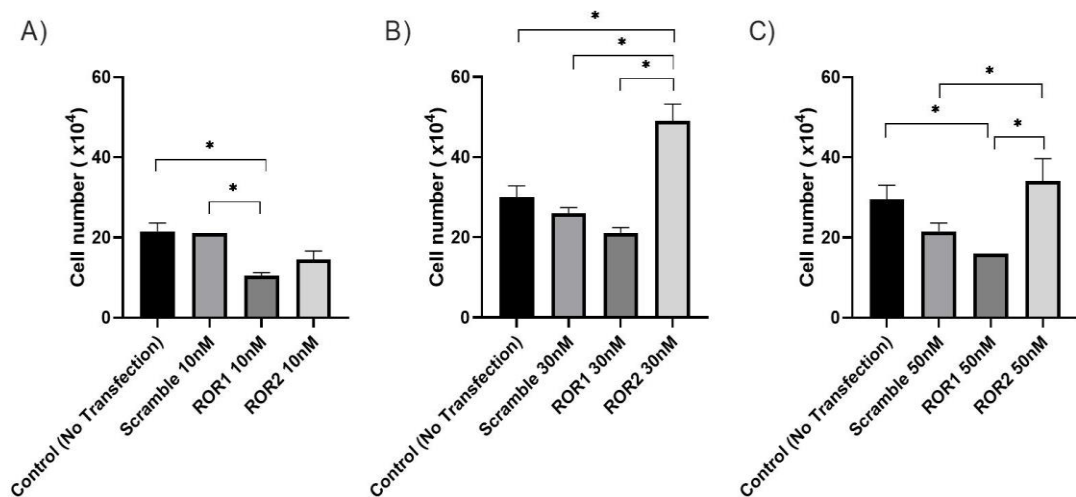
Figure3. 42 OVCAR-3 cell counts post transfection at 72 hours. The graphs show cell counts of OVCAR-3 cell line post siRNA transfection (10nM, 30nM and 50nM) at 72 hours. Cells were counted as described in chapter 2 section 2.1.3. A) Cells were transfected with 10nM of ROR1 and ROR2 siRNA. B) Cells were transfected with 30nM of ROR1 and ROR2 siRNA. C) Cells were transfected with 50nM of ROR1 and ROR2 siRNA. Experiment replicates of n=3 was carried out for reproducibility. A one-way ANOVA test comparing cell counts between each group was carried out where '*'denotes statistical significance of p<0.05. A post hoc analysis using Tukey's test was carried out.

At 120 hours post transfection (Figure 3.43), the cell counts in flasks transfected with 10nM and 30nM had significantly varying counts when compared back to the respective non-transfected controls and scramble. However, there was no significant difference between each other at siRNA concentration of 10nM but not the case at 30nM. There was no significant change in cell counts observed in cells that were transfected with 50nM of siRNA.
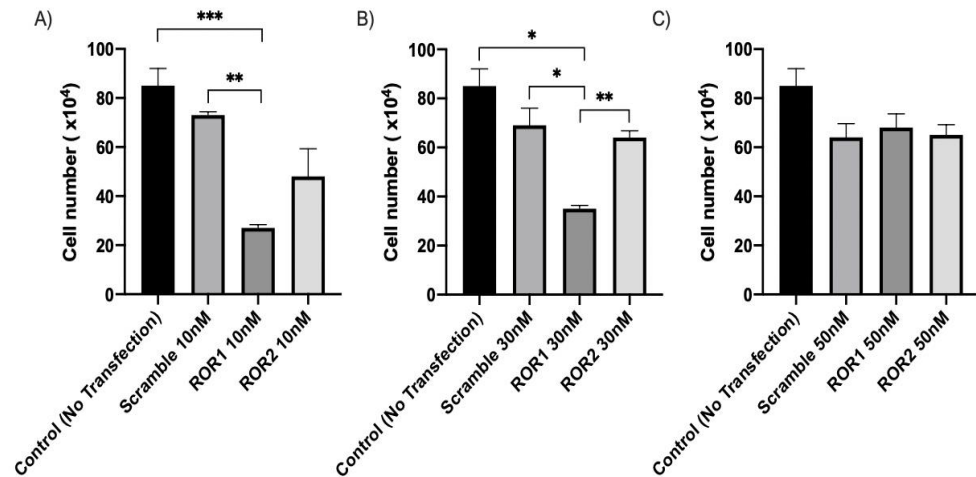
Figure3. 43 OVCAR-3 cell counts post transfection at 120 hours. The graphs show cell counts of OVCAR-3 cell line post siRNA transfection (10nM, 30nM and 50nM) at 120 hours. Cells were counted as described in chapter 2 section 2.1.3. A) Cells were transfected with 10nM of ROR1 and ROR2 siRNA. B) Cells were transfected with 30nM of ROR1 and ROR2 siRNA. C) Cells were transfected with 50nM of ROR1 and ROR2 siRNA. Experiment replicates of n=3 was carried out for reproducibility. A one-way ANOVA test comparing cell counts between each group was carried out where '*', '**' and '***' denotes statistical significance of $p<0.05$, $p<0.01$ and $p<0.001$ respectively. A post hoc analysis using Tukey's test was carried out.

Based on the mRNA expression profile and the cell counts in above figures, the optimal dose of siRNA for ROR1 and ROR2 knockdown are 50nM and 10nM respectively at 72 hours.

3.3.7.2.5 Effect of ROR knockdown on chemotherapy drug sensitivity: HEY cell line

Cells seeded in 96 well plate were treated with varying doses of cisplatin, carboplatin, taxol and talazoparib where cell viability was compared to their ROR1, ROR 2 as well as ROR1 and 2 knock down counter parts. Cells that were not drug treated were also seeded but also underwent transfection and as a result had their singular ROR1, ROR2 and double ROR1 and 2 expression knocked down. This acted as a control to compare whether knockdown affected drug sensitivity of the cells. Transfected cells that were non-drug treated showed no significant difference in their cell viability when normalized to the scramble (100% cell viability). However, upon drug treatment the cell viability of transfected cells significantly reduced to 50% or below when compared to the non-drug treated control cells. This indicates that the overall cell viability of transfected cells decreased with increase in drug dosage.

Figure3.44, shows the effect of treatment with half the IC50 dose of cisplatin (0.69ug/mL), the IC50 dose of cisplatin(1.38ug/mL) and double the IC50 dose of cisplatin (2.76ug/mL).
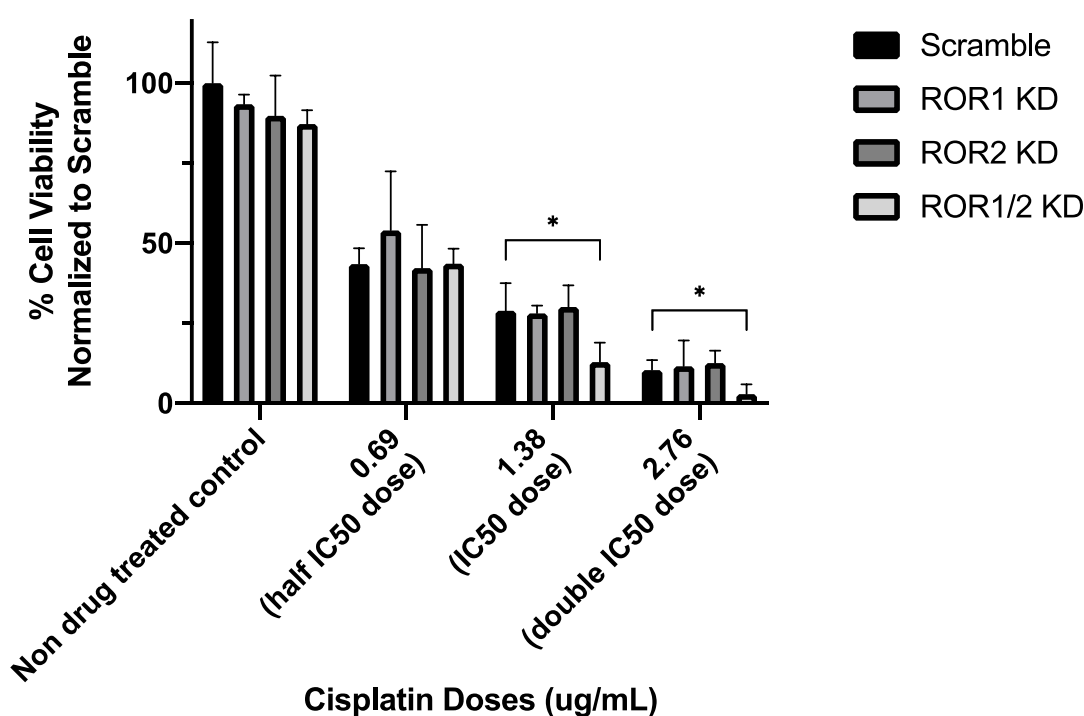
Figure3. 44 Drug treatment of knocked down HEY cell with varying doses of cisplatin (n=3). Transfected cells seeded in 96 well plates as described in section 3.2.1.2 and were treated with three varying doses of cisplatin (section 3.2.1.2.3). Non-drug treated transfected cells were also seeded in 96 well plates acted as a control. Cell viability decreased with increased drug doses. Cell viability was normalized to the respective Scramble for each drug dose where a t-test was carried out to compare effect of knockdown on sensitivity with '*' indicating a significance of $p<0.05$.

KD: Knockdown

In the figure above cell viability was reduced to less than fifty percent in the scramble and ROR1 knocked down cells that were treated with all three doses of cisplatin with the exception of ROR1 knocked down cells treated with half the IC50 dose. The ROR2 knocked down cells also exhibited a decrease in cell viability with increased drug doses. A similar pattern was observed with cells that underwent double knockdown (ROR1/2) however those treated with IC50 and double the IC50 doses exhibited a significant decrease ($p<0.05$) of 70% in viability compared to their respective singular knocked down and scramble counterparts. This suggests the knockdown had an effect on the sensitivity of the cells to cisplatin at these doses.
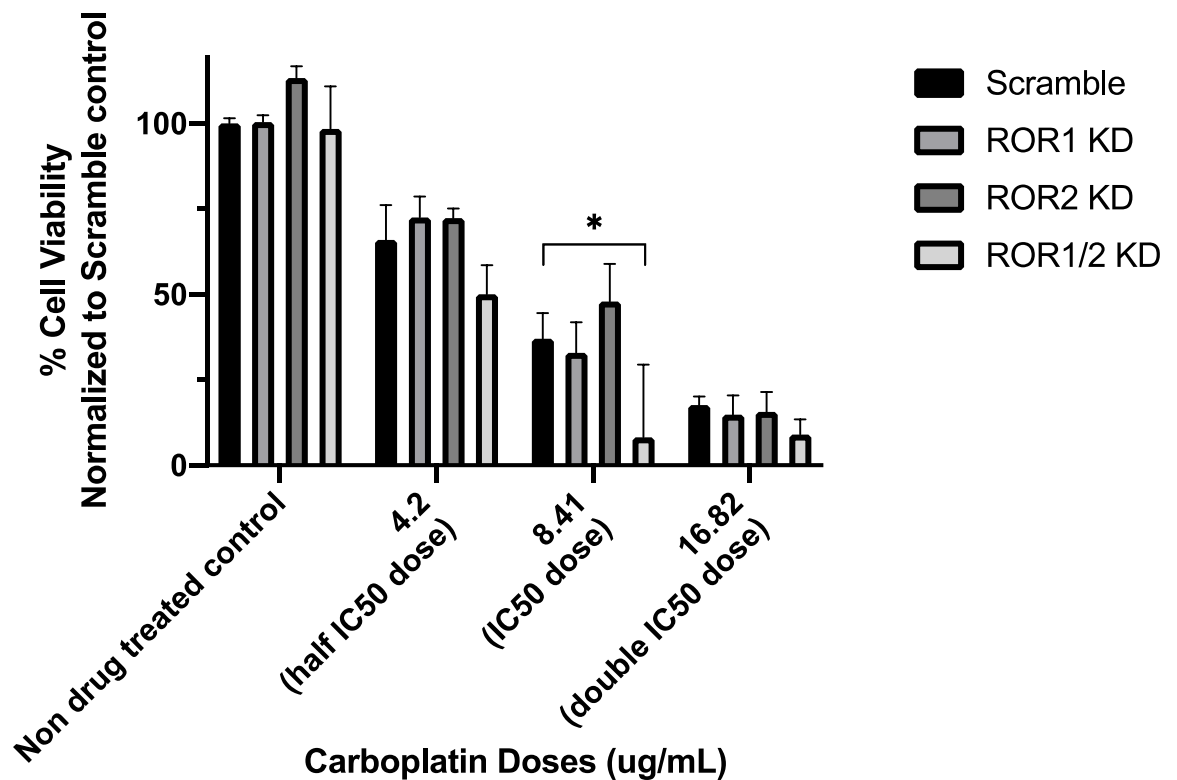
Figure3. 45 Drug treatment of knocked down HEY cell with varying doses of carboplatin (n=3). Transfected cells seeded in 96 well plates as described in section 3.2.1.2 and were treated with three varying doses of carboplatin (section 3.2.1.2.3). Non-drug treated transfected cells were also seeded in 96 well plates acted as a control. Cell viability decreased with increased drug doses. Cell viability was normalized to the respective Scramble for each drug dose where a t-test was carried out to compare effect of knockdown on sensitivity with '*' indicating a significance of $p<0.05$.

KD: Knockdown

Figure 3.45 shows knocked down cells treated with varying doses of carboplatin; half the IC50 dose (4.2 ug/mL), the IC50 dose (8.41ug/mL) and double the IC50 dose (16.82ug/mL). The cell viability once again decreases with increased carboplatin doses. Interestingly, double knocked down cells treated with half the IC50 dose showed decreased cell viability compared to respective singular knockdown and scramble cells but was not statistically significant. However, in the double knocked down cells treated with IC50 dose of carboplatin, a significant decrease of 80% in cell viability compared to respective singular knockdown and scramble cells was observed.
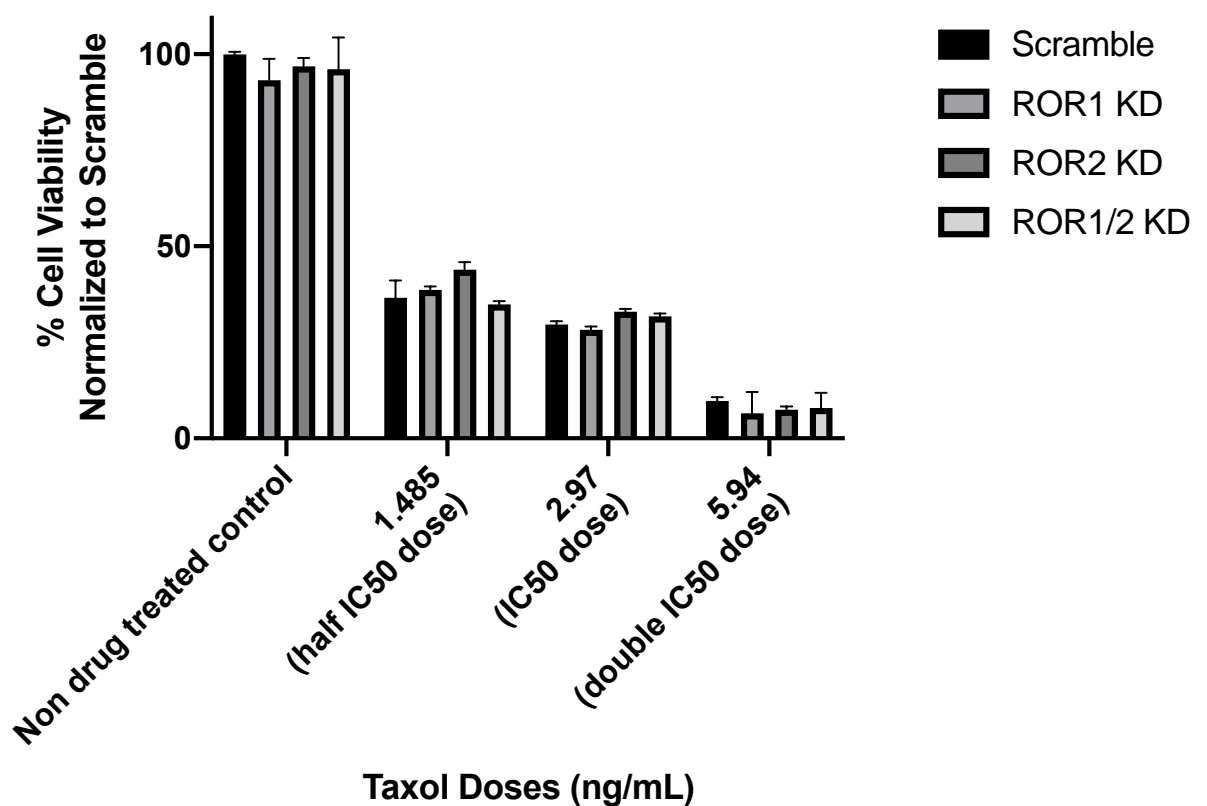
Figure3. 46 Drug treatment of knocked down HEY cell with varying doses of taxol (n=3). Transfected cells seeded in 96 well plates as described in section 3.2.1.2 and were treated with three varying doses of taxol (section 3.2.1.2.3). Non-drug treated transfected cells were also seeded in 96 well plates acted as a control. Cell viability decreased with increased drug doses. Cell viability was normalized to the respective Scramble for each drug dose where a t-test was carried out to compare effect of knockdown on sensitivity. No significant difference was observed.

KD: Knockdown

The HEY cells treated with varying IC50 doses of taxol; half the IC50 dose (1.485 ng/mL), the IC50 dose (2.97 ng/mL) and double the IC50 dose (5.94 ng/mL) are shown in figure 3.46 above. This demonstrated a decrease in cell viability; however, no significant differences were observed between ROR1 and ROR2 singular and double knocked down cells therefore suggesting no impact of knockdown on cell response to taxol treatment.
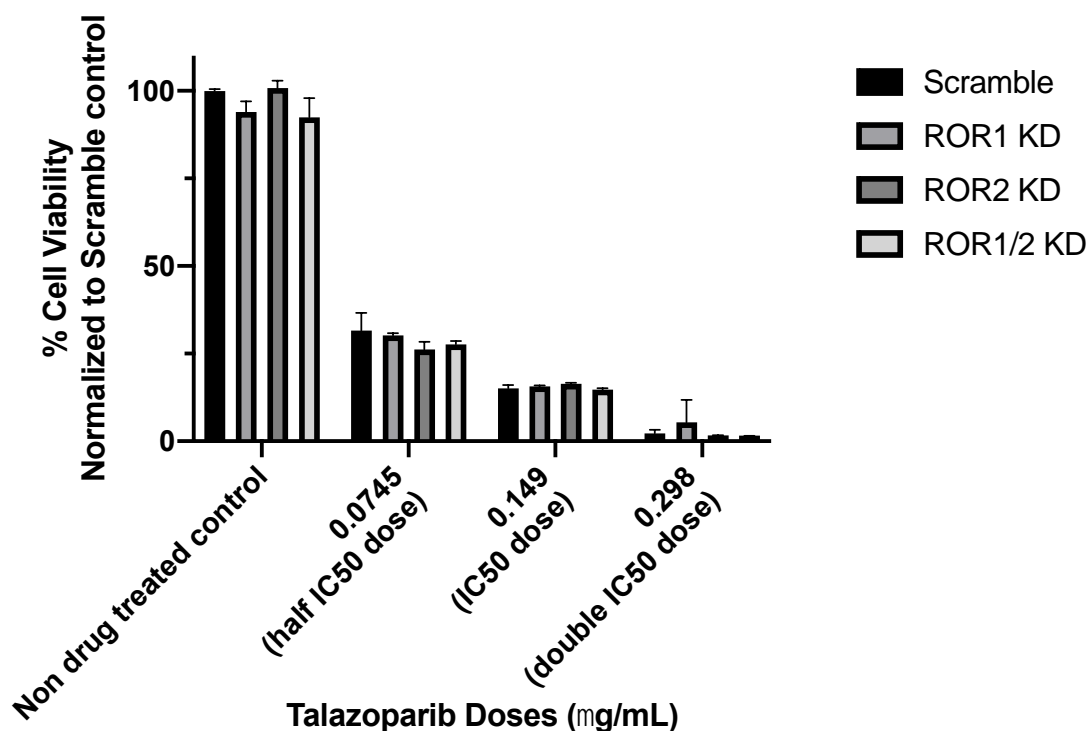
Figure3. 47 Drug treatment of knocked down HEY cell with varying doses of talazoparib (n=3). Transfected cells seeded in 96 well plates as described in section 3.2.1.2 and were treated with three varying doses of talazoparib (section 3.2.1.2.3). Non-drug treated transfected cells were also seeded in 96 well plates acted as a control. Cell viability decreased with increased drug doses. Cell viability was normalized to the respective Scramble for each drug dose where a t-test was carried out to compare effect of knockdown on sensitivity. No significant difference was observed.

KD: Knockdown

Transfected cells treated with varying doses of talazoparib is shown in figure 3.47 above. Cells were treated with half the IC50 dose (0.0745 ug/mL), the IC50 dose (0.149ug/mL) and double the IC50 dose (0.298ug/mL). As with cisplatin and carboplatin treated transfected cells, the cell viability in talazoparib treated transfected cells decreased with increased drug dose. However, no significant difference was observed between the scramble and respective knockdown cells for each drug dose. This suggests that knockdown of ROR1 and 2 has no impact on sensitivity of the cells to the non-platinum-based drug, talazoparib.

3.3.7.2.6 Effect of ROR knockdown on chemotherapy drug sensitivity OVCAR-3 cell line

Similar to the HEY cell line, OVCAR-3 cells were also seeded in a 96 well plate and treated with varying doses of cisplatin, carboplatin and talazoparib where cell viability was compared to their ROR1, ROR 2 as well as ROR1 and 2 knocked down counter parts. Transfected cells that were non-drug treated were also seeded and acted as the control. The cells were normalized to the non-drug treated scramble which represented 100% cell viability.

The ROR1 knocked down OVCAR-3 cells showed varying responses to cisplatin drug treatment. As shown in figure 3.48, cell viability of cells treated with the IC50 dose (0.07 ug/mL) of cisplatin was reduced (less than 50%) when ROR1 and ROR2 was knocked down in these cells compared to the ROR1 and ROR2 knocked down non-drug treated control cells. There was no significant difference observed between the singular and double knockdown of ROR1 and ROR2 in the IC50 dose treated cells. However, cells treated with half IC50 dose (0.035 ug/mL) had a significant 70% decrease in viability ($p < 0.005$) in cells that underwent double knockdown compared to the respective scramble. It was also worth noting that Scramble and ROR1 knocked down cells treated with double the IC50 dose (0.14 ug/mL) were 50% higher ($p < 0.05$) than ROR2 and double knocked down cells treated with the same cisplatin dose.
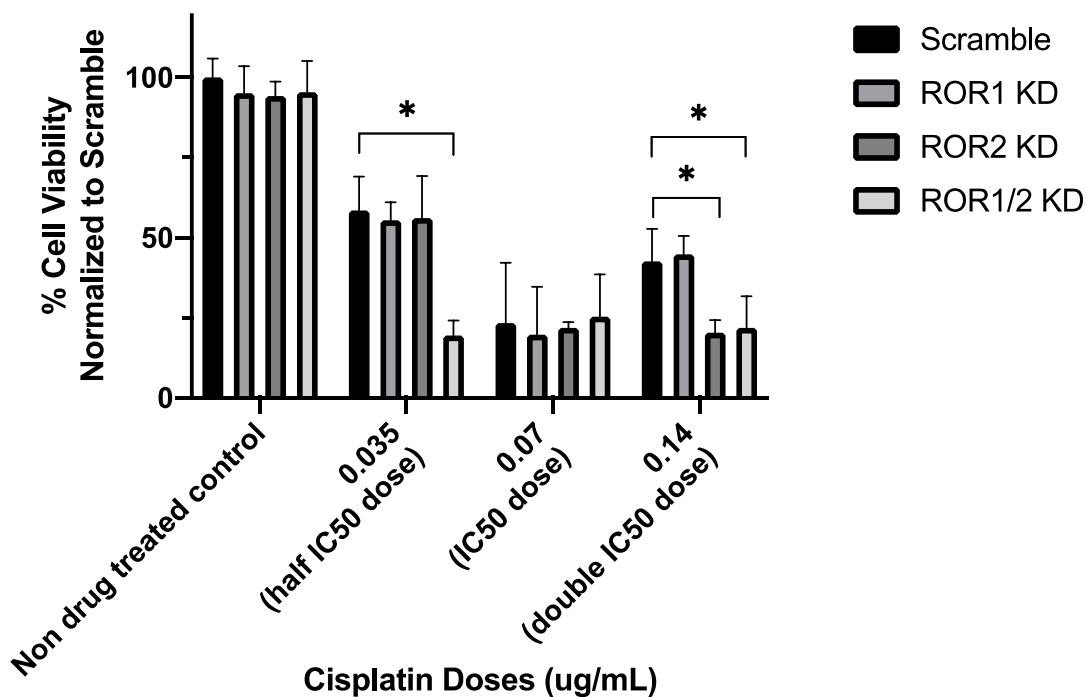
Figure3. 48 Drug treatment of knocked down OVCAR-3 cell with varying doses of cisplatin (n=3). Transfected cells seeded in 96 well plates as described in section 3.2.1.2 and were treated with three varying doses of cisplatin (section 3.2.1.2.3). Non-drug treated transfected cells were also seeded in 96 well plates acted as a control. Cell viability decreased with increased drug doses. Cell viability was normalized to the respective Scramble for each drug dose where a t-test was carried out to compare effect of knockdown on sensitivity with '*' indicating a significance of p<0.05.

KD: Knockdown

In carboplatin treated cells (Figure 3.49) a decrease in cell viability was observed in knocked down cells treated with all three doses of the drug compared to the non-drug treated transfected control cells. No significant difference was observed between the scramble and respective knockdown cells for each drug dose. This suggests that knockdown has no eminent effect on sensitivity in response to carboplatin treatment in the OVCAR-3 cells.
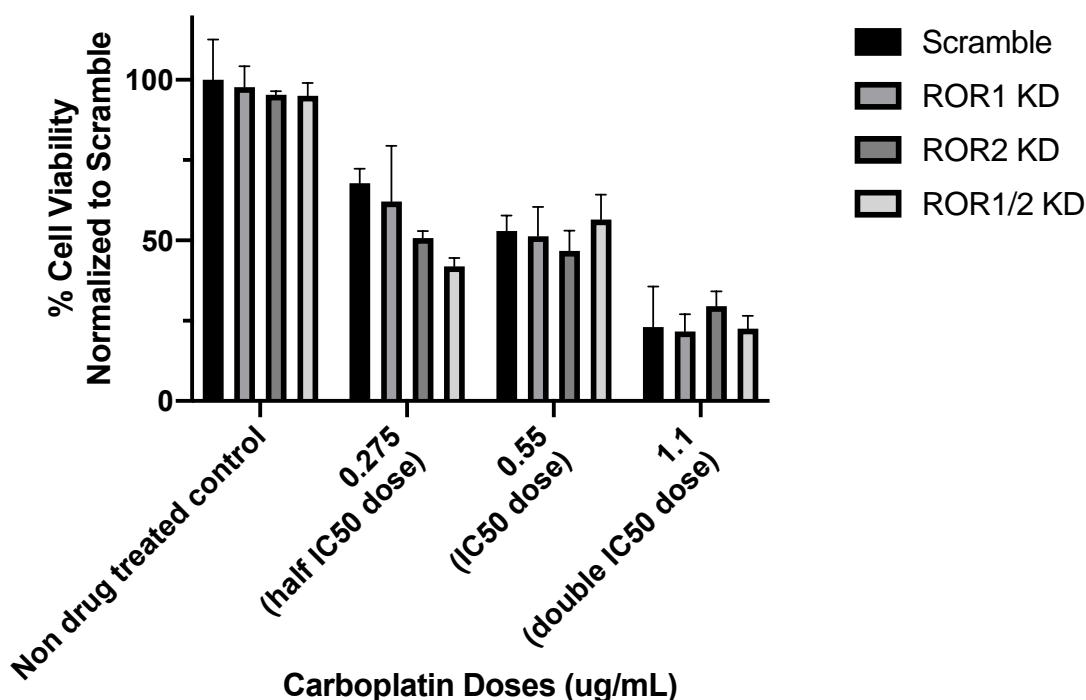
Figure3. 49 Drug treatment of knocked down OVCAR-3 cell with varying doses of carboplatin (n=3). Transfected cells seeded in 96 well plates as described in section 3.2.1.2 and were treated with three varying doses of carboplatin (section 3.2.1.2.3). Non-drug treated transfected cells were also seeded in 96 well plates acted as a control. Cell viability decreased with increased drug doses. Cell viability was normalized to the respective Scramble for each drug dose where a t-test was carried out to compare effect of knockdown on sensitivity. No significant difference was observed.

KD: Knockdown

The OVCAR-3 cells treated with half the IC50 dose (0.64 ng/mL), the IC50 dose (1.28 ng/mL) and double the IC50 dose (2.56 ng/mL) of taxol are shown in figure 3.50 below. Similar to taxol treated transfected HEY cells, a decrease in cell viability was observed. However, there was no significant differences between ROR1 and ROR2 singular and double knocked down cells relative to their respective scramble for each drug dose. Knockdown of ROR1 and ROR2 demonstrated no altered response to taxol treatment in OVCAR-3 cells.
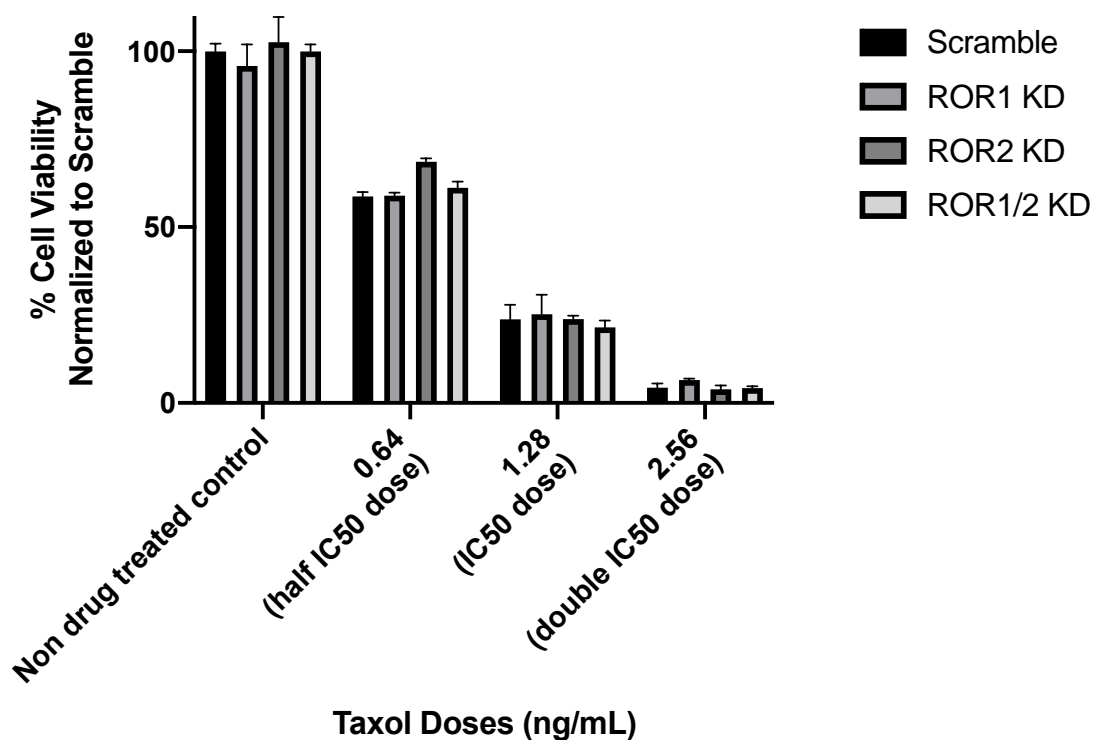
Figure3. 50 Drug treatment of knocked down OVCAR-3 cell with varying doses of taxol (n=3). Transfected cells seeded in 96 well plates as described in section 3.2.1.2 and were treated with three varying doses of taxol (section 3.2.1.2.3). Non-drug treated transfected cells were also seeded in 96 well plates acted as a control. Cell viability decreased with increased drug doses. Cell viability was normalized to the respective Scramble for each drug dose where a t-test was carried out to compare effect of knockdown on sensitivity. No significant difference was observed.

KD: Knockdown

Similar to the carboplatin and taxol treated cells, the OVCAR-3 transfected cells decreased in cell viability when treated with half the IC50 dose (0.0745ug/mL), IC50 dose (0.149ug/mL) and double the IC50 dose (0.298ug/mL) of talazoparib (Figure 3.51). Within each drug dose no significant difference was observed between the knocked down cells and the respective scramble, once again suggesting no effect of knock down on sensitivity of cells to talazoparib treatment.
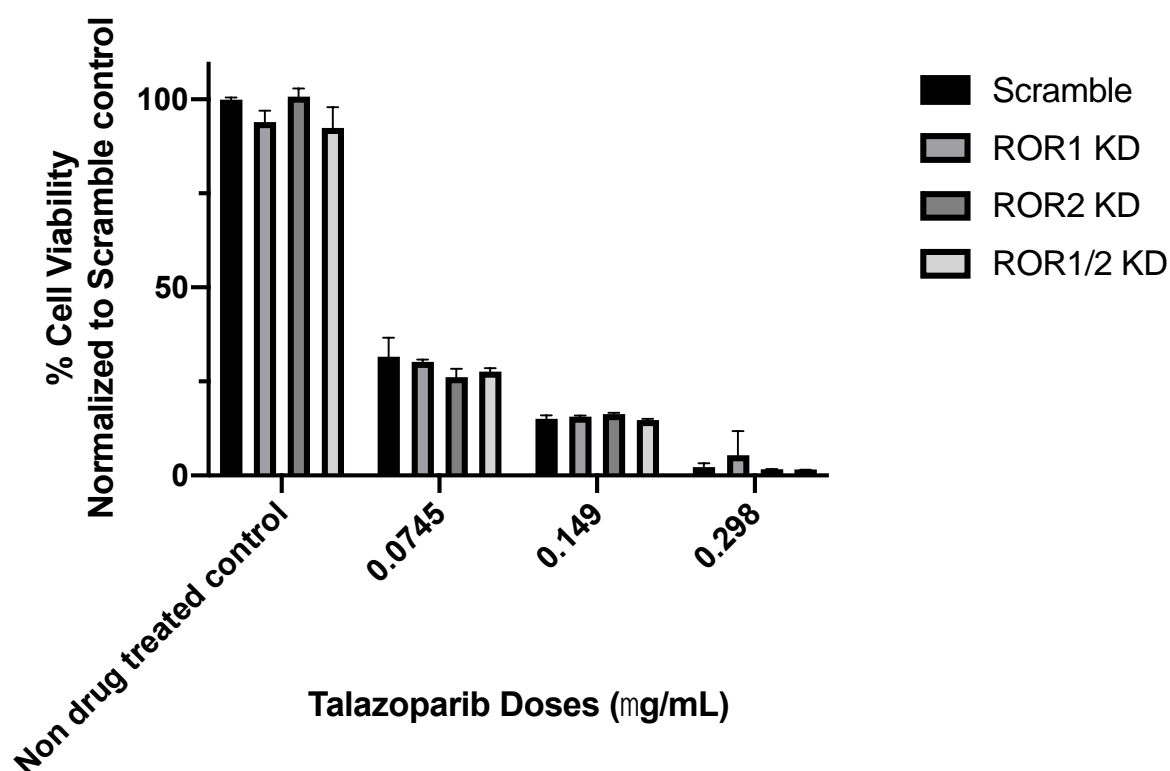
Figure3. 51 Drug treatment of knocked down OVCAR-3 cell with varying doses of talazoparib (n=3). Transfected cells seeded in 96 well plates as described in section 3.2.1.2 and were treated with three varying doses of talazoparib (section 3.2.1.2.3). Non-drug treated transfected cells were also seeded in 96 well plates acted as a control. Cell viability decreased with increased drug doses. Cell viability was normalized to the respective Scramble for each drug dose where a t-test was carried out to compare effect of knockdown on sensitivity. No significant difference was observed.

KD: Knockdown

Overall, from the above results it is evident that transfection does not affect the viability of any of the cell lines. However, with drug treatment, the cell viability considerably reduces and, in some cases, an increased sensitivity to the drugs; cisplatin and carboplatin is observed. This re-sensitisation of sorts was mostly observed in cells that underwent a double knockdown of both ROR1 and ROR2.

3.4 Discussion

3.4.1 Ovarian cancer cell line models with varying resistance profiles

Determining the resistance profile for the ovarian cancer cell lines in the panel represents a step closer to understanding the role of the novel biomarkers in chemoresistance mechanisms and pathways. The results in section 3.3.2 (table 3.5) show a range of dose responses to the platinum based (Cisplatin and Carboplatin), Taxane (Taxol) and PARP inhibitor (Talazoparib) drugs.

It is evident that the cell line most resistant to all four forms of chemotherapy or targeted therapy is the HEY cell line as shown in section 3.3.2. OVCAR-3 falls within the sensitive spectrum as it is sensitive to cisplatin, carboplatin, taxol and talazoparib compared to the other three cell lines. However, OAW42 cell line fluctuates between sensitive to moderately sensitive compared to OVACR-3. An interesting observation was that of the SKOV-3 cell line in its response to drugs compared to the other three cell lines. It exhibited better response to cisplatin than carboplatin but still required a higher dose compared to both OVCAR-3 and OAW42. However, in response to the Taxol and PARPi drug it was more sensitive than OVCAR-3 and OAW42 respectively. This places SKOV-3 within the moderate chemo resistant profile in this panel.

\

According to Sherman-Baust *et al*.(2011) changes in gene expression are associated with drug resistance in ovarian cancer and this depended on which drug is used, cisplatin, paclitaxel or doxorubicin. Their study also suggested that a given drug and condition would likely lean towards similar pathways even though cell lines assumed different resistance mechanisms to different drugs. Another important fact to point out in their study is that the different drug resistance phenotypes possessed different patterns of expression. This is relevant to this project as it further validates selecting a range of cell lines with varying resistance profiles and therefore understanding expression patterns of the selected biomarkers and possibly link it to resistance mechanisms. Pathway analysis could eventually play a big role in identifying the mechanisms involved in the resistance to drugs used to treat ovarian cancer. This would then help better understand the role of the biomarker genes in these pathways.

3.4.2 Modelling ovarian cancer with cell lines

Ovarian cancer is a complex disease to model using cell lines. Studies such as those carried out by Jacob *et al.*(2014), question the reliability of the cancer cell line models used in the past. This is mainly due to the fact that some have had their histological subtype mischaracterised. This, of course, skews the results seen in certain cell line models with regards to drug treatment and resistance. Heterogeneity is also an added complication which needs to be accounted for. Long-established ovarian cancer cell lines have exhibited many drawbacks in terms of their clinical relevance since only a few of them are well defined tumour cell lines (Domcke *et al*., 2013). Frequently used *in vitro* cell line models such as A2780 are often used as HGSOC model while being least likely to be obtained from said cancer (Beaufort *et al.,* 2014; Domcke *et al*., 2013). This warrants a reworking in *in vitro* ovarian cancer research with a focus on the use of well-defined and characterised cell line panels (Anglesio *et al*., 2013; Beaufort *et al*., 2014). Researchers have suggested that investigating large cell line panels is valuable for identifying novel biomarkers (Barretina *et al*., 2012) and studying key players involved in the resistance mechanisms (Alkema *et al*., 2016). Ovarian cancer cell lines generally fail to preserve the phenotype of the original tumour. A study by Ince *et al* (2015) established cell lines from varying subtypes of human ovarian cancer which successfully retained features of the original tumour such as the histopathology, genomic landscape and molecular features. The molecular profile and drug response of these cell lines correlated with distinct types of primary tumours with different outcomes representing improved platforms to study response to therapy.

It has been suggested on numerous occasions, in the context of breast and ovarian cancer; that primary tumours should be used to identify chemotherapy resistance biomarkers and study the mechanisms involved (Gong *et al*., 2010; Jacob *et al*., 2014). Several cases have been made regarding cell lines being mostly acquired from ascites and thus not being an accurate representation of the native tumour. However, most patients that relapse with a chemotherapy resistant form of the disease more often than not undergo cytoreduction. This makes the accessibility of such tumours challenging and consequently the next best alternative is to use cell line models. As mentioned earlier, using said models comes with certain drawbacks. However, establishing a larger panel to conduct the study can be considered a risk reduction strategy.

Chemo-sensitive and resistant cell lines developed *in vitro* by exposing them repeatedly to increasing drug concentrations are largely used to characterize drug-resistant mechanisms (Behrens *et al*., 1987; Jazaeri *et al*., 2013). Although these are well established and have proven to be useful in tumour biology, Cunnea and Stronach (2014) explain that ovarian cancer cell lines should not be used as absolute chemotherapy resistant models for clinical research. This is owing to the fact that the manner in which resistance was created is non-physiological and therefore not completely reliable. A gene expression profiling step was also carried out comparing clinically acquired resistance and resistance derived *in vitro* showing the consistency between the two models was poor (Stronach *et al*., 2011). A 2014 study explored the development of chemotherapy and targeted therapy resistant models *in vitro* (McDermott *et al*., 2014). Here models were divided into clinically relevant or high-level laboratory models. The former was developed in an attempt to mimic conditions of cancer patients during chemotherapy while the latter were developed in order to understand mechanisms of toxicity and resistance to chemotherapy drugs. Both models have their limitations however, the high-level laboratory models are stably resistant and easy to maintain in culture for further research. Additionally, in these models when the level of resistance is higher the molecular changes linked with the resistance mechanisms are larger and therefore making them easily detectable. However, this model becomes less relevant to the clinic the higher the level of resistance (McDermott *et al*., 2014). Therefore, this can be used as a sliding scale to select relevant models to establish the most appropriate cell line panels.

Other comprehensively studied chemotherapy sensitive or resistant ovarian cancer cell lines available tend to acquire phenotypic as well as genotypic alterations as a result of repeated passaging. They therefore do not model the condition they intend to represent clinically (Gillet *et al*., 2013). Recently, chemo resistant cell line models commonly used such as SKOV-3 and A2780 have been considered to be poor HGSOC models (Anglesio *et al*., 2013; Domcke *et al*., 2013). This is because they do not match high grade serous tumours at a molecular level. SKOV-3 cell lines were even shown to possess the hallmarks of the clear cell subtype when it was studied in 3D cultures (Lee *et al*., 2013). Despite SKOV-3 having the above-mentioned limitations it was included in the panel for this study as it can still be utilised as a general ovarian cancer model. SKOV-3 is considered suitable model of AKT driven ovarian cancer since it carries a triggering point mutation in PIK3CA (Domcke *et al*., 2013). PIK3CA mutations is an early-stage tumorigenesis event of clear cell carcinoma and

accounts for 5% of epithelial ovarian cancer (Chan *et al*., 2008). This is especially relevant in this study as the biomarker ROR1 is found to be highly expressed in clear cell carcinoma subtypes and is associated with a poor prognosis (C. E. Henry *et al*., 2017). Although clear cell carcinoma is considered to be rare, it is useful to have a cell-line model representing such tumour behaviour in this study as this could potentially extend to patients also presenting clear cell carcinomas.

Despite all the reservations regarding the use of *in vitro* cell line models to investigate chemo-resistance, it would be unreasonable to cast aside their use in this study. Acquisition of primary tumours in the exact state and stage that is being investigated is challenging. *In vitro* cell line models are the next best thing as they are representative of most if not all tumours being studied. This project is one of the first to establish a panel modelling intrinsic chemotherapy resistance in ovarian cancer cell lines that is as representative as possible of the disease. All the cell lines used are BRCA1/2 wild type that are also BRCA1 un-methylated (Stordal *et al*., 2013). This is useful as 75% of women with recurring ovarian cancer are BRCA wild type (Hollis *et al*., 2017). Since BRCA wild type tumours are harder to treat and show poorer prognosis (Helen E. Bryant *et al*., 2005; Farmer *et al*., 2005b; Hollis *et al*., 2017), selecting cell lines with this genotype was important for this project. With regards to expected sensitivities, the cell line models in this panel had a range of phenotypes; epithelial, intermediate epithelial, intermediate mesenchymal and mesenchymal (Yi *et al*., 2015). Past studies have indicated a higher chemotherapy resistance in models of a mesenchymal phenotype and lower in epithelial phenotype (Haslehurst *et al*., 2012; Zhang *et al*., 2013). The resistance profiles of the cell lines determined from the cytotoxicity assay confirms the above with HEY cell line which is of a mesenchymal phenotype being the most resistant (Figure 3.3). This also showed that the drug doses had the expected effect on the cell line by phenotype thereby validating their position in the cell-line panel.

Consequentially, establishing a cell line panel to investigate chemotherapy resistant and sensitive models in this project proves to be valuable as is evidenced above. It is obvious that there is controversy surrounding the use of certain cell lines such as SKOV-3 however it would be negligent to not consider it in this panel as it can serve as a comparative model. The remaining cell lines in this panel as shown in table 3.5 are well characterised and reliable as this help offset any potential misrepresentations by the SKOV-3 cell line model.

3.4.3 Chemotherapy resistant and invasive ovarian cancer cell line model HEY has highest levels of ROR1 expression

The qPCR data delivered a snapshot of the mRNA levels of ROR1 in the four ovarian cancer cell line models. The qPCR and ELISA results showed a decrease in ROR1 upon drug treatment in the most resistant (HEY) and sensitive (OVCAR-3) cells. Interestingly the cell lines SKOV-3 and OAW42 that demonstrated moderate responses to drug treatment showcased an unexpectedly higher level of ROR1 expression when treated with platinum-based drugs compared to their respective untreated control cells. However, treatment with the taxane and PARP inhibitor drugs did nothing to alter the expression of ROR1 compared to the untreated control cells. The figure 3.52 shows the pattern of expression for ROR1 that are statistically significant across all four cell lines in the qPCR and ELISA results. It is worth noting that mRNA levels are relative while protein levels are absolute and as a result can impact the interpretation of these expression levels. It is apparent that drug treatment has the same effect only on the resistant cell line HEY at both the mRNA and protein level. Although the protein levels of ROR1 expression do not completely replicate the mRNA expression in the sensitive cells; OVCAR-3, it still matches the direction of expression. Here, the cisplatin treated cells have a decreased ROR1 expression. This suggests that when undergoing drug treatment, absolute mesenchymal (HEY) and epithelial (OVCAR-3) cells are impacted with regards to their ROR1 expression. Cell lines with intermediate phenotypes seem to have an elevated ROR1 expression upon drug treatment at the mRNA and protein level.
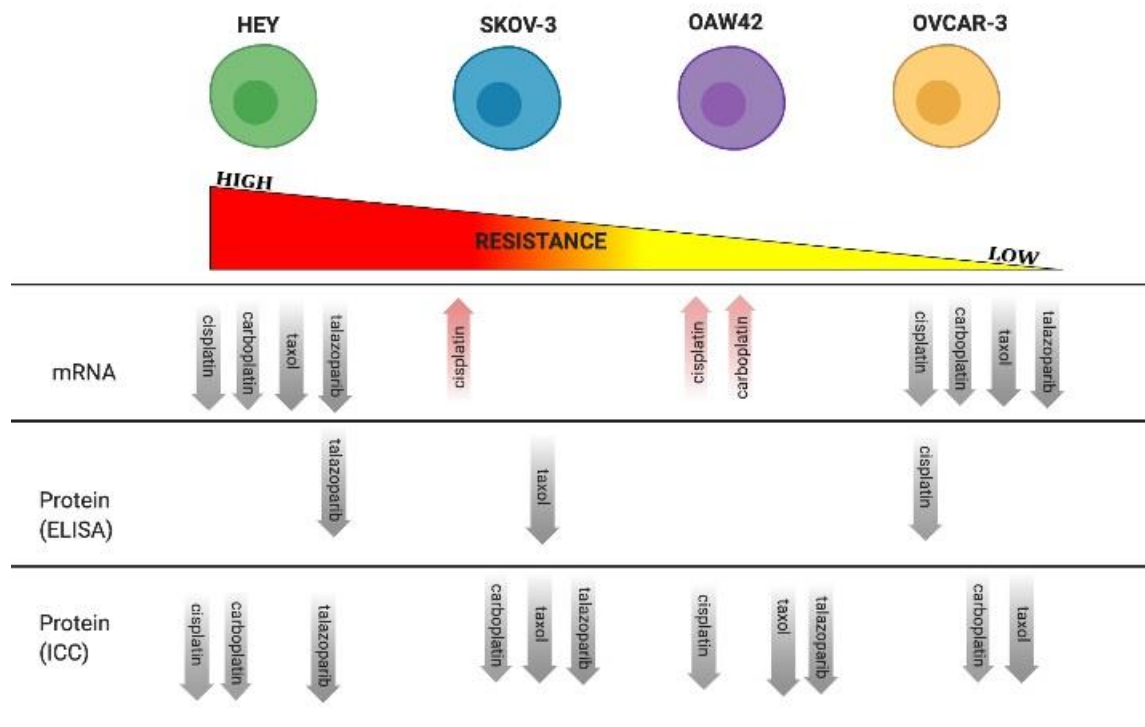
Figure3. 52 Significant changes of ROR1 expression. This is a summary of figures from section 3.3.4. The mRNA level from qPCR results and protein level from ELISA results and Immunocytochemistry (ICC) in each cell line when treated with different drugs. The increase/ decrease of mRNA is relative to the non-drug treated control of each cell line. The increase/ decrease of protein is absolute and depiction in the figure above is in comparison to untreated control cells. The grey arrows depict significant decrease whereas the red arrow depicts significant increase. Only those drugs treated cells that demonstrated a significant change are represented in this figure. Others either did not show any changes with drug treatment or did show change however it was not statistically significant when compared to its respective control.

Based on published literature, ROR1 expression is shown to be elevated in chemotherapy resistant ovarian cancer cell lines (Henry *et al*., 2016). Since HEY cells were the most resistant in our cell line panel ROR1 expression was expected to be highest in these cells. The untreated SKOV3, OVCAR-3 and OAW42 cell lines were compared to untreated HEY cells and demonstrated lower levels of ROR1 validating the rationale of ROR1 expression in the cell line panel. Studies have also established that ROR1 is associated with more aggressive and invasive phenotypes thereby confirming HEY cells association with high ROR1 levels (Cui *et al*., 2013).

Recently there have been more studies investigating the role of ROR1 in chemotherapy resistance. Its prevalence in solid tumours as well as haematological malignancies have been documented (Balakrishnan *et al*., 2017; Cetin *et al*., 2019; Zhang *et al*., 2012a). Previous studies have shown that rise of ROR1 occurs in chemotherapy resistant cells and can

therefore be used as prognostic marker for relapse as well as poor therapeutic outcomes (Chien *et al*., 2016; C. Henry *et al.*, 2017; Jung *et al*., 2016; Wu *et al*., 2019; Zhang *et al.*, 2012a). Analysis of gene expression data from NCBI's Gene Expression Omnibus (GEO) particularly in breast cancer patients suggested that patients with a poor response to chemotherapy drugs had elevated levels of ROR1 (Fultang *et al*., 2020). This suggests a link between ROR1 and chemotherapy resistance. Such an approach was applied to ovarian cancer in this study and thereby validated the expression patterns in the chemotherapy resistant versus the chemotherapy sensitive cell lines in the established cell line panel.

In this study an invasion profile was established to supplement the resistance profile of the cell line models. From the collagen invasion assay (chapter 2 section 2.1.8) it was determined that the invasion profile of the cell line panel was identical to the resistance profile. This placed the HEY cell line as the most invasive, followed by SKOV-3, OAW42 and finally OVCAR-3 as the least invasive. This pattern of invasiveness mirrors ROR1 expression which is depicted in the section 3.3.4.2 figure 3.12. A correlation ($R^2 = 0.8268$) is observed between invasiveness of the cell lines and ROR1 protein expression, with HEY cells having the highest ROR1 levels being the most invasive and OVCAR-3 cells with the lowest ROR1 levels being the least invasive.

As explained in chapter 1 section 1.8.1.1.4, RORs have also been linked to EMT and the Wnt signalling pathway; both of which are implicated in oncogenesis in breast and ovarian cancers (Cui *et al*., 2013; Henry *et al*., 2015). Studies have shown that high levels of ROR1 expression in both ovarian and breast cancers contribute to aggressiveness of the tumour by regulation of EMT gene expression thereby leading to poor prognosis (Cui *et al*., 2013; Tan *et al*., 2016; Zhang *et al*., 2019). Through *in vivo* studies EMT has also been implicated in high-grade serous ovarian cancer invasiveness and chemo-resistance (Ford *et al*., 2014b; Haslehurst *et al*., 2012; Kurrey *et al*., 2005; Miow *et al*., 2015). It was also revealed that EMT profile of the 46 ovarian cancer cell lines in the Miow *et al.* (2015) study were able to predict cisplatin response hence signifying that mesenchymal-type cells are more chemoresistant. It has been acknowledged that EMT induces invasion and metastasis of different cancers (Lamouille *et al*., 2014).

A major signalling cascade involved in EMT regulation is the Wnt signalling pathway. There is increasing data suggesting that the Wnt receptors; RORs (ROR1 and ROR2) are

associated with poor outcome and accelerate EMT in a range of tumour types (Cui *et al.*, 2013; C. Henry *et al.*, 2015; O'Connell *et al.*, 2013, 2010; Sun *et al.*, 2015). It was also reported that the Wnt signalling pathway contributes to EMT in ovarian cancer by way of increased expression of its ligand Wnt5a (Ford *et al.*, 2014b). This study showed the imporatnce of Wnt signalling in development of ovarian cancer. The ROR receptors were found to bind to the ligand Wnt5a (Badiglian Filho *et al.*, 2009; Ford *et al.*, 2014b; Peng *et al.*, 2011). Upregulation of this ligand expression enhanced EMT and in turn correlated with a poorer prognosis (Chen *et al.*, 2013; Qi *et al.*, 2014).

Taken together, it is clear that the EMT drives chemoresistance and invasiveness of the tumour; Wnt signalling regulates the EMT process; RORs function as Wnt receptors which in turn are responsible for upstream regualtion of this pathway. Applying this configuration to our study it is evident that the cell lines with the highest expression of ROR1 possess a mesenchymal phenotype thereby being the most invasive and chemoresistant. Hence, selecting HEY cell line as the chemoresistant and invasive cell line model is valid.

3.4.4 ROR2 expression does not follow same pattern as ROR1

The gene expression levels of ROR2 were also examined in the cell line models. Although ROR2 did not appear in the biomarker discovery for this study, it was considered relevant since it is a ROR1 sister receptor. In addition to this, it also plays a vital role in the Wnt signalling pathway whose aberrant regulation has been implicated in cancer stem cell self-renewal, metastasis, and chemo-resistance (Nguyen *et al.*, 2019). The mRNA expression pattern of ROR2 in the cell line models did not completely match that of ROR1 in all the cell lines.

The OVCAR-3 cells were the only cell line in the panel whose ROR2 expression followed the same pattern as observed in ROR1 expression above (figure 3.52). As shown in the figure 3.53, levels of ROR2 significantly decreased with drug treatment. In the HEY cells, ROR2 also decreased with drug treatment with the exception of taxol treated cells. Although the SKOV-3 and OAW42 cells demonstrated a significant increase in ROR2 expression in drug treated cells this did not follow the same pattern of increase as ROR1.
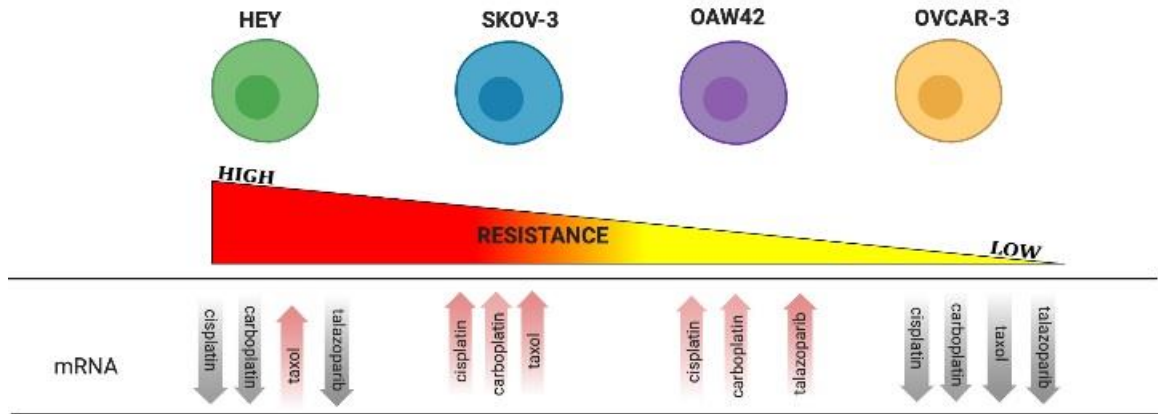
Figure3. 53 Significant changes of ROR2 expression. This is a summary of figures from section 3.3.4. The mRNA level from qPCR results in each cell line when treated with different drugs. The increase/ decrease of mRNA is relative to the non-drug treated control of each cell line. The grey arrows depict significant decrease whereas the red arrow depict significant increase. Only those drugs treated cells that demonstrated a significant change are represented in this figure. Others did not show any changes with drug treatment when compared to its respective control.

It is obvious from these results that the expression of ROR2 after drug treatment does not match the expression of ROR1 in the same cells. Although ROR2 along with ROR1 has been shown to play a role in tumorigenic behaviour such as cell migration and invasion, their expression levels seem to vary from cancer to cancer (Morioka *et al*., 2009; Rebagay *et al*., 2012). According to Gentile *et al* (2009), increased expression of ROR1 was detected among solid tumours as well as B-cell chronic lymphocytic leukaemia, B-cell acute lymphocytic leukaemia and mantle cell leukaemia (Baskar *et al*., 2008; Hudecek *et al*., 2010; Shabani *et al*., 2008). However, ROR2 is overexpressed in osteosarcoma and renal cell carcinoma as well as on primary tumours (Morioka *et al*., 2009; Wright *et al*., 2009). This could explain the varied expression levels between ROR1 and ROR2 among the cell line models in the panel.

In a recent study investigating ROR2 in human ovary tissue microarrays, it was observed that 'malignant' epithelial ovarian cancers had an increased expression however the ROR2 positive rate was extraordinarily higher in 'metastatic' tumour tissues (Xu *et al*., 2017). Similar to ROR1, published data supports the view that as an oncogene, ROR2 stimulates processes such as proliferation, migration and invasion of ovarian cancer cells (Xu *et al*., 2017). Despite studies demonstrating the correlation between high expression of ROR2 and poor prognosis (Huang *et al*., 2015; Lu *et al*., 2015; Mei *et al*., 2014; Sun *et al*., 2015, Lu *et*

al., 2012) there has been a mass of contradicting results. In study carried out by Lara *et al.* (2010), ROR2 in colon cancer cells and tissues was found to be downregulated due to hyper-methylation of promoter sites. This suppression of ROR2 was discovered to have tumour-promoting influence. This was further validated by another study where epigenetically inactivated ROR2 resulted in progression of colorectal cancer (Ma *et al*., 2016). Other studies such as that of O'Connell *et al.* (2013) also reported that ROR2-positive melanoma cells although having more invasive phenotypes were less proliferative. In contrast, the ROR2 gene was shown to be usually methylated in common carcinomas thereby functioning as a tumour suppressor (Li *et al.*, 2014). An association between loss of ROR2 protein and poor prognosis was also established in hepatocellular carcinoma (Geng *et al*., 2012). A 2017 study also indicated that in ovarian cancer ROR2 expression was closely related to the cancer grade (Xu *et al*., 2017). This study (Xu *et al*., 2017) however implied that high grade serous ovarian cancer patients with tumours of advanced FIGO stage more likely expressed lower levels or ROR2. All these studies suggest that perhaps the role of ROR2 is based on the tumour type and context.

3.4.5 Correlation between ROR1 and chemo-resistance

Overall, the HEY cells which is the most chemo-resistant in the cell line panel maintained the highest ROR1 expression at the gene and protein level. This is summarised in figure 3.52 above. Following the gene expression data of ROR1 in the cell lines, protein levels were also determined in drug treated and control untreated cells. The HEY cells maintained the highest ROR1 protein levels with decreasing expression with drug treatment. This was confirmed in immunocytochemistry using confocal microscopy (section 3.3.4.3, figure 3.13). This corresponds with what was observed in the qPCR results. ROR1 expression at the gene and protein level matched across all techniques and this consistency in the results confirm a clear correlation with chemoresistance

Similarly, in the sensitive OVCAR-3 cells ROR1 expression decreased with drug treatment at mRNA level (section 3.3.4.1 Figure 3.8). The protein levels vary between ELISA (section 3.3.4.2, Figure 3.10) and the immunocytochemistry (section 3.3.4.3, Figure 3.17) however, any changes observed were only significant in decreased ROR1 levels upon drug treatment. Unlike HEY and OVCAR-3, the other two cell lines exhibited differences in expression at the mRNA and protein level. The significant changes from qPCR data observed in both

SKOV-3 and OAW42 showed increase in ROR1 upon treatment with the platinum-based drugs. This was in contrast with the ROR1 expression of these two cell lines at the protein level where any significant changes observed were in the decrease of ROR1.

 It is evident that the mRNA expression levels from these experiments do not necessarily translate into their corresponding protein levels. This could be due to several reasons one of them largely owing to the fact that the ROR1 protein can undergo complex post translational modifications (Kaucká *et al*., 2011). These include the glycosylation and mono-ubiquitination of ROR1 which in turn regulate their localization and signalling (Kaucká *et al*., 2011). It has been shown ROR1 that is endogenous or overexpressed are both N-glycosylated and mono-ubiquitinated. This variability in modifications was observed mainly in CLL patients (Kaucká *et al*., 2011) that otherwise express unfluctuating amounts of ROR1 at mRNA and protein levels. However, this phenomenon could very well extend to other malignancies and explain the inconsistencies in ROR1 expression. According to Karvonen *et al*.(2017), mutations in the canonical motifs of RORs affects their kinase activities thereby rendering RORs into what are known as pseudokinases. This can result in them having low to no detectable catalytic activity which could also explain its varying expression in the above experiments.

Another factor which could explain the conflicting expression of ROR1 captured in the confocal images is that commercially available antibodies lack sensitivity to detect endogenous cell surface ROR1 levels. Previous studies investigating ROR1 expression focused on tissue sections (H. Zhang *et al*., 2014a; S. Zhang *et al*., 2012a) whereas here, ROR1 in cell lines were the targets. Balakrishnan *et al*. (2017) explain that transcriptional profiling and immunohistochemistry reveals 50% of ovarian cancers express ROR1 transcripts. However, immunohistochemistry analysis showed ROR1 localized in the tumour cytoplasm and nucleus while in tumour cell lines they were expressed on the cell surface. ROR1 has been described to have different splice variants. These variants either lack the extracellular domain or the transmembrane and intracellular domain (Rebagay *et al*., 2012). The ROR1 antibody used in our project had an observed molecular weight of 140 KDa. This is indicative of the presence of an N-glycosylation site (Kaucka *et al*., 2011). These post-translational modifications were observed to regulate ROR1 localization and signalling in CLL patients, therefore the same effect in ovarian cancer is not impossible (Kaucka *et al*., 2011; Hojjat-Farsangi *et al*., 2013). Additionally, these glycosylated isoforms were

suggested to be surface bound in CLL which could also explain the difference in ROR1 localization in our ovarian cancer tissues (Hojjat-Farsangi *et al*., 2013).

ROR1 is notable for selectively being highly expressed in various blood and solid malignancies as compared to low expression in normal tissues (Karvonen *et al*., 2017) To date there has been no functional studies on ROR1 in a cell line panel consisting of more than two cell lines. It is evident that ELISA experiments are necessary to further validate ROR1 protein expression which has been achieved through our study. Through these ELISA results the ROR1 protein levels were found to be strongly correlated ($R^2 = 0.99$) to chemo-resistance in cisplatin treated cells. Similarly, cells treated with carboplatin, taxol and talazoparib also strongly correlated with ROR1 protein expression (section 3.3.4.2, Figure 3.12).

Several studies have been cited above describing the role ROR1 plays in regulating EMT and additionally the role EMT plays in chemo-resistance. Therefore, it is possible to infer a link, although indirect, between ROR1, EMT and chemo-resistance. A 2020 study described how ROR1 regulates chemo-resistance which indicated a direct relation between the two (Kaucká *et al*., 2011). Although this study was conducted on breast cancer cells it provides insight into the mechanism of chemo-resistance, nevertheless. Studies that investigated the role of ROR1 in ovarian cancer explored its effects on processes that are involved in the regulation of EMT and by extension chemo-resistance (Henry *et al*., 2015; Henry *et al*., 2016; Zhang *et al*., 2014). Our study is one of the first to directly associate ROR1 expression with chemo-resistance in ovarian cancer.

3.4.6 Epithelial to mesenchymal transition markers are prevalent in chemo-resistant ovarian cancer cell line models

It has been well documented that EMT influences organized processes such as embryonic development and maintenance of adult tissue haemostasis (Nisticò *et al*., 2012; Wang *et al*., 2016). However, it also is responsible for contributing to several pathological conditions by responding to alterations in the microenvironment through inappropriate activation and abnormal stimuli (Nisticò *et al*., 2012). These disease conditions include fibrosis and cancer progression (Craene and Berx, 2013; Kalluri and Weinberg, 2009; Lamouille *et al*., 2014;

Thiery *et al*., 2009). Recent studies proving that EMT; which is reactivated during cancer progression, is linked to chemo-resistance (van Staalduinen *et al*., 2018).

As demonstrated in section 3.3.5 (figure 3.21), the inherent expression of mesenchymal EMT markers is higher in the cells with the mesenchymal phenotype while the epithelial EMT marker was higher in the cells with epithelial phenotype. Figure 3.54 provides an overall pattern of expression of EMT markers in the drug treated cells used in this project. Here, expression of key EMT molecules such as Vimentin, E-Cadherin and N-Cadherin were observed in the established ovarian cancer cell line models. As mentioned in chapter 1, the downregulation of epithelial; E-cadherin and expression of mesenchymal; Vimentin and N-Cadherin molecules were cited to be associated with EMT. The gene expression data in section 3.3.5 revealed the effect of resistance profiles on the expression of the above mentioned EMT markers. The HEY and SKOV-3 cells, which represent mesenchymal and intermediate mesenchymal phenotypes respectively demonstrated no significant change in vimentin expression in drug treated cells relative to its non-drug treated control cells. However, in both cell lines cisplatin treatment was associated with an increase in vimentin. In contrast, mesenchymal markers were significantly decreased in the chemotherapy sensitive OVCAR3 and OAW2 cells following drug treatment.
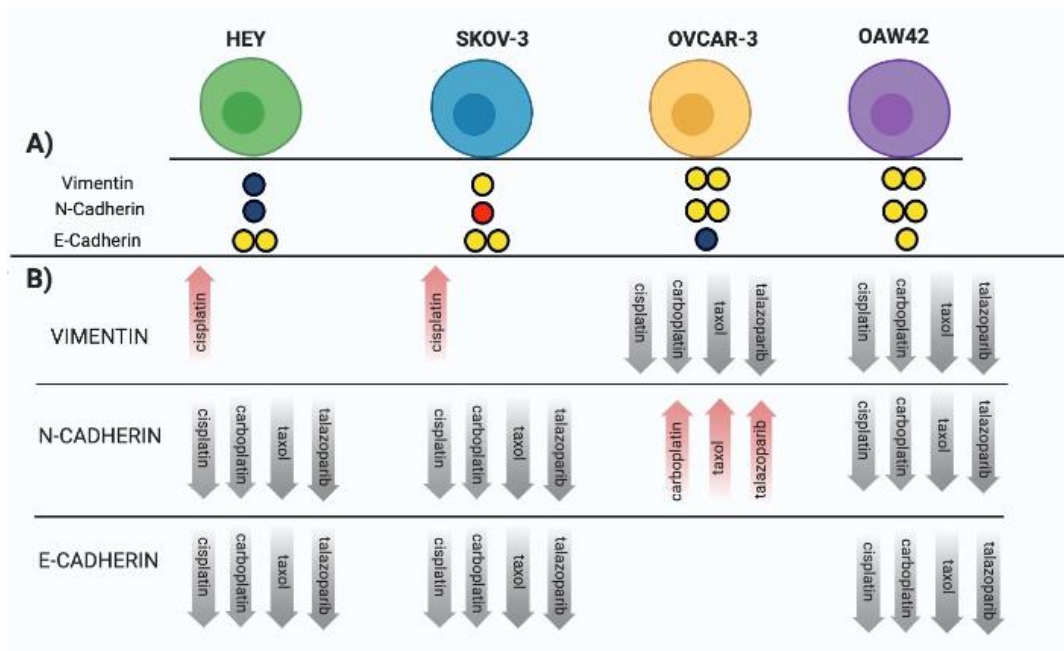
Figure 3.54 Significant changes of EMT markers expression. This is a summary of figures from section 3.3.5. A) The top row represents cell lines (untreated) expressing either mesenchymal or epithelial markers relative to the control. The circle filled in black represent the cell line selected as the control. The circle in red represents increase while yellow signifies decrease in expression. Two circles indicate statistical significance. B) The mRNA level of Vimentin, N-Cadherin and E-Cadherin from qPCR results in each cell line when treated with different drugs. The increase/ decrease of mRNA is relative to the non-drug treated control of each cell line. The grey arrows depict significant decrease whereas the red arrow depict significant increase. Only those drugs treated cells that demonstrated a significant change are represented in this figure. Others did not show any changes with drug treatment when compared to its respective control.

With HEY cells experiencing a two-fold increase after cisplatin treatment, it exhibited highest expression of vimentin across the cell line panel. This result aligns with the suggestion that EMT is linked to chemo-resistance which is validated by the case that HEY cells being the most resistant had the highest level of expression for the mesenchymal marker, vimentin. N-Cadherin which is considered to also be a mesenchymal marker and a hallmark of EMT (Loh *et al*., 2019) displayed significantly lower expression with drug treatment relative to the untreated control in all the cell lines (section 3.3.5, Figures 3.22-3.25). Interestingly, the expression levels of N-Cadherin in cisplatin treated OVCAR-3 cells showed no significant change in expression when compared to the untreated control. This is relevant as the expectation was that this mesenchymal marker should match the outcome seen with vimentin and more specifically in chemotherapy resistant HEY cells. Since OVCAR-3 cells fall within the chemotherapy sensitive category of the cell line panel it was expected to have lower expression levels of N-Cadherin. This signifies that tracking the phenotype switch during EMT based on the expression of a single gene marker does not

completely represent the complicated nature of the process and is not sufficient to validate whether cells undergoing EMT are chemo-resistant (Wang *et al.*, 2016). As such the approach taken in our study overcomes this limitation by examining the three EMT markers considered.

The expression of the epithelial marker E-cadherin has been reported to also be a hallmark of EMT. E-Cadherin's downregulation indicates EMT and as such enhances metastasis, chemo-resistance and tumour stem-ness (Loh *et al.*, 2019). In all the cell lines of the panel a significant downregulation in E-cadherin was observed except for the chemo-sensitive cell line; OVCAR-3. The cell line HEY displayed the lowest expression of the epithelial marker once again confirming the suggestion that repression of E-cadherin results in the transition to mesenchymal phenotype in EMT and development of chemo-resistance (Russell and Pranjol, 2018; Wang *et al.*, 2017). According to Miow *et al.* (2015), ovarian cancer cell lines with mesenchymal type cells are more chemo-resistant and therefore can help predict responses to platinum-based drugs such as cisplatin.

3.4.7 Simultaneous knockdown of ROR1 and ROR2 re-sensitizes ovarian cancer cells to platinum

The results from our project demonstrated sensitization of cells to platinum-based drugs when undergoing double knockdown of ROR1 and ROR2. Additionally, it demonstrates the impact of ROR on more reliable cell line models since HEY and OVCAR-3 cells underwent an elaborate process for selecting it as the resistant and sensitive ovarian cancer cell line models. However, what sets our study apart is that the individual and simultaneous knockdowns of ROR1 and ROR2 were carried out in a chemo-resistant and a chemo-sensitive cell line model; HEY and OVCAR-3 respectively. These knocked-down cells were also drug treated with a range of drugs in addition to cisplatin. This allowed for a more clinically appropriate model in order to investigate development of chemo-resistance in ovarian cancer patients. The chemo-resistant cell line model HEY showed significant sensitivity to cisplatin when subjected to a simultaneous knockdown of ROR1 and ROR2 when treated with the IC50 dose of cisplatin. Similar sensitivity to double the IC50 dose of cisplatin was observed with the identical simultaneous knockdown conditions. In addition to cisplatin, the HEY cells were also treated with carboplatin and chemo-sensitization was

once again observed. This occurred when treated with the IC50 dose of carboplatin in cells that underwent simultaneous knockdown of ROR1 and ROR2.

In the chemo-sensitive cell line model; OVCAR-3, cells appeared to have an improved response to the IC50 dose cisplatin when they underwent simultaneous ROR1 and ROR2 knockdown. This response to cisplatin was also evident when cells were treated with double the IC50 dose. Unlike the chemo-resistant cell model, the OVCAR-3 cells were sensitised to double the IC50 dose of cisplatin when singular knockdown of ROR2 was carried out. In the Henry *et al.* (2015) study, it was hypothesised that ROR2 expression was upregulated in ovarian-cancer patients. The ovarian cancer cell line model used in the study for knockdown assays was also OVCAR-3 as it expresses both ROR1 and ROR2. It was shown that ROR1 and ROR2 both regulated invasion and migration. There was significant reduction in these processes when knocked down individually. Additionally, it was shown that ROR1 and ROR2 synergistically regulated these processes upon simultaneous knockdown where once again there was significant reduction. However, it must be noted that the exact mode of signalling of ROR1 and ROR2 are still unclear although Henry *et al.*'s (2015) functional results propose ROR1 and ROR2 may in fact be operating in separate pathways to deliver different invasion and migration results. This same approach can be applied to the drug response seen in the results of our study. Having used the cell line model (OVCAR-3) this somewhat validates the effect of ROR2 knockdown to different cisplatin doses.

The effects of ROR1 knockdown has been observed in different cancers including ovarian cancer (Cetin *et al.*, 2019; Cui *et al.*, 2013; C. E. Henry *et al.*, 2016a; S. Zhang *et al.*, 2012a). ROR1 has been implicated in processes such as enhanced tumour cell growth, epithelial to mesenchymal transition and metastasis (Hojjat-Farsangi *et al.*, 2013; S. Zhang *et al.*, 2012b, 2012a). However, limited information is available regarding the role of ROR1 in chemo-resistance. As mentioned earlier (section 3.3.4.1), in the cell line panel with varying drug resistance profiles, resistant cell line model (HEY) presented with highest expression of ROR1. This cell line also exhibited highest percentage of invasion among other cell lines in the panel.

Studies have been carried out examining the role of ROR1 and its sister receptor ROR2 in metastasis by investigating important characteristics, adhesion, invasion and migration (Henry *et al.*, 2015; Henry *et al.*, 2016). It was observed in these studies that upon

knockdown of ROR1 and ROR2, cell migration and invasion was significantly inhibited in a cisplatin resistant cell line model (A2780-cis). So far there has been only one study that explored the association of ROR1 and ROR2 with chemo-resistance (Henry *et al.*, 2016) It reported that the simultaneous knockdown of both ROR1 and ROR2 had a minor but significant sensitizing effect on the A2780-cis cells to cisplatin. However, it was mentioned in earlier the lack of appropriateness of using A2780 cells as a standard HGSOC model (Beaufort *et al.,* 2014; Domcke *et al.*, 2013). Therefore, knockdown results using a resistant model of A2780 cells may present a level of unreliability. Our project overcomes this limitation through the development of the cell line panel thereby selecting a more appropriate cell line model to study knockdown effects of RORs.

The results from our study aligned with the results demonstrated in the Henry *et al.* (2016) study indicating that ROR1 and ROR2 do affect chemo-resistance. This is further validated by the correlation observed between ROR1 and chemo-resistance discussed above and shown in section 3.3.4.2 figure 3.12. In another Henry *et al.* (2015) study it was confirmed that singular knockdown of either ROR1 and ROR2 had no significant effect on the proliferation and adhesion of cells. The effect of individual and double knockdown of ROR1 and ROR2 on migration and invasion was significant suggesting that these receptors have play a major role in the progression of ovarian cancer. Additionally, EMT markers were also evaluated post knockdown. It revealed singular knockdown of ROR1 and ROR2 significantly decreased the expression of vimentin. Oddly, double knockdown resulted in an increased expression of vimentin although this was not significant. Our project exclusively reviewed the gene expression levels of EMT markers prior to ROR1 and ROR2 knockdown as a means to build the phenotypic profiles of the selected cell line models. We emphasised earlier the necessity of including more than one EMT marker as reliable evidence for the involvement of EMT regulation. Although we did not profile EMT markers post knockdown it is evident that a pre-knockdown profile such as the one created in our study would have supplemented the post knockdown EMT data produced in the 2015 study (Henry *et al.*, 2015).

Kajiyama *et al.* (2007) described EMT as a characteristic of chemo-resistant cells *in vitro.* Silencing of EMT transcription factors (Snail and Snug) induced chemo-sensitivity in cisplatin resistant ovarian cancer cell line models (Henry *et al.*, 2016). These transcription factors are believed to strongly repress E-cadherin and induce EMT in ovarian cancer

(Kurrey *et al*., 2005). Taking into account these transcription factors and the effect simultaneous knockdown of ROR1 and ROR2 has on chemo-resistant ovarian cancer cells, it was hypothesised that these knockdowns result in the reversion of EMT (Henry *et al*., 2016). Perhaps a post knockdown EMT profile as presented in the above-mentioned study (Henry *et al*., 2015) would have further assisted in understanding the link between EMT and RORs in ovarian cancer cells.

Although both HEY and OVCAR-3 models presented increased sensitivity to cisplatin upon knockdown of ROR 1 and 2, no such sensitisation effect was observed when individually treated with carboplatin and talazoparib in the OVCAR-3 cells. However, the HEY cells showed an increased response to carboplatin with simultaneous ROR1 and ROR2 knockdown. This may be due to the different mechanism of action of each drug and therefore the pathways which ROR knockdown interrupts may not directly impact response of the cells to the drug treatment.

ROR1 and ROR2 *in vitro* modulation emphasised the distinct role each receptor plays as well as their synergistic effects. Therefore, in our project it is necessary to recognize that neither receptor was completely silenced although they were drastically reduced. Since studies have shown that the efficacy of silencing regulates the extent of invasion and migration inhibition, further studies would benefit from stable knockdown cell lines through short hairpin RNA (shRNA) (Henry *et al*., 2017) . Therefore, the results of our project can function as a vital roadmap for what to expect with these further studies.

Chapter 4

Investigation of Rab27b as a potential second biomarker

4.1 Introduction

Rab27b expression has been reported to correlate with cancer development and progression (Dong *et al*., 2012; Hendrix *et al*., 2010b). It is expressed in different secretory epithelial cells and functions as important elements involved in exosome secretion which is essential in progression and metastasis of cancer (Li *et al*., 2017; Rajagopal and Harikumar, 2018; Weidle *et al*., 2016; Zhao *et al*., 2016). A 2020 systematic review and meta-analysis (Koh *et al*., 2020) revealed that high expression of both Rab27a and Rab27b were significantly associated with metastasis in seven types of cancer (renal cell carcinoma, lung cancer, ovarian cancer, pancreatic cancer, colorectal cancer, breast cancer and hepatocellular cancer). Although this was the first meta-analysis conducted to evaluate the association between the expression of Rab27b with survival in solid cancers, it presents several limitations. These include the small sample population and sizes of the cancer types investigated and the cut off values selected to determine expression in the different studies. In ovarian cancer, the expression of Rab27b was found to associate with certain clinic-pathological features (Ren *et al*., 2016). This study also revealed that Rab27b was expressed in malignant ovarian tumours, borderline ovarian tumours and benign ovarian adenoid tumours however, level of expression reduced in borderline ovarian tumours. This suggests that increase in Rab27b expression occurs with development of tumours in the ovarian tissues further increases with the incidence of cancer.

In the biomarker discovery stage Rab27b was identified as one of the genes that was differentially expressed as described in chapter 1 section 1.8.1. The validation of Rab27b as a potential biomarker for chemoresistance was carried out by examining its expression in publically available ovarian cancer gene expression datasets using OvMark (Madden *et al*., 2014). The OvMark analysis was initially carried out in combination with ROR1 and demonstrated improved survival outcome in patients with increased expression of Rab27b as shown in chapter 1 figure 1.7. This was contrary to several of the published studies where increased Rab27b expression was associated with poorer survival outcome.

Further Ovmark analysis of Rab27b expression in all ovarian cancer patient datasets revealed that the pattern of expression supported the initial hypothesis set out at the biomarker discovery stage of this project (chapter 1 section 1.8.1). Lower Rab27b expression was associated with poor progression free survival (hazard ratio = 0.86, p = 0.049) as shown in

figure 4.1 (A) suggesting a link between Rab27b expression and platinum drug resistance. When data was filtered into FIGO stage 3 ovarian cancer the same pattern of (low) expression was observed (Figure 4.1 B). However, this analysis was not significant, presumably due to the low patient numbers. Patients grouped into FIGO stage 4 (metastatic) showed low Rab27b expression when analysed and these patients had an improved prognosis (Figure 4.1 C). This matched what was observed in the Ren *et al* (2016) study cited earlier, where increased distant metastasis was associated with increased Rab27b expression.
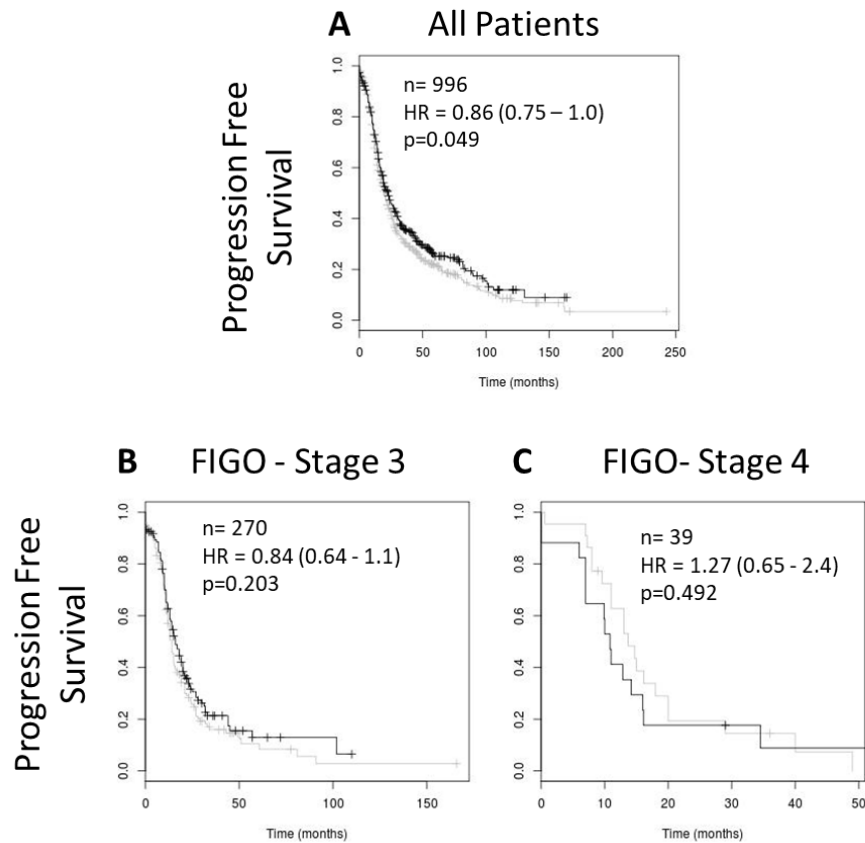
Figure4. 1 Progression-Free Survival Analysis of RAB27B Gene Expression in Ovarian Cancer Patients from Ovmark platform. A) All Patients B) FIGO Stage 3 C) FIGO Stage 4. Patient samples are divided on the median into high and low expressers of each given gene. The black line indicates expression above the median and grey indicates expression below the median.

HR: Hazard ratio, p: P-value, n: number of patients

The contradiction in Rab27b expression in different studies emphasises the need to investigate it as a potential biomarker. This can perhaps provide greater insight into the role of Rab27b in ovarian cancer and more importantly chemoresistance.

4.2 Methods

4.2.1 cDNA conversion and qPCR

Expression levels of Rab27b in the cell lines were assessed using qPCR as described in chapter 2. Both drug treated and untreated samples of each cell line underwent cDNA conversion prior to qPCR as described in chapter 2 section 2.2 Results were analysed using Roche LightCycler 96 software and statistical analysis was performed as described in chapter 2 section 2.4.

4.2.2 Enzyme-linked immunosorbent assay: Rab27b

The cell pellets were prepared as described in chapter 2 section 2.1.7 for a sandwich ELISA kit (Abbexa Ltd). to detect levels of the RAB27B protein in both control and drug treated cells for each cell line. A 1mL standard solution of 2.5ng/mL was prepared and serially diluted (1:2) seven times so as to form an eight-point standard curve. A 96-well plate pre-coated with a RAB27B specific antibody was seeded with 100 µL of the diluted standards as well as cell lysate samples (drug treated and untreated of four cell lines) in duplicates.

The standard diluent buffer (provided by the kit) was also added to the wells set up as the control (zero). The plate was then sealed with a cover film and incubated at 37°C for one hour. The contents of the plate were discarded and 100µL of 1X detection reagent A (provided by kit) was added to each well. The plate was sealed and incubated again for an hour at 37°C. The solution in the plate was discarded followed by washing three times with a wash buffer provided by the kit. Each well was filled with 350µL of wash buffer followed by a 1-2-minute soak between each wash. This is followed by adding a 100uL of detection reagent B (provided by kit) to each well and the plate was incubated for 30 min at 37°C. The plate was washed 5 times each time letting the wash buffer soak for 1-2 minutes. After discarding the wash buffer, the plate was thoroughly dried before adding 90 µL of the TMB substrate into each well. The plate was sealed and incubated at 37°C for 10-20 minutes while avoiding exposure to light. To each well 50 µL of stop solution provided by the kit was added while gently tapping the plate to ensure thorough mixing. Using the Omega FLUOStar (BMG Labtech) plate reader, the optical density of each well was determined. The wavelength was set to 450nm with a correction set to 570nm.

4.2.3 Immunocytochemistry and confocal microscopy (ICC)

Cells were prepared for visualization and examination of Rab27b protein using the protocol described in chapter 2 section 2.3

4.2.4 Statistical Analysis

Minitab was used to carry out statistical analysis to investigate mRNA expression of Rab27b from qPCR. A one sample t-test was used to account for statistical significance of mRNA expression from qPCR. GraphPad Prism was also used to interpolate values of Rab27b in drug treated and untreated cells in ELISA. The one-way ANOVA was used to compare expression levels. The correlation between resistance and Rab27b expression was determined by the Pearson's correlation coefficient. The one-way ANOVA test was used to account for statistical significance in both ELISA in the expression levels of the biomarkers in the cell lines (with each drug treatment). A one sample t test was carried out to examine the significant expression levels of Rab27b protein visualized in the (drug-treated) cells by ICC.

4.3 Results

4.3.1 Expression of Rab27b in cell line panel

4.3.1.1 mRNA expression levels of Rab27b in cell line panel

In order to determine whether Rab27b expression was related to chemoresistance, mRNA expression studies using a qPCR assay was undertaken for each of the four cell lines: HEY, SKOV-3, OVCAR-3 and OAW42. Similar to chapter 3 section 3.3.4.1 the expression profile of Rab27b was first normalized and compared against the most resistant cell line HEY (Figure 4.2). The mRNA levels of Rab27b were significantly (-2.5-fold) lower in SKOV-3 ($p<0.05$), -2-fold in OVCAR-3 and OAW42 ($p<0.001$) compared to HEY.
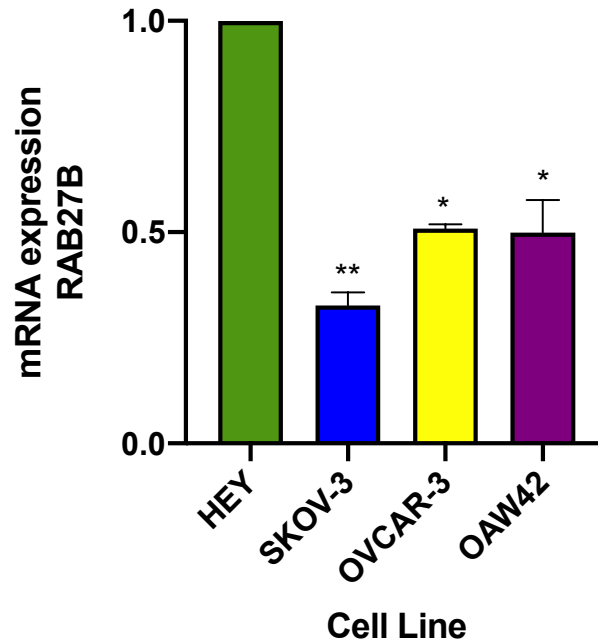
Figure4. 2 qPCR of all four cell lines demonstrating Rab27b expression. Relative mRNA expression of all cells is untreated and reflect the expression profile relative to the most resistant. cell line; HEY. Experiment repeats of n=3 was carried out. HEY cell line set to a constant of 1.0 on the Y-axis. A one-sample t-test was carried out with '*' and '**' denoting significance of $p<0.05$ and $p<0.01$ respectively.

The bar graphs below (Figure 4.3) show varying levels of expression in drug treated and control (untreated) cells for each cell line. The expression levels were normalized to their respective controls. The expression of Rab27b in cisplatin treated HEY cells had an increase in expression relative to the control however this was not statistically significant. Other drug treated HEY cells also did not show any significant change in expression compared to the control. Similar to the cisplatin treated HEY cells, the cisplatin treated SKOV-3 cells showed an increase (2.5-fold) in Rab27b expression however it was significant ($p<0.001$) relative to the control. Other drug treated cells were did not exhibit any significant change in expression. In the OVCAR-3 cell line, all the drug treated cells showed a significant -3-downregulation ($p<0.01$) of Rab27b compared to the control. OAW42 cells displayed a similar pattern to the HEY cells. The cisplatin and carboplatin treated cells showed an increase in Rab27b expression than the control but was not significant.
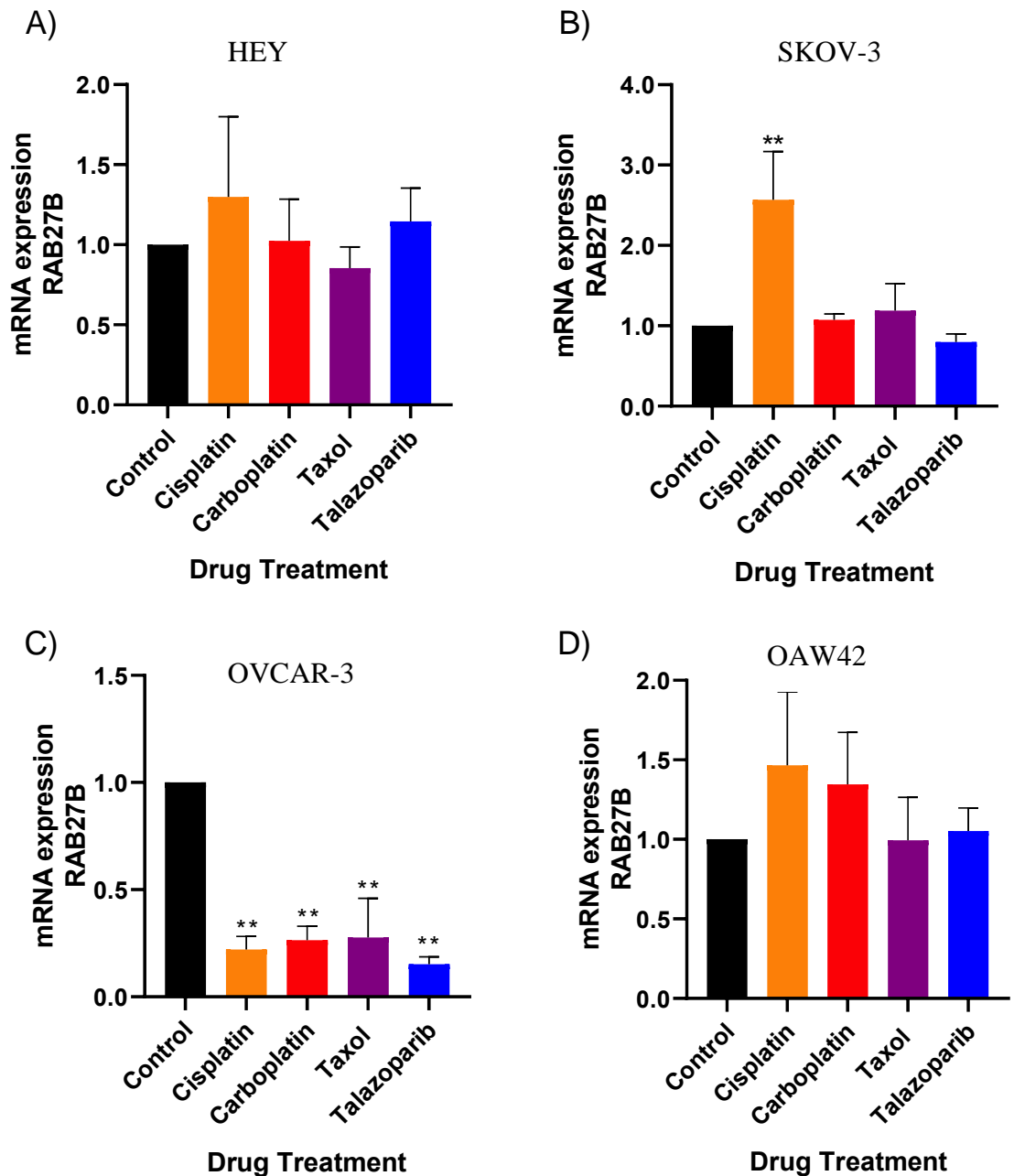
Figure4. 3 A qPCR assay shows varying levels of Rab27b expression in response to drug treatment in cell line panel. Relative mRNA expression of Rab27b in A) HEY, B) SKOV-3, C) OVCAR-3 and D) OAW42 cell lines treated with four drugs: cisplatin, carboplatin, taxol and talazoparib. Experiment repeats of n=3 was carried out. Cells treated with drugs are compared to their respective control (non-drug treated) to determine the change. Control cells set to a constant of 1.0 on the Y-axis. A one-sample t-test was carried out with '**' denoting significance of $p < 0.01$.

4.3.1.2 Analysis of Enzyme Linked Immunosorbent Assay (ELISA): Rab27b

An eight-point standard curve was plotted shown in the figure 4.4 following the protocol described in section 4.2.2.
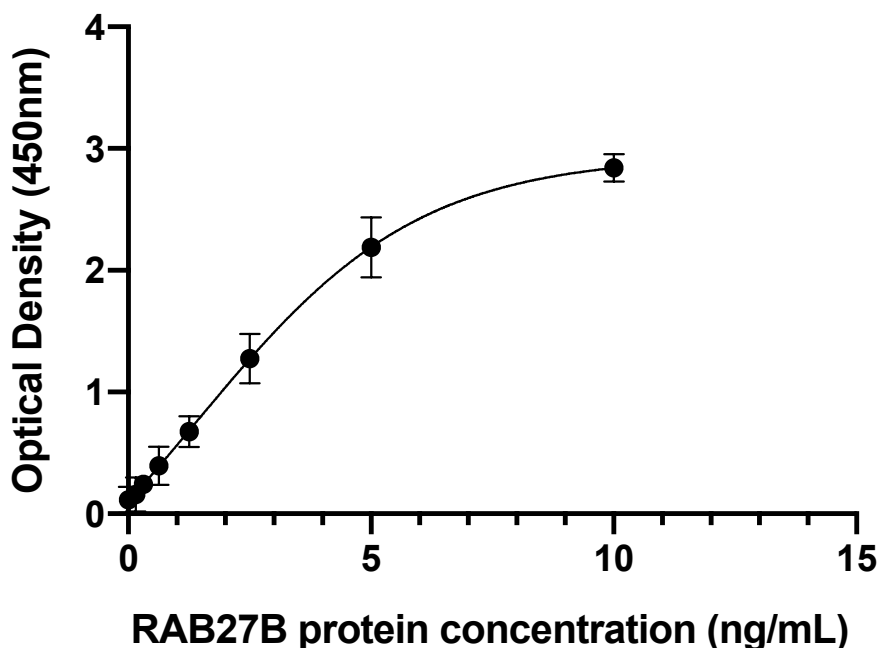
Figure4. 4 Standard curve plotted of Rab27b standards in sandwich ELISA. An eight-point standard curve plotted to interpolate Rab27b protein concentration in the four cell lines (n=2).

Rab27b protein expression in the four cell lines (HEY, SKOV-3, OVCAR-3 and OAW42) was quantified using a sandwich ELISA.. The protein concentrations in the non-drug treated control and drug treated cells were interpolated (figure 4.5) from the seven-point standard curve shown above. No significant difference in Rab27b protein concentrations was observed between the drug treated and control cells. In the SKOV-3 cells, the taxol treated cells expressed higher ($p < 0.01$) levels of Rab27b protein by 2.5-fold than the control cells, cisplatin, carboplatin and talazoparib treated cells. Control cells of the OVCAR-3 cell line comprised of significantly lower ($p < 0.01$) levels of Rab27b protein by -2-fold in comparison to its drug treated cells. However, protein levels were not significantly different between cisplatin treated and carboplatin treated cells but were both significantly ($p < 0.01$) higher than taxol and talazoparib treated cells by 1.5-fold.

In control OAW42 cells, Rab27b protein was higher ($p < 0.05$) than all the drug treated cells except taxol treated cells. These (taxol-treated) cells exhibited higher ($p < 0.05$) Rab27b

protein levels than the cells treated with cisplatin and carboplatin. Although the cells lines showed varying levels of Rab27b protein, interestingly Rab27b was higher in the HEY cell lines compared to the other cell lines tested.
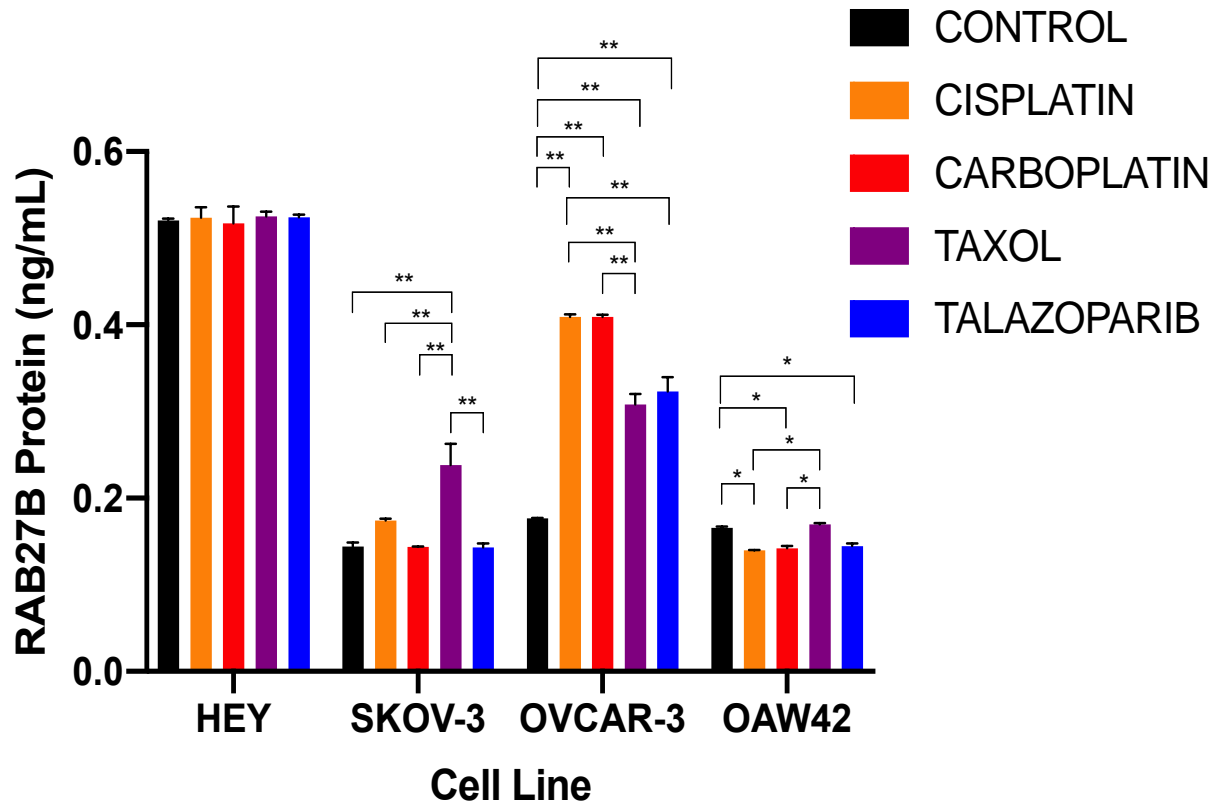
Figure4. 5 Protein levels of Rab27b in each cell line with different drug treatments was determined using a sandwich ELISA (n=2). Each cell line showed varying levels of Rab27b protein level with drug treatment. A one-way ANOVA comparing Rab27b levels in drug treated and untreated cells for each cell line was carried out. '*' and '**' denotes statistical significance of $p<0.05$ and $p<0.01$ respectively. A post hoc analysis using Tukey's test was carried out.

Similar to ROR1, correlation graphs were plotted (Figure 4.6) to determine if Rab27b was associated with chemoresistance. A weakly positive correlation was observed between the expression of Rab27b, and cisplatin ($R^2 = 0.3988$) and carboplatin ($R^2 = 0.2430$) treated cells. The weaker correlation is largely due to the relatively high level of Rab27b protein present in OVCAR3 cells. There was a positive strong correlation between Rab27b levels and both taxol ($R^2 = 0.9632$) and talazoparib ($R^2 = 0.9235$) treated cells. In all cases, HEY cells exhibited the highest levels of Rab27b and since it has been established as the most resistant cell line (chapter 3 section 3.3.2) there is validity in the strong association between chemoresistance and Rab27b. However, it is interesting that this association lies with taxol and talazoparib resistance.
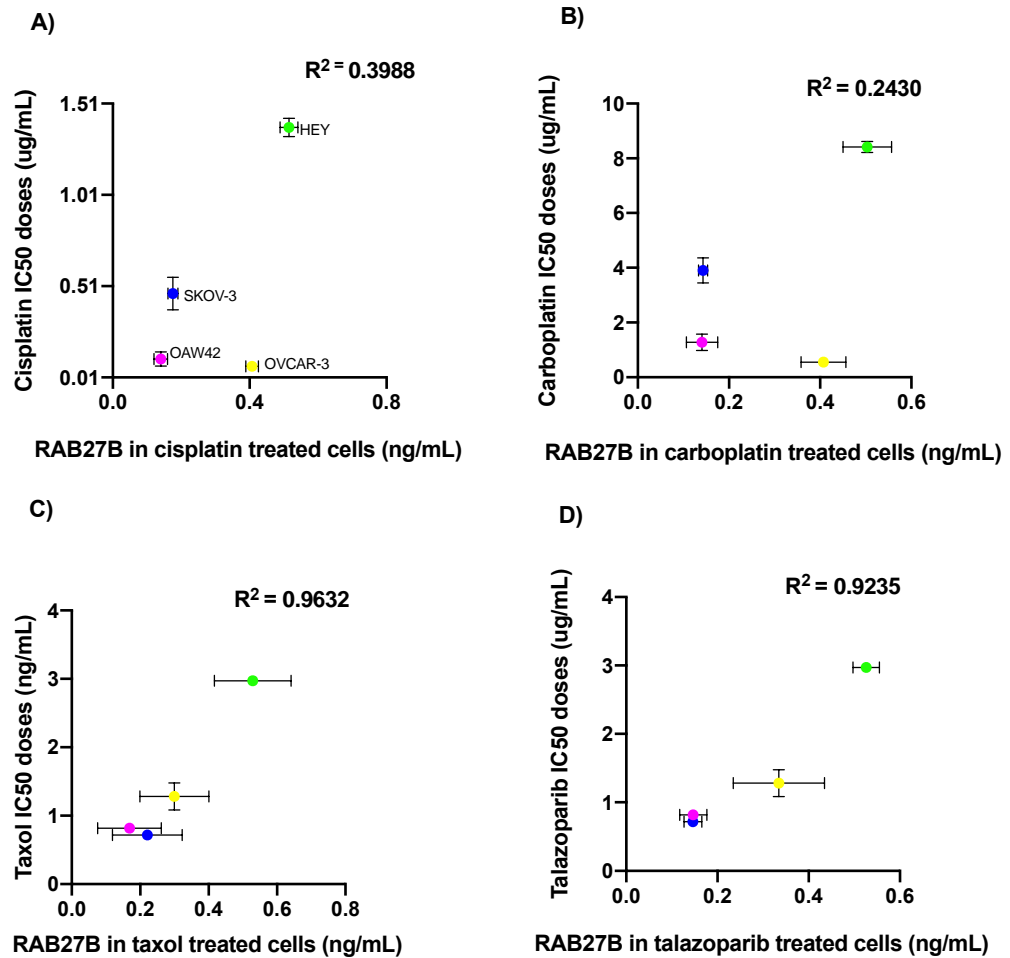
Figure4. 6 Correlation between the expression of Rab27b and the IC50 doses of all drug treatments in the cell line panel. There is a weakly positive correlation between Rab27b and chemoresistance in A) cisplatin and B) carboplatin but with p values of 0.3685 and 0.5071 representing no significance respectively. However, a strong positive correlation was observed in C) taxol (p<0.0186) and D) talazoparib (p<0.0390) treated cells. The x-axis represents the Rab27b protein levels interpolated from the ELISA described in section 4.3.1.2. The y axis represents the IC50 doses of each drug determined through cytotoxicity assay as described in chapter 2 section 2.1.6. The Pearson coefficient is displayed on top right corner of each correlation graph.

4.3.1.3 Confocal microscopy of cells after Immunocytochemistry (Rab27b)

Confocal images captured below (Figure 4.7) show the Rab27b expression in HEY control and drug treated cell line. The FITC label (green) indicates the Rab27b expression increases with drug treatment compared to the control.

FITC · DAPI · Merged FITC + DAPI

Carboplatin

50 uM · 50 uM · 50 uM

FITC · DAPI · Merged FITC + DAPI

Taxol

50 uM · 50 uM · 50 uM
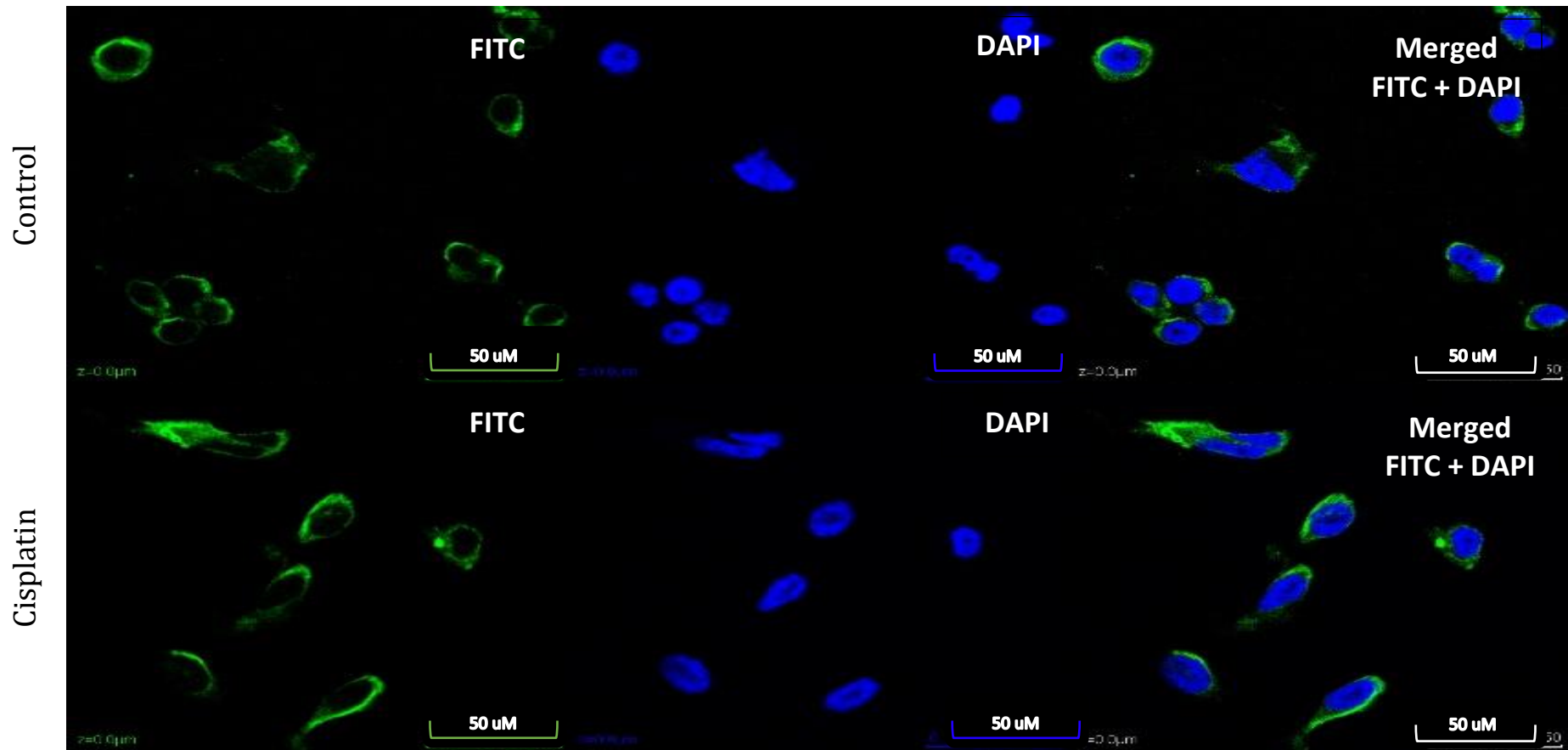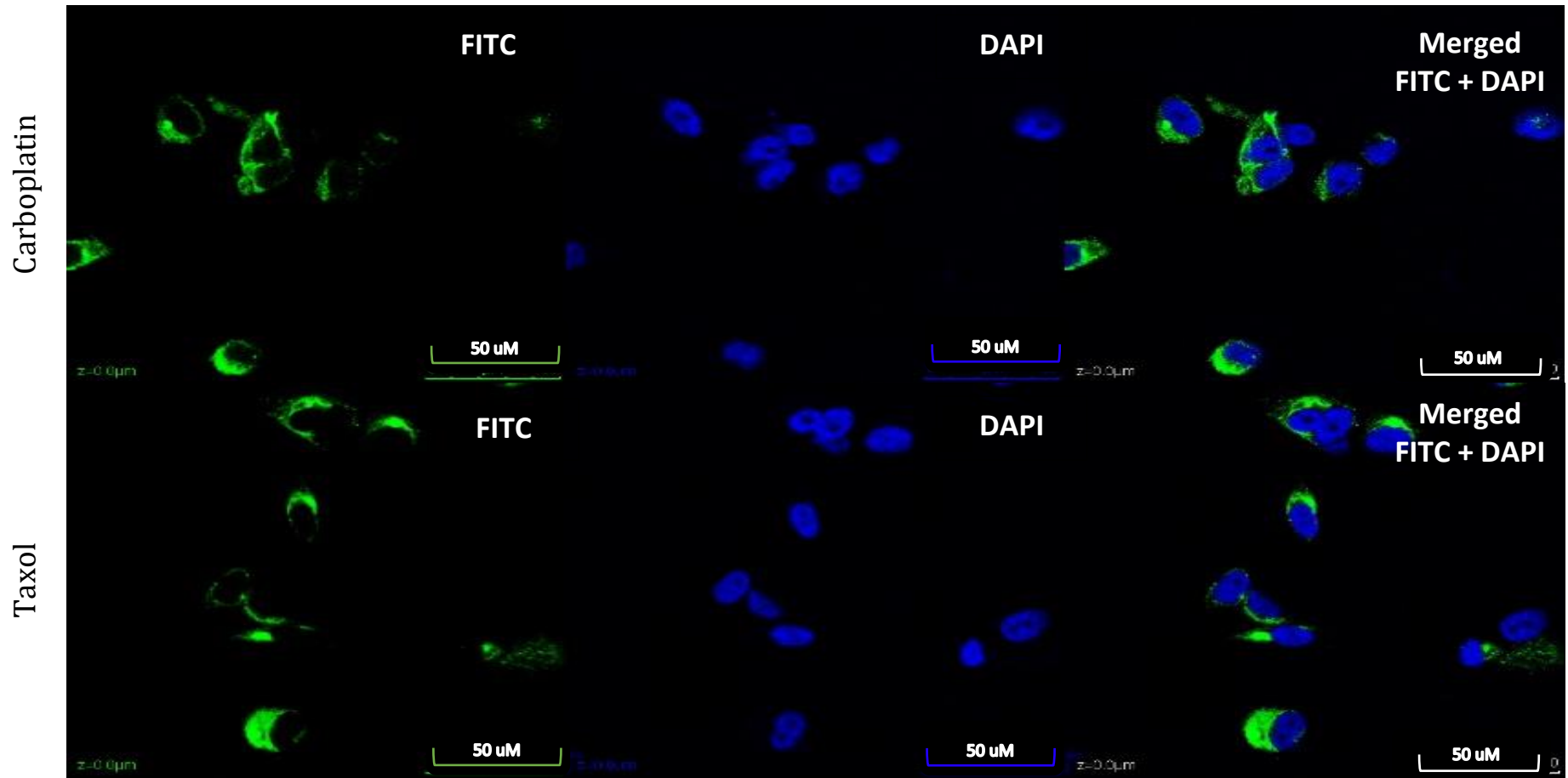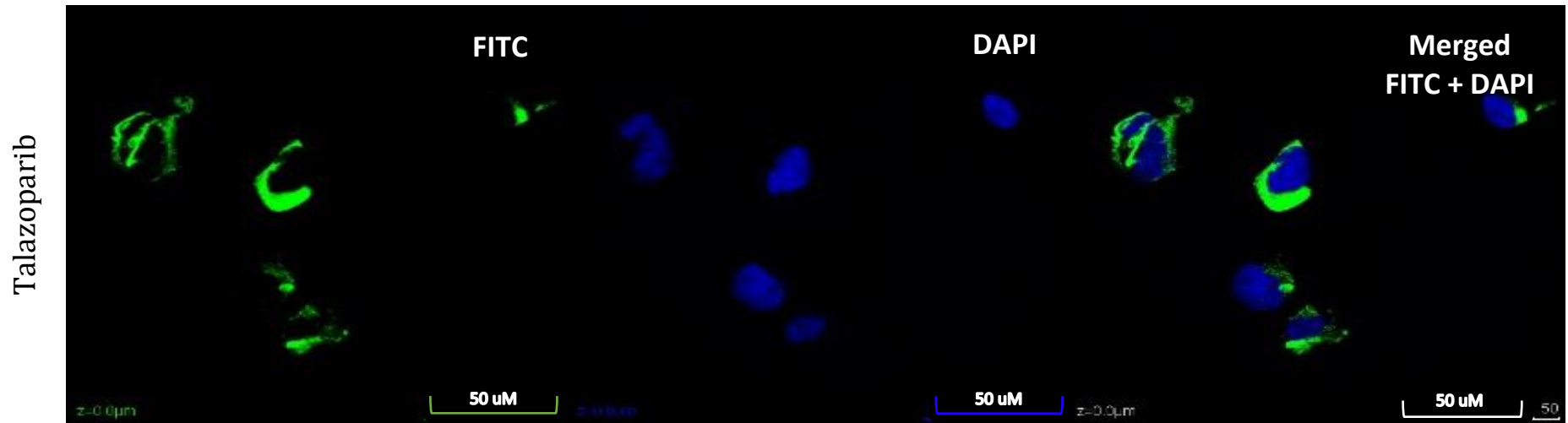
Figure4. 7 Confocal microscopic images of Rab27b expression (green) in HEY cell lines with drug treatments. Cells were counterstained with DAPI to show the localization of the nucleus. Images were captured at 10X magnification.
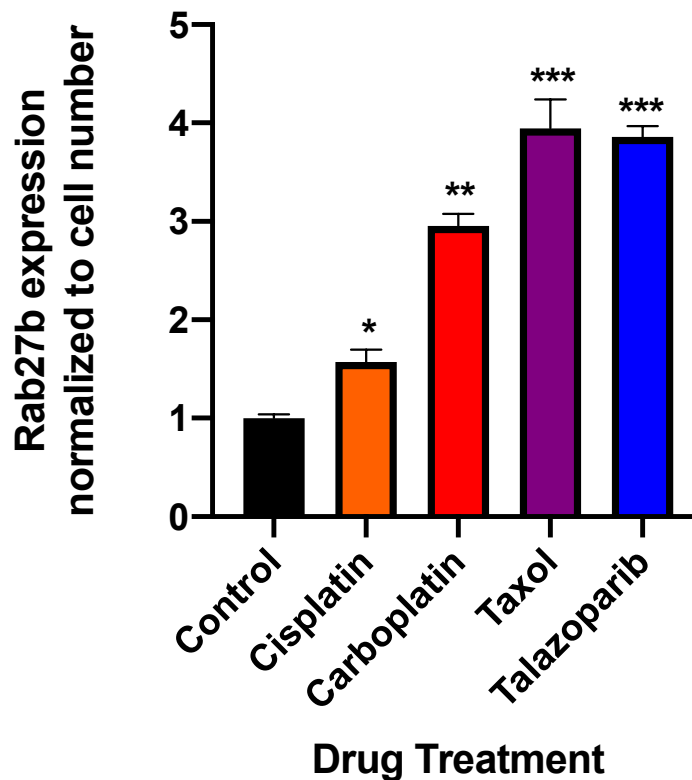
Figure4. 8 Measurement of Rab27b expression of drug treated HEY cells from confocal microscopy images. Intensity of ROR1 in drug treated cells measured relative to control untreated cells and normalized to cell number. A one sample t-test was carried out with '*', '**' and '***' denotes statistical significance of $p<0.5$, $p<0.01$ and $p<0.001$.

Rab27b expression was normalized to cell number in drug treated cells and all drug treated cells showed a significant increase in expression relative to control (untreated) cells (cisplatin; $p<0.05$, carboplatin; $p<0.01$, taxol and talazoparib; $p<0.001$). These increases in Rab27b expression ranged from two to four-fold. (Figure 4.8).

Confocal images captured below (Figure 4.9) show the Rab27b expression in SKOV-3 control and drug treated cell line. The FITC label (green) indicates the Rab27b expressed in the cisplatin, carboplatin and taxol treated cells. Talazoparib treated cell visually appear to have negligible protein expression.
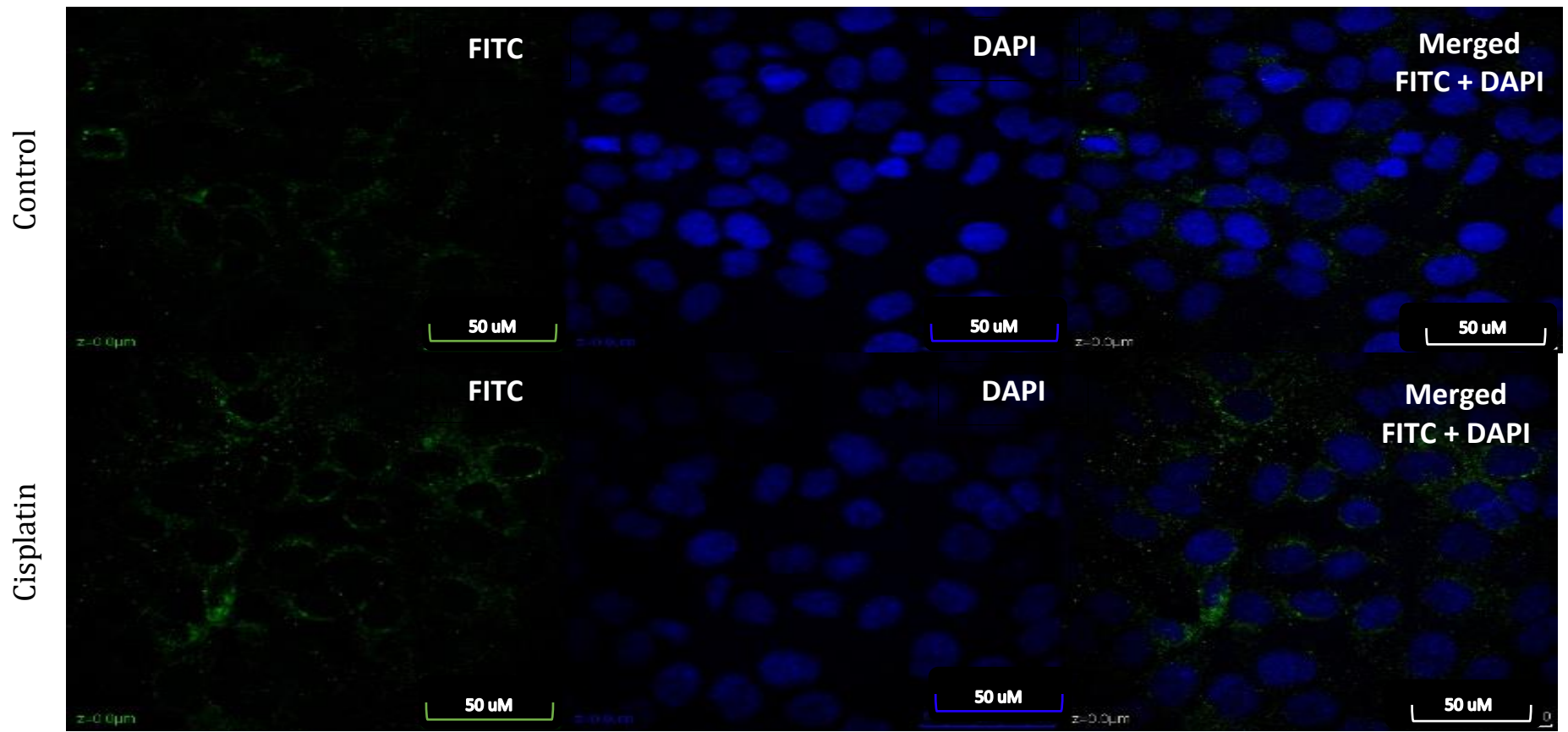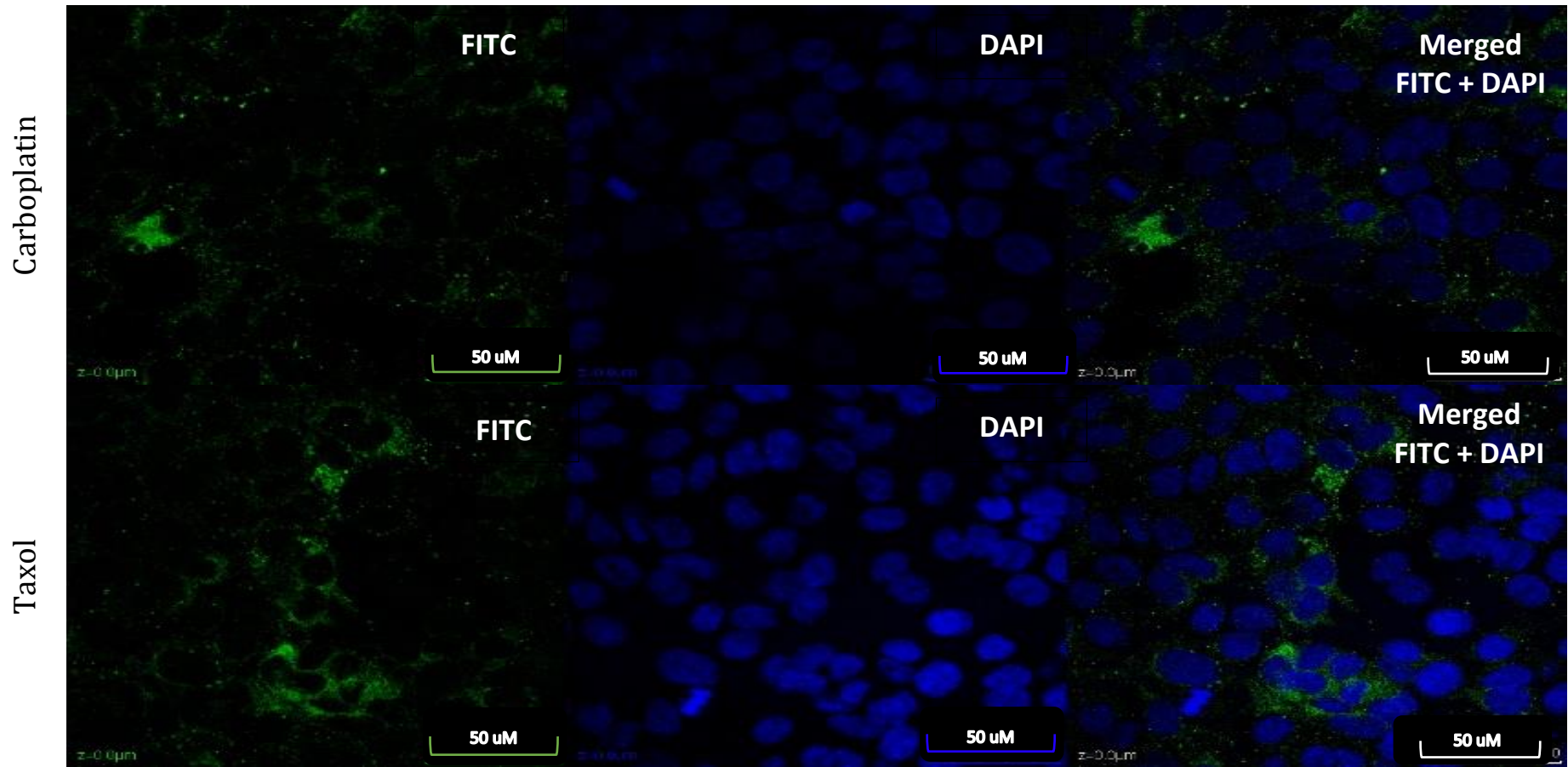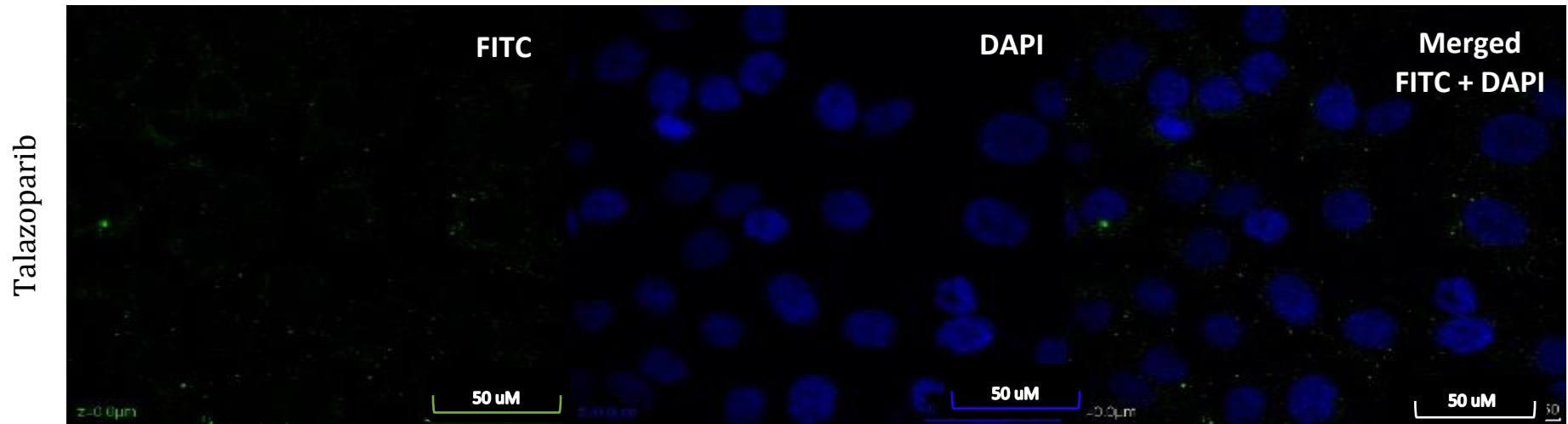
Figure4. 9 Measurement of Rab27b expression of drug treated SKOV-3 cells from confocal microscopy images. Cells were counterstained with DAPI to show the localization of the nucleus. Images were captured at 10X magnification.
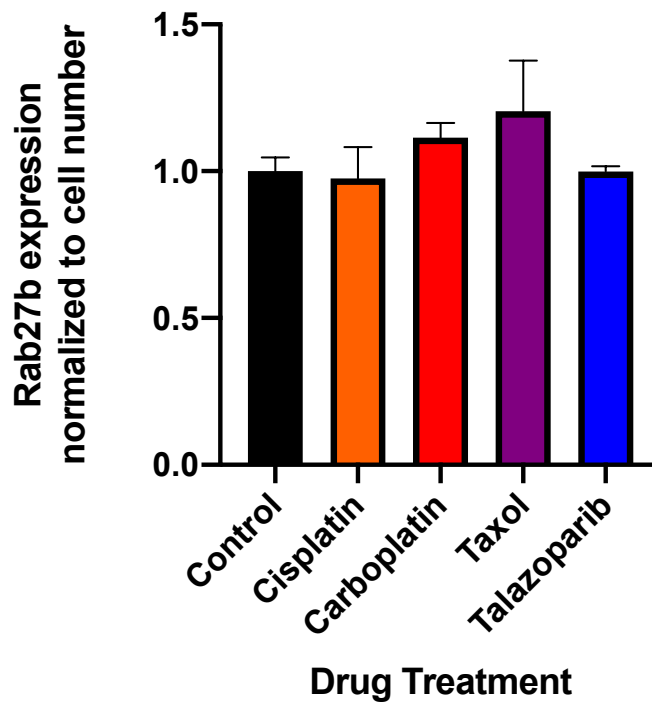
Figure4. 10 Measurement of Rab27b expression of drug treated SKOV-3 cells from confocal microscopy images. Intensity of ROR1 in drug treated cells measured relative to control untreated cells and normalized to cell number. A one sample t-test was carried out with no statistical significance observed.

Rab27b expression was normalized to cell number in drug treated SKOV-3 cells. Although protein levels seem to increase with drug treatment in the confocal image (figure 4.10), the graph shows there was no significant increase in any of the drug treated cells.

Confocal images captured below (Figure 4.11) show the Rab27b expression in OVCAR3 control and drug treated cell line. The FITC label (green) indicates the Rab27b expression increases with drug treatment compared to the control similar to HEY cells.

Carboplatin

FITC

DAPI

Merged
FITC + DAPI

50 uM

50 uM

50 uM

Taxol

FITC

DAPI

Merged
FITC + DAPI

50 uM

50 uM

50 uM
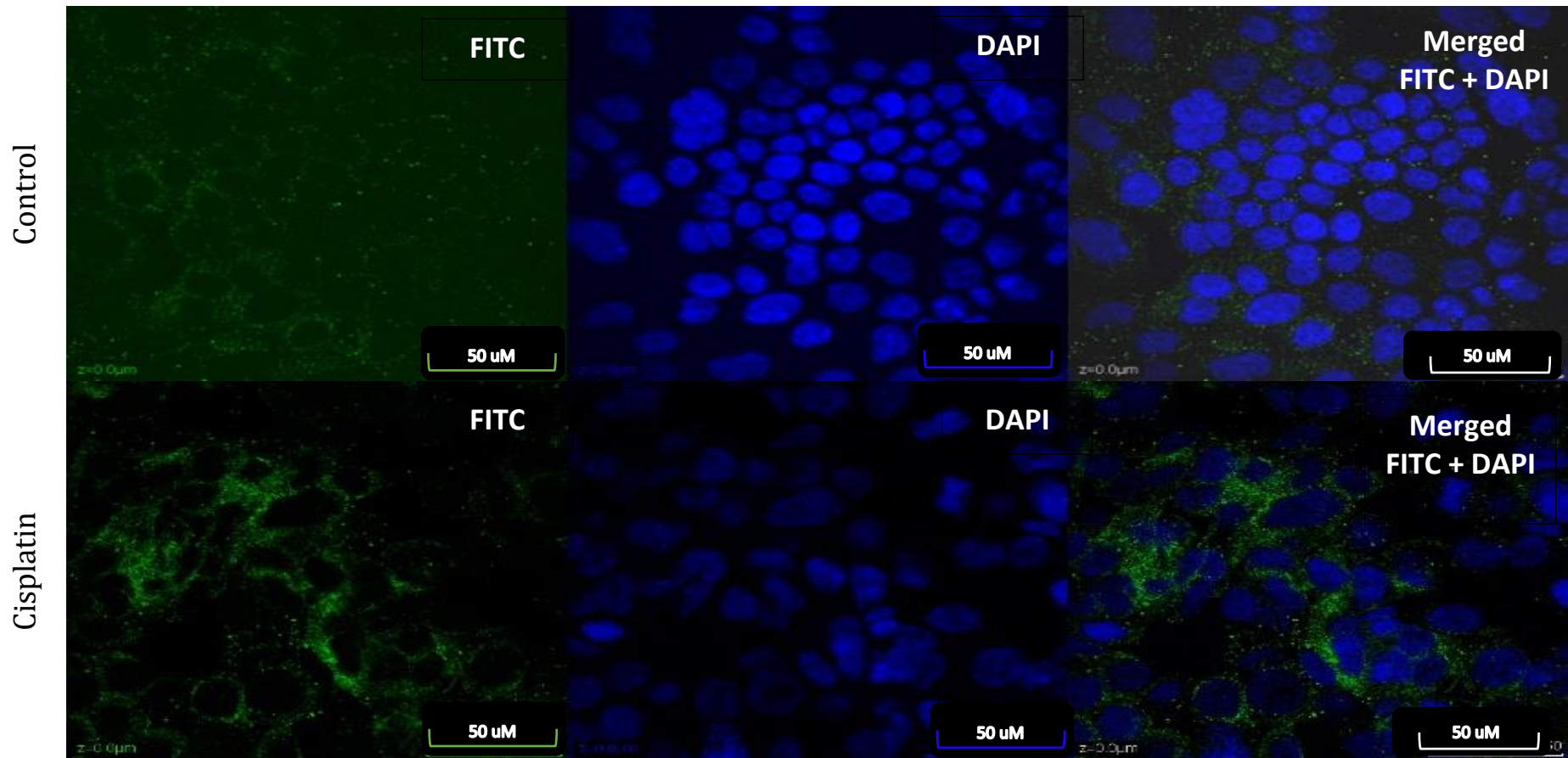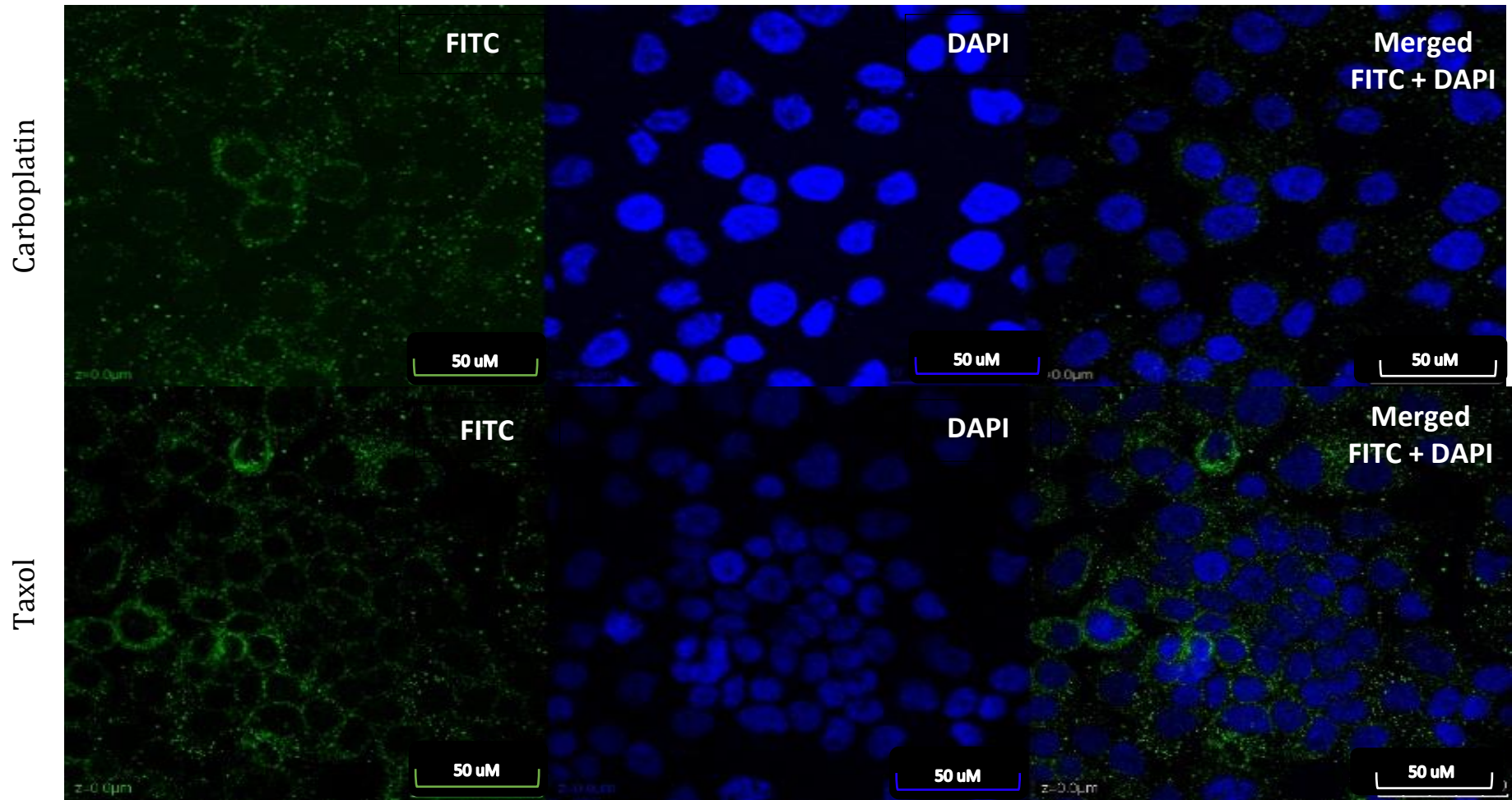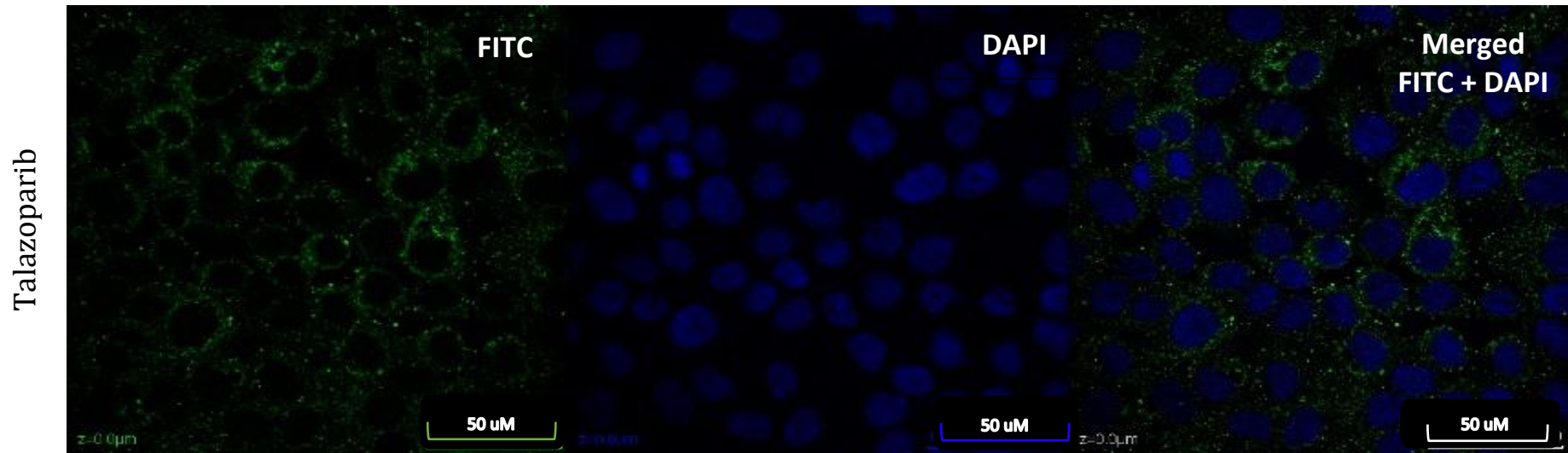
Figure4. 11 Confocal microscopic images of Rab27b expression (green) in OVCAR-3 cell lines with drug treatments. Cells were counterstained with DAPI to show the localization of the nucleus. Images were captured at 10X magnification.
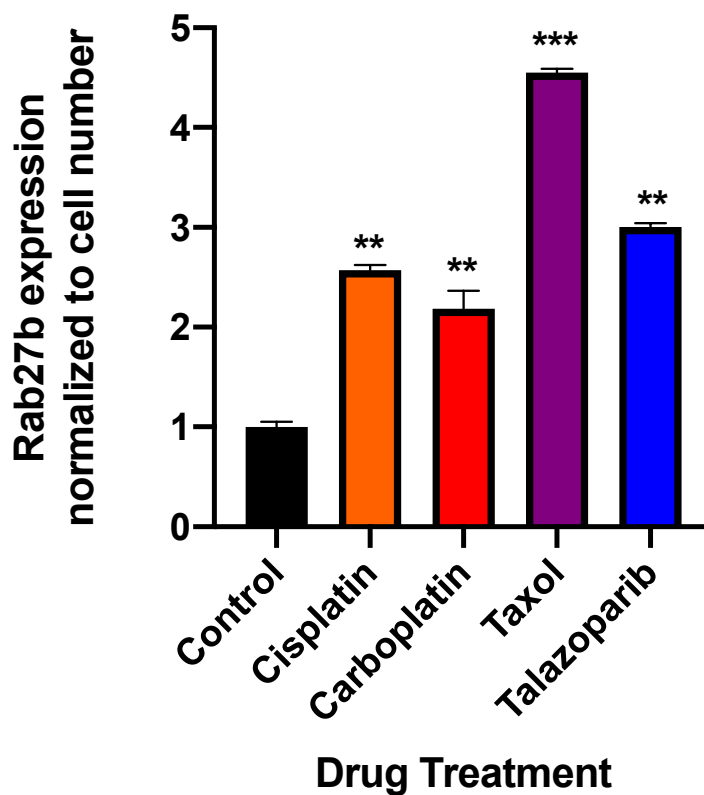
Figure4. 12 Measurement of Rab27b expression of drug treated OVCAR-3 cells from confocal microscopy images. Intensity of ROR1 in drug treated cells measured relative to control untreated cells and normalized to cell number. A one sample t-test was carried out with '**', '***' denotes statistical significance of $p<0.01$ and $p<0.001$.

Rab27b expression was normalized to cell number in drug treated OVCAR-3 cells (Figure 4.12). Protein levels significantly increased in all drug treated cells. Cisplatin and carboplatin treated cells saw a significant 2.5fold increase ($p<0.01$) while taxol and talazoparib saw a 4.5- and 3-fold increase ($p<0.001$) respectively of protein level compared to the untreated control.

Confocal images captured below (Figure 4.13) show the Rab27b expression in OAW42 control and drug treated cell line. The FITC label (green) indicates visible Rab27b expression in all but cisplatin and talazoparib treated cells.
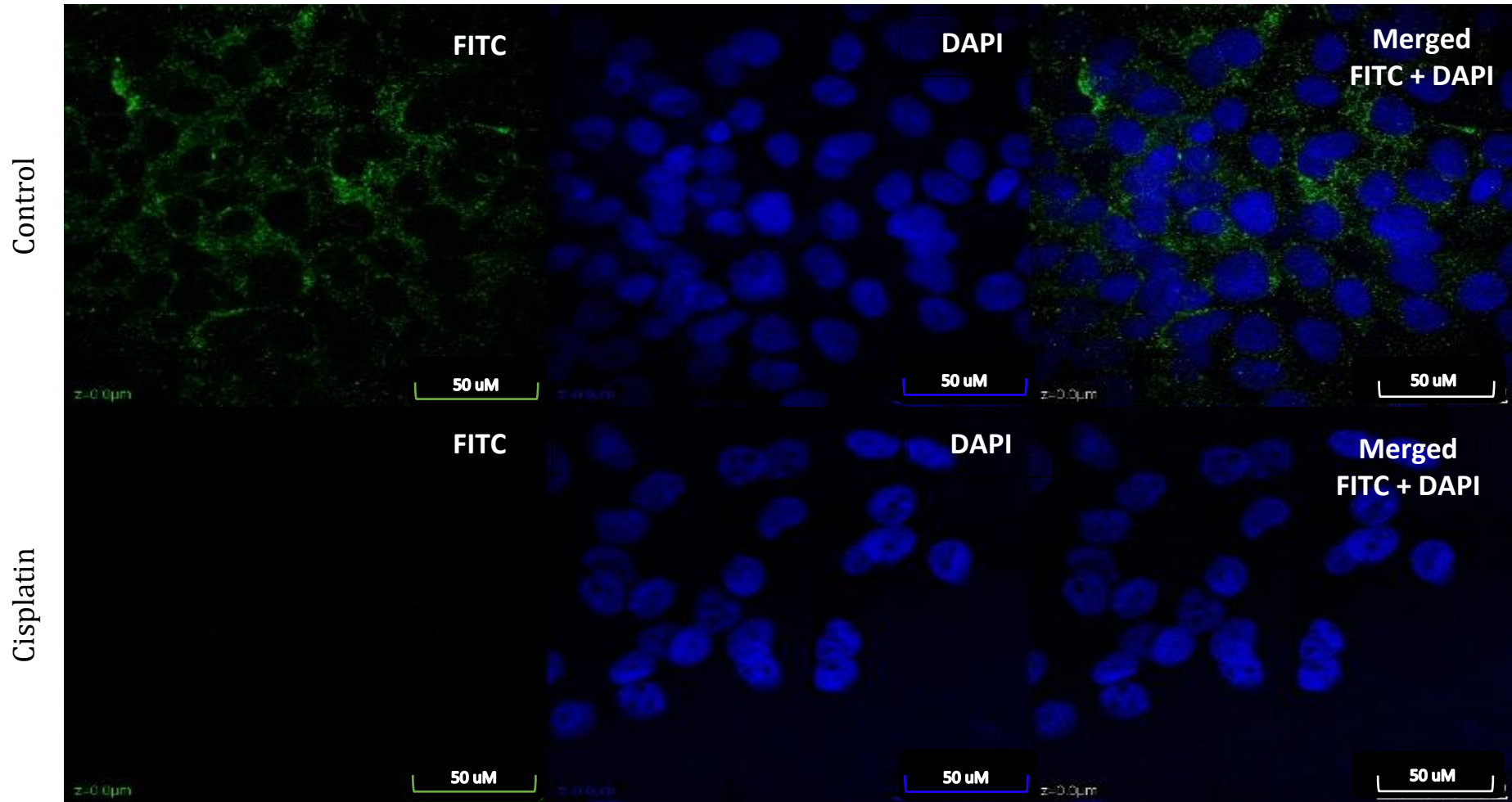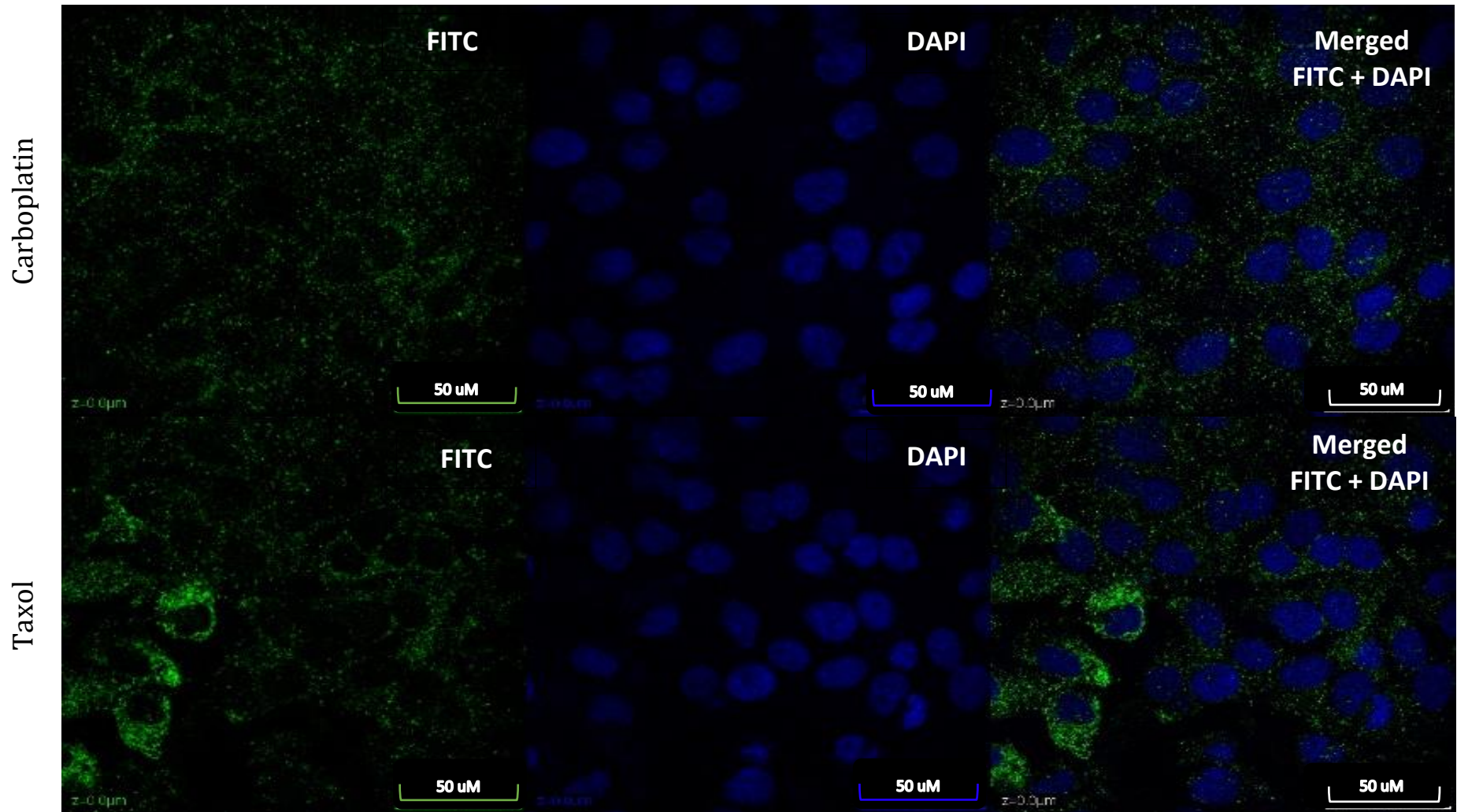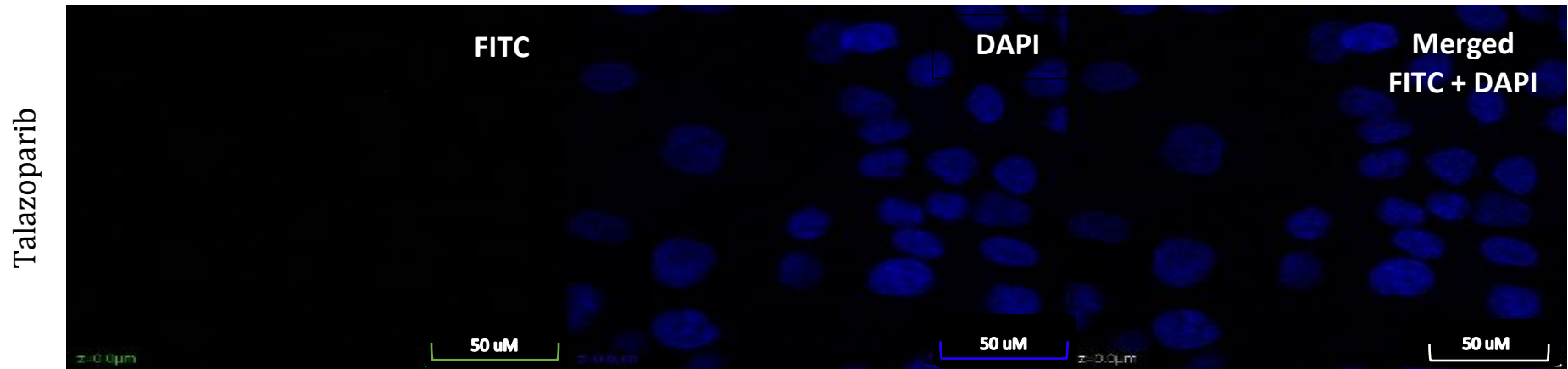
Figure4. 13 Confocal microscopic images of Rab27b expression (green) in OAW42 cell lines with drug treatments. Cells were counterstained with DAPI to show the localization of the nucleus. Images were captured at 10X magnification.
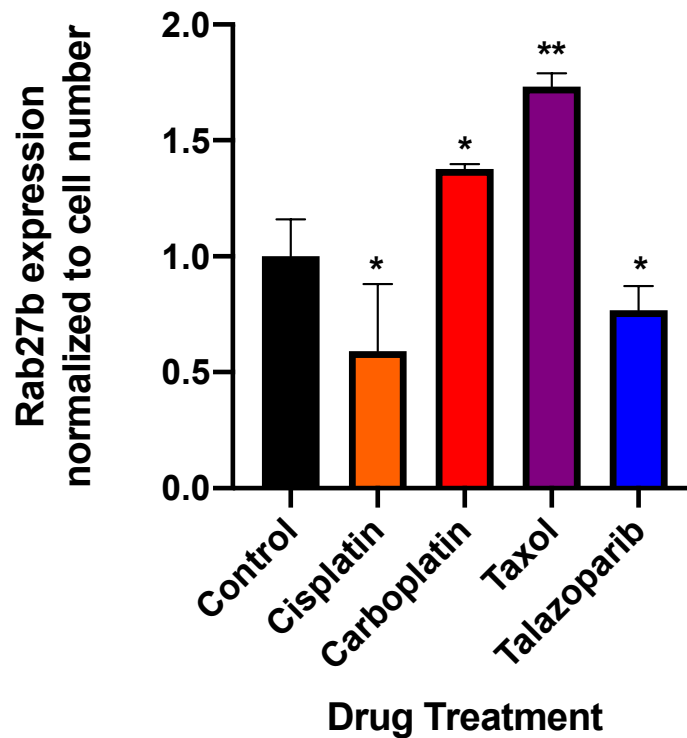
Figure4. 14 Measurement of Rab27b expression of drug treated OAW42 cells from confocal microscopy images. Intensity of ROR1 in drug treated cells measured relative to control untreated cells and normalized to cell number. A one sample t-test was carried out with '*', '**' denotes statistical significance of $p<0.05$ and $p<0.01$.

Rab27b expression was normalized to cell number in drug treated OAW42 cells (Figure 4.14). Protein levels significantly increased in carboplatin ($p<0.05$) and taxol ($p<0.01$) treated cells. Cisplatin and talazoparib treated cells saw a significant decrease ($p<0.05$) in Rab27b protein levels compared to the control.

4.4 Discussion

4.4.1 Rab27b: contradiction in expression

There is mounting evidence that suggests genes associated with trafficking of vesicles and exocytosis contribute to cancer progression. Much of this evidence implicates the Rab family; a subfamily of the Ras superfamily of small G proteins (Palmer *et al*., 2002; Wright, 2008). Several members of the Rab family such as Rab4, Rab11, Rab14, Rab23, Rab25, Rab35, as well as the Rab27 subfamily have been studied in cancer (Tzeng and Wang, 2016). A set of Rab proteins were identified promoting tumour cell migration and invasion by controlling intracellular signal transductions (Cheng *et al*., 2004; Hendrix *et al*., 2010b; Tzeng and Wang, 2016; Wheeler *et al*., 2015; Yoon *et al*., 2005). This show cases the role they play in tumorigenesis and metastasis. As described in chapter 1 (section 1.8.2), Rab27 consists of two isoforms: Rab27a and Rab27b. Although both have 71% of the amino acid sequence identical (Pereira-Leal and Seabra, 2001) and employ the same effector proteins (Fukuda, 2003), they were shown to possess different functions even within the same cell type (Johnson *et al*., 2010).

The selection of Rab27b from the biomarker discovery stage of this project (Chapter 1, section 1.8) hypothesised that lower expression was associated with poor prognosis in all ovarian cancer patients (Chapter 1, figure 1.7). However, this seems to be in contradiction to most of the literature that has been published so far. A 2010 study by Ostrowski *et al*., described the different roles of Rab27a and Rab27b in HeLa cells with the former regulating docking and membrane fusion of multi-vesicular endosomes whereas the latter is involved in transferring membranes to the multi-vesicular endosomes from the trans-Golgi network. Since the role of Rab27a and Rab27b are crucial for the maintenance of cellular function, their aberrant expression may result in the development of cancers (Li *et al*., 2018).

Several cancers have demonstrated association of oncogenic traits with the overexpression of Rab27b. In estrogen receptor (ER)-positive breast cancer cells the upregulation of Rab27b stimulates metastasis both *in vitro* and *in vivo* (Hendrix *et al*., 2010a, 2010b; Zhang *et al*., 2012). In hepatocellular cancer (HCC), Rab27b proteins were found to be upregulated in drug resistant cells and extracellularly transported drugs by exosome mediated efflux (Li *et al*., 2020). Another study demonstrated that Rab27b expression was correlated with tumour progression in HCC patients(Dong *et al*., 2012). In squamous cell carcinoma of the lung,

high Rab27b expression was shown to be an unfavourable prognostic factor. Tumours with distant metastasis also showed higher expression levels of both Rab27a and Rab27b (Koh and Song, 2019). In pancreatic ductal adenocarcinoma (PDAC), high protein expression of Rab27b as well as p53 were found to be associated with invasion and distant metastasis. Furthermore, high Rab27b expression showed a strong correlation with poor overall patient survival (Zhao *et al*., 2016). Similar Rab27b results were observed in colorectal cancer (CRC) where high elevated level of Rab27b led to tumour metastasis and poor patient prognosis (Bao *et al*., 2014).

So far, there is only one study investigating the role of Rab27b in ovarian cancer (Ren *et al*., 2016). The results from this study were consistent with previous findings described in the studies above. In the Ren *et al* (2016) study, poorly differentiated patient tissue specimens showed higher levels of Rab27b compared to well differentiated specimens. Other clinical features such as histological type, tumour grade and tumour stage were also found to be associated with Rab27b expression. Similar to the 2012 study (J.-X. Zhang *et al*., 2012) described earlier, lymph node and distant metastasis were also linked to increased Rab27b in ovarian cancer patients. The results from the Ren *et al* (2016) study also described Rab27b as a novel predictor for metastasis in ovarian cancer. When patient samples were grouped based on the Rab27b expression, a Kaplan Meier curve revealed that 80% of those with low expression had 5-year survival rate. In contrast, only 29% of patients with high Rab27b expression had a cumulative 5-year survival rate. This confirms the significant correlation Rab27b -positive tumours have with poor overall survival. These results present strong clinical value in Rab27b for the assessment of ovarian cancer patient prognosis.

There are limited number of studies that are in agreement with the hypothesis set out in this project regarding Rab27b expression. In 2017, Worst *et al*. validated *in silico* data that showed Rab27b as well as Rab27a, consistently under expressed in metastatic prostate cancer. The dataset from Tomlins *et al.* (2007) also demonstrated both genes being under-expressed in localized prostate cancer. According to Worst *et al*. (2017) the contrast in the expression of Rab27b may be attributed to assay and readout conditions. In addition to this, the cell lines used represent entities of different cancers which differentially regulate the expression and function of Rab27a and Rab27b. Because cell lines originate from different micro environmental conditions, the role of extracellular vesicles of malignant cells remains unclear. This particularly applies in the context of immune evasion (Yanfang Liu *et al*., 2015;

Lundholm *et al*., 2014) and the activation of the immune system against the tumour cells (W. Li *et al*., 2013). Therefore, this indicates that there is a component of regulation on extracellular vesicle biogenesis and secretion.

Montel *et al* (2005) showed that Rab27a and other genes associated with metastasis play a significant role in vesicle trafficking and are differentially expressed in breast cancer murine xenograft models (Montel *et al*., 2005). Additionally, the invasive and metastatic potential of human breast cancer cells was associated with overexpression of Rab27a and showed a strong correlation to lymph node metastasis and poor patient prognosis. Interestingly, there was no detection of Rab27b expression reported in these breast cancer cells (Wang *et al*., 2008). However, other studies such as those mentioned earlier (Hendrix *et al*., 2010a, 2010b; Zhang *et al*., 2012) reported increased expression of Rab27b and described its role in invasion, size of the tumour and metastasis of ER positive breast cancer cells. The data from this study is inconsistent with Wang *et al*.'s (2008) study and could be due to several factors such as the different research models and varied sample sizes.

4.4.2 Rab27b mRNA and protein expression is varied across the cell lines

The level of Rab27b expression was first compared within the cell line panel in untreated cells. Since the HEY cell line was established as the most resistant it was normalized as the control. The chemotherapy-sensitive cells OVCAR-3 and OAW42 displayed higher levels of Rab27b compared to SKOV-3 cells although all were lower compared to HEY cells. Following on from the updated Ovmark analysis described earlier, it can be assumed this is in line with what was hypothesized; the lower the expression of Rab27b the greater the link to resistance. The figure below represents the expression patterns at the mRNA level and protein level.
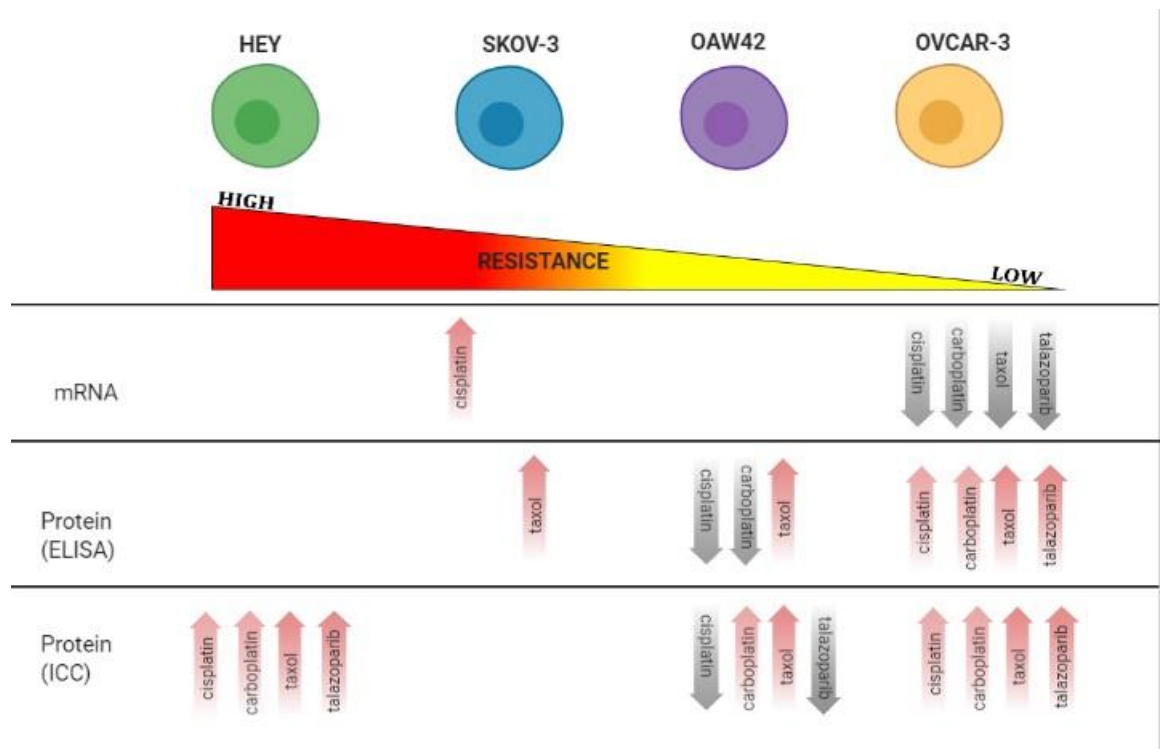
Figure4. 15 Significant changes of Rab27b expression. The mRNA level from qPCR results and protein level from ELISA and immunocytochemistry (ICC) results in each cell line when treated with different drugs. The increase/ decrease of mRNA is relative to the non-drug treated control of each cell line. The increase/ decrease of protein is absolute and depiction in the figure above is in comparison to untreated control cells. The grey arrows depict significant decrease whereas the red arrow depicts significant increase. Only those drugs treated cells that demonstrated a significant change are represented in this figure. Others did not show any changes with drug treatment when compared to its respective control.

With drug treatment, most cells at the mRNA level showed no significant change relative to their respective untreated controls. Only the cisplatin treated SKOV-3 cells showed a significant increase in Rab27b expression compared to its control. Additionally, the sensitive cell line OVCAR-3 showed a dramatic decrease in Rab27b expression when subjected to drug treatment (Figure 4.15). Although the changes were not significant the remaining cell lines presented slightly elevated levels of Rab27b. This presents as a complication in the understanding of Rab27b expression patterns. The drug treatments seem to switch Rab27b expression in the same direction as those described in previously mentioned studies (Ren *et al*, 2016). Comparison of Rab27b expression in the untreated control cells normalized to HEY (section 4.3.1.1, figure 4.2) showed patterns similar to what was hypothesised when Rab27b was identified in chapter 1 section 1.8.1.

From the ELISA results, the protein levels of Rab27b in the cell line panel did not match the expression pattern at the mRNA level. The resistant cell line HEY; untreated and drug treated, showed the highest Rab27b protein expression although there were no significant changes with treatment. All other cell lines had at least one drug treatment resulting in the increase of Rab27b expression compared to the untreated control cells. However, the OVCAR-3 cell line stood out due to the fact that it showed protein levels second to HEY cells. Furthermore, the drug treated OVCAR-3 cells showed a significant increase in Rab27b with drug treatment. Unlike the qPCR data, these results align more with the hypothesis of Rab27b expression. Analysis of confocal microscopy images revealed Rab27b expression mostly followed the pattern of expression observed in the ELISAs. Perhaps what is most interesting is that almost all drug treated cells of the three cell lines showed a significant increase in Rab27b protein expression compared to the control cells (section 4.3.1.2 and 4.3.1.3). This concurs with the findings from the biomarker discovery stage described earlier.

It is worth mentioning that a correlation was observed between resistance and Rab27b protein expression (figure 4.6). However, this link was observed in taxol and talazoparib treated cells whereas the link between platinum drug treated cells and Rab27b expression showed a weak correlation. This again presents a complexity in understanding Rab27b. since the earlier Ovmark analysis builds on linking poor prognosis with platinum resistance in cells with decreased Rab27b expression. Since Rab27b promotes drug efflux resulting in chemotherapy resistance, these mechanisms maybe dependant on the kind of drug treatment (Li *et al.*, 2020). It is apparent that there is a clear disconnect between mRNA and protein levels of Rab27b which is not an uncommon event occurring between assays (Vogel and Marcotte, 2012). However, the inconsistency in expression between resistant and sensitive cell lines could be attributed to the fact that the cell lines exhibit properties that mimic certain FIGO stages. The HEY cells being the most invasive and possessing mesenchymal phenotype suggests that it has undergone EMT and therefore metastatic. This can be further validated by the increased level of vimentin in these cells as described in earlier sections. Consequentially this showcases HEY cells having similar characteristics as the FIGO stage 4 ovarian cancer and in agreement with most of the literature. In contrast, the OVCAR-3 cells being the sensitive cell line and of an epithelial phenotype responds to drug treatment with higher Rab27b levels. Perhaps OVCAR-3 can be considered a FIGO stage 3 ovarian

cancer model. This could explain why OVCAR-3 cells profile is more in sync with the Ovmark analysis than HEY cells.

These discrepancies underline the need to investigate Rab27b in clinical tissue samples as were done for ROR1. This would help establish whether *in vitro* data translates to clinical data. Perhaps there is a need to expand on the existing cell line panel in order to understand the role of Rab27b in conjunction with ROR1. It is widely recognised that Rab27b is linked to EMT and metastasis (Bao *et al*., 2014; Ren *et al*., 2016; J.-X. Zhang *et al*., 2012) which have also been linked to ROR1 as established in this project

Chapter 5

Tissue Microarray Analysis – ROR1 and Vimentin

5.1 Introduction

Traditionally immuno-histochemical staining was carried out on entire tissue sections from paraffin blocks to examine proteins as potential markers. This process is particularly time consuming when investigating large number of tumour samples or markers as this requires processing and staining of hundreds to thousands of slides. Tissue microarray (TMA) technology was introduced in 1998 by Kononen *et al*. which enabled analysis of large number of archival formalin-fixed, paraffin-embedded samples. This technology has facilitated simultaneous processing of hundreds of specimens using identical conditions (Khouja *et al*., 2010). Additionally, identification of associations between several markers can be aided by analysis of serial TMA sections (Korsching *et al*., 2002; Tolgay Ocal *et al*., 2003). In chapter 3 it was observed that ROR1 expression was correlated with chemo-resistance and also impacted chemo-response when knocked down *in vitro*. However, in this chapter TMA analysis was carried out in order to investigate expression of ROR1 in clinical samples and its association with survival. Although there have been several studies analysing ROR1 expression in cancer tissue samples (Balakrishnan *et al*., 2017; S. Zhang *et al*., 2012b; Zheng *et al*., 2016), only a few have investigated them in ovarian cancer tissues (Yin *et al*., 2019; H. Zhang *et al*., 2014b; S. Zhang *et al*., 2014). One particular study investigated the expression of ROR1and its sister receptor ROR2 in the same ovarian cancer clinical cohort (Henry *et al*., 2017). The results from this study showed ROR1 and ROR2 were expressed in all the histological subtypes specifically in the stroma regions of the tumours. (Henry *et al*., 2017). The TMAs for this project were obtained from the same source as the Henry *et al*., (2017) study. Although ROR1 expression was investigated with its sister receptor ROR2 in these clinical samples, there were no studies of other markers such EMT. Since EMT markers were prevalent in the chemo-resistant ovarian cancer cell line models (chapter 3 section 3.4.6) it was decided to include Vimentin along with ROR1 in expression and survival analysis of the TMAs.

Although *in vitro* studies can deliver certain insights into the role of selected markers these still require validation at the clinical level. TMAs provide the ability to study possible associations between molecular changes and clinico-pathological characteristics of tumours (Khouja *et al*., 2007; Sapino *et al*., 2006; Tolgay Ocal *et al*., 2003). A 2010 study by Khouja *et al*. showed ovarian cancer TMA cores as small as 0.6mm significantly represented a whole section as the score of three cores from the same TMA. These results concur with a previous

study where the outcome of up to two breast cancer TMA cores per case were similar (95%) to outcomes achieved using conventional tissue sections (Camp *et al*., 2000). However, other TMA validation studies suggested analysis of two to three 0.6mm cores offers reliable similarity than analysis of one core (Fernebro *et al*., 2002; Fons *et al*., 2007; Griffin *et al*., 2003; Kallioniemi *et al*., 2001). Here, the TMAs analysed consisted of two cores per case therefore keeping in line with the optimal conditions for scoring.

5.2 Methods

5.2.1 Immunohistochemistry

Immunohistochemistry (IHC) was performed on tissue microarrays (TMA) fixed on slides that were constructed as described in Henry *et al*. (2017) and provided by Westmead Hospital, Sydney. The TMA cohort consisted of 144 patient samples (two cores each) with ovarian cancer. Tumour stage was classified according to the International Federation of Gynaecologists and Obstetricians (FIGO) criteria.

The TMAs were deparaffinized in xylene baths twice for 10 minutes each. This was followed by rehydration by sequentially dipping them for 5 minutes each in 100%, 95%, 80% and 60% ethanol. The sections were then rinsed with tap water three times for 3 minutes each before undergoing an antigen retrieval step. For the antigen retrieval, citrate buffer (pH6) was the buffer of choice and was prepared by adding 2.9g of 10mM Tris-sodium citrate.$2H_20$(Fisher) and 0.4g of 1.9mM Citric acid.$2H_20$ (Fisher Scientific) to 1000mL of distilled water. The pH was adjusted accordingly. In order to expose epitopes, the citrate buffer was poured into a microwavable container and heated in 20 second bursts at a 100W till the buffer temperature raised to 90°C. The TMAs were then transferred into the citrate buffer container and heated in the microwave at 80W for 10 minutes in 30 second bursts. The slides were allowed to cool down for 30 minutes before proceeding to the next step. (For observing Vimentin expression, antigen retrieval step was not required, and the below protocol was carried out as usual).

The slides were washed in PBS (Fisher) three times for 3 minutes each. The slides were then incubated in 3% H_2O_2 for 10 minutes. This was done in order to quench peroxidase activity that may occur endogenously. Again, the slides were washed as previously described before undergoing a blocking step for one hour. The blocking solution consisted of 5% Bovine

Serum Albumin in 1X PBS. This was followed by incubating the slides in the primary antibody; ROR1 and Vimentin, at the recommended dilutions shown in Table 5.1 at 4°C overnight. Staining for ROR2 was excluded as it was already analysed in TMAs of the same source in another study conducted by Henry *et al*. (2017). Due to limited availability of ROR2, N-Cadherin and E-Cadherin antibody it was decided to only stain for ROR1 and Vimentin.

Antibody	Source/Clonality	Dilution
ROR1(Proteintech)	Rabbit Polyclonal	1:50
RAB27B(Proteintech)	Rabbit Polyclonal	1:100
VIMENTIN(Dako)	Mouse Monoclonal	1:100

Table5. 1 Primary Antibodies used for IHC

Slides were washed as described above followed by the application of diluted biotinylated secondary antibody (1: 1000 dilution of Anti-Mouse IgG/Rabbit IgG Vectastain universal ABC kit) for 30 minutes at room temperature. The slides were washed and then incubated for 30 minutes with Vectastain Elite ABC reagent which is comprised of Avidin DH and Biotinylated Horseradish Peroxidase provided in the same Vectastain Universal ABC kit. Following another wash step, liquid 1X DAB substrate (Sigma) was applied onto the slides for 20 minutes till the desired brown colour developed.

Prior to and following counterstaining the slides with Haematoxylin for 10 minutes, the slides were gently rinsed with distilled water. They were then transferred into an acid-alcohol solution (1% HCl and 99% ethanol) for 10 seconds and then immediately into distilled water for 20 – 30 seconds. Following this the slides were dehydrated by immersing them sequentially for 5 minutes each in 60%, 80%,90% and 100% ethanol baths and then in xylene baths twice for 5 minutes each. Finally, the TMA sections on the slides were mounted with a small drop of mounting medium Dibutylphthalate Polystyrene Xylene (DPX)(Fisher) and a coverslip and left to air dry in the hood for a few hours before viewing under the microscope.

5.2.2 IHC scoring and evaluation

Tissue sections stained were scored in a blinded manner by three independent observers with no knowledge of the clinical or pathological features of patient cohort. Tissues were scored based on a) percentage of overall positive stain and b) intensity of the stain. These were each given a score according to an in-house scoring system detailed in Table 5.2 below. The overall score was then calculated by multiplying the percentage of overall positive stain score and the intensity score. This gave a range of 0-12 which were dichotomized based on expression and stratified for subsequent analysis accordingly. The percentage cut off for stained tissues were based on an in-house assessment which seemed to represent a fairer distribution of the staining. This semi quantitative scoring system was also adapted from Liu *et al.*, (2015) and Zheng *et al.* (2016) for scoring ROR1.

A.	%age of Positively stained cells	Score	B.	Intensity of Stain	Score
	0-20%	0		**Negative**	0
	21-40%	1		**Low Positive**	1
	41%-60%	2		**Positive**	2
	61-80%	3		**High Positive**	3
	81-100%	4			

Table5. 2 Scoring percentage coverage of positively stained tissues. Scoring intensity of positively stained tissues.

Another scoring procedure used to compare to the above was the ImageJ software plugin; IHC profiler (Varghese *et al.*, 2014). The percentage of positive stain was represented as the sum of the positive contribution produced from the plugin histogram profile. The intensity was represented by the score output. Similar to the above manual scoring method, the in-house scoring system was also used to assign a score to images processed through the ImageJ software.

5.2.3 Survival analysis

For survival analysis, ROR1/Vimentin expression in patient tissues were dichotomized based on expression score and grouped as high and low scores. Progression free and Overall survival by Kaplan Meier curves were performed to assess association between ROR1/Vimentin expression and patient outcome. Similar curves were produced to assess patient outcome with FIGO stage of the tumour using the Chi square test. These were plotted using GraphPad Prism

Using the R statistical package surv, survminer and dplyr a multivariate analysis was performed. This was done through the Cox's proportional hazards regression models using the coxph and ggforest function to visualize the forest plot. These functions helped to determine factors that were independently associated with progression-free and overall survival.

5.3 Results

5.3.1 Tissue microarrays

A tissue microarray cohort consisting of 144 tissue samples of patients diagnosed with (serous) epithelial ovarian cancer were obtained from Westmead Hospital, Sydney. The clinical and histological features are detailed in table 5.3 below.

	Adenocarcinoma, serous (n=144)	
Grade		
High	133	92%
Low	11	8%
FIGO stage		
I	4	3%
II	7	5%
III	119	83%
IV	14	10%
Primary site		
Ovary	111	77%
Fallopian tube	8	5%
Ovary/fallopian tube can't distinguish	2	1%
Peritoneum	18	13%
Ovary/peritoneum can't distinguish	6	4%
Ovary/fallopian tube/peritoneum can't distinguish	0	0%
AGE		
≤60 years	69	48%
>60 years	75	52%

Residual disease		
Nil	30	21%
Any	114	79%
Neoadjuvant therapy		
No	143	99%
Yes	1	1%
Primary treatment		
Platinum	17	12%
Platinum/taxol	94	65%
Platinum/ cyclophosphamide	14	10%
Platinum/taxol/other	16	11%
Other/none	3	2%

Table5. 3 Clinical and pathological characteristics of tissue microarray cohort. Tissue sections of epithelial ovarian cancer patients obtained from Westmead Hospital; Sydney were fixed on slides in the form of tissue microarrays. These microarrays consisted of a total of 144 patients.

5.3.2 Survival analysis based on FIGO stage

A Kaplan Meier curve was plotted as described in section 5.2.3 to demonstrate survival outcomes in patients with different FIGO stages of the tumours. Figure 5.1 below represents progression free and overall survival rate while table 5.4 represents the univariate analysis outcome. Patients with later stage of the tumour (Stage 3 and 4) had a significantly poor survival outcome compared to patients in earlier stages of the tumour (Stage 1 and 2).
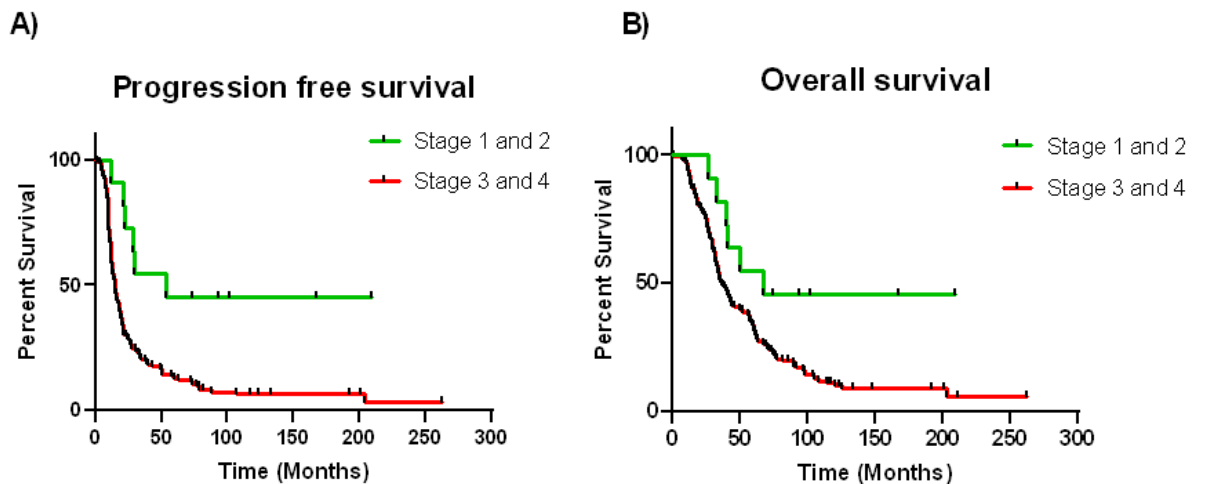
Figure5. 1 Survival analysis by Kaplan-Meier method of ovarian cancer patients (n=144) with different FIGO stages. (A) Progression free survival rate in patients with FIGO stage 3 and 4 (red line n= 133) tumours were lower than patients with FIGO stage 1 and 2 tumours (green line n=11). A significant separation of the curves was observed (p =0.0017) (B) Overall survival rate in patients with FIGO stage 3 and 4 (red line = 133) was lower than patients with FIGO stage 1 and 2 (green line n=11). The separation of the curves was also significant with a p value of 0.0257. A log rank (Mantel-Cox test) was used to determine the p value.

\

	Hazard ratio	95% CI	Chi-square	P value
Progression free survival				
FIGO Stage	3.382	2.062 to 5.545	9.851	0.0017
Overall Survival				
FIGO Stage	2.459	1.405 to 4.301	4.977	0.0257

Table5. 4 Univariate analysis of FIGO stage for PFS and OS in TMA cohort.

5.3.3 Immunohistochemistry -Scoring tissue microarrays for ROR1 and Vimentin.

Tissue microarrays stained for ROR1 and Vimentin were scored manually and independently by three individuals as described in section 5.2.2. The same tissues were scored using the ImageJ software plugin called IHC profiler (Varghese *et al*., 2014) and compared against the scores obtained manually.

The images that were manually examined were scored based on coverage of positive ROR1/ Vimentin percentage and intensity of the stain in the tissue samples. The scoring system used was an in house developed scoring model as shown in section 5.2.2. The overall score was determined as a product of percentage of positive cells and the intensity shown in table 5.5. A comparative score between the three manual independent scores is represented in figure 5.2.
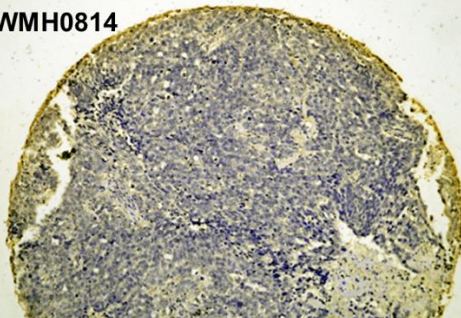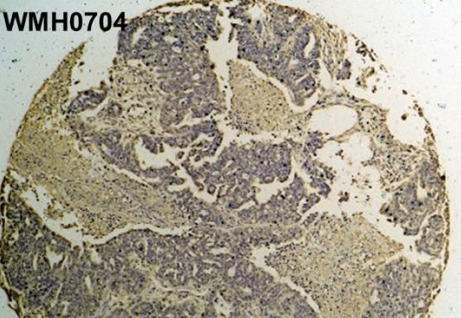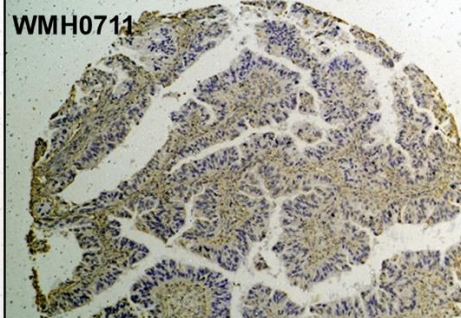
A.	Score 1			Score 2			Score 3		
	+ve ROR %age	Intensity	Overall score	+ve ROR %age	Intensity	Overall Score	+ve ROR %age	Intensity	Overall Score
WMH0814	0	2	0	0	0	0	0	0	0
WMH0704	1	1	1	1	1	1	1	1	1
WMH0711	2	1	2	2	2	4	2	1	2
WMH0788	3	1	3	3	1	3	3	1	3
WMH0724	4	2	8	4	2	8	4	2	8
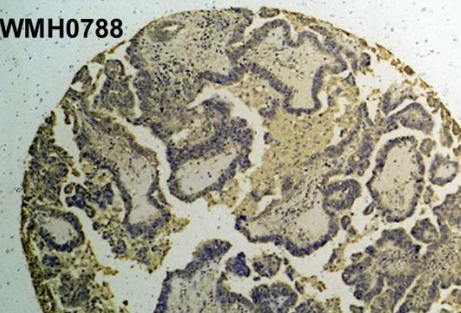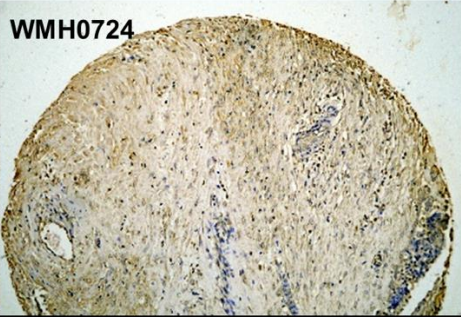
B.	+ve Vimentin %age	Intensity	Overall score	+ve Vimentin %age	Intensity	Overall Score	+ve Vimentin %age	Intensity	Overall Score
WMH0814	1	1	1	1	1	1	1	1	1
WMH0704	2	2	4	2	2	4	2	4	8
WMH0711	3	2	6	2	3	6	2	3	6
WMH0788	3	3	9	2	2	4	3	2	6
WMH0724	4	2	8	2	2	4	1	2	2

Table5. 5 Overall scores of the tissue sections for (A)ROR1 and (B)Vimentin. The scores indicate the percentage of cells positively stained for ROR1 and Vimentin based on an in-house developed scoring system as described in section 5.2.2. The intensity of the DAB stain was also manually scored based on another in-house developed scoring system (Table 5.2). The overall score is represented as the product of the score from percentage of positively stained cells and the intensity score.

A.

ROR1

Score 1	Score 2	Score 3	Score 1	Score 2	Score 3	Score 1	Score 2	Score 3
0	0	0	1	1	1	2	2	2

WMH0814 WMH0704 WMH0711

Score 1	Score 2	Score 3	Score 1	Score 2	Score 3
3	3	2	4	4	3

WMH0788 WMH0724

B.

VIMENTIN

Score 1	Score 2	Score 3
1	1	1

WMH0814

Score 1	Score 2	Score 3
2	2	2

WMH0704

Score 1	Score 2	Score 3
3	2	2

WMH0711

Score 1	Score 2	Score 3
1	2	1

WMH0788

Score 1	Score 2	Score 3
4	2	1

WMH0724
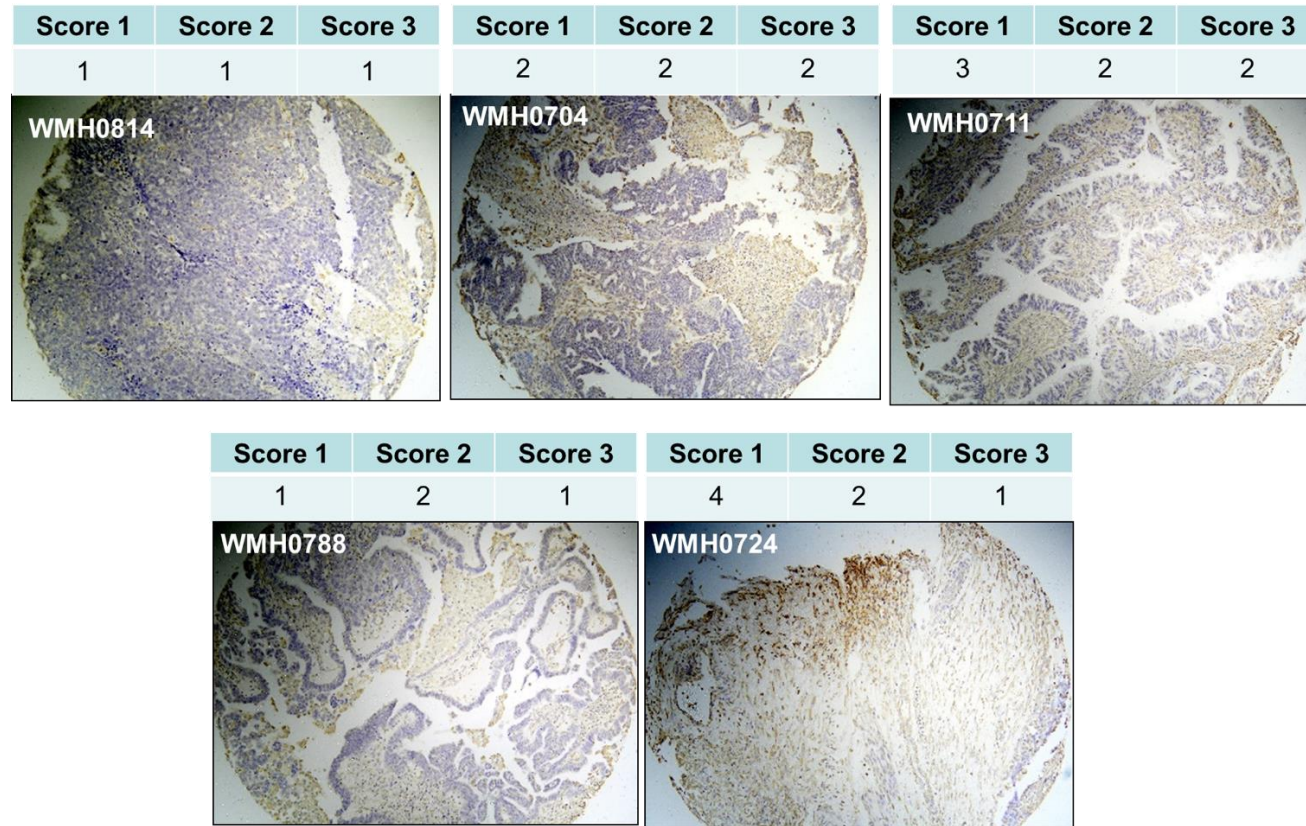
Figure5. 2 Representative scores for DAB-stained tissue images with varying levels of ROR1 and Vimentin expression. Images of tissue samples independently and manually scored for overall positively stained ROR1 (A) and Vimentin (B). The scores range from 0 to 4 with 0 being the least and 4 being the highest expression level. The samples selected represent tissues with closest score match between the three scorers in ROR1 stained tissues. The corresponding tissues scored for vimentin do not necessarily match the score for ROR1.

The correlation between the three scores is also demonstrated in the form of Pearson's coefficient with the R^2 values tabulated below (Table 5.6). The correlation is positive confirming reliability within the independent scoring.

ROR1	Scorer 1		Scorer 2	
	R^2	P-value	R^2	P-value
Scorer 2	0.959	0.010		
Scorer 3	1	*	0.959	0.010
Vimentin	Scorer 1		Scorer 2	
	R^2	P-value	R^2	P-value
Scorer 2	0.636	0.249		
Scorer 3	0.268	0.663	0.641	0.244

Table5. 6 Correlation between independent scores for ROR1 and Vimentin. Tissue sections of the same patient were scored for ROR1 and Vimentin by three independent scorers manually. The scores for ROR1 demonstrated a strong positive correlation while those for Vimentin were not as high.

For images analysed with the ImageJ plugin, the sum of percentage of the positive contribution in images from Figure 5.3 are scored against the in-house developed scoring system in table 5.2. The output scores were compared against in-house scoring system for stain intensity. Similar to the manual scoring, the overall score was represented as the product of sum percentage of positively stained cells and the intensity score (Table 5.7).

A.

ROR1

B.

VIMENTIN

WMH0814

Pixel Count: 5898240
Percentage contribution of High Positive: 2.4738
Percentage contribution of Positive: 7.3413
Percentage contribution of Low Positive: 50.92
Percentage contribution of Negative: 39.2649
The score is Low Positive

Score: 2

Pixel Count: 5898240
Percentage contribution of High Positive: 1.9101
Percentage contribution of Positive: 4.9644
Percentage contribution of Low Positive: 31.3464
Percentage contribution of Negative: 61.7791
The score is Low Positive

Score: 1

WMH0704

Pixel Count: 5898240
Percentage contribution of High Positive: 3.6738
Percentage contribution of Positive: 18.2598
Percentage contribution of Low Positive: 48.1191
Percentage contribution of Negative: 29.9472
The score is Positive

Score: 3

Pixel Count: 5898240
Percentage contribution of High Positive: 2.8199
Percentage contribution of Positive: 6.665
Percentage contribution of Low Positive: 31.9106
Percentage contribution of Negative: 58.6046
The score is Low Positive

Score: 1

WMH0711

Pixel Count: 5898240
Percentage contribution of High Positive: 3.1882
Percentage contribution of Positive: 16.386
Percentage contribution of Low Positive: 48.312
Percentage contribution of Negative: 32.1138
The score is Low Positive

Score: 3

Pixel Count: 5898240
Percentage contribution of High Positive: 1.7497
Percentage contribution of Positive: 5.8757
Percentage contribution of Low Positive: 26.1494
Percentage contribution of Negative: 66.2252
The score is Negative

Score: 1

Figure5. 3 Representative scores for DAB-stained tissue images with varying levels of ROR1 and Vimentin expression. Profile of the same tissues as in Figure 5.2 using an ImageJ software plugin; IHC Profiler (Varghese *et al*.,2014)are shown for ROR1 (A) and Vimentin expression (B). The DAB-stained cytoplasmic image sample is profiled for each sample through a colour deconvolution step. The image is separated into a DAB-stained image (brown) and Haematoxylin image (blue). A histogram profile is also produced which corresponds to the pixel intensity value vs. corresponding number counts of a pixel intensity. Below the histogram profile the percentage of the pixels present in each zone of pixel intensity and the respective computed score is produced.

A.	ROR1		
	+ve ROR1 %age	**Intensity**	**Overall score**
WMH0814	2	1	2
WMH0704	3	2	6
WMH0711	3	1	3
WMH0788	2	1	2
WMH0724	2	1	2
B.	Vimentin		
	+ve Vimentin %age	**Intensity**	**Overall score**
WMH0814	1	1	1
WMH0704	1	1	1
WMH0711	1	0	0
WMH0788	1	0	0
WMH0724	1	0	0

Table5. 7 Overall scores of the tissue sections for (A)ROR1 and (B)Vimentin analysed using the ImageJ plugin. The scores indicate the percentage of cells positively stained for ROR1 and Vimentin analysed by the plugin. The intensity of the DAB stain was also scored based on in-house developed scoring system (Table 5.2). The overall score is represented as the product of the score from percentage of positively stained cells and the intensity score.

A poor correlation between the manual and automated scores was observed as shown in table 5.8 below. Tissue images scored using the IHC profiler plugin for the ImageJ software produced scores that did not match those scored manually. For both ROR1 and Vimentin, Pearson coefficient was in the negative range suggesting a very poor similarity. Therefore, the manual scores were used for further analysis.

ROR1	**Scorer 1**		**Scorer 2**		**Scorer 3**	
	R^2	**P-value**	R^2	**P-value**	R^2	**P-value**
IHC Profiler	-0.323	0.596	-0.395	0.511	-0.323	0.596
Vimentin	**Scorer 1**		**Scorer 2**		**Scorer 3**	
	R^2	**P-value**	R^2	**P-value**	R^2	**P-value**
IHC Profiler	-0.882	0.048	-0.663	0.222	-0.031	0.961

Table5. 8 Correlation between manual and ImageJ plugin scores for ROR1 and Vimentin. Tissue sections of the same patient scored manually were also scored for ROR1 and Vimentin using IHC profiler. There was a negative correlation between IHC profiler scores and all the manual scores.

Pearson correlation	0.563
P value	0.0001

Table5. 9 Correlation between scores for ROR1 and Vimentin. The median of overall scores for ROR1 and Vimentin showed a moderate association.

Further analysis also revealed a moderate correlation between ROR1 and vimentin expression. The median of the scores from three independent scorers for ROR1 and vimentin were analysed against each other and the Pearson's correlation coefficient showed a moderate correlation as detailed in the table 5.9 above.

5.3.4 Survival analysis of ROR1 and Vimentin

A Kaplan Meier curve was plotted to demonstrate survival outcomes in patients with low/high ROR1 and Vimentin expression. Figure 5.4 below represents progression free survival rate while table 5.10 represents the univariate analysis outcome.

Progression free survival
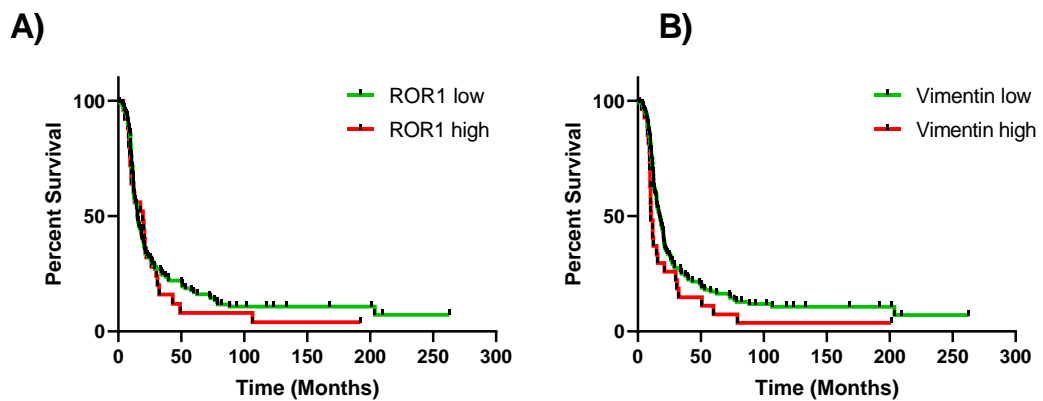
Figure5. 4 Survival analysis by Kaplan-Meier method of ovarian cancer patients (n=144) with ROR1 and Vimentin expression. Tissues with a score less than 6 was considered low expression and greater than 8 was high expression (A) Progression free survival rate in patients with high ROR1 expression (red line n=25) was lower than patients with low ROR1 expression (green line n= 119). However, there was no significant separation of the curves (B) Progression free survival rate in patients with high Vimentin expression (red line n=25) was lower than patients with low Vimentin expression (green line n=119). The separation of the curves was borderline significant with a p value of 0.0512. A log rank (Mantel-Cox test) was used to determine the p value.

	Hazard ratio	95% CI	Chi-square	P value
ROR1				
High vs Low	1.170	0.7341 to 1.866	0.4923	0.4829
Vimentin				
High vs Low	1.525	0.9303 to 2.500	3.801	0.0512

Table5. 10 Univariate analysis of ROR1/ Vimentin expression and PFS in TMA cohort.

The overall survival rate for patients with ROR1/Vimentin expression is shown in figure 5.5 along with the outcome of the univariate analysis detailed in table 5.11 below.

Overall survival
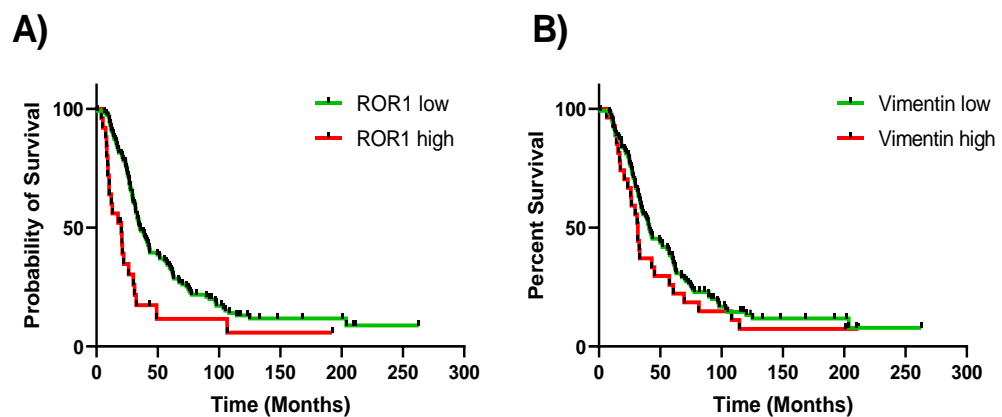
Figure5. 5 Survival analysis by Kaplan-Meier method of ovarian cancer patients (n = 144) with ROR1 and Vimentin expression. Tissues with a score less than 6 was considered low expression and greater than 8 was high expression (A) Overall survival rate in patients with high ROR1 expression (red line n= 26) was lower than patients with low ROR1 expression (green line=119). A significant separation (p=0.0006) of the curves observed (B) Overall survival rate in patients with high expression of Vimentin (red line= 26) was also lower in patients low Vimentin expression (green line=119) however there was no significance in the separation of the curves. A Mantel-Cox test was used to determine the p value.

	Hazard ratio	95% CI	Chi-square	P value
ROR1				
High vs Low	2.190	1.183 to 4.056	11.92	0.0006
Vimentin				
High vs Low	1.323	0.8193 to 2.136	1.588	0.2076

Table5. 11 Univariate analysis of ROR1/ Vimentin expression and OS in TMA cohort.

A multivariate analysis was carried out using a cox proportional hazards model. This test was carried out using the coxph function and visualized using the ggforest function in R. For this the dataset was divided into low and high score extremities. The middle data (scores greater 4 and less than 8) was extracted and not included in the analysis. The analysis for progression free and overall survival are shown below in figure 5.6 and 5.7 respectively.
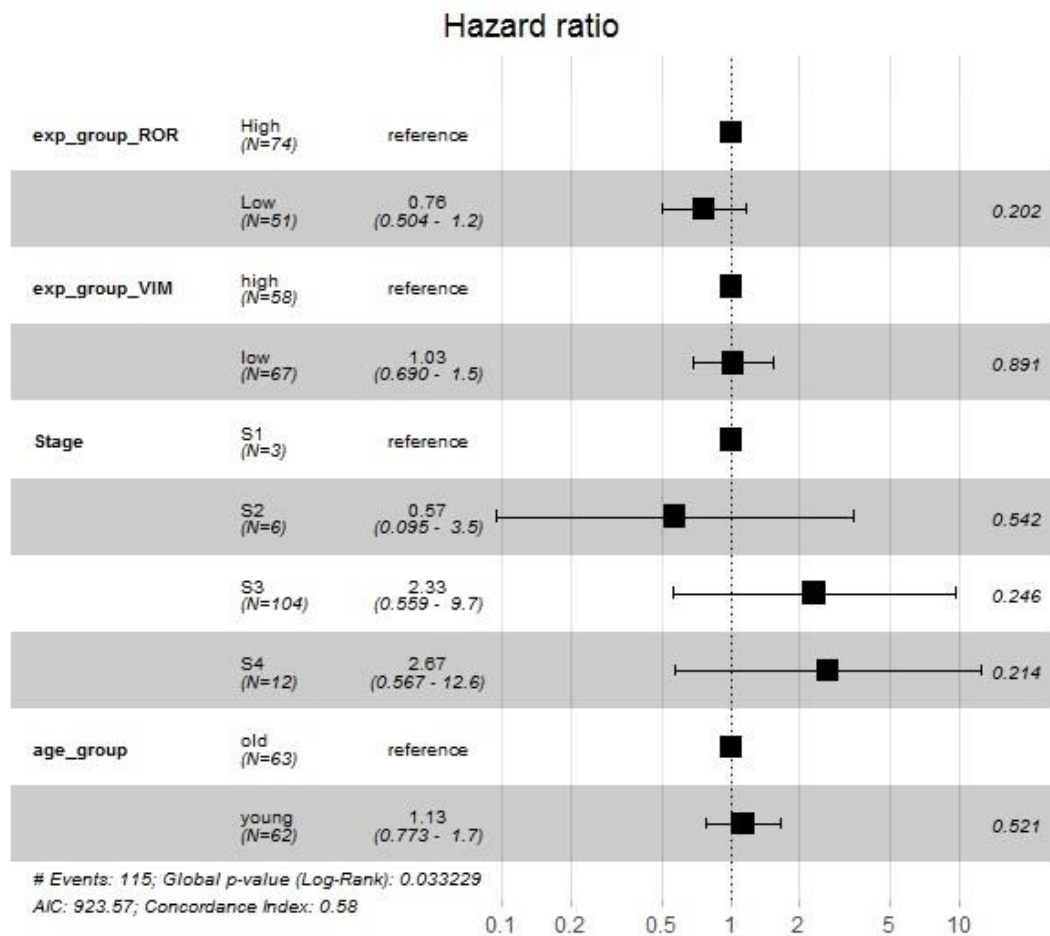
Figure5. 6 Multivariate analysis of prognostic factors for progression free survival. Forest plot produced in R studio represents the hazard ratios and p values of different prognostic factors for progression free survival. exp_group_ROR- tissues scored for ROR1, exp_group_VIM- tissues score for vimentin, Stage- FIGO stage of the tumour. The p value is represented on the right side of the plot for each prognostic factor. The bottom scale represents the hazard ratio range with any outcome above 1 being increased risk of death. The patient dataset is separated into low and high scores with scores below 4 as low and above 8 as high. These scores are calculated as described in section 5.2.3.

The different covariates such as vimentin expression, stage and age group of the data show no significant prognostic value in progression free survival. However, the patient groups that express low ROR1, vimentin and patient cohort that possess a lower FIGO stage (S2) tumour

have a hazard ratio of 1 or lower. This indicates a reduced risk of dying compared to the higher expression, stage patient group. Interestingly, younger patients showed a slightly increased hazard ratio of 1.13 indicating an increased risk of death.
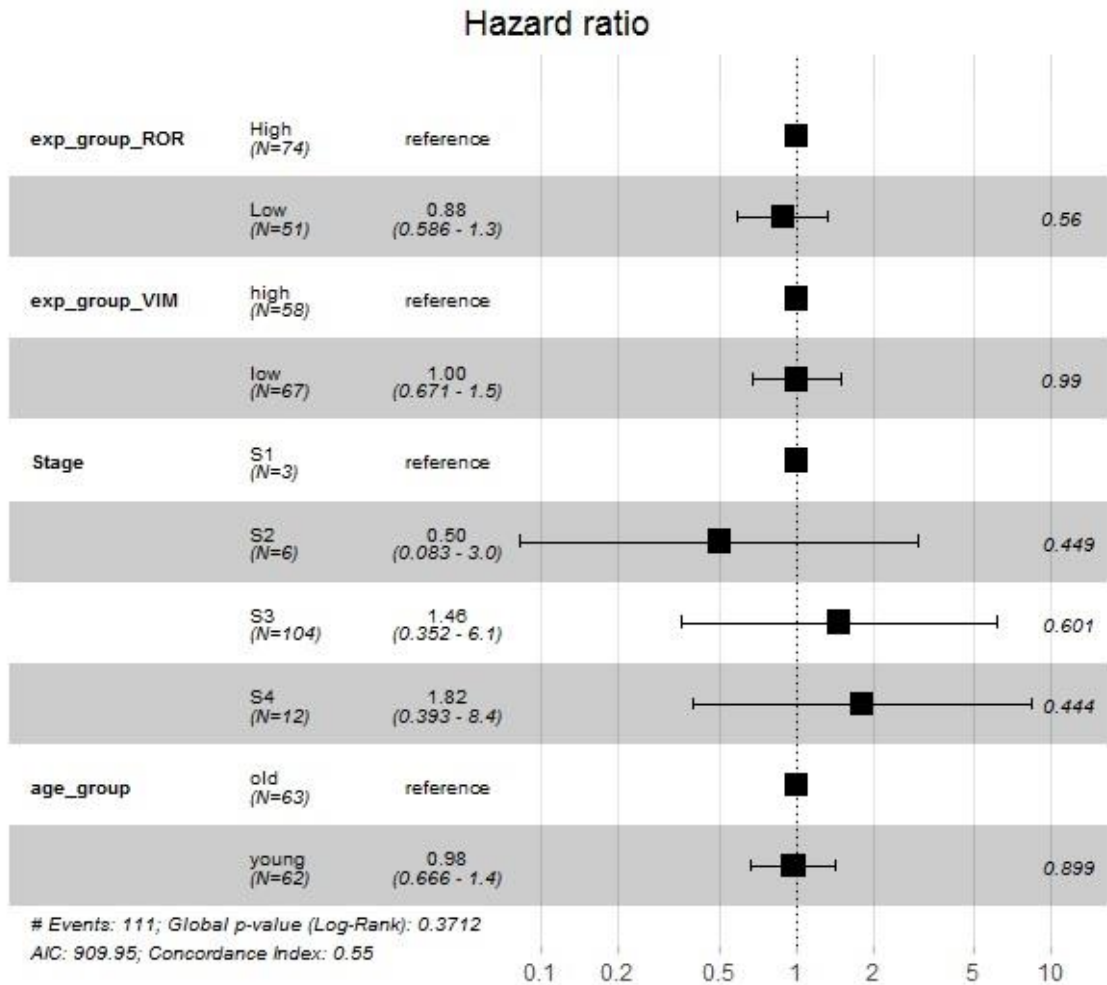
Figure5. 7 Multivariate analysis of prognostic factors for overall survival. Forest plot produced in R studio represents the hazard ratios and p values of different prognostic factors for overall survival. exp_group_ROR- tissues scored for ROR1, exp_group_VIM- tissues score for vimentin. The p value is represented on the right side of the plot for each prognostic factor. The bottom scale represents the hazard ratio range with any outcome above 1 being increased risk of death. The patient dataset is separated into low and high scores with scores below 4 as low and above 8 as high. These scores are calculated as described in section 5.2.3.

Similar to progression free survival, there was no significant contribution of potential prognostic indicators on overall survival. However, the covariates did follow the same pattern of reduced hazard ratios in cohorts with low expression of ROR1, vimentin and lower FIGO stage tumours. Unlike the previous analysis, patients within the younger age group showed a reduced hazard ratio.

5.4 Discussion

5.4.1 Scoring of TMA cohort for protein expression is subjective

It is apparent sample scoring that was carried out manually varied from those scored through the ImageJ software. Scores produced from the software had an inverse correlation with scores produced manually thereby making the automated scores unreliable. There are possible contributing factors to this observation. According to Varghese *et al*. (2014) while validating the use of the ImageJ plugin, cases in which the scores differed by 1 or 2 degrees on the score scale were due to low tumour to stroma ratio. This variation is common in cancer tissue samples where expert pathologists scoring the slides usually ignore the stromal staining and only consider intensity staining of the tumour cells. Varghese *et al*. (2014) further explains that in these cases a manual judgment to use higher magnification images (40X) for analysis provides a higher accuracy score thereby minimizing the averaging effect. Other factors such as staining of non-neoplastic cells, issues with tissue necrosis, uneven fixation of the tissue samples, etc., contribute to technical errors beyond the scope of the ImageJ plugin. Such cases would also require the opinion of a trained pathologist. Taking into account all these factors, manual scoring was the method of choice.

5.4.2 ROR is associated with Vimentin in the TMAs

The pattern of expression of both ROR1 and vimentin varied across the patient cohort. However, a significant correlation was observed between ROR1 and vimentin scores (section 5.3.2, table 5.9). This suggests that increase in ROR1 is typically accompanied by the increase in the mesenchymal marker vimentin. This further validates the link between ROR1 and EMT. In the cell line models of this project, it was established that increased ROR1 expression is prevalent in the chemotherapy resistance models. Elevated expression of mesenchymal EMT markers were also prevalent in the same chemotherapy resistant models. This in effect once again advocates the association of ROR1 and EMT with chemotherapy resistance. From the results of the TMA cohort, it is evident that results observed in the cell lines models translates to patient samples to a large extent.

A Cui *et al*. (2013) study in breast cancer linked ROR1 and EMT, where silencing of ROR1 showed a suppression in vimentin. This indicated that ROR1 is required to maintain a mesenchymal phenotype (Cui *et al*., 2013). ROR1 and Vimentin have both been associated with the p-Akt pathway which promotes tumour proliferation and invasion in several cancers

(Chang *et al*., 2015; Jiang *et al*., 2014; Yanchun Liu *et al*., 2015; S. Zhang *et al*., 2012b). Perhaps this could explain the close link observed in our study between ROR1 and vimentin expression.

There have been conflicting results reported in the context of vimentin in ovarian cancer. A study of clinical ovarian tissue samples undergoing EMT reported the overexpression of EMT-associated transcriptional factors; Snail, Slug, Twist but not vimentin (Yi *et al*., 2015). This study further established that Snail affects the EMT process in ovarian cancer development and invasiveness along with the downregulation of E-cadherin. A more recent study suggested that higher vimentin levels were associated with an improved overall survival in ovarian cancer patients (Szubert *et al*., 2019). Interestingly, Szubert *et al* reported better survival outcome when vimentin expression was low in the stroma and high in the tumour. Although a majority of the published literature is aligned with what was established in this project further investigation into vimentin expression is worth considering in future clinical ovarian cancer studies (Du *et al*., 2018; Liu *et al*., 2017; Ngan *et al*., 2007; Yin *et al*., 2018).

5.4.3 Impact of inclusion of ROR2 in TMA studies

Studies mentioned in earlier sections of this chapter have confirmed the role of ROR1 in the progression of ovarian cancer in cell lines thereby emphasising the invasive nature of the disease (Henry *et al*., 2015). However, the same studies investigated the role of the ROR1 sister receptor; ROR2 and described its possible role in cancer progression. Another study investigating the role of ROR2 in cervical cancer found its upregulation was associated with tumour progression and subsequently poor patient prognosis (Sun *et al*., 2015). Taking into account Henry *et al* (2015) and several other studies it is evident that both ROR1 and ROR2 may be over expressed in gynaecological cancers and impact disease progression (. Zhang *et al*., 2014; Zhang *et al*., 2012a).It is therefore imperative that comparative studies be carried out on clinical samples to investigate synergistic effects of not only ROR1 and Vimentin but also ROR2.

Although this project investigated only ROR1 and vimentin in the clinical cohort, the impact ROR2 would have had on the narrative of ROR in chemotherapy resistant tumours is not overlooked. Appropriately, the TMAs which were investigated in this project originated from the same clinical cohort in which Henry *et al* (2017) investigated ROR2.

The serous adenocarcinomas made up 63% of the cohort which matched the profile of samples investigated in this project. Similar to observations in this project, Henry *et al* (2017) indicated that cellular localization of ROR1 was primarily cytoplasmic. However, ROR2 exhibited some membranous patterns. Data for ROR2 from this study can be evaluated in conjunction with ROR1 data from our project however variation in TMA sections need to be considered. Although Henry *et al* (2017) reported worse overall and progression-free survival in patients positively stained for ROR1 and ROR2 in the same TMA cohort, difference in staining, scoring and analysis need to be accounted for. One such example is the relationship between ovarian tumour and stroma expression of ROR1 and ROR2. The Henry *et al* (2017) study described the range of ROR expression in different subtypes of ovarian cancer in which ROR2 was found to be overexpressed in the serous subtype. When the serous stroma showed the strongest ROR2 expression, no expression was found in the patient tumour cells. This indicates that ROR2 has a significant role in stromal signalling which further supports the need to account for its expression in detail when studying its role in metastasis and recurrence along with ROR1.

Our project would have benefitted from in house ROR2 staining however other results from the Henry *et al* (2017) study support the other findings in out project so far therefore not significantly impacting the overall analysis.

5.4.4 Survival outcome of patients impacted by FIGO stage, ROR1 and Vimentin expression

An initial assessment of survival based on FIGO stage was carried out in this project in section 5.3.2. A Kaplan Meier curve demonstrated that patients with FIGO stage 3 and 4 tumours had worse survival outcome (progression free and overall) compared to FIGO 1 and 2 patients (Figure 5.1). The univariate analysis also produced a hazard ratio above 3 thereby implying that patients with FIGO stage 3 and 4 have a higher death rate compared to patients with FIGO stage 1 and 2 (table 5.4). This poses the theory that the later the stage the higher the ROR1 expression and thus the worse the prognosis. The results from these analyses align with recently published studies that have evaluated the association of high FIGO stage of the ovarian tumour with poor survival (Paik *et al*., 2015; Sartorius *et al*., 2018). ROR1 expression has also been associated with FIGO stage along with tumour grade and lymph

node metastasis (Henry *et al*., 2015; Zhang *et al*., 2014) further reinforcing the survival data of our project mentioned above.

ROR1 and survival outcome has already been established in previous studies. Zhang *et al*. (2014) confirmed that patients with high ROR1 levels had a poor prognosis. Similarly, another study established poor survival outcomes in patient data from the publicly available database Gene Expression Omnibus that had high ROR1expression (Zhang *et al*., 2014). Additionally, it was found that these high ROR1 expressing ovarian cancer cells presented stem cell like gene signatures. Keeping in line with these studies, survival analysis of patients expressing high ROR1 versus low ROR1 were carried out. A Kaplan Meier curve demonstrated that patients with high ROR1 expression had a poor survival outcome. Both progression free and overall survival displayed a separation in the curve between high and low ROR patients (section 5.3.4, figure 5.4-5.5). However, only the overall survival showed a significant separation (p<0.001).

From the univariate analysis, overall survival hazard ratio was 2.1 which indicates that the rate of death in high ROR1 group was twice that of the low ROR1 group. (table 5.11). Similar to ROR1, the progression free and overall survival for patients with high vimentin showed a poorer outcome. However, in progression free survival the separation of the curves was borderline significant. The univariate analysis also showed a hazard ratio slightly greater than 1 implying increased death in patients with higher vimentin expression (table 5.11). This suggests that patients with high vimentin have possibly undergone or undergoing EMT thereby decreasing their survival rate thus qualifying vimentin as a potential combination prognostic marker. Multivariate analysis indicated no covariate functioned as significant independent prognostic factors for survival in ovarian cancer patients (Figure 5.6-5.7). However, patients with low expression of ROR1 had a reduced hazard ratio of 0.88 which implies a better survival rate than patients with high ROR1 expression. Additionally, patients with FIGO stage 3 and 4 had a higher hazard ratio (1.46 and 1.82 respectively) which suggests poorer survival outcome. This supports the survival analysis described earlier. The vimentin expression did not seem to have an impact in survival outcome and as such did not qualify as an independent prognostic matter. Although no significant impact of variables on survival was observed, it is evident from the hazard ratios that our findings concerning the effectiveness of ROR1 as predictive signature is compelling.

Along with the novelty of this project, it is necessary to address certain confounding factors that may have led to divergences in the expected result. Although the univariate analysis of TMA data yielded the expected survival outcome, the multivariate analysis fell short of the expected result when accounting for the covariates in the Cox regression model. A major contributing factor may have been the variation of the scores that were assigned manually. This in turn may have had an impact on stratification of data for analysis. Additionally, the sample size of the TMA cohort also can be considered a contributing factor. However, these are circumstantial conditions and do not diminish the results obtained during the course of this project.

Chapter 6

General Discussion

6.1 Discussion and Limitations

As mentioned in earlier sections, ovarian cancer is a complex disease and even more complicated to model *in vitro* using cell lines. Several studies have indicated origins of ovarian cancers from different tissues with distinct histological and epidemiological features (Cardenas *et al*., 2016; Matz *et al*., 2017; Momenimovahed *et al*., 2019; Reid *et al*., 2017). Based on gene and microRNA expression, large studies have established multiple molecular subtypes of high grade serous cancers (Bell *et al*., 2011; Tothill *et al*., 2008). For example, a stromal subtype defined by Tothill *et al*. (2008), indicates associations with specific biological processes (such as reactive stroma, mesenchymal, immunoreactive, and proliferation) and poor prognosis. Further research into the clinical characteristics of these biological subtypes and the best treatment approaches may contribute to the development of new therapeutic strategies. In order to test specific treatment methods, it is important that experimentally reliable *in vitro* models, such as cell lines, accurately reflect the different histological and molecular subtypes.

A study carried out by Beaufort *et al*. (2014) provided structured data resource for a panel of 39 ovarian cancer cell lines (Beaufort *et al*., 2014). The group discovered histological and morphological subtypes of ovarian carcinomas that were linked to clinical, pathological, and molecular characteristics as well as prognosis. As a result, those searching for better defined model systems that are compatible with valid clinical phenotypes benefited greatly from this analysis, this project being no exception. The cell lines selected for this study were done so based on criteria that would be as clinically representative as possible. This allowed the establishment of a cell line panel with varying resistance to a list of drugs (Platinum-based, taxol and PARP inhibitor) to carry further expression analysis of biomarkers downstream.

Certain limitations regarding the use of cell lines were acknowledged in chapter 3, section 3.4.2 along with the importance of cells retaining features of the original tumour (Ince *et al*., 2015). The cell lines selected were done so as to function as high level laboratory models. These types of *in vitro* models were selected on the premise that they would help understand resistance mechanisms as described in McDermott *et al*. (2014). Although the cell line for this project proved to be reasonably representative, it needs to be acknowledged that these models may be appropriate only for studying certain biomarkers and not others. Another limitation regarding the use of cell line models for investigating ROR1 and Rab27b

expression is the exclusion of positive controls. Determining a suitable cell line that would function as a positive control could contribute to broader understanding to the patterns of expression between the biomarkers in the cell line panel.

From the four-cell line panel, the most resistant and invasive cell line (HEY) exhibited highest expression of ROR1. As explained in chapter 3, the expression of ROR1 was found to be correlated with chemo-resistance. Additionally, knockdown studies have shown that both ROR1 and ROR2 play a role in chemoresponse in the resistant (HEY) and sensitive (OVCAR-3) cell lines. However, the rationale to include ROR2 in the knockdown experiments was based on evidence from other studies (Henry *et al*., 2015, 2016, 2017) implicating ROR2 in mechanisms linked to chemoresistance. Although the results from the knockdown studies (chapter 3 section 3.47) were promising, it is worth noting that some conditions may have been excluded. One such condition involves not testing additional siRNA to rule out off target effects of the knockdown. However, this is somewhat compensated through the cell count and viability records for each experimental condition tested in order to validate actual knockdown effects observed. Another notable limitation is the exclusion of ROR2 at the protein quantification step (ELISA) as this would have provided additional backing to the results obtained.

The process of EMT has been linked to several mechanisms associated with cancer (Ahmed *et al*., 2010). In ovarian cancer, EMT has been implicated as a key player in cancer invasion and metastasis (Vergara *et al*., 2010). Several *in vitro* and *in vivo* studies have shown that cancer cells resistant to carboplatin and/or paclitaxel develop a mesenchymal phenotype, pointing to EMT as a driver of therapy resistance (Baribeau *et al*., 2014; Brozovic *et al*., 2015; Chowanadisai *et al*., 2016; Haslehurst *et al*., 2012; Zhu *et al*., 2016). There are different EMT driven mechanisms leading to chemoresistance (Loret *et al*., 2019). Platinum resistant mesenchymal ovarian cancer cell lines have been shown to express lower levels of CTR1 than platinum-sensitive and more epithelial counterparts suggesting an EMT link to lower drug uptake (Sonego *et al*., 2017). Additionally, the drug efflux pump P-glycoprotein was found to be expressed at higher levels in mesenchymal and therapy resistant ovarian cancer cells than the epithelial and chemo-sensitive cell lines (Feng *et al*., 2017). Other mechanisms involved linking EMT to chemoresistance include enhanced repair of platinum drug induced DNA damage (Abubaker *et al*., 2013; Bae *et al*., 2018; Samardzija *et al*., 2017), inhibition of p-53 mediated apoptosis where mesenchymal phenotypes had an increased

expression of apoptosis inhibitors (Chowanadisai *et al*., 2016; Guoyan Liu *et al*., 2015; Vega *et al*., 2004), changes in different signalling pathways such as EGFR, PI3-K/AKT/NF-κB and JAK/STAT (Altomare *et al*., 2004; Hou *et al*., 2017; Sakata *et al*., 2017) and the tumour microenvironment (Hansen *et al*., 2016; B. Zhang *et al*., 2018). As described ealier, EMT has clear links to chemoresistance, and this validates the decision to investigate the gene expression of EMT markers in this project. It is evident that the expression of these markers in the cell line panel differs due to the difference in the phenotypic state. The mesenchymal cell line such as HEY was the most resistant while the epithelial cell line OVCAR-3 was the most sensitive in the panel. This indicates that the mechanisms by which these cells respond to drug treatment is due to the EMT state of said cells thereby linking EMT to chemoresistance. However, there are factors that need to be accounted for such as the types of EMT markers that were analysed for this project. A larger panel of EMT signatures would have been beneficial to further validate whether certain cell line phenotypes were due to one specific signature or a combination. It could also account for the differential expression of the EMT markers in the cell line panel to drug treatment.

Segueing into ROR1, its expression in ovarian cancer has been shown to inhibit apoptosis, activate EFGR signalling among other pathways and more interestingly induce EMT (Borcherding *et al*., 2014b; Cui *et al*., 2013; Yamaguchi *et al*., 2012b). It is evident that ROR1 and EMT are involved in several similar pathways and mechanisms which suggests they directly or indirectly play a role in chemoresistance. From the gene expression analysis (chapter 3 section 3.3.5) mesenchymal markers were more prevalent in the resistant cell line HEY which also was shown to have the highest expression of ROR1 among the other cell lines in the panel. This confirms that ROR1 and EMT perhaps work synergistically. A study by Henry *et al* (2015) showed that silencing of ROR1 as well as its sister receptor ROR2 inhibited the expression of the EMT marker vimentin therefore further validating the link between ROR1 and EMT.

The investigation of ROR1 *in vitro* revealed itself as a promising biomarker and therefore necessitated exploring its impact on patient outcome in clinical tissue samples. It was evident from the TMAs Kaplan Meier curves that higher ROR1 expression resulted in a significantly poor overall survival outcome which is validated by other studies that have been published (Henry *et al*., 2017; Zhang *et al*., 2014) . In chapter 5 section 5.4.3 the impact of including

ROR2 in these TMA studies were discussed and although was clear it would provide additional perspective; it does not take away from the value of the overall TMA analysis. The EMT marker vimentin was also analysed in the TMA's and the Kaplan Meier curves showed a poor overall survival outcome although it was not as significant as ROR1. Multivariate analyses showed none of the covariates such as vimentin expression, stage of the tumour or age group of the patients functioned as independent prognostic factors for survival. However, the hazard ratios for patients with ROR1 and Vimentin expression were high suggesting a possible link to poor survival outcome. As with other sections of this project there are limitations that need to be addressed. Staining the TMAs with other EMT markers such as E-Cadherin would have been useful as there is recent evidence to suggest that normal or malignant ovarian cancers strongly expressed vimentin while E-Cadherin was barely expressed (Yi *et al*., 2015). The decreased expression of E-Cadherin has been observed in more invasive tumours and associated with high tumour grade and poor overall survival (Vergara *et al*., 2010). The clinical data of the patients in the TMA cores used in this project were made of those presenting high tumour grades and therefore it would have been useful to include E-Cadherin in the univariate as well as the multivariate analysis. Other immunohistochemical staining's of ovarian cancer patient samples have demonstrated that the serous subtype are typically double positive for E-cadherin and vimentin (Hudson *et al*., 2008). This underlines the importance of including E-Cadherin staining in our TMA analysis since a majority of the patient sample size are made of the serous subtype.

In addition to ROR1 a second biomarker, Rab27b that was investigated in this project showed differential expression patterns in the cell line panel. The gene expression analysis also showed a variation in expression upon drug treatment across the four cell lines. However, the protein expression from the ELISA and ICC experiments did not translate therefore presenting complications in understanding the impact of Rab27b on chemoresistance. A factor that may have contributed to this is that cell lines selected may not have been ideal and representative enough to investigate the role of Rab27b. Unlike ROR1, knockdown experiments to silence Rab27b were not carried out which is one of the limitations encountered during this stage of the project. As mentioned in chapter 4 section 4.4.1, different studies reported contradictory survival outcomes in association with Rab27b expression. This is also evident from the biomarker discovery stage when Rab27b was identified for this project. The follow up in the investigation of Rab27b should include the TMA analysis as this would perhaps provide a better understanding of the direction of

expression in the clinical samples. This could possibly validate the results observed in the OvMark analysis at the biomarker discovery stage. Although the results of Rab27b in this project did not present any significant role in chemoresistance it does not negate our findings described in chapter 4.

6.2 Conclusion and Future direction:

Overall, it is evident that ROR1 has an essential role in the resistance mechanism of cancer, specifically in the context of ovarian cancer. Studies investigating the role of ROR1 in other cancers has greatly informed the studies conducted in evaluating its role in ovarian cancer. It is therefore unsurprising that it was selected during the biomarker discovery. As is proven through this project, ROR1 has links to several mechanisms contributing to the progression, invasion, metastasis of cancer and also more recently chemotherapy resistance. The schematic diagram below (Figure 6.1) summarises its role and shows how different processes are interlinked and can also work independently.
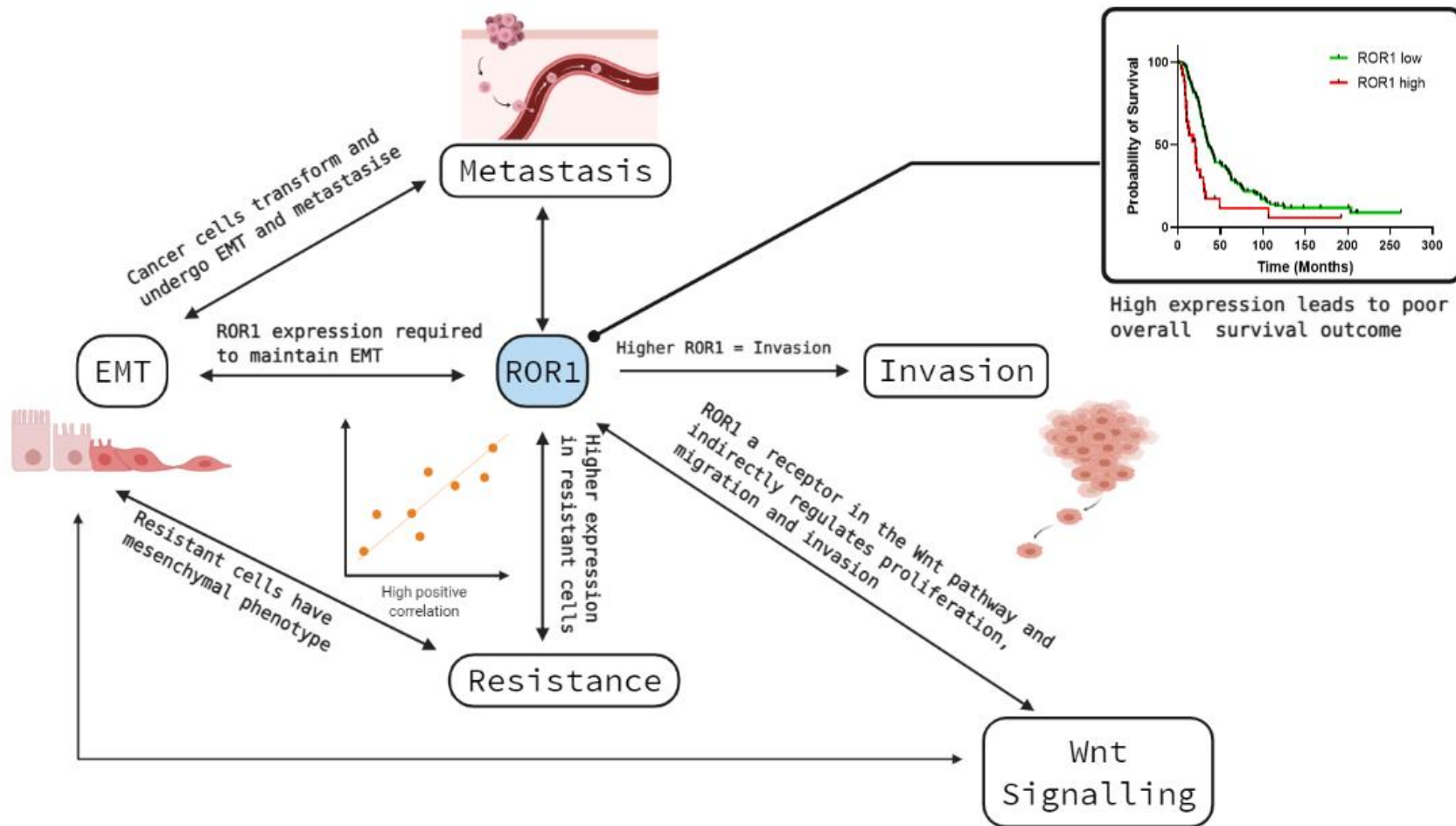
Figure6. 1 Schematic diagram summarizing the overall role of ROR1 and Rab27b in ovarian cancer. The solid lines represent direct link between ROR1 and other mechanism.

Future work in addressing the role of ROR1 in chemoresistance should involve the use of commercialized ROR1 antibodies. Several studies have developed and investigated ROR1 antibodies in different cancers. In 2018, Hojjat-Farsangi *et al*. developed a small molecule inhibitor (KAN0439834) targeting the tyrosine kinase domain of ROR1 which induced apoptosis in CLL cells (Hojjat-Farsangi *et al*., 2018). Another study reported the use of a humanized anti-ROR1 monoclonal antibody; cirmtuzumab which reduced the activation of Rho-GTPases and Hippo-YAP/TAZ as well as stem-ness in breast cancer (Zhang *et al*., 2019). Furthermore, Liu *et al*. (2019) constructed a ROR1 inhibitor (AR1-1) which was able to suppress non-small cell lung cancer development (Liu *et al*., 2019). These studies mentioned above all demonstrated the potential ROR1 inhibitors have to manage treatment in different types of cancer. However, so far one study has constructed and demonstrated the use of a fully chimeric anti-ROR1 IgG antibody against tumour activity in ovarian cancer (Yin *et al*., 2019). The results from this study showed the ROR1 Ig-G has the potential to specifically bind to ROR1 positive cells with great affinity. Functional studies also demonstrated that these antibodies inhibited malignant behaviour in cells that were ROR1 positive in a time and dose dependant manner. Since ROR1 IgG were validated *in vitro*, using this in conjunction with knockdown studies could prove to be a promising approach to improve survival in patients with highly ROR1 positive ovarian cancer.

Another approach would be inhibiting the induction of EMT. As previously described, EMT is linked to ROR1. Therefore, targeting EMT in future projects may function as a therapeutic strategy. A pathway known to induce EMT is the MAPK/ERK pathway and has also been associated with platinum resistance (Brozovic, 2017; Dongre and Weinberg, 2019). Studies have shown how certain genes induce platinum drug resistance in ovarian cancer cells by activating MAPK and AKT pathway (Rosanò *et al*., 2011) and promote EMT in cell lines OVCAR-3 and HEY by triggering the ERK/MAPK pathway (Y. Zhang *et al*., 2018). Similarly another study demonstrated how MEK inhibitors in SKOV-3 cells inhibited ERK phosphorylation , EMT induction and above all decreased platinum resistance (Latifi *et al*., 2011). As these studies were carried out on three of the same cell lines used in this project, using inhibitors that target EMT would be an appropriate step in the future direction of this project.

Keeping in line with the objectives of this project it can be concluded that ROR1 expression correlates with drug resistance (platinum based, taxanes and PARP inhibitors). It also plays a role in other mechanisms which mediate chemotherapy resistance. This can occur either through its role as a receptor for the Wnt signalling pathway or its role in EMT and by extension promote invasion and metastasis. Additionally, Rab27b is also linked to some of the same mechanisms as ROR1 which brands it as a potential chemoresistance biomarker. However, this still requires further validation through *in vitro* and clinical sample studies. Although there are several studies investigating Rab27b in cancer, this is only the second study that has been conducted in ovarian cancer. However, this is the first time Rab27b has been studied in conjunction with another biomarker.

Finally, the results from this project demonstrate promising potential of ROR1 as a predictive biomarker for chemotherapy resistance in ovarian cancer.

REFERENCES

Abubaker, K., Latifi, A., Luwor, R., Nazaretian, S., Zhu, H., Quinn, M.A., Thompson, E.W., Findlay, J.K., Ahmed, N., 2013. Short-term single treatment of chemotherapy results in the enrichment of ovarian cancer stem cell-like cells leading to an increased tumor burden. Mol Cancer 12, 24. https://doi.org/10.1186/1476-4598-12-24

Aghajanian, C., Blank, S.V., Goff, B.A., Judson, P.L., Teneriello, M.G., Husain, A., Sovak, M.A., Yi, J., Nycum, L.R., 2012. OCEANS: A Randomized, Double-Blind, Placebo-Controlled Phase III Trial of Chemotherapy With or Without Bevacizumab in Patients With Platinum-Sensitive Recurrent Epithelial Ovarian, Primary Peritoneal, or Fallopian Tube Cancer. J Clin Oncol 30, 2039–2045. https://doi.org/10.1200/JCO.2012.42.0505

Aghajanian, C., Goff, B., Nycum, L.R., Wang, Y.V., Husain, A., Blank, S.V., 2015. Final overall survival and safety analysis of OCEANS, a phase 3 trial of chemotherapy with or without bevacizumab in patients with platinum-sensitive recurrent ovarian cancer. Gynecologic Oncology 139, 10–16. https://doi.org/10.1016/j.ygyno.2015.08.004

Ahmed, N., Abubaker, K., Findlay, J., Quinn, M., 2010. Epithelial mesenchymal transition and cancer stem cell-like phenotypes facilitate chemoresistance in recurrent ovarian cancer. Curr Cancer Drug Targets 10, 268–278. https://doi.org/10.2174/156800910791190175

Alkema, N.G., Wisman, G.B.A., van der Zee, A.G.J., van Vugt, M.A.T.M., de Jong, S., 2016. Studying platinum sensitivity and resistance in high-grade serous ovarian cancer: Different models for different questions. Drug Resist. Updat. 24, 55–69. https://doi.org/10.1016/j.drup.2015.11.005

Allen, J.D., Brinkhuis, R.F., van Deemter, L., Wijnholds, J., Schinkel, A.H., 2000. Extensive contribution of the multidrug transporters P-glycoprotein and Mrp1 to basal drug resistance. Cancer Res. 60, 5761–5766.

Altomare, D.A., Wang, H.Q., Skele, K.L., De Rienzo, A., Klein-Szanto, A.J., Godwin, A.K., Testa, J.R., 2004. AKT and mTOR phosphorylation is frequently detected in ovarian cancer and can be targeted to disrupt ovarian tumor cell growth. Oncogene 23, 5853–5857. https://doi.org/10.1038/sj.onc.1207721

Alves, M.R., Do Amaral, N.S., Marchi, F.A., Silva, F.I.D.B., Da Costa, A.A.B.A., Carvalho, K.C., Baiocchi, G., Soares, F.A., De Brot, L., Rocha, R.M., 2019. Prostaglandin D2 expression is prognostic in high-grade serous ovarian cancer. Oncol. Rep. 41, 2254–2264. https://doi.org/10.3892/or.2019.6984

Aly, A., Ganesan, S., 2011. BRCA1, PARP, and 53BP1: conditional synthetic lethality and synthetic viability. J Mol Cell Biol 3, 66–74. https://doi.org/10.1093/jmcb/mjq055

Anglesio, M.S., Wiegand, K.C., Melnyk, N., Chow, C., Salamanca, C., Prentice, L.M., Senz, J., Yang, W., Spillman, M.A., Cochrane, D.R., Shumansky, K., Shah, S.P., Kalloger, S.E., Huntsman, D.G., 2013. Type-Specific Cell Line Models for Type-Specific Ovarian Cancer Research. PLOS ONE 8, e72162. https://doi.org/10.1371/journal.pone.0072162

Anwar, M., Aslam, H.M., Anwar, S., 2015. PARP inhibitors. Hereditary cancer in clinical practice 13, 4. https://doi.org/10.1186/s13053-014-0024-8

Armstrong, D.K., Bundy, B., Wenzel, L., Huang, H.Q., Baergen, R., Lele, S., Copeland, L.J., Walker, J.L., Burger, R.A., Gynecologic Oncology Group, 2006.

Intraperitoneal cisplatin and paclitaxel in ovarian cancer. N. Engl. J. Med. 354, 34–43. https://doi.org/10.1056/NEJMoa052985

Arnaudeau, C., Lundin, C., Helleday, T., 2001. DNA double-strand breaks associated with replication forks are predominantly repaired by homologous recombination involving an exchange mechanism in mammalian cells11Edited by J. Karn. Journal of Molecular Biology 307, 1235–1245. https://doi.org/10.1006/jmbi.2001.4564

Ashworth, A., 2008. A synthetic lethal therapeutic approach: poly(ADP) ribose polymerase inhibitors for the treatment of cancers deficient in DNA double-strand break repair. J. Clin. Oncol. 26, 3785–3790. https://doi.org/10.1200/JCO.2008.16.0812

Aubertin, K., Silva, A.K.A., Luciani, N., Espinosa, A., Djemat, A., Charue, D., Gallet, F., Blanc-Brude, O., Wilhelm, C., 2016. Massive release of extracellular vesicles from cancer cells after photodynamic treatment or chemotherapy. Sci Rep 6, 35376. https://doi.org/10.1038/srep35376

Badiglian Filho, L., Oshima, C.T.F., De Oliveira Lima, F., De Oliveira Costa, H., De Sousa Damião, R., Gomes, T.S., Gonçalves, W.J., 2009. Canonical and noncanonical Wnt pathway: A comparison among normal ovary, benign ovarian tumor and ovarian cancer. Oncology Reports 21, 313–320. https://doi.org/10.3892/or_00000223

Bae, J.S., Noh, S.J., Kim, K.M., Park, S.-H., Hussein, U.K., Park, H.S., Park, B.-H., Ha, S.H., Lee, H., Chung, M.J., Moon, W.S., Cho, D.H., Jang, K.Y., 2018. SIRT6 Is Involved in the Progression of Ovarian Carcinomas via β-Catenin-Mediated Epithelial to Mesenchymal Transition. Front Oncol 8, 538. https://doi.org/10.3389/fonc.2018.00538

Baekelandt, M.M., Holm, R., Nesland, J.M., Tropé, C.G., Kristensen, G.B., 2000. P-glycoprotein expression is a marker for chemotherapy resistance and prognosis in advanced ovarian cancer. Anticancer Res. 20, 1061–1067.

Baekelandt, M.M., Holm, R., Nesland, J.M., Tropé, C.G., Kristensen, G.B.,. P-glycoprotein expression is a marker for chemotherapy resistance and prognosis in advanced ovarian cancer. Anticancer research 20, 1061–7.

Balakrishnan, A., Goodpaster, T., Randolph-Habecker, J., Hoffstrom, B.G., Jalikis, F.G., Koch, L.K., Berger, C., Kosasih, P.L., Rajan, A., Sommermeyer, D., Porter, P.L., Riddell, S.R., 2017. Analysis of ROR1 protein expression in human cancer and normal tissues. Clin Cancer Res 23, 3061–3071. https://doi.org/10.1158/1078-0432.CCR-16-2083

Banerjee, S., Bookman, M.A., Gore, M., 2011. Systemic therapy for ovarian cancer, current treatment, recent advances, and unmet needs, in: Emerging Therapeutic Targets in Ovarian Cancer. Springer, pp. 1–33.

Bao, J., Ni, Y., Qin, H., Xu, L., Ge, Z., Zhan, F., Zhu, H., Zhao, J., Zhou, X., Tang, X., Tang, L., 2014. Rab27b Is a Potential Predictor for Metastasis and Prognosis in Colorectal Cancer [WWW Document]. Gastroenterology Research and Practice. https://doi.org/10.1155/2014/913106

Barber, L.J., Sandhu, S., Chen, L., Campbell, J., Kozarewa, I., Fenwick, K., Assiotis, I., Rodrigues, D.N., Reis Filho, J.S., Moreno, V., Mateo, J., Molife, L.R., De Bono, J., Kaye, S., Lord, C.J., Ashworth, A., 2013. Secondary mutations in BRCA2 associated with clinical resistance to a PARP inhibitor. J. Pathol. 229, 422–429. https://doi.org/10.1002/path.4140

Barbolina, M.V., Burkhalter, R.J., Stack, M.S., 2011. Diverse mechanisms for activation of Wnt signalling in the ovarian tumour microenvironment. Biochemical Journal 437, 1–12. https://doi.org/10.1042/BJ20110112

Baribeau, S., Chaudhry, P., Parent, S., Asselin, É., 2014. Resveratrol inhibits cisplatin-induced epithelial-to-mesenchymal transition in ovarian cancer cell lines. PLoS One 9, e86987. https://doi.org/10.1371/journal.pone.0086987

Barna, G., Mihalik, R., Timár, B., Tömböl, J., Csende, Z., Sebestyén, A., Bödör, C., Csernus, B., Reiniger, L., Peták, I., Matolcsy, A., 2011. ROR1 expression is not a unique marker of CLL. Hematol. Oncol. 29, 17–21. https://doi.org/10.1002/hon.948

Barr, F., Lambright, D.G., 2010. Rab GEFs and GAPs. Current Opinion in Cell Biology, Membranes and organelles 22, 461–470. https://doi.org/10.1016/j.ceb.2010.04.007

Barretina, J., Caponigro, G., Stransky, N., Venkatesan, K., Margolin, A.A., Kim, S., Wilson, C.J., Lehár, J., Kryukov, G.V., Sonkin, D., Reddy, A., Liu, M., Murray, L., Berger, M.F., Monahan, J.E., Morais, P., Meltzer, J., Korejwa, A., Jané-Valbuena, J., Mapa, F.A., Thibault, J., Bric-Furlong, E., Raman, P., Shipway, A., Engels, I.H., Cheng, J., Yu, G.K., Yu, J., Aspesi, P., Silva, M. de, Jagtap, K., Jones, M.D., Wang, L., Hatton, C., Palescandolo, E., Gupta, S., Mahan, S., Sougnez, C., Onofrio, R.C., Liefeld, T., MacConaill, L., Winckler, W., Reich, M., Li, N., Mesirov, J.P., Gabriel, S.B., Getz, G., Ardlie, K., Chan, V., Myer, V.E., Weber, B.L., Porter, J., Warmuth, M., Finan, P., Harris, J.L., Meyerson, M., Golub, T.R., Morrissey, M.P., Sellers, W.R., Schlegel, R., Garraway, L.A., 2012. The Cancer Cell Line Encyclopedia enables predictive modelling of anticancer drug sensitivity. Nature 483, nature11003. https://doi.org/10.1038/nature11003

Bashashati, A., Ha, G., Tone, A., Ding, J., Prentice, L.M., Roth, A., Rosner, J., Shumansky, K., Kalloger, S., Senz, J., Yang, W., McConechy, M., Melnyk, N., Anglesio, M., Luk, M.T.Y., Tse, K., Zeng, T., Moore, R., Zhao, Y., Marra, M.A., Gilks, B., Yip, S., Huntsman, D.G., McAlpine, J.N., Shah, S.P., 2013. Distinct evolutionary trajectories of primary high-grade serous ovarian cancers revealed through spatial mutational profiling. J. Pathol. 231, 21–34. https://doi.org/10.1002/path.4230

Baskar, S., Kwong, K.Y., Hofer, T., Levy, J.M., Kennedy, M.G., Lee, E., Staudt, L.M., Wilson, W.H., Wiestner, A., Rader, C., 2008. Unique cell surface expression of receptor tyrosine kinase ROR1 in human B-cell chronic lymphocytic leukemia. Clin. Cancer Res. 14, 396–404. https://doi.org/10.1158/1078-0432.CCR-07-1823

Basu, A., Krishnamurthy, S., 2010a. Cellular responses to cisplatin-induced DNA damage. Journal of nucleic acids 2010.

Basu, A., Krishnamurthy, S., 2010b. Cellular Responses to Cisplatin-Induced DNA Damage. Journal of Nucleic Acids 2010, e201367. https://doi.org/10.4061/2010/201367

Baum, B., Settleman, J., Quinlan, M.P., 2008. Transitions between epithelial and mesenchymal states in development and disease. Semin. Cell Dev. Biol. 19, 294–308. https://doi.org/10.1016/j.semcdb.2008.02.001

Beaufort, C.M., Helmijr, J.C.A., Piskorz, A.M., Hoogstraat, M., Ruigrok-Ritstier, K., Besselink, N., Murtaza, M., IJcken, W.F.J. van, Heine, A.A.J., Smid, M., Koudijs, M.J., Brenton, J.D., Berns, E.M.J.J., Helleman, J., 2014. Ovarian Cancer Cell Line Panel (OCCP): Clinical Importance of *In vitro* Morphological Subtypes. PLOS ONE 9, e103988. https://doi.org/10.1371/journal.pone.0103988

Begg, C.B., Rice, M.S., Zabor, E.C., Tworoger, S.S., 2017. Examining the common aetiology of serous ovarian cancers and basal-like breast cancers using double primaries. British Journal of Cancer 116, 1088–1091. https://doi.org/10.1038/bjc.2017.73

Behrens, B.C., Hamilton, T.C., Masuda, H., Grotzinger, K.R., Whang-Peng, J., Louie, K.G., Knutsen, T., McKoy, W.M., Young, R.C., Ozols, R.F., 1987.

Characterization of a cis-diamminedichloroplatinum(II)-resistant human ovarian cancer cell line and its use in evaluation of platinum analogues. Cancer Res. 47, 414–418.

Bell, D., Berchuck, A., Birrer, M., Chien, J., Cramer, D.W., Dao, F., Dhir, R., DiSaia, P., Gabra, H., Glenn, P., Godwin, A.K., Gross, J., Hartmann, L., Huang, M., Huntsman, D.G., Iacocca, M., Imielinski, M., Kalloger, S., Karlan, B.Y., Levine, D.A., Mills, G.B., Morrison, C., Mutch, D., Olvera, N., Orsulic, S., Park, K., Petrelli, N., Rabeno, B., Rader, J.S., Sikic, B.I., Smith-McCune, K., Sood, A.K., Bowtell, D., Penny, R., Testa, J.R., Chang, K., Creighton, C.J., Dinh, H.H., Drummond, J.A., Fowler, G., Gunaratne, P., Hawes, A.C., Kovar, C.L., Lewis, L.R., Morgan, M.B., Newsham, I.F., Santibanez, J., Reid, J.G., Trevino, L.R., Wu, Y.-Q., Wang, M., Muzny, D.M., Wheeler, D.A., Gibbs, R.A., Getz, G., Lawrence, M.S., Cibulskis, K., Sivachenko, A.Y., Sougnez, C., Voet, D., Wilkinson, J., Bloom, T., Ardlie, K., Fennell, T., Baldwin, J., Nichol, R., Fisher, S., Gabriel, S., Lander, E.S., Ding, L., Fulton, R.S., Koboldt, D.C., McLellan, M.D., Wylie, T., Walker, J., O'Laughlin, M., Dooling, D.J., Fulton, L., Abbott, R., Dees, N.D., Zhang, Q., Kandoth, C., Wendl, M., Schierding, W., Shen, D., Harris, C.C., Schmidt, H., Kalicki, J., Delehaunty, K.D., Fronick, C.C., Demeter, R., Cook, L., Wallis, J.W., Lin, L., Magrini, V.J., Hodges, J.S., Eldred, J.M., Smith, S.M., Pohl, C.S., Vandin, F., Upfal, E., Raphael, B.J., Weinstock, G.M., Mardis, E.R., Wilson, R.K., Meyerson, M., Winckler, W., Getz, G., Verhaak, R.G.W., Carter, S.L., Mermel, C.H., Saksena, G., Nguyen, H., Onofrio, R.C., Lawrence, M.S., Hubbard, D., Gupta, S., Crenshaw, A., Ramos, A.H., Ardlie, K., Chin, L., Protopopov, A., Zhang, Juinhua, Kim, T.M., Perna, I., Xiao, Y., Zhang, H., Ren, G., Sathiamoorthy, N., Park, R.W., Lee, E., Park, P.J., Kucherlapati, R., Absher, D.M., Waite, L., Sherlock, G., Brooks, J.D., Li, J.Z., Xu, J., Myers, R.M., Laird, P.W., Cope, L., Herman, J.G., Shen, H., Weisenberger, D.J., Noushmehr, H., Pan, F., Triche Jr, T., Berman, B.P., Van Den Berg, D.J., Buckley, J., Baylin, S.B., Spellman, P.T., Purdom, E., Neuvial, P., Bengtsson, H., Jakkula, L.R., Durinck, S., Han, J., Dorton, S., Marr, H., Choi, Y.G., Wang, V., Wang, N.J., Ngai, J., Conboy, J.G., Parvin, B., Feiler, H.S., Speed, T.P., Gray, J.W., Levine, D.A., Socci, N.D., Liang, Y., Taylor, B.S., Schultz, N., Borsu, L., Lash, A.E., Brennan, C., Viale, A., Sander, C., Ladanyi, M., Hoadley, K.A., Meng, S., Du, Y., Shi, Y., Li, L., Turman, Y.J., Zang, D., Helms, E.B., Balu, S., Zhou, X., Wu, J., Topal, M.D., Hayes, D.N., Perou, C.M., Getz, G., Voet, D., Saksena, G., Zhang, Junihua, Zhang, H., Wu, C.J., Shukla, S., Cibulskis, K., Lawrence, M.S., Sivachenko, A., Jing, R., Park, R.W., Liu, Y., Park, P.J., Noble, M., Chin, L., Carter, H., Kim, D., Samayoa, J., Karchin, R., Spellman, P.T., Purdom, E., Neuvial, P., Bengtsson, H., Durinck, S., Han, J., Korkola, J.E., Heiser, L.M., Cho, R.J., Hu, Z., Parvin, B., Speed, T.P., Gray, J.W., Schultz, N., Cerami, E., Taylor, B.S., Olshen, A., Reva, B., Antipin, Y., Shen, R., Mankoo, P., Sheridan, R., Ciriello, G., Chang, W.K., Bernanke, J.A., Borsu, L., Levine, D.A., Ladanyi, M., Sander, C., Haussler, D., Benz, C.C., Stuart, J.M., Benz, S.C., Sanborn, J.Z., Vaske, C.J., Zhu, J., Szeto, C., Scott, G.K., Yau, C., Hoadley, K.A., Du, Y., Balu, S., Hayes, D.N., Perou, C.M., Wilkerson, M.D., Zhang, N., Akbani, R., Baggerly, K.A., Yung, W.K., Mills, G.B., Weinstein, J.N., Penny, R., Shelton, T., Grimm, D., Hatfield, M., Morris, S., Yena, P., Rhodes, P., Sherman, M., Paulauskis, J., Millis, S., Kahn, A., Greene, J.M., The Cancer Genome Atlas Research Network, (Participants are arranged by area of contribution and then by institution.), Disease working group and tissue source sites, Genome sequencing centres: Baylor College of Medicine, Broad Institute, Washington

University in St Louis, Cancer genome characterization centres: Broad Institute/Dana-Farber Cancer Institute, Harvard Medical School, HudsonAlpha Institute/Stanford University, University of Southern California/Johns Hopkins University, Lawrence Berkeley National Laboratory, Memorial Sloan-Kettering Cancer Center, University of North Carolina at Chapel Hill, Genome data analysis centres: Broad Institute, Johns Hopkins University, University of California Santa Cruz/Buck Institute, The University of Texas MD Anderson Cancer Center, Biospecimen core resource, Data coordination centre, 2011. Integrated genomic analyses of ovarian carcinoma. Nature 474, 609–615. https://doi.org/10.1038/nature10166

Bergamini, A., Candiani, M., Taccagni, G., Rabaiotti, E., Viganò, R., Marzi, P.D., Ferrari, D., Mangili, G., 2016. Different Patterns of Disease Spread between Advanced-Stage Type I and II Epithelial Ovarian Cancer. GOI 81, 10–14. https://doi.org/10.1159/000381261

Bicocca, V.T., Chang, B.H., Masouleh, B.K., Muschen, M., Loriaux, M.M., Druker, B.J., Tyner, J.W., 2012. Crosstalk between ROR1 and the Pre-B cell receptor promotes survival of t(1;19) acute lymphoblastic leukemia. Cancer Cell 22, 656–667. https://doi.org/10.1016/j.ccr.2012.08.027

Bitler, B.G., Watson, Z.L., Wheeler, L.J., Behbakht, K., 2017. PARP inhibitors: Clinical utility and possibilities of overcoming resistance. Gynecologic Oncology 147, 695–704. https://doi.org/10.1016/j.ygyno.2017.10.003

Boggaram, V., 2009. Thyroid transcription factor-1 (TTF-1/Nkx2.1/TITF1) gene regulation in the lung. Clin. Sci. 116, 27–35. https://doi.org/10.1042/CS20080068

Bookman, M.A., Brady, M.F., McGuire, W.P., Harper, P.G., Alberts, D.S., Friedlander, M., Colombo, N., Fowler, J.M., Argenta, P.A., De Geest, K., Mutch, D.G., Burger, R.A., Swart, A.M., Trimble, E.L., Accario-Winslow, C., Roth, L.M., 2009. Evaluation of new platinum-based treatment regimens in advanced-stage ovarian cancer: a Phase III Trial of the Gynecologic Cancer Intergroup. J. Clin. Oncol. 27, 1419–1425. https://doi.org/10.1200/JCO.2008.19.1684

Borcherding, N., Kusner, D., Liu, G.-H., Zhang, W., 2014a. ROR1, an embryonic protein with an emerging role in cancer biology. Protein Cell 5, 496–502. https://doi.org/10.1007/s13238-014-0059-7

Borcherding, N., Kusner, D., Liu, G.-H., Zhang, W., 2014b. ROR1, an embryonic protein with an emerging role in cancer biology. Protein Cell 5, 496–502. https://doi.org/10.1007/s13238-014-0059-7

Borst, P., 2012. Cancer drug pan-resistance: pumps, cancer stem cells, quiescence, epithelial to mesenchymal transition, blocked cell death pathways, persisters or what? Open Biol 2, 120066. https://doi.org/10.1098/rsob.120066

Bosquet, J.G., Marchion, D.C., Chon, H., Lancaster, J.M., Chanock, S., 2014. Analysis of chemotherapeutic response in ovarian cancers using publicly available high-throughput data. Cancer research 74, 3902–12. https://doi.org/10.1158/0008-5472.CAN-14-0186

Brabec, V., Kasparkova, J., 2005. Modifications of DNA by platinum complexes: Relation to resistance of tumors to platinum antitumor drugs. Drug Resistance Updates 8, 131–146. https://doi.org/10.1016/j.drup.2005.04.006

Brown, C.W., Brodsky, A.S., Freiman, R.N., 2015. Notch3 Overexpression Promotes Anoikis Resistance in Epithelial Ovarian Cancer via Upregulation of COL4A2. Mol Cancer Res 13, 78–85. https://doi.org/10.1158/1541-7786.MCR-14-0334

Browning, R.J., Reardon, P.J.T., Parhizkar, M., Pedley, R.B., Edirisinghe, M., Knowles, J.C., Stride, E., 2017. Drug Delivery Strategies for Platinum-Based Chemotherapy. ACS Nano 11, 8560–8578. https://doi.org/10.1021/acsnano.7b04092

Brozovic, A., 2017. The relationship between platinum drug resistance and epithelial-mesenchymal transition. Arch. Toxicol. 91, 605–619. https://doi.org/10.1007/s00204-016-1912-7

Brozovic, A., Duran, G.E., Wang, Y.C., Francisco, E.B., Sikic, B.I., 2015. The miR-200 family differentially regulates sensitivity to paclitaxel and carboplatin in human ovarian carcinoma OVCAR-3 and MES-OV cells. Mol Oncol 9, 1678–1693. https://doi.org/10.1016/j.molonc.2015.04.015

Bryant, Helen E, Schultz, N., Thomas, H.D., Parker, K.M., Flower, D., Lopez, E., Kyle, S., Meuth, M., Curtin, N.J., Helleday, T., 2005. Specific killing of BRCA2-deficient tumours with inhibitors of poly(ADP-ribose) polymerase. Nature 434, 913–7. https://doi.org/10.1038/nature03443

Bryant, Helen E., Schultz, N., Thomas, H.D., Parker, K.M., Flower, D., Lopez, E., Kyle, S., Meuth, M., Curtin, N.J., Helleday, T., 2005. Specific killing of BRCA2-deficient tumours with inhibitors of poly(ADP-ribose) polymerase. Nature 434, 913–917. https://doi.org/10.1038/nature03443

Budiana, I.N.G., Angelina, M., Pemayun, T.G.A., 2019. Ovarian cancer: Pathogenesis and current recommendations for prophylactic surgery. J Turk Ger Gynecol Assoc 20, 47–54. https://doi.org/10.4274/jtgga.galenos.2018.2018.0119

Burger, H., Loos, W.J., Eechoute, K., Verweij, J., Mathijssen, R.H.J., Wiemer, E.A.C., 2011. Drug transporters of platinum-based anticancer agents and their clinical significance. Drug Resistance Updates 14, 22–34. https://doi.org/10.1016/j.drup.2010.12.002

Burger, R.A., Brady, M.F., Bookman, M.A., Fleming, G.F., Monk, B.J., Huang, H., Mannel, R.S., Homesley, H.D., Fowler, J., Greer, B.E., Boente, M., Birrer, M.J., Liang, S.X., Gynecologic Oncology Group, 2011. Incorporation of bevacizumab in the primary treatment of ovarian cancer. N. Engl. J. Med. 365, 2473–2483. https://doi.org/10.1056/NEJMoa1104390

Burstein, H.J., Mangu, P.B., Somerfield, M.R., Schrag, D., Samson, D., Holt, L., Zelman, D., Ajani, J.A., American Society of Clinical Oncology, 2011. American Society of Clinical Oncology clinical practice guideline update on the use of chemotherapy sensitivity and resistance assays. J. Clin. Oncol. 29, 3328–3330. https://doi.org/10.1200/JCO.2011.36.0354

Callaghan, R., Luk, F., Bebawy, M., 2014. Inhibition of the Multidrug Resistance P-Glycoprotein: Time for a Change of Strategy? Drug Metab Dispos 42, 623–631. https://doi.org/10.1124/dmd.113.056176

Camp, R.L., Charette, L.A., Rimm, D.L., 2000. Validation of tissue microarray technology in breast carcinoma. Lab Invest 80, 1943–1949. https://doi.org/10.1038/labinvest.3780204

Cardenas, C., Alvero, A.B., Yun, B.S., Mor, G., 2016. Redefining the origin and evolution of ovarian cancer: a hormonal connection. Endocrine-Related Cancer 23, R411–R422. https://doi.org/10.1530/ERC-16-0209

Carper, M.B., Denvir, J., Boskovic, G., Primerano, D.A., Claudio, P.P., 2014. RGS16, a novel p53 and pRb cross-talk candidate inhibits migration and invasion of pancreatic cancer cells. Genes Cancer 5, 420–435.

Cetin, M., Odabas, G., Douglas, L.R., Duriez, P.J., Balcik-Ercin, P., Yalim-Camci, I., Sayan, A.E., Yagci, T., 2019. ROR1 Expression and Its Functional Significance in Hepatocellular Carcinoma Cells. Cells 8. https://doi.org/10.3390/cells8030210

Chan, J.K., Teoh, D., Hu, J.M., Shin, J.Y., Osann, K., Kapp, D.S., 2008. Do clear cell ovarian carcinomas have poorer prognosis compared to other epithelial cell types? A study of 1411 clear cell ovarian cancers. Gynecol. Oncol. 109, 370–376. https://doi.org/10.1016/j.ygyno.2008.02.006

Chang, H., Jung, W.Y., Kang, Y., Lee, H., Kim, A., Kim, B., 2015. Expression of ROR1, pAkt, and pCREB in gastric adenocarcinoma. Ann Diagn Pathol 19, 330–334. https://doi.org/10.1016/j.anndiagpath.2015.06.010

Chen, S., Wang, J., Gou, W.-F., Xiu, Y.-L., Zheng, H.-C., Zong, Z.-H., Takano, Y., Zhao, Y., 2013. The Involvement of RhoA and Wnt-5a in the Tumorigenesis and Progression of Ovarian Epithelial Carcinoma. International Journal of Molecular Sciences 14, 24187–24199. https://doi.org/10.3390/ijms141224187

Cheng, K.W., Lahad, J.P., Kuo, W., Lapuk, A., Yamada, K., Auersperg, N., Liu, J., Smith-McCune, K., Lu, K.H., Fishman, D., Gray, J.W., Mills, G.B., 2004. The RAB25 small GTPase determines aggressiveness of ovarian and breast cancers. Nature Medicine 10, 1251–1256. https://doi.org/10.1038/nm1125

Chiarugi, A., 2012. A snapshot of chemoresistance to PARP inhibitors. Trends Pharmacol. Sci. 33, 42–48. https://doi.org/10.1016/j.tips.2011.10.001

Chien, A.J., Conrad, W.H., Moon, R.T., 2009. A Wnt Survival Guide: From Flies to Human Disease. Journal of Investigative Dermatology 129, 1614–1627. https://doi.org/10.1038/jid.2008.445

Chien, H.-P., Ueng, S.-H., Chen, S.-C., Chang, Y.-S., Lin, Y.-C., Lo, Y.-F., Chang, H.-K., Chuang, W.-Y., Huang, Y.-T., Cheung, Y.-C., Shen, S.-C., Hsueh, C., 2016. Expression of ROR1 has prognostic significance in triple negative breast cancer. Virchows Arch 468, 589–595. https://doi.org/10.1007/s00428-016-1911-3

Chien, J., Poole, E.M., 2017. Ovarian Cancer Prevention, Screening, and Early Detection: Report From the 11th Biennial Ovarian Cancer Research Symposium. International Journal of Gynecologic Cancer 27, S20–S22. https://doi.org/10.1097/IGC.0000000000001118

Chowanadisai, W., Messerli, S.M., Miller, D.H., Medina, J.E., Hamilton, J.W., Messerli, M.A., Brodsky, A.S., 2016. Cisplatin Resistant Spheroids Model Clinically Relevant Survival Mechanisms in Ovarian Tumors. PLoS One 11, e0151089. https://doi.org/10.1371/journal.pone.0151089

Clevers, H., Nusse, R., 2012. Wnt/β-Catenin Signaling and Disease. Cell 149, 1192–1205. https://doi.org/10.1016/j.cell.2012.05.012

Coleman, R.L., Oza, A.M., Lorusso, D., Aghajanian, C., Oaknin, A., Dean, A., Colombo, N., Weberpals, J.I., Clamp, A., Scambia, G., Leary, A., Holloway, R.W., Gancedo, M.A., Fong, P.C., Goh, J.C., O'Malley, D.M., Armstrong, D.K., Garcia-Donas, J., Swisher, E.M., Floquet, A., Konecny, G.E., McNeish, I.A., Scott, C.L., Cameron, T., Maloney, L., Isaacson, J., Goble, S., Grace, C., Harding, T.C., Raponi, M., Sun, J., Lin, K.K., Giordano, H., Ledermann, J.A., ARIEL3 investigators, 2017. Rucaparib maintenance treatment for recurrent ovarian carcinoma after response to platinum therapy (ARIEL3): a randomised, double-blind, placebo-controlled, phase 3 trial. Lancet 390, 1949–1961. https://doi.org/10.1016/S0140-6736(17)32440-6

Craene, B.D., Berx, G., 2013. Regulatory networks defining EMT during cancer initiation and progression. Nat Rev Cancer 13, 97–110. https://doi.org/10.1038/nrc3447

Cree, I.A., Kurbacher, C.M., Lamont, A., Hindley, A.C., Love, S., TCA Ovarian Cancer Trial Group, 2007. A prospective randomized controlled trial of tumour chemosensitivity assay directed chemotherapy versus physician's choice in patients with recurrent platinum-resistant ovarian cancer. Anticancer Drugs 18, 1093–1101. https://doi.org/10.1097/CAD.0b013e3281de727e

Cristea, M., Han, E., Salmon, L., Morgan, R.J., 2010. Review: Practical considerations in ovarian cancer chemotherapy. Therapeutic advances in medical oncology 2, 175–187.

Cui, B., Zhang, S., Chen, L., Yu, J., Widhopf, G.F., Fecteau, J.-F., Rassenti, L.Z., Kipps, T.J., 2013. Targeting ROR1 inhibits epithelial-mesenchymal transition and metastasis. Cancer Res. 73, 3649–3660. https://doi.org/10.1158/0008-5472.CAN-12-3832

Cunnea, P., Stronach, E.A., 2014. Modeling Platinum Sensitive and Resistant High-Grade Serous Ovarian Cancer: Development and Applications of Experimental Systems. Front Oncol 4. https://doi.org/10.3389/fonc.2014.00081

DaneshManesh, A.H., Mikaelsson, E., Jeddi-Tehrani, M., Bayat, A.A., Ghods, R., Ostadkarampour, M., Akhondi, M., Lagercrantz, S., Larsson, C., Österborg, A., Shokri, F., Mellstedt, H., Rabbani, H., 2008. Ror1, a cell surface receptor tyrosine kinase is expressed in chronic lymphocytic leukemia and may serve as a putative target for therapy. Int. J. Cancer 123, 1190–1195. https://doi.org/10.1002/ijc.23587

Daneshmanesh, A.H., Porwit, A., Hojjat-Farsangi, M., Jeddi-Tehrani, M., Tamm, K.P., Grandér, D., Lehmann, S., Norin, S., Shokri, F., Rabbani, H., Mellstedt, H., Österborg, A., 2013. Orphan receptor tyrosine kinases ROR1 and ROR2 in hematological malignancies. Leuk. Lymphoma 54, 843–850. https://doi.org/10.3109/10428194.2012.731599

Dasari, S., Tchounwou, P.B., 2014. Cisplatin in cancer therapy: molecular mechanisms of action. Eur. J. Pharmacol. 740, 364–378. https://doi.org/10.1016/j.ejphar.2014.07.025

Deo, A., Mukherjee, S., Rekhi, B., Ray, P., 2020. Subtype specific biomarkers associated with chemoresistance in epithelial ovarian cancer. Indian Journal of Pathology and Microbiology 63, 64. https://doi.org/10.4103/IJPM.IJPM_872_19

DiSilvestro, P.A., 2019. Shaping the standard of care in ovarian cancer management: A review of Gynecologic Oncology Group (GOG)/NRG oncology clinical trials of the past twenty years. Gynecologic Oncology 153, 479–486. https://doi.org/10.1016/j.ygyno.2019.02.020

Doherty, B., Lawlor, D., Gillet, J.-P., Gottesman, M., O'leary, J.J., Stordal, B., 2014. Collateral Sensitivity to Cisplatin in KB-8-5-11 Drug-resistant Cancer Cells. Anticancer Res 34, 503–507.

Domcke, S., Sinha, R., Levine, D.A., Sander, C., Schultz, N., 2013. Evaluating cell lines as tumour models by comparison of genomic profiles. Nature Communications 4, ncomms3126. https://doi.org/10.1038/ncomms3126

Dong, W.-W., Mou, Q., Chen, J., Cui, J.-T., Li, W.-M., Xiao, W.-H., 2012. Differential expression of Rab27A/B correlates with clinical outcome in hepatocellular carcinoma. World J. Gastroenterol. 18, 1806–1813. https://doi.org/10.3748/wjg.v18.i15.1806

Dongre, A., Weinberg, R.A., 2019. New insights into the mechanisms of epithelial-mesenchymal transition and implications for cancer. Nat Rev Mol Cell Biol 20, 69–84. https://doi.org/10.1038/s41580-018-0080-4

Dorayappan, K.D.P., Wanner, R., Wallbillich, J.J., Saini, U., Zingarelli, R., Suarez, A.A., Cohn, D.E., Selvendiran, K., 2018. Hypoxia-induced exosomes contribute to a more aggressive and chemoresistant ovarian cancer phenotype: a novel mechanism linking STAT3/Rab proteins. Oncogene 37, 3806–3821. https://doi.org/10.1038/s41388-018-0189-0

Drew, Y., 2015. The development of PARP inhibitors in ovarian cancer: from bench to bedside. British Journal of Cancer 113, S3–S9. https://doi.org/10.1038/bjc.2015.394

Du Bois, A., Floquet, A., Kim, J.W., Rau, J., Del Campo, J.M., Friedlander, M., Pignata, S., Fujiwara, K., Vergote, I., Colombo, N., Mirza, M.R., Monk, B.J., Wimberger, P., Ray-Coquard, I., Zang, R., Diaz-Padilla, I., Baumann, K.H., Kim, J.H., Harter, P., 2013. Randomized, double-blind, phase III trial of pazopanib versus placebo in women who have not progressed after first-line chemotherapy for advanced epithelial ovarian, fallopian tube, or primary peritoneal cancer (AEOC): Results of an international Intergroup trial (AGO-OVAR16). JCO 31, LBA5503–LBA5503. https://doi.org/10.1200/jco.2013.31.18_suppl.lba5503

Du, L., Li, J., Lei, L., He, H., Chen, E., Dong, J., Yang, J., 2018. High Vimentin Expression Predicts a Poor Prognosis and Progression in Colorectal Cancer: A Study with Meta-Analysis and TCGA Database. Biomed Res Int 2018, 6387810. https://doi.org/10.1155/2018/6387810

Duan, Z., Lamendola, D.E., Duan, Y., Yusuf, R.Z., Seiden, M.V., 2005. Description of paclitaxel resistance-associated genes in ovarian and breast cancer cell lines. Cancer Chemother. Pharmacol. 55, 277–285. https://doi.org/10.1007/s00280-004-0878-y

Durmus, S., Sparidans, R.W., van Esch, A., Wagenaar, E., Beijnen, J.H., Schinkel, A.H., 2015. Breast Cancer Resistance Protein (BCRP/ABCG2) and P-glycoprotein (P-GP/ABCB1) Restrict Oral Availability and Brain Accumulation of the PARP Inhibitor Rucaparib (AG-014699). Pharm Res 32, 37–46. https://doi.org/10.1007/s11095-014-1442-z

Edwards, S.L., Brough, R., Lord, C.J., Natrajan, R., Vatcheva, R., Levine, D.A., Boyd, J., Reis-Filho, J.S., Ashworth, A., 2008. Resistance to therapy caused by intragenic deletion in BRCA2. Nature 451, 1111–1115. https://doi.org/10.1038/nature06548

Eisenhauer, E.A., Vermorken, J.B., van Glabbeke, M., 1997. Predictors of response to subsequent chemotherapy in platinum pretreated ovarian cancer: a multivariate analysis of 704 patients [seecomments]. Ann. Oncol. 8, 963–968. https://doi.org/10.1023/a:1008240421028

Elattar, A., Bryant, A., Winter-Roach, B.A., Hatem, M., Naik, R., 2011. Optimal primary surgical treatment for advanced epithelial ovarian cancer. Cochrane Database Syst Rev CD007565. https://doi.org/10.1002/14651858.CD007565.pub2

Erickson, B.K., Conner, M.G., Landen, C.N., 2013. The role of the fallopian tube in the origin of ovarian cancer. American Journal of Obstetrics and Gynecology 209, 409–414. https://doi.org/10.1016/j.ajog.2013.04.019

Fagotti, A., Ferrandina, G., Fanfani, F., Ercoli, A., Lorusso, D., Rossi, M., Scambia, G., 2006. A laparoscopy-based score to predict surgical outcome in patients with advanced ovarian carcinoma: a pilot study. Ann Surg Oncol 13, 1156–1161. https://doi.org/10.1245/ASO.2006.08.021

Faratian, D., Zweemer, A.J.M., Nagumo, Y., Sims, A.H., Muir, M., Dodds, M., Mullen, P., Um, I., Kay, C., Hasmann, M., Harrison, D.J., Langdon, S.P., 2011. Trastuzumab and Pertuzumab Produce Changes in Morphology and Estrogen Receptor Signaling in Ovarian Cancer Xenografts Revealing New Treatment Strategies. Clin Cancer Res 17, 4451–4461. https://doi.org/10.1158/1078-0432.CCR-10-2461

Farmer, H., McCabe, N., Lord, C.J., Tutt, A.N.J., Johnson, D.A., Richardson, T.B., Santarosa, M., Dillon, K.J., Hickson, I., Knights, C., Martin, N.M.B., Jackson, S.P., Smith, G.C.M., Ashworth, A., 2005a. Targeting the DNA repair defect in BRCA

mutant cells as a therapeutic strategy. Nature 434, 917–21.
https://doi.org/10.1038/nature03445

Farmer, H., McCabe, N., Lord, C.J., Tutt, A.N.J., Johnson, D.A., Richardson, T.B., Santarosa, M., Dillon, K.J., Hickson, I., Knights, C., Martin, N.M.B., Jackson, S.P., Smith, G.C.M., Ashworth, A., 2005b. Targeting the DNA repair defect in BRCA mutant cells as a therapeutic strategy. Nature 434, 917–921.
https://doi.org/10.1038/nature03445

Feng, T., Wang, Y., Lang, Y., Zhang, Y., 2017. KDM5A promotes proliferation and EMT in ovarian cancer and closely correlates with PTX resistance. Mol Med Rep 16, 3573–3580. https://doi.org/10.3892/mmr.2017.6960

Ferlini, C., Cicchillitti, L., Raspaglio, G., Bartollino, S., Cimitan, S., Bertucci, C., Mozzetti, S., Gallo, D., Persico, M., Fattorusso, C., Campiani, G., Scambia, G., 2009. Paclitaxel Directly Binds to Bcl-2 and Functionally Mimics Activity of Nur77. Cancer Res 69, 6906–6914. https://doi.org/10.1158/0008-5472.CAN-09-0540

Fernebro, E., Dictor, M., Bendahl, P.-O., Fernö, M., Nilbert, M., 2002. Evaluation of the tissue microarray technique for immunohistochemical analysis in rectal cancer. Arch Pathol Lab Med 126, 702–705. https://doi.org/10.1043/0003-9985(2002)126<0702:EOTTMT>2.0.CO;2

Fischer, K.R., Durrans, A., Lee, S., Sheng, J., Li, F., Wong, S.T.C., Choi, H., Rayes, T.E., Ryu, S., Troeger, J., Schwabe, R.F., Vahdat, L.T., Altorki, N.K., Mittal, V., Gao, D., 2015. Epithelial-to-mesenchymal transition is not required for lung metastasis but contributes to chemoresistance. Nature 527, 472–476.
https://doi.org/10.1038/nature15748

Fons, G., Hasibuan, S.M., van der Velden, J., ten Kate, F.J.W., 2007. Validation of tissue microarray technology in endometrioid cancer of the endometrium. J Clin Pathol 60, 500–503. https://doi.org/10.1136/jcp.2006.040170

Ford, C.E., Henry, C.E., Llamosas, E., Djordjevic, A., Hacker, N.F., Heinzelmann-Schwarz, V.A., Ward, R.L., 2014a. Hear the Ror! the Role of Wnt Signalling in Ovarian Cancer [WWW Document]. International Journal of Gynecological Cancer. URL http://ocrf.com.au/static/media/uploads/dr_caroline_ford_2014updated.pdf (accessed 5.10.16).

Ford, C.E., Jary, E., Ma, S.S.Q., Nixdorf, S., Heinzelmann-Schwarz, V.A., Ward, R.L., 2013. The Wnt Gatekeeper SFRP4 Modulates EMT, Cell Migration and Downstream Wnt Signalling in Serous Ovarian Cancer Cells. PLOS ONE 8, e54362. https://doi.org/10.1371/journal.pone.0054362

Ford, C.E., Punnia-Moorthy, G., Henry, C.E., Llamosas, E., Nixdorf, S., Olivier, J., Caduff, R., Ward, R.L., Heinzelmann-Schwarz, V., 2014b. The non-canonical Wnt ligand, Wnt5a, is upregulated and associated with epithelial to mesenchymal transition in epithelial ovarian cancer. Gynecol. Oncol. 134, 338–345.
https://doi.org/10.1016/j.ygyno.2014.06.004

Forrester, W.C., Kim, C., Garriga, G., 2004. The Caenorhabditis elegans Ror RTK CAM-1 Inhibits EGL-20/Wnt Signaling in Cell Migration. Genetics 168, 1951–1962.
https://doi.org/10.1534/genetics.104.031781

Fuertes, M.A., Alonso, C., Pérez, J.M., 2003. Biochemical modulation of Cisplatin mechanisms of action: enhancement of antitumor activity and circumvention of drug resistance. Chem. Rev. 103, 645–662. https://doi.org/10.1021/cr020010d

Fukuda, M., 2008. Regulation of secretory vesicle traffic by Rab small GTPases. Cell. Mol. Life Sci. 65, 2801–2813. https://doi.org/10.1007/s00018-008-8351-4

Fukuda, M., 2003. Distinct Rab Binding Specificity of Rim1, Rim2, Rabphilin, and Noc2 IDENTIFICATION OF A CRITICAL DETERMINANT OF Rab3A/Rab27A RECOGNITION BY Rim2. J. Biol. Chem. 278, 15373–15380. https://doi.org/10.1074/jbc.M212341200

Fukuda, T., Chen, L., Endo, T., Tang, L., Lu, D., Castro, J.E., Widhopf, G.F., Rassenti, L.Z., Cantwell, M.J., Prussak, C.E., Carson, D.A., Kipps, T.J., 2008. Antisera induced by infusions of autologous Ad-CD154-leukemia B cells identify ROR1 as an oncofetal antigen and receptor for Wnt5a. Proc. Natl. Acad. Sci. U.S.A. 105, 3047–3052. https://doi.org/10.1073/pnas.0712148105

Fultang, N., Illendula, A., Chen, B., Wu, C., Jonnalagadda, S., Baird, N., Klase, Z., Peethambaran, B., 2019. Strictinin, a novel ROR1-inhibitor, represses triple negative breast cancer survival and migration via modulation of PI3K/AKT/GSK3ß activity. PLOS ONE 14, e0217789. https://doi.org/10.1371/journal.pone.0217789

Fultang, N., Illendula, A., Lin, J., Pandey, M.K., Klase, Z., Peethambaran, B., 2020. ROR1 regulates chemoresistance in Breast Cancer via modulation of drug efflux pump ABCB1. Scientific Reports 10, 1–12. https://doi.org/10.1038/s41598-020-58864-0

Gadducci, A., Guarneri, V., Peccatori, F.A., Ronzino, G., Scandurra, G., Zamagni, C., Zola, P., Salutari, V., 2019. Current strategies for the targeted treatment of high-grade serous epithelial ovarian cancer and relevance of BRCA mutational status. Journal of Ovarian Research 12, 9. https://doi.org/10.1186/s13048-019-0484-6

Galluzzi, L., Senovilla, L., Vitale, I., Michels, J., Martins, I., Kepp, O., Castedo, M., Kroemer, G., 2012. Molecular mechanisms of cisplatin resistance. Oncogene 31, 1869–1883. https://doi.org/10.1038/onc.2011.384

Ganguly, A., Yang, H., Cabral, F., 2010. Paclitaxel-Dependent Cell Lines Reveal a Novel Drug Activity. Mol Cancer Ther 9, 2914–2923. https://doi.org/10.1158/1535-7163.MCT-10-0552

Geng, M., Cao, Y.-C., Chen, Y.-J., Jiang, H., Bi, L.-Q., Liu, X.-H., 2012. Loss of Wnt5a and Ror2 protein in hepatocellular carcinoma associated with poor prognosis. World J. Gastroenterol. 18, 1328–1338. https://doi.org/10.3748/wjg.v18.i12.1328

Gentile, A., Lazzari, L., Benvenuti, S., Trusolino, L., Comoglio, P.M., 2011. Ror1 Is a Pseudokinase That Is Crucial for Met-Driven Tumorigenesis. Cancer Res 71, 3132–3141. https://doi.org/10.1158/0008-5472.CAN-10-2662

Gershenson, D.M., 2012. Current advances in the management of malignant germ cell and sex cord-stromal tumors of the ovary. Gynecologic Oncology 125, 515–517. https://doi.org/10.1016/j.ygyno.2012.03.019

Ghosal, G., Chen, J., 2013. DNA damage tolerance: a double-edged sword guarding the genome. Translational cancer research 2, 107–129. https://doi.org/10.3978/j.issn.2218-676X.2013.04.01

Gillet, J.-P., Calcagno, A.M., Varma, S., Marino, M., Green, L.J., Vora, M.I., Patel, C., Orina, J.N., Eliseeva, T.A., Singal, V., Padmanabhan, R., Davidson, B., Ganapathi, R., Sood, A.K., Rueda, B.R., Ambudkar, S.V., Gottesman, M.M., 2011. Redefining the relevance of established cancer cell lines to the study of mechanisms of clinical anti-cancer drug resistance. PNAS 108, 18708–18713. https://doi.org/10.1073/pnas.1111840108

Gillet, J.-P., Varma, S., Gottesman, M.M., 2013. The clinical relevance of cancer cell lines. J. Natl. Cancer Inst. 105, 452–458. https://doi.org/10.1093/jnci/djt007

Glazer, R.I., Rohlff, C., 1994. Transcriptional regulation of multidrug resistance in breast cancer. Breast Cancer Res Tr 31, 263–271. https://doi.org/10.1007/BF00666159

Gong, C., Yao, H., Liu, Q., Chen, J., Shi, J., Su, F., Song, E., 2010. Markers of tumor-initiating cells predict chemoresistance in breast cancer. PLoS ONE 5, e15630. https://doi.org/10.1371/journal.pone.0015630

Gong, J., Luk, F., Jaiswal, R., George, A.M., Grau, G.E.R., Bebawy, M., 2013. Microparticle drug sequestration provides a parallel pathway in the acquisition of cancer drug resistance. European Journal of Pharmacology 721, 116–125. https://doi.org/10.1016/j.ejphar.2013.09.044

González-Martín, A.J., Calvo, E., Bover, I., Rubio, M.J., Arcusa, A., Casado, A., Ojeda, B., Balañá, C., Martínez, E., Herrero, A., Pardo, B., Adrover, E., Rifá, J., Godes, M.J., Moyano, A., Cervantes, A., 2005. Randomized phase II trial of carboplatin versus paclitaxel and carboplatin in platinum-sensitive recurrent advanced ovarian carcinoma: a GEICO (Grupo Espanol de Investigacion en Cancer de Ovario) study. Ann. Oncol. 16, 749–755. https://doi.org/10.1093/annonc/mdi147

Goodsell, D.S., 2006. The Molecular Perspective: Cisplatin. STEM CELLS 24, 514–515. https://doi.org/10.1634/stemcells.2006-CSC2

Gordon, A.N., Fleagle, J.T., Guthrie, D., Parkin, D.E., Gore, M.E., Lacave, A.J., 2001. Recurrent epithelial ovarian carcinoma: a randomized phase III study of pegylated liposomal doxorubicin versus topotecan. J. Clin. Oncol. 19, 3312–3322. https://doi.org/10.1200/JCO.2001.19.14.3312

Gottesman, M.M., Ludwig, J., Xia, D., Szakacs, G., 2009. Defeating Drug Resistance in Cancer. Discovery Medicine 6, 18–23.

Green, J., Nusse, R., Amerongen, R. van, 2014. The Role of Ryk and Ror Receptor Tyrosine Kinases in Wnt Signal Transduction. Cold Spring Harb Perspect Biol 6, a009175. https://doi.org/10.1101/cshperspect.a009175

Griffin, M.C., Robinson, R.A., Trask, D.K., 2003. Validation of tissue microarrays using p53 immunohistochemical studies of squamous cell carcinoma of the larynx. Mod Pathol 16, 1181–1188. https://doi.org/10.1097/01.MP.0000097284.40421.D6

Grimm, C., Polterauer, S., Zeillinger, R., Tong, D., Heinze, G., Wolf, A., Natter, C., Reinthaller, A., Hefler, L.A., 2010. Two Multidrug-resistance (ABCB1) Gene Polymorphisms as Prognostic Parameters in Women with Ovarian Cancer. Anticancer Res 30, 3487–3491.

Gross, A.L., Kurman, R.J., Vang, R., Shih, I.-M., Visvanathan, K., 2010. Precursor lesions of high-grade serous ovarian carcinoma: morphological and molecular characteristics. J Oncol 2010, 126295. https://doi.org/10.1155/2010/126295

Grosshans, B.L., Ortiz, D., Novick, P., 2006. Rabs and their effectors: achieving specificity in membrane traffic. Proc. Natl. Acad. Sci. U.S.A. 103, 11821–11827. https://doi.org/10.1073/pnas.0601617103

Grünert, S., Jechlinger, M., Beug, H., 2003. Diverse cellular and molecular mechanisms contribute to epithelial plasticity and metastasis. Nat. Rev. Mol. Cell Biol. 4, 657–665. https://doi.org/10.1038/nrm1175

Gschwind, A., Fischer, O.M., Ullrich, A., 2004. The discovery of receptor tyrosine kinases: targets for cancer therapy. Nat. Rev. Cancer 4, 361–370. https://doi.org/10.1038/nrc1360

Guerra, F., Paiano, A., Migoni, D., Girolimetti, G., Perrone, A.M., De Iaco, P., Fanizzi, F.P., Gasparre, G., Bucci, C., 2019. Modulation of RAB7A Protein Expression Determines Resistance to Cisplatin through Late Endocytic Pathway Impairment and Extracellular Vesicular Secretion. Cancers 11, 52. https://doi.org/10.3390/cancers11010052

Guo, C., Song, C., Zhang, J., Gao, Y., Qi, Y., Zhao, Z., Yuan, C., 2020. Revisiting chemoresistance in ovarian cancer: Mechanism, biomarkers, and precision medicine. Genes & Diseases. https://doi.org/10.1016/j.gendis.2020.11.017

Guo, N., Peng, Z., 2017. Does serum CA125 have clinical value for follow-up monitoring of postoperative patients with epithelial ovarian cancer? Results of a 12-year study. Journal of Ovarian Research 10, 14. https://doi.org/10.1186/s13048-017-0310-y

Hagopian, G.S., Mills, G.B., Khokhar, A.R., Bast, R.C., Siddik, Z.H., 1999. Expression of p53 in cisplatin-resistant ovarian cancer cell lines: modulation with the novel platinum analogue (1R, 2R-diaminocyclohexane)(trans-diacetato)(dichloro)-platinum (IV). Clinical cancer research 5, 655–663.

Hah, S.S., Stivers, K.M., de Vere White, R.W., Henderson, P.T., 2006. Kinetics of Carboplatin−DNA Binding in Genomic DNA and Bladder Cancer Cells As Determined by Accelerator Mass Spectrometry. Chem. Res. Toxicol. 19, 622–626. https://doi.org/10.1021/tx060058c

Hansen, J.M., Coleman, R.L., Sood, A.K., 2016. Targeting the tumour microenvironment in ovarian cancer. Eur J Cancer 56, 131–143. https://doi.org/10.1016/j.ejca.2015.12.016

Haroon, S., Zia, A., Idrees, R., Memon, A., Fatima, S., Kayani, N., 2013. Clinicopathological spectrum of ovarian sex cord-stromal tumors; 20 years' retrospective study in a developing country. J Ovarian Res 6, 87. https://doi.org/10.1186/1757-2215-6-87

Harter, P., du Bois, A., Hahmann, M., Hasenburg, A., Burges, A., Loibl, S., Gropp, M., Huober, J., Fink, D., Schröder, W., Muenstedt, K., Schmalfeldt, B., Emons, G., Pfisterer, J., Wollschlaeger, K., Meerpohl, H.-G., Breitbach, G.-P., Tanner, B., Sehouli, J., Arbeitsgemeinschaft Gynaekologische Onkologie Ovarian Committee, AGO Ovarian Cancer Study Group, 2006. Surgery in recurrent ovarian cancer: the Arbeitsgemeinschaft Gynaekologische Onkologie (AGO) DESKTOP OVAR trial. Ann. Surg. Oncol. 13, 1702–1710. https://doi.org/10.1245/s10434-006-9058-0

Harter, P., Hahmann, M., Lueck, H.J., Poelcher, M., Wimberger, P., Ortmann, O., Canzler, U., Richter, B., Wagner, U., Hasenburg, A., Burges, A., Loibl, S., Meier, W., Huober, J., Fink, D., Schroeder, W., Muenstedt, K., Schmalfeldt, B., Emons, G., du Bois, A., 2009. Surgery for recurrent ovarian cancer: role of peritoneal carcinomatosis: exploratory analysis of the DESKTOP I Trial about risk factors, surgical implications, and prognostic value of peritoneal carcinomatosis. Ann. Surg. Oncol. 16, 1324–1330. https://doi.org/10.1245/s10434-009-0357-0

Harter, P., Sehouli, J., Reuss, A., Hasenburg, A., Scambia, G., Cibula, D., Mahner, S., Vergote, I., Reinthaller, A., Burges, A., Hanker, L., Pölcher, M., Kurzeder, C., Canzler, U., Petry, K.U., Obermair, A., Petru, E., Schmalfeldt, B., Lorusso, D., du Bois, A., 2011. Prospective validation study of a predictive score for operability of recurrent ovarian cancer: the Multicenter Intergroup Study DESKTOP II. A project of the AGO Kommission OVAR, AGO Study Group, NOGGO, AGO-Austria, and MITO. Int. J. Gynecol. Cancer 21, 289–295. https://doi.org/10.1097/IGC.0b013e31820aaafd

Hasan, N., Ohman, A.W., Dinulescu, D.M., 2015. The promise and challenge of ovarian cancer models. Transl Cancer Res 4, 14–28. https://doi.org/10.3978/j.issn.2218-676X.2015.01.02

Haslehurst, A.M., Koti, M., Dharsee, M., Nuin, P., Evans, K., Geraci, J., Childs, T., Chen, J., Li, J., Weberpals, J., Davey, S., Squire, J., Park, P.C., Feilotter, H., 2012. EMT transcription factors snail and slug directly contribute to cisplatin resistance in ovarian cancer. BMC Cancer 12, 91. https://doi.org/10.1186/1471-2407-12-91

Havrilesky, L.J., Yang, J.-C., Lee, P.S., Secord, A.A., Ehrisman, J.A., Davidson, B., Berchuck, A., Darcy, K.M., Maxwell, G.L., Reed, S.D., 2019. Patient preferences for attributes of primary surgical debulking versus neoadjuvant chemotherapy for treatment of newly diagnosed ovarian cancer. Cancer 125, 4399–4406. https://doi.org/10.1002/cncr.32447

Heintz, A.P.M., Odicino, F., Maisonneuve, P., Quinn, M.A., Benedet, J.L., Creasman, W.T., Ngan, H.Y.S., Pecorelli, S., Beller, U., 2006. Carcinoma of the Ovary. International Journal of Gynecology & Obstetrics 95, Supple, S161–S192. http://dx.doi.org/10.1016/S0020-7292(06)60033-7

Helleday, T., 2011. The underlying mechanism for the PARP and BRCA synthetic lethality: Clearing up the misunderstandings. Molecular Oncology, Genetic Instability and Cancer 5, 387–393. https://doi.org/10.1016/j.molonc.2011.07.001

Helm, C.W., States, J.C., 2009. Enhancing the efficacy of cisplatin in ovarian cancer treatment – could arsenic have a role. Journal of Ovarian Research 2, 1–7. https://doi.org/10.1186/1757-2215-2-2

Hendrix, A., Braems, G., Bracke, M., Seabra, M., Gahl, W., De Wever, O., Westbroek, W., 2010a. The secretory small GTPase Rab27B as a marker for breast cancer progression. Oncotarget 1, 304–308. https://doi.org/10.18632/oncotarget.100809

Hendrix, A., Maynard, D., Pauwels, P., Braems, G., Denys, H., Van den Broecke, R., Lambert, J., Van Belle, S., Cocquyt, V., Gespach, C., Bracke, M., Seabra, M.C., Gahl, W.A., De Wever, O., Westbroek, W., 2010b. Effect of the Secretory Small GTPase Rab27B on Breast Cancer Growth, Invasion, and Metastasis. J Natl Cancer Inst 102, 866–880. https://doi.org/10.1093/jnci/djq153

Hennessy, B.T., Coleman, R.L., Markman, M., 2009. Ovarian cancer. The Lancet 374, 1371–1382. https://doi.org/10.1016/S0140-6736(09)61338-6

Hennessy, B.T.J., Timms, K.M., Carey, M.S., Gutin, A., Meyer, L.A., Flake, D.D., Abkevich, V., Potter, J., Pruss, D., Glenn, P., Li, Y., Li, J., Gonzalez-Angulo, A.M., McCune, K.S., Markman, M., Broaddus, R.R., Lanchbury, J.S., Lu, K.H., Mills, G.B., 2010. Somatic mutations in BRCA1 and BRCA2 could expand the number of patients that benefit from poly (ADP ribose) polymerase inhibitors in ovarian cancer. Journal of clinical oncology : official journal of the American Society of Clinical Oncology 28, 3570–6. https://doi.org/10.1200/JCO.2009.27.2997

Henry, C., Hacker, N., Ford, C., 2017. Silencing ROR1 and ROR2 inhibits invasion and adhesion in an organotypic model of ovarian cancer metastasis. Oncotarget 8, 112727–112738. https://doi.org/10.18632/oncotarget.22559

Henry, Claire, Llamosas, E., Knipprath-Mészáros, A., Schoetzau, A., Obermann, E., Fuenfschilling, M., Caduff, R., Fink, D., Hacker, N., Ward, R., Heinzelmann-Schwarz, V., Ford, C., 2015. Targeting the ROR1 and ROR2 receptors in epithelial ovarian cancer inhibits cell migration and invasion. Oncotarget 6, 40310–40326.

Henry, C., Quadir, A., Hawkins, N.J., Jary, E., Llamosas, E., Kumar, D., Daniels, B., Ward, R.L., Ford, C.E., 2015. Expression of the novel Wnt receptor ROR2 is increased in breast cancer and may regulate both β-catenin dependent and independent Wnt signalling. J. Cancer Res. Clin. Oncol. 141, 243–254. https://doi.org/10.1007/s00432-014-1824-y

Henry, C.E., Emmanuel, C., Lambie, N., Loo, C., Kan, B., Kennedy, C.J., de Fazio, A., Hacker, N.F., Ford, C.E., 2017. Distinct Patterns of Stromal and Tumor Expression of ROR1 and ROR2 in Histological Subtypes of Epithelial Ovarian Cancer. Translational Oncology 10, 346–356. https://doi.org/10.1016/j.tranon.2017.01.014

Henry, C E, Llamosas, E., Djordjevic, A., Hacker, N.F., Ford, C.E., 2016. Migration and invasion is inhibited by silencing ROR1 and ROR2 in chemoresistant ovarian cancer. Oncogenesis 5, e226. https://doi.org/10.1038/oncsis.2016.32

Henry, C. E., Llamosas, E., Djordjevic, A., Hacker, N.F., Ford, C.E., 2016a. Migration and invasion is inhibited by silencing ROR1 and ROR2 in chemoresistant ovarian cancer. Oncogenesis 5, e226. https://doi.org/10.1038/oncsis.2016.32

Henry, C. E., Llamosas, E., Djordjevic, A., Hacker, N.F., Ford, C.E., 2016b. Migration and invasion is inhibited by silencing ROR1 and ROR2 in chemoresistant ovarian cancer. Oncogenesis 5, e226. https://doi.org/10.1038/oncsis.2016.32

Herrinton, L.J., Stanford, J.L., Schwartz, S.M., Weiss, N.S., 1994. Ovarian cancer incidence among Asian migrants to the United States and their descendants. J. Natl. Cancer Inst. 86, 1336–1339. https://doi.org/10.1093/jnci/86.17.1336

Hills, C.A., Kelland, L.R., Abel, G., Siracky, J., Wilson, A.P., Harrap, K.R., 1989. Biological properties of ten human ovarian carcinoma cell lines: calibration *in vitro* against four platinum complexes. British journal of cancer 59, 527–34.

Hojjat-Farsangi, M., Daneshmanesh, A.H., Khan, A.S., Shetye, J., Mozaffari, F., Kharaziha, P., Rathje, L.-S., Kokhaei, P., Hansson, L., Vågberg, J., Byström, S., Olsson, E., Löfberg, C., Norström, C., Schultz, J., Norin, M., Olin, T., Österborg, A., Mellstedt, H., Moshfegh, A., 2018. First-in-class oral small molecule inhibitor of the tyrosine kinase ROR1 (KAN0439834) induced significant apoptosis of chronic lymphocytic leukemia cells. Leukemia 32, 2291–2295. https://doi.org/10.1038/s41375-018-0113-1

Hojjat-Farsangi, M., Ghaemimanesh, F., Daneshmanesh, A.H., Bayat, A.-A., Mahmoudian, J., Jeddi-Tehrani, M., Rabbani, H., Mellstedt, H., 2013. Inhibition of the receptor tyrosine kinase ROR1 by anti-ROR1 monoclonal antibodies and siRNA induced apoptosis of melanoma cells. PLoS ONE 8, e61167. https://doi.org/10.1371/journal.pone.0061167

Hojjat-Farsangi, M., Moshfegh, A., Daneshmanesh, A.H., Khan, A.S., Mikaelsson, E., Österborg, A., Mellstedt, H., 2014. The receptor tyrosine kinase ROR1 – An oncofetal antigen for targeted cancer therapy. Seminars in Cancer Biology, Oncofetal signaling as a target for cancer therapy 29, 21–31. https://doi.org/10.1016/j.semcancer.2014.07.005

Hollestelle, A., Peeters, J.K., Smid, M., Timmermans, M., Verhoog, L.C., Westenend, P.J., Heine, A.A.J., Chan, A., Sieuwerts, A.M., Wiemer, E.A.C., Klijn, J.G.M., van der Spek, P.J., Foekens, J.A., Schutte, M., den Bakker, M.A., Martens, J.W.M., 2013. Loss of E-cadherin is not a necessity for epithelial to mesenchymal transition in human breast cancer. Breast Cancer Res. Treat. 138, 47–57. https://doi.org/10.1007/s10549-013-2415-3

Hollis, R.L., Churchman, M., Gourley, C., 2017. Distinct implications of different BRCA mutations: efficacy of cytotoxic chemotherapy, PARP inhibition and clinical outcome in ovarian cancer. Onco Targets Ther 10, 2539–2551. https://doi.org/10.2147/OTT.S102569

Holschneider, C.H., Berek, J.S., 2000. Ovarian cancer: epidemiology, biology, and prognostic factors. Semin Surg Oncol 19, 3–10.

Holzer, A.K., Howell, S.B., 2006. The Internalization and Degradation of Human Copper Transporter 1 following Cisplatin Exposure. Cancer Research 66, 10944–10952. https://doi.org/10.1158/0008-5472.CAN-06-1710

Holzer, A.K., Manorek, G.H., Howell, S.B., 2006. Contribution of the major copper influx transporter CTR1 to the cellular accumulation of cisplatin, carboplatin, and

oxaliplatin. Molecular pharmacology 70, 1390–4. https://doi.org/10.1124/mol.106.022624

Hoogstraat, M., de Pagter, M.S., Cirkel, G.A., van Roosmalen, M.J., Harkins, T.T., Duran, K., Kreeftmeijer, J., Renkens, I., Witteveen, P.O., Lee, C.C., Nijman, I.J., Guy, T., van 't Slot, R., Jonges, T.N., Lolkema, M.P., Koudijs, M.J., Zweemer, R.P., Voest, E.E., Cuppen, E., Kloosterman, W.P., 2014. Genomic and transcriptomic plasticity in treatment-naive ovarian cancer. Genome Res. 24, 200–211. https://doi.org/10.1101/gr.161026.113

Hooks, S.B., Callihan, P., Altman, M.K., Hurst, J.H., Ali, M.W., Murph, M.M., 2010. Regulators of G-Protein signaling RGS10 and RGS17 regulate chemoresistance in ovarian cancer cells. Molecular cancer 9, 289. https://doi.org/10.1186/1476-4598-9-289

Hope, J.M., Blank, S.V., 2010. Current status of maintenance therapy for advanced ovarian cancer. Int J Womens Health 1, 173–180.

Horta, M., Cunha, T.M., 2015. Sex cord-stromal tumors of the ovary: a comprehensive review and update for radiologists. Diagn Interv Radiol 21, 277–286. https://doi.org/10.5152/dir.2015.34414

Horvath, L.G., Lelliott, J.E., Kench, J.G., Lee, C.-S., Williams, E.D., Saunders, D.N., Grygiel, J.J., Sutherland, R.L., Henshall, S.M., 2007. Secreted frizzled-related protein 4 inhibits proliferation and metastatic potential in prostate cancer. The Prostate 67, 1081–1090. https://doi.org/10.1002/pros.20607

Hoskins, P.J., Le, N., Gilks, B., Tinker, A., Santos, J., Wong, F., Swenerton, K.D., 2012. Low-stage ovarian clear cell carcinoma: population-based outcomes in British Columbia, Canada, with evidence for a survival benefit as a result of irradiation. J. Clin. Oncol. 30, 1656–1662. https://doi.org/10.1200/JCO.2011.40.1646

Hou, L., Hou, X., Wang, L., Li, Z., Xin, B., Chen, J., Gao, X., Mu, H., 2017. PD98059 impairs the cisplatin-resistance of ovarian cancer cells by suppressing ERK pathway and epithelial mesenchymal transition process. Cancer Biomark 21, 187–194. https://doi.org/10.3233/CBM-170644

Howe, J.R., Conlon, K.C., 1997. The molecular genetics of pancreatic cancer. Surg Oncol 6, 1–18. https://doi.org/10.1016/s0960-7404(97)00001-7

Hu, Y., Xing, J., Chen, L., Guo, X., Du, Y., Zhao, C., Zhu, Y., Lin, M., Zhou, Z., Sha, J., 2008. RGS22, a novel testis-specific regulator of G-protein signaling involved in human and mouse spermiogenesis along with GNA12/13 subunits. Biol. Reprod. 79, 1021–1029. https://doi.org/10.1095/biolreprod.107.067504

Huang, J., Fan, X., Wang, X., Lu, Y., Zhu, H., Wang, W., Zhang, S., Wang, Z., 2015. High ROR2 expression in tumor cells and stroma is correlated with poor prognosis in pancreatic ductal adenocarcinoma. Sci Rep 5, 12991. https://doi.org/10.1038/srep12991

Huang, J., Hu, W., Sood, A.K., 2010. Prognostic Biomarkers in Ovarian Cancer. Cancer Biomark 8, 231–251. https://doi.org/10.3233/CBM-2011-0212

Huang, N., Xia, Y., Zhang, D., Wang, S., Bao, Y., He, R., Teng, J., Chen, J., 2017. Hierarchical assembly of centriole subdistal appendages via centrosome binding proteins CCDC120 and CCDC68. Nature Communications 8, 15057. https://doi.org/10.1038/ncomms15057

Huber, M.A., Kraut, N., Beug, H., 2005. Molecular requirements for epithelial-mesenchymal transition during tumor progression. Curr. Opin. Cell Biol. 17, 548–558. https://doi.org/10.1016/j.ceb.2005.08.001

Hudecek, M., Schmitt, T.M., Baskar, S., Lupo-Stanghellini, M.T., Nishida, T., Yamamoto, T.N., Bleakley, M., Turtle, C.J., Chang, W.-C., Greisman, H.A., Wood, B.,

Maloney, D.G., Jensen, M.C., Rader, C., Riddell, S.R., 2010. The B-cell tumor–associated antigen ROR1 can be targeted with T cells modified to express a ROR1-specific chimeric antigen receptor. Blood 116, 4532–4541. https://doi.org/10.1182/blood-2010-05-283309

Hudson, L.G., Zeineldin, R., Stack, M.S., 2008. Phenotypic Plasticity of Neoplastic Ovarian Epithelium: Unique Cadherin Profiles in Tumor Progression. Clin Exp Metastasis 25, 643–655. https://doi.org/10.1007/s10585-008-9171-5

Hugo, H., Ackland, M.L., Blick, T., Lawrence, M.G., Clements, J.A., Williams, E.D., Thompson, E.W., 2007. Epithelial--mesenchymal and mesenchymal--epithelial transitions in carcinoma progression. J. Cell. Physiol. 213, 374–383. https://doi.org/10.1002/jcp.21223

Ince, T.A., Sousa, A.D., Jones, M.A., Harrell, J.C., Agoston, E.S., Krohn, M., Selfors, L.M., Liu, W., Chen, K., Yong, M., Buchwald, P., Wang, B., Hale, K.S., Cohick, E., Sergent, P., Witt, A., Kozhekbaeva, Z., Gao, S., Agoston, A.T., Merritt, M.A., Foster, R., Rueda, B.R., Crum, C.P., Brugge, J.S., Mills, G.B., 2015. Characterization of twenty-five ovarian tumour cell lines that phenocopy primary tumours. Nature Communications 6, 7419. https://doi.org/10.1038/ncomms8419

Ishida, S., Lee, J., Thiele, D.J., Herskowitz, I., 2002. Uptake of the anticancer drug cisplatin mediated by the copper transporter Ctr1 in yeast and mammals. PNAS 99, 14298–14302. https://doi.org/10.1073/pnas.162491399

Ishida, S., McCormick, F., Smith-McCune, K., Hanahan, D., 2010. Enhancing tumor-specific uptake of the anticancer drug cisplatin with a copper chelator. Cancer cell 17, 574–83. https://doi.org/10.1016/j.ccr.2010.04.011

Iwatsuki, M., Mimori, K., Yokobori, T., Ishi, H., Beppu, T., Nakamori, S., Baba, H., Mori, M., 2010. Epithelial-mesenchymal transition in cancer development and its clinical significance. Cancer Sci. 101, 293–299. https://doi.org/10.1111/j.1349-7006.2009.01419.x

Jacob, F., Nixdorf, S., Hacker, N.F., Heinzelmann-Schwarz, V.A., 2014. Reliable *in vitro* studies require appropriate ovarian cancer cell lines. J Ovarian Res 7, 60. https://doi.org/10.1186/1757-2215-7-60

Jacobs, I., Oram, D., Fairbanks, J., Turner, J., Frost, C., Grudzinskas, J.G., 1990. A risk of malignancy index incorporating CA 125, ultrasound and menopausal status for the accurate preoperative diagnosis of ovarian cancer. BJOG: An International Journal of Obstetrics & Gynaecology 97, 922–929. https://doi.org/10.1111/j.1471-0528.1990.tb02448.x

Jayson, G.C., Kohn, E.C., Kitchener, H.C., Ledermann, J.A., 2014. Ovarian cancer. The Lancet 384, 1376–1388. https://doi.org/10.1016/S0140-6736(13)62146-7

Jazaeri, A.A., Shibata, E., Park, J., Bryant, J.L., Conaway, M.R., Modesitt, S.C., Smith, P.G., Milhollen, M.A., Berger, A.J., Dutta, A., 2013. Overcoming platinum resistance in preclinical models of ovarian cancer using the neddylation inhibitor MLN4924. Mol. Cancer Ther. 12, 1958–1967. https://doi.org/10.1158/1535-7163.MCT-12-1028

Jekerle, V., Klinkhammer, W., Scollard, D.A., Breitbach, K., Reilly, R.M., Piquette-Miller, M., Wiese, M., 2006. *In vitro* and *in vivo* evaluation of WK-X-34, a novel inhibitor of P-glycoprotein and BCRP, using radio imaging techniques. International Journal of Cancer 119, 414–422. https://doi.org/10.1002/ijc.21827

Jelovac, D., Armstrong, D.K., 2011. Recent progress in the diagnosis and treatment of ovarian cancer. CA: A Cancer Journal for Clinicians 61, 183–203. https://doi.org/10.3322/caac.20113

Ji, X., Lu, Y., Tian, H., Meng, X., Wei, M., Cho, W.C., 2019. Chemoresistance mechanisms of breast cancer and their countermeasures. Biomedicine & Pharmacotherapy 114, 108800. https://doi.org/10.1016/j.biopha.2019.108800

Jiang, H., Gao, M., Shen, Z., Luo, B., Li, R., Jiang, X., Ding, R., Ha, Y., Wang, Z., Jie, W., 2014. Blocking PI3K/Akt signaling attenuates metastasis of nasopharyngeal carcinoma cells through induction of mesenchymal-epithelial reverting transition. Oncology Reports 32, 559–566. https://doi.org/10.3892/or.2014.3220

Johnatty, S.E., Beesley, J., Gao, B., Chen, X., Lu, Y., Law, M.H., Henderson, M.J., Russell, A.J., Hedditch, E.L., Emmanuel, C., Fereday, S., Webb, P.M., Goode, E.L., Vierkant, R.A., Fridley, B.L., Cunningham, J.M., Fasching, P.A., Beckmann, M.W., Ekici, A.B., Hogdall, E., Kjaer, S.K., Jensen, A., Hogdall, C., Brown, R., Paul, J., Lambrechts, S., Despierre, E., Vergote, I., Lester, J., Karlan, B.Y., Heitz, F., Bois, A. du, Harter, P., Schwaab, I., Bean, Y., Pejovic, T., Levine, D.A., Goodman, M.T., Camey, M.E., Thompson, P.J., Lurie, G., Shildkraut, J., Berchuck, A., Terry, K.L., Cramer, D.W., Norris, M.D., Haber, M., MacGregor, S., deFazio, A., Chenevix-Trench, G., 2013. ABCB1 (MDR1) polymorphisms and ovarian cancer progression and survival: A comprehensive analysis from the Ovarian Cancer Association Consortium and The Cancer Genome Atlas. Gynecologic Oncology 131, 8–14. https://doi.org/10.1016/j.ygyno.2013.07.107

Johnson, J.L., Brzezinska, A.A., Tolmachova, T., Munafo, D.B., Ellis, B.A., Seabra, M.C., Hong, H., Catz, S.D., 2010. Rab27a and Rab27b Regulate Neutrophil Azurophilic Granule Exocytosis and NADPH oxidase Activity by Independent Mechanisms. Traffic 11, 533–547. https://doi.org/10.1111/j.1600-0854.2009.01029.x

Jung, E.-H., Lee, H.-N., Han, G.-Y., Kim, M.-J., Kim, C.-W., 2016. Targeting ROR1 inhibits the self-renewal and invasive ability of glioblastoma stem cells. Cell Biochemistry and Function 34, 149–157. https://doi.org/10.1002/cbf.3172

Jung, J.-G., Shih, I.-M., Park, J.T., Gerry, E., Kim, T.H., Ayhan, A., Handschuh, K., Davidson, B., Fader, A.N., Selleri, L., Wang, T.-L., 2016. Ovarian Cancer Chemoresistance Relies on the Stem Cell Reprogramming Factor PBX1. Cancer Res 76, 6351–6361. https://doi.org/10.1158/0008-5472.CAN-16-0980

Kaelin, W.G., 2005. The Concept of Synthetic Lethality in the Context of Anticancer Therapy | Nature Reviews Cancer. Nature Reviews Cancer 5, 689–698. https://doi.org/10.1038/nrc1691

Kajiyama, H., Shibata, K., Terauchi, M., Yamashita, M., Ino, K., Nawa, A., Kikkawa, F., 2007. Chemoresistance to paclitaxel induces epithelial-mesenchymal transition and enhances metastatic potential for epithelial ovarian carcinoma cells. International Journal of Oncology 31, 277–283. https://doi.org/10.3892/ijo.31.2.277

Kallioniemi, O.P., Wagner, U., Kononen, J., Sauter, G., 2001. Tissue microarray technology for high-throughput molecular profiling of cancer. Hum Mol Genet 10, 657–662. https://doi.org/10.1093/hmg/10.7.657

Kalluri, R., Weinberg, R.A., 2009. The basics of epithelial-mesenchymal transition. J Clin Invest 119, 1420–1428. https://doi.org/10.1172/JCI39104

Kampan, N.C., Madondo, M.T., McNally, O.M., Quinn, M., Plebanski, M., 2015. Paclitaxel and Its Evolving Role in the Management of Ovarian Cancer [WWW Document]. BioMed Research International. https://doi.org/10.1155/2015/413076

Karvonen, H., Niininen, W., Murumägi, A., Ungureanu, D., 2017. Targeting ROR1 identifies new treatment strategies in hematological cancers. Biochemical Society Transactions 45, 457–464. https://doi.org/10.1042/BST20160272

Kasherman, Y., Sturup, S., Gibson, D., 2009. Is glutathione the major cellular target of cisplatin? A study of the interactions of cisplatin with cancer cell extracts. Journal of medicinal chemistry 52, 4319–28. https://doi.org/10.1021/jm900138u

Kaucká, M., Krejčí, P., Plevová, K., Pavlová, S., Procházková, J., Janovská, P., Valnohová, J., Kozubík, A., Pospíšilová, S., Bryja, V., 2011. Post-translational modifications regulate signalling by Ror1. Acta Physiol (Oxf) 203, 351–362. https://doi.org/10.1111/j.1748-1716.2011.02306.x

Kauff, N.D., Satagopan, J.M., Robson, M.E., Scheuer, L., Hensley, M., Hudis, C.A., Ellis, N.A., Boyd, J., Borgen, P.I., Barakat, R.R., Norton, L., Castiel, M., Nafa, K., Offit, K., 2002. Risk-Reducing Salpingo-oophorectomy in Women with a BRCA1 or BRCA2 Mutation. New England Journal of Medicine 346, 1609–1615. https://doi.org/10.1056/NEJMoa020119

Kaufman, B., Shapira-Frommer, R., Schmutzler, R.K., Audeh, M.W., Friedlander, M., Balmaña, J., Mitchell, G., Fried, G., Stemmer, S.M., Hubert, A., Rosengarten, O., Steiner, M., Loman, N., Bowen, K., Fielding, A., Domchek, S.M., 2015. Olaparib monotherapy in patients with advanced cancer and a germline BRCA1/2 mutation. J Clin Oncol 33, 244–250. https://doi.org/10.1200/JCO.2014.56.2728

Kaye, S.B., Brown, R., Gabra, H., Gore, M., 2011. Emerging therapeutic targets in ovarian cancer. Springer.

Kehoe, S., Hook, J., Nankivell, M., Jayson, G.C., Kitchener, H., Lopes, T., Luesley, D., Perren, T., Bannoo, S., Mascarenhas, M., Dobbs, S., Essapen, S., Twigg, J., Herod, J., McCluggage, G., Parmar, M., Swart, A.-M., 2015. Primary chemotherapy versus primary surgery for newly diagnosed advanced ovarian cancer (CHORUS): an open-label, randomised, controlled, non-inferiority trial. Lancet 386, 249–257. https://doi.org/10.1016/S0140-6736(14)62223-6

Kelemen, L.E., Köbel, M., 2011. Mucinous carcinomas of the ovary and colorectum: different organ, same dilemma. Lancet Oncol. 12, 1071–1080. https://doi.org/10.1016/S1470-2045(11)70058-4

Kelland, L.R., Barnard, F.J., Evans, I.G., Murrer, B.A., Theobald, B.R.C., Wyer, S.B., Goddard, P.M., Jones, M., Valenti, M., 1995. Synthesis and *in vitro* and *in vivo* Antitumor Activity of a Series of Trans Platinum Antitumor Complexes. Journal of Medicinal Chemistry 38, 3016–3024. https://doi.org/10.1021/jm00016a004

Khoo, X.-H., Paterson, I.C., Goh, B.-H., Lee, W.-L., 2019. Cisplatin-Resistance in Oral Squamous Cell Carcinoma: Regulation by Tumor Cell-Derived Extracellular Vesicles. Cancers 11, 1166. https://doi.org/10.3390/cancers11081166

Khouja, M.H., Baekelandt, M., Nesland, J.M., Holm, R., 2007. The clinical importance of Ki-67, p16, p14, and p57 expression in patients with advanced ovarian carcinoma. Int J Gynecol Pathol 26, 418–425. https://doi.org/10.1097/pgp.0b013e31804216a0

Khouja, M.H., Baekelandt, M., Sarab, A., Nesland, J.M., Holm, R., 2010. Limitations of tissue microarrays compared with whole tissue sections in survival analysis. Oncol Lett 1, 827–831. https://doi.org/10.3892/ol_00000145

Kilari, D., Guancial, E., Kim, E.S., 2016. Role of copper transporters in platinum resistance. World J Clin Oncol 7, 106–113. https://doi.org/10.5306/wjco.v7.i1.106

Kim, J.H., Lee, J.Y., Lee, K.T., Lee, J.K., Lee, K.H., Jang, K.-T., Heo, J.S., Choi, S.H., Rhee, J.C., 2010. RGS16 and FosB underexpressed in pancreatic cancer with lymph node metastasis promote tumor progression. Tumour Biol. 31, 541–548. https://doi.org/10.1007/s13277-010-0067-z

King, M.-C., Marks, J.H., Mandell, J.B., Group, T.N.Y.B.C.S., 2003. Breast and Ovarian Cancer Risks Due to Inherited Mutations in BRCA1 and BRCA2. Science 302, 643–646. https://doi.org/10.1126/science.1088759

Kliewer, E.V., Smith, K.R., 1995. Ovarian cancer mortality among immigrants in Australia and Canada. Cancer Epidemiol. Biomarkers Prev. 4, 453–458.

Koh, H.M., Jang, B.G., Kim, D.C., 2020. Prognostic significance of Rab27 expression in solid cancer: a systematic review and meta-analysis. Scientific Reports 10, 14136. https://doi.org/10.1038/s41598-020-71104-9

Koh, H.M., Song, D.H., 2019. Prognostic role of Rab27A and Rab27B expression in patients with non-small cell lung carcinoma. Thoracic Cancer 10, 143–149. https://doi.org/10.1111/1759-7714.12919

Kononen, J., Bubendorf, L., Kallioniemi, A., Bärlund, M., Schraml, P., Leighton, S., Torhorst, J., Mihatsch, M.J., Sauter, G., Kallioniemi, O.P., 1998. Tissue microarrays for high-throughput molecular profiling of tumor specimens. Nat Med 4, 844–847. https://doi.org/10.1038/nm0798-844

Kool, M., de Haas, M., Scheffer, G.L., Scheper, R.J., van Eijk, M.J., Juijn, J.A., Baas, F., Borst, P., 1997. Analysis of expression of cMOAT (MRP2), MRP3, MRP4, and MRP5, homologues of the multidrug resistance-associated protein gene (MRP1), in human cancer cell lines. Cancer Res. 57, 3537–3547.

Korsching, E., Packeisen, J., Agelopoulos, K., Eisenacher, M., Voss, R., Isola, J., van Diest, P.J., Brandt, B., Boecker, W., Buerger, H., 2002. Cytogenetic alterations and cytokeratin expression patterns in breast cancer: integrating a new model of breast differentiation into cytogenetic pathways of breast carcinogenesis. Lab Invest 82, 1525–1533. https://doi.org/10.1097/01.lab.0000038508.86221.b3

Koshiyama, M., Matsumura, N., Konishi, I., 2014. Recent Concepts of Ovarian Carcinogenesis: Type I and Type II. Biomed Res Int 2014. https://doi.org/10.1155/2014/934261

Kothandapani, A., Dangeti, V.S.M.N., Brown, A.R., Banze, L.A., Wang, X.-H., Sobol, R.W., Patrick, S.M., 2011. Novel Role of Base Excision Repair in Mediating Cisplatin Cytotoxicity. J Biol Chem 286, 14564–14574. https://doi.org/10.1074/jbc.M111.225375

Kreuzinger, C., Gamperl, M., Wolf, A., Heinze, G., Geroldinger, A., Lambrechts, D., Boeckx, B., Smeets, D., Horvat, R., Aust, S., Hamilton, G., Zeillinger, R., Cacsire Castillo-Tong, D., 2015. Molecular characterization of 7 new established cell lines from high grade serous ovarian cancer. Cancer Lett. 362, 218–228. https://doi.org/10.1016/j.canlet.2015.03.040

Kruse, V., Rottey, S., Backer, O. De, Belle, S. Van, Cocquyt, V., Denys, H., 2014. PARP INHIBITORS IN ONCOLOGY: A NEW SYNTHETIC LETHAL APPROACH TO CANCER THERAPY. Acta Clinica Belgica.

Kurman, R.J., Shih, I.-M., 2010. The Origin and Pathogenesis of Epithelial Ovarian Cancer- a Proposed Unifying Theory. Am J Surg Pathol 34, 433–443. https://doi.org/10.1097/PAS.0b013e3181cf3d79

Kurrey, N.K., K, A., Bapat, S.A., 2005. Snail and Slug are major determinants of ovarian cancer invasiveness at the transcription level. Gynecol. Oncol. 97, 155–165. https://doi.org/10.1016/j.ygyno.2004.12.043

Labidi-Galy, S.I., Papp, E., Hallberg, D., Niknafs, N., Adleff, V., Noe, M., Bhattacharya, R., Novak, M., Jones, S., Phallen, J., Hruban, C.A., Hirsch, M.S., Lin, D.I., Schwartz, L., Maire, C.L., Tille, J.-C., Bowden, M., Ayhan, A., Wood, L.D., Scharpf, R.B., Kurman, R., Wang, T.-L., Shih, I.-M., Karchin, R., Drapkin, R., Velculescu, V.E., 2017. High grade serous ovarian carcinomas originate in the fallopian tube. Nat Commun 8. https://doi.org/10.1038/s41467-017-00962-1

Lagas, J.S., Damen, C.W.N., Waterschoot, R.A.B. van, Iusuf, D., Beijnen, J.H., Schinkel, A.H., 2012. P-Glycoprotein, Multidrug-Resistance Associated Protein 2, Cyp3a,

and Carboxylesterase Affect the Oral Availability and Metabolism of Vinorelbine. Mol Pharmacol 82, 636–644. https://doi.org/10.1124/mol.111.077099

Lamouille, S., Xu, J., Derynck, R., 2014. Molecular mechanisms of epithelial–mesenchymal transition. Nat Rev Mol Cell Biol 15, 178–196. https://doi.org/10.1038/nrm3758

Lara, E., Calvanese, V., Huidobro, C., Fernández, A.F., Moncada-Pazos, A., Obaya, A.J., Aguilera, O., González-Sancho, J.M., Sánchez, L., Astudillo, A., Muñoz, A., López-Otín, C., Esteller, M., Fraga, M.F., 2010. Epigenetic repression of ROR2 has a Wnt-mediated, pro-tumourigenic role in colon cancer. Mol. Cancer 9, 170. https://doi.org/10.1186/1476-4598-9-170

Latifi, A., Abubaker, K., Castrechini, N., Ward, A.C., Liongue, C., Dobill, F., Kumar, J., Thompson, E.W., Quinn, M.A., Findlay, J.K., Ahmed, N., 2011. Cisplatin treatment of primary and metastatic epithelial ovarian carcinomas generates residual cells with mesenchymal stem cell-like profile. J Cell Biochem 112, 2850–2864. https://doi.org/10.1002/jcb.23199

Lawlor, D., Martin, P., Busschots, S., Thery, J., O'leary, J.J., Hennessy, B.T., Stordal, B., 2014. PARP Inhibitors as P-glyoprotein Substrates. Journal of Pharmaceutical Sciences 103, 1913–1920. https://doi.org/10.1002/jps.23952

Ledermann, J., Harter, P., Gourley, C., Friedlander, M., Vergote, I., Rustin, G., Scott, C., Meier, W., Shapira-Frommer, R., Safra, T., Matei, D., Macpherson, E., Watkins, C., Carmichael, J., Matulonis, U., 2012. Olaparib Maintenance Therapy in Platinum-Sensitive Relapsed Ovarian Cancer. New England Journal of Medicine 366, 1382–1392. https://doi.org/10.1056/NEJMoa1105535

Ledermann, J., Harter, P., Gourley, C., Friedlander, M., Vergote, I., Rustin, G., Scott, C.L., Meier, W., Shapira-Frommer, R., Safra, T., Matei, D., Fielding, A., Spencer, S., Dougherty, B., Orr, M., Hodgson, D., Barrett, J.C., Matulonis, U., 2014. Olaparib maintenance therapy in patients with platinum-sensitive relapsed serous ovarian cancer: a preplanned retrospective analysis of outcomes by BRCA status in a randomised phase 2 trial. The Lancet Oncology 15, 852–861. https://doi.org/10.1016/S1470-2045(14)70228-1

Ledermann, Jonathan A., Drew, Y., Kristeleit, R.S., 2016. Homologous recombination deficiency and ovarian cancer. European Journal of Cancer 60, 49–58. https://doi.org/10.1016/j.ejca.2016.03.005

Ledermann, Jonathan A, Harter, P., Gourley, C., Friedlander, M., Vergote, I., Rustin, G., Scott, C., Meier, W., Shapira-Frommer, R., Safra, T., Matei, D., Fielding, A., Spencer, S., Rowe, P., Lowe, E., Hodgson, D., Sovak, M.A., Matulonis, U., 2016. Overall survival in patients with platinum-sensitive recurrent serous ovarian cancer receiving olaparib maintenance monotherapy: an updated analysis from a randomised, placebo-controlled, double-blind, phase 2 trial. The Lancet Oncology 17, 1579–1589. https://doi.org/10.1016/S1470-2045(16)30376-X

Lee, J.M., Mhawech-Fauceglia, P., Lee, N., Parsanian, L.C., Lin, Y.G., Gayther, S.A., Lawrenson, K., 2013. A three-dimensional microenvironment alters protein expression and chemosensitivity of epithelial ovarian cancer cells in vitro. Lab. Invest. 93, 528–542. https://doi.org/10.1038/labinvest.2013.41

Lemmon, M.A., Schlessinger, J., 2010. Cell signaling by receptor tyrosine kinases. Cell 141, 1117–1134. https://doi.org/10.1016/j.cell.2010.06.011

Li, J., Jin, Q., Huang, F., Tang, Z., Huang, J., 2017. Effects of Rab27A and Rab27B on Invasion, Proliferation, Apoptosis, and Chemoresistance in Human Pancreatic Cancer Cells. Pancreas 46, 1173–1179. https://doi.org/10.1097/MPA.0000000000000910

Li, L., Ying, J., Tong, X., Zhong, L., Su, X., Xiang, T., Shu, X., Rong, R., Xiong, L., Li, H., Chan, A.T.C., Ambinder, R.F., Guo, Y., Tao, Q., 2014. Epigenetic identification of receptor tyrosine kinase-like orphan receptor 2 as a functional tumor suppressor inhibiting β-catenin and AKT signaling but frequently methylated in common carcinomas. Cell. Mol. Life Sci. 71, 2179–2192. https://doi.org/10.1007/s00018-013-1485-z

Li, R., Dong, C., Jiang, K., Sun, R., Zhou, Y., Yin, Z., Lv, J., Zhang, J., Wang, Q., Wang, L., 2020. Rab27B enhances drug resistance in hepatocellular carcinoma by promoting exosome-mediated drug efflux. Carcinogenesis. https://doi.org/10.1093/carcin/bgaa029

Li, W., Mu, D., Tian, F., Hu, Y., Jiang, T., Han, Y., Chen, J., Han, G., Li, X., 2013. Exosomes derived from Rab27a-overexpressing tumor cells elicit efficient induction of antitumor immunity. Mol Med Rep 8, 1876–1882. https://doi.org/10.3892/mmr.2013.1738

Li, X., Li, J., Yang, Y., Hou, R., Liu, R., Zhao, X., Yan, X., Yin, G., An, P., Wang, Y., Zhang, K., 2013. Differential gene expression in peripheral blood T cells from patients with psoriasis, lichen planus, and atopic dermatitis. J. Am. Acad. Dermatol. 69, e235-243. https://doi.org/10.1016/j.jaad.2013.06.030

Li, Z., Fang, R., Fang, J., He, S., Liu, T., 2018. Functional implications of Rab27 GTPases in Cancer. Cell Communication and Signaling 16, 44. https://doi.org/10.1186/s12964-018-0255-9

Liang, G., Bansal, G., Xie, Z., Druey, K.M., 2009. RGS16 Inhibits Breast Cancer Cell Growth by Mitigating Phosphatidylinositol 3-Kinase Signaling. J Biol Chem 284, 21719–21727. https://doi.org/10.1074/jbc.M109.028407

Liebmann, J.E., Cook, J.A., Lipschultz, C., Teague, D., Fisher, J., Mitchell, J.B., 1993. Cytotoxic studies of paclitaxel (Taxol®) in human tumour cell lines. British Journal of Cancer 68, 1104. https://doi.org/10.1038/bjc.1993.488

Lin, K.K., Harrell, M.I., Oza, A.M., Oaknin, A., Ray-Coquard, I., Tinker, A.V., Helman, E., Radke, M.R., Say, C., Vo, L.-T., Mann, E., Isaacson, J.D., Maloney, L., O'Malley, D.M., Chambers, S.K., Kaufmann, S.H., Scott, C.L., Konecny, G.E., Coleman, R.L., Sun, J.X., Giordano, H., Brenton, J.D., Harding, T.C., McNeish, I.A., Swisher, E.M., 2019. BRCA Reversion Mutations in Circulating Tumor DNA Predict Primary and Acquired Resistance to the PARP Inhibitor Rucaparib in High-Grade Ovarian Carcinoma. Cancer Discov 9, 210–219. https://doi.org/10.1158/2159-8290.CD-18-0715

Liu, Guoyan, Yang, D., Rupaimoole, R., Pecot, C.V., Sun, Y., Mangala, L.S., Li, X., Ji, P., Cogdell, D., Hu, L., Wang, Y., Rodriguez-Aguayo, C., Lopez-Berestein, G., Shmulevich, I., De Cecco, L., Chen, K., Mezzanzanica, D., Xue, F., Sood, A.K., Zhang, W., 2015. Augmentation of response to chemotherapy by microRNA-506 through regulation of RAD51 in serous ovarian cancers. J Natl Cancer Inst 107. https://doi.org/10.1093/jnci/djv108

Liu, J.F., Barry, W.T., Birrer, M., Lee, J.-M., Buckanovich, R.J., Fleming, G.F., Rimel, B., Buss, M.K., Nattam, S., Hurteau, J., Luo, W., Quy, P., Whalen, C., Obermayer, L., Lee, H., Winer, E.P., Kohn, E.C., Ivy, S.P., Matulonis, U.A., 2014. Combination cediranib and olaparib versus olaparib alone for women with recurrent platinum-sensitive ovarian cancer: a randomised phase 2 study. Lancet Oncol 15, 1207–1214. https://doi.org/10.1016/S1470-2045(14)70391-2

Liu, L.-G., Yan, X.-B., Xie, R.-T., Jin, Z.-M., Yang, Y., 2017. Stromal Expression of Vimentin Predicts the Clinical Outcome of Stage II Colorectal Cancer for High-

Risk Patients. Med. Sci. Monit. 23, 2897–2905.
https://doi.org/10.12659/msm.904486

Liu, X., Han, E.K., Anderson, M., Shi, Y., Semizarov, D., Wang, G., McGonigal, T., Roberts, L., Lasko, L., Palma, J., Zhu, G.-D., Penning, T., Rosenberg, S., Giranda, V.L., Luo, Y., Leverson, J., Johnson, E.F., Shoemaker, A.R., 2009. Acquired resistance to combination treatment with temozolomide and ABT-888 is mediated by both base excision repair and homologous recombination DNA repair pathways. Mol. Cancer Res. 7, 1686–1692. https://doi.org/10.1158/1541-7786.MCR-09-0299

Liu, X., Pu, W., He, H., Fan, X., Zheng, Yuanyuan, Zhou, J.-K., Ma, R., He, J., Zheng, Yuzhu, Wu, K., Zhao, Y., Yang, S.-Y., Wang, C., Wei, Y.-Q., Wei, X.-W., Peng, Y., 2019. Novel ROR1 inhibitor ARI-1 suppresses the development of non-small cell lung cancer. Cancer Letters 458, 76–85. https://doi.org/10.1016/j.canlet.2019.05.016

Liu, Yanfang, Gu, Y., Cao, X., 2015. The exosomes in tumor immunity. Oncoimmunology 4, e1027472. https://doi.org/10.1080/2162402X.2015.1027472

Liu, Yanchun, Yang, H., Chen, T., Luo, Y., Xu, Z., Li, Y., Yang, J., 2015. Silencing of Receptor Tyrosine Kinase ROR1 Inhibits Tumor-Cell Proliferation via PI3K/AKT/mTOR Signaling Pathway in Lung Adenocarcinoma. PLOS ONE 10, e0127092. https://doi.org/10.1371/journal.pone.0127092

Loh, C.-Y., Chai, J.Y., Tang, T.F., Wong, W.F., Sethi, G., Shanmugam, M.K., Chong, P.P., Looi, C.Y., 2019. The E-Cadherin and N-Cadherin Switch in Epithelial-to-Mesenchymal Transition: Signaling, Therapeutic Implications, and Challenges. Cells 8. https://doi.org/10.3390/cells8101118

Loh, S.Y., Mistry, P., Kelland, L.R., Abel, G., Harrap, K.R., 1992. Reduced drug accumulation as a major mechanism of acquired resistance to cisplatin in a human ovarian carcinoma cell line: circumvention studies using novel platinum (II) and (IV) ammine/amine complexes. British journal of cancer 66, 1109–15.

Loret, N., Denys, H., Tummers, P., Berx, G., 2019. The Role of Epithelial-to-Mesenchymal Plasticity in Ovarian Cancer Progression and Therapy Resistance. Cancers (Basel) 11. https://doi.org/10.3390/cancers11060838

Lu, B.-J., Wang, Y.-Q., Wei, X.-J., Rong, L.-Q., Wei, D., Yan, C.-M., Wang, D.-J., Sun, J.-Y., 2012. Expression of WNT-5a and ROR2 correlates with disease severity in osteosarcoma. Molecular Medicine Reports 5, 1033–1036. https://doi.org/10.3892/mmr.2012.772

Lu, C., Wang, X., Zhu, H., Feng, J., Ni, S., Huang, J., 2015. Over-expression of ROR2 and Wnt5a cooperatively correlates with unfavorable prognosis in patients with non-small cell lung cancer. Oncotarget 6, 24912–24921.

Lundholm, M., Schröder, M., Nagaeva, O., Baranov, V., Widmark, A., Mincheva-Nilsson, L., Wikström, P., 2014. Prostate Tumor-Derived Exosomes Down-Regulate NKG2D Expression on Natural Killer Cells and CD8+ T Cells: Mechanism of Immune Evasion. PLOS ONE 9, e108925. https://doi.org/10.1371/journal.pone.0108925

Ma, S.S.Q., Srivastava, S., Llamosas, E., Hawkins, N.J., Hesson, L.B., Ward, R.L., Ford, C.E., 2016. ROR2 is epigenetically inactivated in the early stages of colorectal neoplasia and is associated with proliferation and migration. BMC Cancer 16, 508. https://doi.org/10.1186/s12885-016-2576-7

MacKeigan, J.P., Murphy, L.O., Blenis, J., 2005. Sensitized RNAi screen of human kinases and phosphatases identifies new regulators of apoptosis and chemoresistance. Nature Cell Biology 7, 591. https://doi.org/10.1038/ncb1258

Madden, S.F., Clarke, C., Stordal, B., Carey, M.S., Broaddus, R., Gallagher, W.M., Crown, J., Mills, G.B., Hennessy, B.T., 2014. OvMark: a user-friendly system for the identification of prognostic biomarkers in publically available ovarian cancer gene expression datasets. Molecular cancer 13, 241. https://doi.org/10.1186/1476-4598-13-241

Malander, S., Ridderheim, M., Måsbäck, A., Loman, N., Kristoffersson, U., Olsson, H., Nilbert, M., Borg, A., 2004. One in 10 ovarian cancer patients carry germ line BRCA1 or BRCA2 mutations: results of a prospective study in Southern Sweden. Eur. J. Cancer 40, 422–428. https://doi.org/10.1016/j.ejca.2003.09.016

Mallen, A., Soong, T.R., Townsend, M.K., Wenham, R.M., Crum, C.P., Tworoger, S.S., 2018. Surgical prevention strategies in ovarian cancer. Gynecologic Oncology 151, 166–175. https://doi.org/10.1016/j.ygyno.2018.08.005

Manchana, T., Phoolcharoen, N., Tantbirojn, P., 2019. BRCA mutation in high grade epithelial ovarian cancers. Gynecol Oncol Rep 29, 102–105. https://doi.org/10.1016/j.gore.2019.07.007

Manfredi, J.J., Horwitz, S.B., 1984. Taxol: an antimitotic agent with a new mechanism of action. Pharmacology & Therapeutics 25, 83–125. https://doi.org/10.1016/0163-7258(84)90025-1

Markman, M., 2011. Docetaxel plus trabectedin appears active in recurrent or persistent ovarian and primary peritoneal cancer after up to three prior regimes: A phase II study of the Gynecologic Oncology Group. Gynecologic Oncology 122, 462. https://doi.org/10.1016/j.ygyno.2011.04.053

Markman, M., Rothman, R., Hakes, T., Reichman, B., Hoskins, W., Rubin, S., Jones, W., Almadrones, L., Lewis, J.L., 1991. Second-line platinum therapy in patients with ovarian cancer previously treated with cisplatin. J. Clin. Oncol. 9, 389–393. https://doi.org/10.1200/JCO.1991.9.3.389

Masiakowski, P., Carroll, R.D., 1992. A novel family of cell surface receptors with tyrosine kinase-like domain. J. Biol. Chem. 267, 26181–26190.

Matz, M., Coleman, M.P., Sant, M., Chirlaque, M.D., Visser, O., Gore, M., Allemani, C., 2017. The Histology of Ovarian Cancer: Worldwide Distribution and Implications for International Survival Comparisons (CONCORD-2). Gynecol Oncol 144, 405–413. https://doi.org/10.1016/j.ygyno.2016.10.019

Mavaddat, N., Peock, S., Frost, D., Ellis, S., Platte, R., Fineberg, E., Evans, D.G., Izatt, L., Eeles, R.A., Adlard, J., Davidson, R., Eccles, D., Cole, T., Cook, J., Brewer, C., Tischkowitz, M., Douglas, F., Hodgson, S., Walker, L., Porteous, M.E., Morrison, P.J., Side, L.E., Kennedy, M.J., Houghton, C., Donaldson, A., Rogers, M.T., Dorkins, H., Miedzybrodzka, Z., Gregory, H., Eason, J., Barwell, J., McCann, E., Murray, A., Antoniou, A.C., Easton, D.F., 2013. Cancer Risks for BRCA1 and BRCA2 Mutation Carriers: Results From Prospective Analysis of EMBRACE. J Natl Cancer Inst 105, 812–822. https://doi.org/10.1093/jnci/djt095

May, T., Comeau, R., Sun, P., Kotsopoulos, J., Narod, S.A., Rosen, B., Ghatage, P., 2017. A Comparison of Survival Outcomes in Advanced Serous Ovarian Cancer Patients Treated With Primary Debulking Surgery Versus Neoadjuvant Chemotherapy. International Journal of Gynecologic Cancer 27, 668–674. https://doi.org/10.1097/IGC.0000000000000946

McCluggage, W.G., Hirschowitz, L., Gilks, C.B., Wilkinson, N., Singh, N., 2017. The Fallopian Tube Origin and Primary Site Assignment in Extrauterine High-grade Serous Carcinoma: Findings of a Survey of Pathologists and Clinicians. Int. J. Gynecol. Pathol. 36, 230–239. https://doi.org/10.1097/PGP.0000000000000336

McDermott, M., Eustace, A.J., Busschots, S., Breen, L., Crown, J., Clynes, M., O'Donovan, N., Stordal, B., 2014. *In vitro* Development of Chemotherapy and Targeted Therapy Drug-Resistant Cancer Cell Lines: A Practical Guide with Case Studies. Front Oncol 4. https://doi.org/10.3389/fonc.2014.00040

McGuire, W.P., Hoskins, W.J., Brady, M.F., Kucera, P.R., Partridge, E.E., Look, K.Y., Clarke-Pearson, D.L., Davidson, M., 1996. Cyclophosphamide and cisplatin compared with paclitaxel and cisplatin in patients with stage III and stage IV ovarian cancer. N. Engl. J. Med. 334, 1–6. https://doi.org/10.1056/NEJM199601043340101

McWhinney, S.R., Goldberg, R.M., McLeod, H.L., 2009. Platinum neurotoxicity pharmacogenetics. Mol Cancer Ther 8, 10–16. https://doi.org/10.1158/1535-7163.MCT-08-0840

Mechetner, E., Kyshtoobayeva, A., Zonis, S., Kim, H., Stroup, R., Garcia, R., Parker, R.J., Fruehauf, J.P., 1998. Levels of multidrug resistance (MDR1) P-glycoprotein expression by human breast cancer correlate with *in vitro* resistance to taxol and doxorubicin. Clin Cancer Res 4, 389–398.

Mei, H., Lian, S., Zhang, S., Wang, W., Mao, Q., Wang, H., 2014. High expression of ROR2 in cancer cell correlates with unfavorable prognosis in colorectal cancer. Biochemical and Biophysical Research Communications 453, 703–709. https://doi.org/10.1016/j.bbrc.2014.09.141

Meyer, T., Nelstrop, A.E., Mahmoudi, M., Rustin, G.J., 2001. Weekly cisplatin and oral etoposide as treatment for relapsed epithelial ovarian cancer. Ann. Oncol. 12, 1705–1709. https://doi.org/10.1023/a:1013558501425

Miow, Q.H., Tan, T.Z., Ye, J., Lau, J.A., Yokomizo, T., Thiery, J.-P., Mori, S., 2015. Epithelial-mesenchymal status renders differential responses to cisplatin in ovarian cancer. Oncogene 34, 1899–1907. https://doi.org/10.1038/onc.2014.136

Mirza, M.R., Monk, B.J., Herrstedt, J., Oza, A.M., Mahner, S., Redondo, A., Fabbro, M., Ledermann, J.A., Lorusso, D., Vergote, I., Ben-Baruch, N.E., Marth, C., Mądry, R., Christensen, R.D., Berek, J.S., Dørum, A., Tinker, A.V., du Bois, A., González-Martín, A., Follana, P., Benigno, B., Rosenberg, P., Gilbert, L., Rimel, B.J., Buscema, J., Balser, J.P., Agarwal, S., Matulonis, U.A., 2016. Niraparib Maintenance Therapy in Platinum-Sensitive, Recurrent Ovarian Cancer. New England Journal of Medicine 375, 2154–2164. https://doi.org/10.1056/NEJMoa1611310

Miyoshi, N., Ishii, H., Sekimoto, M., Doki, Y., Mori, M., 2009. RGS16 is a marker for prognosis in colorectal cancer. Ann. Surg. Oncol. 16, 3507–3514. https://doi.org/10.1245/s10434-009-0690-3

Momenimovahed, Z., Tiznobaik, A., Taheri, S., Salehiniya, H., 2019. Ovarian cancer in the world: epidemiology and risk factors. Int J Womens Health 11, 287–299. https://doi.org/10.2147/IJWH.S197604

Montel, V., Huang, T.-Y., Mose, E., Pestonjamasp, K., Tarin, D., 2005. Expression profiling of primary tumors and matched lymphatic and lung metastases in a xenogeneic breast cancer model. Am. J. Pathol. 166, 1565–1579. https://doi.org/10.1016/S0002-9440(10)62372-3

Montoni, A., Robu, M., Pouliot, E., Shah, G.M., 2013. Resistance to PARP-Inhibitors in Cancer Therapy. Front Pharmacol 4, 18. https://doi.org/10.3389/fphar.2013.00018

Moore, K., Colombo, N., Scambia, G., Kim, B.-G., Oaknin, A., Friedlander, M., Lisyanskaya, A., Floquet, A., Leary, A., Sonke, G.S., Gourley, C., Banerjee, S., Oza, A., González-Martín, A., Aghajanian, C., Bradley, W., Mathews, C., Liu, J., Lowe, E.S., Bloomfield, R., DiSilvestro, P., 2018. Maintenance Olaparib in

Patients with Newly Diagnosed Advanced Ovarian Cancer. New England Journal of Medicine 379, 2495–2505. https://doi.org/10.1056/NEJMoa1810858

More, S.S., Akil, O., Ianculescu, A.G., Geier, E.G., Lustig, L.R., Giacomini, K.M., 2010. Role of the copper transporter, CTR1, in platinum-induced ototoxicity. The Journal of neuroscience : the official journal of the Society for Neuroscience 30, 9500–9. https://doi.org/10.1523/JNEUROSCI.1544-10.2010

Morgan, R.J., Alvarez, R.D., Armstrong, D.K., Boston, B., Burger, R.A., Chen, L., Copeland, L., Crispens, M.A., Gershenson, D., Gray, H.J., Grigsby, P.W., Hakam, A., Havrilesky, L.J., Johnston, C., Lele, S., Matulonis, U.A., O'Malley, D.M., Penson, R.T., Remmenga, S.W., Sabbatini, P., Schilder, R.J., Schink, J.C., Teng, N., Werner, T.L., 2011. Epithelial Ovarian Cancer. Journal of the National Comprehensive Cancer Network 9, 82–113.

Morioka, K., Tanikawa, C., Ochi, K., Daigo, Y., Katagiri, T., Kawano, H., Kawaguchi, H., Myoui, A., Yoshikawa, H., Naka, N., Araki, N., Kudawara, I., Ieguchi, M., Nakamura, K., Nakamura, Y., Matsuda, K., 2009. Orphan receptor tyrosine kinase ROR2 as a potential therapeutic target for osteosarcoma. Cancer Science 100, 1227–1233. https://doi.org/10.1111/j.1349-7006.2009.01165.x

Muralidharan-Chari, V., Kohan, H.G., Asimakopoulos, A.G., Sudha, T., Sell, S., Kannan, K., Boroujerdi, M., Davis, P.J., Mousa, S.A., 2016. Microvesicle removal of anticancer drugs contributes to drug resistance in human pancreatic cancer cells. Oncotarget 7, 50365–50379. https://doi.org/10.18632/oncotarget.10395

Murthy, P., Muggia, F., 2019. PARP inhibitors: clinical development, emerging differences, and the current therapeutic issues. Cancer Drug Resistance 2, 665–679. https://doi.org/10.20517/cdr.2019.002

Negri, E., Pelucchi, C., Franceschi, S., Montella, M., Conti, E., Dal Maso, L., Parazzini, F., Tavani, A., Carbone, A., La Vecchia, C., 2003. Family history of cancer and risk of ovarian cancer. Eur. J. Cancer 39, 505–510. https://doi.org/10.1016/s0959-8049(02)00743-8

Ng, I.O., Liu, C.L., Fan, S.T., Ng, M., 2000. Expression of P-glycoprotein in hepatocellular carcinoma. A determinant of chemotherapy response. Am. J. Clin. Pathol. 113, 355–363. https://doi.org/10.1309/AC1M-4TY4-U0TN-EN7T

Ngan, C.Y., Yamamoto, H., Seshimo, I., Tsujino, T., Man-i, M., Ikeda, J.-I., Konishi, K., Takemasa, I., Ikeda, M., Sekimoto, M., Matsuura, N., Monden, M., 2007. Quantitative evaluation of vimentin expression in tumour stroma of colorectal cancer. Br. J. Cancer 96, 986–992. https://doi.org/10.1038/sj.bjc.6603651

Nguyen, V.H.L., Hough, R., Bernaudo, S., Peng, C., 2019. Wnt/β-catenin signalling in ovarian cancer: Insights into its hyperactivation and function in tumorigenesis. Journal of Ovarian Research 12, 122. https://doi.org/10.1186/s13048-019-0596-z

Nisticò, P., Bissell, M.J., Radisky, D.C., 2012. Epithelial-Mesenchymal Transition: General Principles and Pathological Relevance with Special Emphasis on the Role of Matrix Metalloproteinases. Cold Spring Harb Perspect Biol 4, a011908. https://doi.org/10.1101/cshperspect.a011908

O'Connell, M.P., Fiori, J.L., Xu, M., Carter, A.D., Frank, B.P., Camilli, T.C., French, A.D., Dissanayake, S.K., Indig, F.E., Bernier, M., Taub, D.D., Hewitt, S.M., Weeraratna, A.T., 2010. The orphan tyrosine kinase receptor, ROR2, mediates Wnt5A signaling in metastatic melanoma. Oncogene 29, 34. https://doi.org/10.1038/onc.2009.305

O'Connell, M.P., Marchbank, K., Webster, M.R., Valiga, A.A., Kaur, A., Vultur, A., Li, L., Herlyn, M., Villanueva, J., Liu, Q., Yin, X., Widura, S., Nelson, J., Ruiz, N., Camilli, T.C., Indig, F.E., Flaherty, K.T., Wargo, J.A., Frederick, D.T., Cooper,

Z.A., Nair, S., Amaravadi, R.K., Schuchter, L.M., Karakousis, G.C., Xu, W., Xu, X., Weeraratna, A.T., 2013. Hypoxia induces phenotypic plasticity and therapy resistance in melanoma via the tyrosine kinase receptors ROR1 and ROR2. Cancer Discov 3, 1378–1393. https://doi.org/10.1158/2159-8290.CD-13-0005

Oishi, I., Takeuchi, S., Hashimoto, R., Nagabukuro, A., Ueda, T., Liu, Z.-J., Hatta, T., Akira, S., Matsuda, Y., Yamamura, H., Otani, H., Minami, Y., 1999. Spatio-temporally regulated expression of receptor tyrosine kinases, mRor1, mRor2, during mouse development: implications in development and function of the nervous system. Genes to Cells 4, 41–56. https://doi.org/10.1046/j.1365-2443.1999.00234.x

Okoye, E., Euscher, E.D., Malpica, A., 2016. Ovarian Low-grade Serous Carcinoma: A Clinicopathologic Study of 33 Cases With Primary Surgery Performed at a Single Institution. Am. J. Surg. Pathol. 40, 627–635. https://doi.org/10.1097/PAS.0000000000000615

Onda, T., Satoh, T., Ogawa, G., Saito, T., Kasamatsu, T., Nakanishi, T., Mizutani, T., Takehara, K., Okamoto, A., Ushijima, K., Kobayashi, H., Kawana, K., Yokota, H., Takano, M., Kanao, H., Watanabe, Y., Yamamoto, K., Yaegashi, N., Kamura, T., Yoshikawa, H., Japan Clinical Oncology Group, 2020. Comparison of survival between primary debulking surgery and neoadjuvant chemotherapy for stage III/IV ovarian, tubal and peritoneal cancers in phase III randomised trial. Eur J Cancer 130, 114–125. https://doi.org/10.1016/j.ejca.2020.02.020

Oplustilova, L., Wolanin, K., Mistrik, M., Korinkova, G., Simkova, D., Bouchal, J., Lenobel, R., Bartkova, J., Lau, A., O'Connor, M.J., Lukas, J., Bartek, J., 2012. Evaluation of candidate biomarkers to predict cancer cell sensitivity or resistance to PARP-1 inhibitor treatment. Cell Cycle 11, 3837–3850. https://doi.org/10.4161/cc.22026

Orr, G.A., Verdier-Pinard, P., McDaid, H., Horwitz, S.B., 2003. Mechanisms of Taxol resistance related to microtubules. Oncogene 22, 7280. https://doi.org/10.1038/sj.onc.1206934

Osaki, M., Oshimura, M., Ito, H., 2004. PI3K-Akt pathway: its functions and alterations in human cancer. Apoptosis 9, 667–676. https://doi.org/10.1023/B:APPT.0000045801.15585.dd

O'Shannessy, D.J., Jackson, S.M., Twine, N.C., Hoffman, B.E., Dezso, Z., Agoulnik, S.I., Somers, E.B., 2013. Gene expression analyses support fallopian tube epithelium as the cell of origin of epithelial ovarian cancer. International journal of molecular sciences 14, 13687–703. https://doi.org/10.3390/ijms140713687

Ostrowski, M., Carmo, N.B., Krumeich, S., Fanget, I., Raposo, G., Savina, A., Moita, C.F., Schauer, K., Hume, A.N., Freitas, R.P., Goud, B., Benaroch, P., Hacohen, N., Fukuda, M., Desnos, C., Seabra, M.C., Darchen, F., Amigorena, S., Moita, L.F., Thery, C., 2010. Rab27a and Rab27b control different steps of the exosome secretion pathway. Nature Cell Biology 12, 19–30. https://doi.org/10.1038/ncb2000

Oza, A.M., Cibula, D., Benzaquen, A.O., Poole, C., Mathijssen, R.H.J., Sonke, G.S., Colombo, N., Špaček, J., Vuylsteke, P., Hirte, H., Mahner, S., Plante, M., Schmalfeldt, B., Mackay, H., Rowbottom, J., Lowe, E.S., Dougherty, B., Barrett, J.C., Friedlander, M., 2015. Olaparib combined with chemotherapy for recurrent platinum-sensitive ovarian cancer: a randomised phase 2 trial. Lancet Oncol 16, 87–97. https://doi.org/10.1016/S1470-2045(14)71135-0

Ozols, R.F., 2003. Maintenance therapy in advanced ovarian cancer: progression-free survival and clinical benefit. J. Clin. Oncol. 21, 2451–2453. https://doi.org/10.1200/JCO.2003.03.039

Ozols, R.F., Bundy, B.N., Greer, B.E., Fowler, J.M., Clarke-Pearson, D., Burger, R.A., Mannel, R.S., DeGeest, K., Hartenbach, E.M., Baergen, R., Gynecologic Oncology Group, 2003. Phase III trial of carboplatin and paclitaxel compared with cisplatin and paclitaxel in patients with optimally resected stage III ovarian cancer: a Gynecologic Oncology Group study. J. Clin. Oncol. 21, 3194–3200. https://doi.org/10.1200/JCO.2003.02.153

Paik, E.S., Lee, Y.-Y., Lee, E.-J., Choi, C.H., Kim, T.-J., Lee, J.-W., Bae, D.-S., Kim, B.-G., 2015. Survival analysis of revised 2013 FIGO staging classification of epithelial ovarian cancer and comparison with previous FIGO staging classification. Obstet Gynecol Sci 58, 124–134. https://doi.org/10.5468/ogs.2015.58.2.124

Paley, P.J., Swisher, E.M., Garcia, R.L., Agoff, S.N., Greer, B.E., Peters, K.L., Goff, B.A., 2001. Occult cancer of the fallopian tube in BRCA-1 germline mutation carriers at prophylactic oophorectomy: a case for recommending hysterectomy at surgical prophylaxis. Gynecol. Oncol. 80, 176–180. https://doi.org/10.1006/gyno.2000.6071

Palmer, R.E., Lee, S.B., Wong, J.C., Reynolds, P.A., Zhang, H., Truong, V., Oliner, J.D., Gerald, W.L., Haber, D.A., 2002. Induction of BAIAP3 by the EWS-WT1 chimeric fusion implicates regulated exocytosis in tumorigenesis. Cancer Cell 2, 497–505. https://doi.org/10.1016/s1535-6108(02)00205-2

Parkin, D.M., Bray, F., Ferlay, J., Pisani, P., 2005. Global cancer statistics, 2002. Ca-A Cancer Journal for Clinicians 55, 74–108.

Parmar, M.K.B., Ledermann, J.A., Colombo, N., du Bois, A., Delaloye, J.-F., Kristensen, G.B., Wheeler, S., Swart, A.M., Qian, W., Torri, V., Floriani, I., Jayson, G., Lamont, A., Tropé, C., ICON and AGO Collaborators, 2003. Paclitaxel plus platinum-based chemotherapy versus conventional platinum-based chemotherapy in women with relapsed ovarian cancer: the ICON4/AGO-OVAR-2.2 trial. Lancet 361, 2099–2106. https://doi.org/10.1016/s0140-6736(03)13718-x

Patel, A.G., Sarkaria, J.N., Kaufmann, S.H., 2011. Nonhomologous end joining drives poly(ADP-ribose) polymerase (PARP) inhibitor lethality in homologous recombination-deficient cells. Proc. Natl. Acad. Sci. U.S.A. 108, 3406–3411. https://doi.org/10.1073/pnas.1013715108

Paul, P., Simm, S., Mirus, O., Scharf, K.-D., Fragkostefanakis, S., Schleiff, E., 2014. The complexity of vesicle transport factors in plants examined by orthology search. PLoS ONE 9, e97745. https://doi.org/10.1371/journal.pone.0097745

Pauli-Magnus, C., Kroetz, D.L., 2004. Functional Implications of Genetic Polymorphisms in the Multidrug Resistance Gene MDR1 (ABCB1). Pharm Res 21, 904–913. https://doi.org/10.1023/B:PHAM.0000029276.21063.0b

Peng, C., Zhang, X., Yu, H., Wu, D., Zheng, J., 2011. Wnt5a as a predictor in poor clinical outcome of patients and a mediator in chemoresistance of ovarian cancer. Int. J. Gynecol. Cancer 21, 280–288. https://doi.org/10.1097/IGC.0b013e31820aaadb

Pepa, C.D., Tonini, G., Pisano, C., Di Napoli, M., Cecere, S.C., Tambaro, R., Facchini, G., Pignata, S., 2015. Ovarian cancer standard of care: are there real alternatives? Chin J Cancer 34, 17–27. https://doi.org/10.5732/cjc.014.10274

Pereira-Leal, J.B., Seabra, M.C., 2001. Evolution of the rab family of small GTP-binding proteins11Edited by J. Thornton. Journal of Molecular Biology 313, 889–901. https://doi.org/10.1006/jmbi.2001.5072

Peres, L.C., Moorman, P.G., Alberg, A.J., Bandera, E.V., Barnholtz-Sloan, J., Bondy, M., Cote, M.L., Funkhouser, E., Peters, E.S., Schwartz, A.G., Terry, P.D., Abbott, S.E., Camacho, F., Wang, F., Schildkraut, J.M., 2017. Lifetime number of ovulatory cycles and epithelial ovarian cancer risk in African American women. Cancer Causes Control 28, 405–414. https://doi.org/10.1007/s10552-017-0853-7

Permuth-Wey, J., Sellers, T., 2009. Epidemiology of Ovarian Cancer, in: Verma, M. (Ed.), Cancer Epidemiology. Humana Press, pp. 413–437. https://doi.org/10.1007/978-1-60327-492-0_20

Perren, T.J., Swart, A.M., Pfisterer, J., Ledermann, J.A., Pujade-Lauraine, E., Kristensen, G., Carey, M.S., Beale, P., Cervantes, A., Kurzeder, C., du Bois, A., Sehouli, J., Kimmig, R., Stähle, A., Collinson, F., Essapen, S., Gourley, C., Lortholary, A., Selle, F., Mirza, M.R., Leminen, A., Plante, M., Stark, D., Qian, W., Parmar, M.K.B., Oza, A.M., ICON7 Investigators, 2011. A phase 3 trial of bevacizumab in ovarian cancer. N. Engl. J. Med. 365, 2484–2496. https://doi.org/10.1056/NEJMoa1103799

Pfeffer, S., 2005. A model for Rab GTPase localization. Biochem. Soc. Trans. 33, 627–630. https://doi.org/10.1042/BST0330627

Pfeffer, S.R., 2005. Structural clues to Rab GTPase functional diversity. J. Biol. Chem. 280, 15485–15488. https://doi.org/10.1074/jbc.R500003200

Pfisterer, J., Plante, M., Vergote, I., du Bois, A., Hirte, H., Lacave, A.J., Wagner, U., Stähle, A., Stuart, G., Kimmig, R., Olbricht, S., Le, T., Emerich, J., Kuhn, W., Bentley, J., Jackisch, C., Lück, H.-J., Rochon, J., Zimmermann, A.H., Eisenhauer, E., AGO-OVAR, NCIC CTG, EORTC GCG, 2006. Gemcitabine plus carboplatin compared with carboplatin in patients with platinum-sensitive recurrent ovarian cancer: an intergroup trial of the AGO-OVAR, the NCIC CTG, and the EORTC GCG. J. Clin. Oncol. 24, 4699–4707. https://doi.org/10.1200/JCO.2006.06.0913

Pieretti, M., Hopenhayn-Rich, C., Khattar, N.H., Cao, Y., Huang, B., Tucker, T.C., 2002. Heterogeneity of ovarian cancer: relationships among histological group, stage of disease, tumor markers, patient characteristics, and survival. Cancer Invest. 20, 11–23. https://doi.org/10.1081/cnv-120000361

Pokhriyal, R., Hariprasad, R., Kumar, L., Hariprasad, G., 2019. Chemotherapy Resistance in Advanced Ovarian Cancer Patients. Biomark�Cancer 11, 1179299X19860815. https://doi.org/10.1177/1179299X19860815

Polyak, K., Weinberg, R.A., 2009. Transitions between epithelial and mesenchymal states: acquisition of malignant and stem cell traits. Nat Rev Cancer 9, 265–273. https://doi.org/10.1038/nrc2620

Prat, J., 2012. Pathology of cancers of the female genital tract. International Journal of Gynecology & Obstetrics 119, S137–S150. https://doi.org/10.1016/S0020-7292(12)60027-7

Prislei, S., Martinelli, E., Zannoni, G.F., Petrillo, M., Filippetti, F., Mariani, M., Mozzetti, S., Raspaglio, G., Scambia, G., Ferlini, C., 2015. Role and prognostic significance of the epithelial-mesenchymal transition factor ZEB2 in ovarian cancer. Oncotarget 6, 18966–18979.

Pujade-Lauraine, E., Hilpert, F., Weber, B., Reuss, A., Poveda, A., Kristensen, G., Sorio, R., Vergote, I.B., Witteveen, P., Bamias, A., Pereira, D., Wimberger, P., Oaknin, A., Mirza, M.R., Follana, P., Bollag, D.T., Ray-Coquard, I., 2012. AURELIA: A randomized phase III trial evaluating bevacizumab (BEV) plus chemotherapy (CT) for platinum (PT)-resistant recurrent ovarian cancer (OC). JCO 30, LBA5002–LBA5002. https://doi.org/10.1200/jco.2012.30.18_suppl.lba5002

Pujade-Lauraine, E., Ledermann, J.A., Selle, F., Gebski, V., Penson, R.T., Oza, A.M., Korach, J., Huzarski, T., Poveda, A., Pignata, S., Friedlander, M., Colombo, N., Harter, P., Fujiwara, K., Ray-Coquard, I., Banerjee, S., Liu, J., Lowe, E.S., Bloomfield, R., Pautier, P., Korach, J., Huzarski, T., Byrski, T., Pautier, P., Friedlander, M., Harter, P., Colombo, N., Pignata, S., Scambia, G., Nicoletto, M., Nussey, F., Clamp, A., Penson, R., Oza, A., Velasco, A.P., Rodrigues, M., Lotz, J.-

P., Selle, F., Ray-Coquard, I., Provencher, D., Aparicio, A.P., Boixader, L.V., Scott, C., Tamura, K., Yunokawa, M., Lisyanskaya, A., Medioni, J., Pécuchet, N., Dubot, C., Rouge, T. de la M., Kaminsky, M.-C., Weber, B., Lortholary, A., Parkinson, C., Ledermann, J., Williams, S., Banerjee, S., Cosin, J., Hoffman, J., Penson, R., Plante, M., Covens, A., Sonke, G., Joly, F., Floquet, A., Banerjee, S., Hirte, H., Amit, A., Park-Simon, T.-W., Matsumoto, K., Tjulandin, S., Kim, J.H., Gladieff, L., Sabbatini, R., O'Malley, D., Timmins, P., Kredentser, D., Milagro, N.L., Ginesta, M.P.B., Martorell, A.T., Lista, A.G. de L., González, B.O., Mileshkin, L., Mandai, M., Boere, I., Ottevanger, P., Nam, J.-H., Filho, E., Hamizi, S., Cognetti, F., Warshal, D., Dickson-Michelson, E., Kamelle, S., McKenzie, N., Rodriguez, G., Armstrong, D., Chalas, E., Celano, P., Behbakht, K., Davidson, S., Welch, S., Helpman, L., Fishman, A., Bruchim, I., Sikorska, M., Słowińska, A., Rogowski, W., Bidziński, M., Śpiewankiewicz, B., Herraez, A.C., Fernández, C.M., Gropp-Meier, M., Saito, T., Takehara, K., Enomoto, T., Watari, H., Choi, C.H., Kim, B.-G., Kim, J.W., Hegg, R., Vergote, I., 2017. Olaparib tablets as maintenance therapy in patients with platinum-sensitive, relapsed ovarian cancer and a BRCA1/2 mutation (SOLO2/ENGOT-Ov21): a double-blind, randomised, placebo-controlled, phase 3 trial. The Lancet Oncology 18, 1274–1284. https://doi.org/10.1016/S1470-2045(17)30469-2

Pujade-Lauraine, E., Wagner, U., Aavall-Lundqvist, E., Gebski, V., Heywood, M., Vasey, P.A., Volgger, B., Vergote, I., Pignata, S., Ferrero, A., Sehouli, J., Lortholary, A., Kristensen, G., Jackisch, C., Joly, F., Brown, C., Le Fur, N., du Bois, A., 2010. Pegylated liposomal Doxorubicin and Carboplatin compared with Paclitaxel and Carboplatin for patients with platinum-sensitive ovarian cancer in late relapse. J. Clin. Oncol. 28, 3323–3329. https://doi.org/10.1200/JCO.2009.25.7519

Purdie, D.M., Bain, C.J., Siskind, V., Webb, P.M., Green, A.C., 2003. Ovulation and risk of epithelial ovarian cancer. International Journal of Cancer 104, 228–232. https://doi.org/10.1002/ijc.10927

Qi, H., Sun, B., Zhao, X., Du, J., Gu, Q., Liu, Y., Cheng, R., Dong, X., 2014. Wnt5a promotes vasculogenic mimicry and epithelial-mesenchymal transition via protein kinase Cα in epithelial ovarian cancer. Oncology Reports 32, 771–779. https://doi.org/10.3892/or.2014.3229

Quirk, J.T., Natarajan, N., 2005. Ovarian cancer incidence in the United States, 1992-1999. Gynecol. Oncol. 97, 519–523. https://doi.org/10.1016/j.ygyno.2005.02.007

Rabban, J.T., Zaloudek, C.J., 2013. A practical approach to immunohistochemical diagnosis of ovarian germ cell tumours and sex cord–stromal tumours. Histopathology 62, 71–88. https://doi.org/10.1111/his.12052

Rabbani, H., Ostadkarampour, M., Danesh Manesh, A.H., Basiri, A., Jeddi-Tehrani, M., Forouzesh, F., 2010. Expression of ROR1 in patients with renal cancer--a potential diagnostic marker. Iran. Biomed. J. 14, 77–82.

Radulovich, N, Leung, L., Ibrahimov, E., Navab, R., Sakashita, S., Zhu, C.-Q., Kaufman, E., Lockwood, W.W., Thu, K.L., Fedyshyn, Y., Moffat, J., Lam, W.L., Tsao, M.-S., 2015. Coiled-coil domain containing 68 (CCDC68) demonstrates a tumor-suppressive role in pancreatic ductal adenocarcinoma. Oncogene 34, 4238–47. https://doi.org/10.1038/onc.2014.357

Radulovich, N., Leung, L., Ibrahimov, E., Navab, R., Sakashita, S., Zhu, C.-Q., Kaufman, E., Lockwood, W.W., Thu, K.L., Fedyshyn, Y., Moffat, J., Lam, W.L., Tsao, M.-S., 2015. Coiled-coil domain containing 68 (CCDC68) demonstrates a tumor-suppressive role in pancreatic ductal adenocarcinoma. Oncogene 34, 4238. https://doi.org/10.1038/onc.2014.357

Rajagopal, C., Harikumar, K.B., 2018. The Origin and Functions of Exosomes in Cancer. Front Oncol 8. https://doi.org/10.3389/fonc.2018.00066

Rauh-Hain, J.A., Melamed, A., Wright, A., Gockley, A., Clemmer, J.T., Schorge, J.O., Del Carmen, M.G., Keating, N.L., 2017. Overall Survival Following Neoadjuvant Chemotherapy vs Primary Cytoreductive Surgery in Women With Epithelial Ovarian Cancer: Analysis of the National Cancer Database. JAMA Oncol 3, 76–82. https://doi.org/10.1001/jamaoncol.2016.4411

Rebagay, G., Yan, S., Liu, C., Cheung, N.-K., 2012. ROR1 and ROR2 in Human Malignancies: Potentials for Targeted Therapy. Front Oncol 2, 34. https://doi.org/10.3389/fonc.2012.00034

Reddy, U.R., Phatak, S., Allen, C., Nycum, L.M., Sulman, E.P., White, P.S., Biegel, J.A., 1997. Localization of the human Ror1 gene (NTRKR1) to chromosome 1p31-p32 by fluorescence in situ hybridization and somatic cell hybrid analysis. Genomics 41, 283–285. https://doi.org/10.1006/geno.1997.4653

Reed, E., 1998. Platinum-DNA adduct, nucleotide excision repair and platinum based anti-cancer chemotherapy. Cancer Treatment Reviews 24, 331–344. https://doi.org/10.1016/S0305-7372(98)90056-1

Reid, B.M., Permuth, J.B., Sellers, T.A., 2017. Epidemiology of ovarian cancer: a review. Cancer Biol Med 14, 9–32. https://doi.org/10.20892/j.issn.2095-3941.2016.0084

Ren, P., Yang, X.-Q., Zhai, X.-L., Zhang, Y.-Q., Huang, J.-F., 2016. Overexpression of Rab27B is correlated with distant metastasis and poor prognosis in ovarian cancer. Oncol Lett 12, 1539–1545. https://doi.org/10.3892/ol.2016.4801

Renneberg, R., 2007. Biotech History: Yew trees, paclitaxel synthesis and fungi. Biotechnology Journal 2, 1207–1209. https://doi.org/10.1002/biot.200790106

Reuss, A., du Bois, A., Harter, P., Fotopoulou, C., Sehouli, J., Aletti, G., Guyon, F., Greggi, S., Mosgaard, B.J., Reinthaller, A., Hilpert, F., Schade-Brittinger, C., Chi, D.S., Mahner, S., 2019. TRUST: Trial of Radical Upfront Surgical Therapy in advanced ovarian cancer (ENGOT ov33/AGO-OVAR OP7). Int J Gynecol Cancer 29, 1327–1331. https://doi.org/10.1136/ijgc-2019-000682

Ricci, F., Affatato, R., Carrassa, L., Damia, G., 2018. Recent Insights into Mucinous Ovarian Carcinoma. Int J Mol Sci 19. https://doi.org/10.3390/ijms19061569

Rocha, C.R.R., Silva, M.M., Quinet, A., Cabral-Neto, J.B., Menck, C.F.M., 2018. DNA repair pathways and cisplatin resistance: an intimate relationship. Clinics (Sao Paulo) 73. https://doi.org/10.6061/clinics/2018/e478s

Rohena, C.C., Mooberry, S.L., 2014. Recent progress with microtubule stabilizers: new compounds, binding modes and cellular activities. Nat Prod Rep 31, 335–355. https://doi.org/10.1039/c3np70092e

Rosanò, L., Cianfrocca, R., Spinella, F., Di Castro, V., Nicotra, M.R., Lucidi, A., Ferrandina, G., Natali, P.G., Bagnato, A., 2011. Acquisition of chemoresistance and EMT phenotype is linked with activation of the endothelin A receptor pathway in ovarian carcinoma cells. Clin Cancer Res 17, 2350–2360. https://doi.org/10.1158/1078-0432.CCR-10-2325

Ross, E.M., Wilkie, T.M., 2000. GTPase-activating proteins for heterotrimeric G proteins: regulators of G protein signaling (RGS) and RGS-like proteins. Annu. Rev. Biochem. 69, 795–827. https://doi.org/10.1146/annurev.biochem.69.1.795

Roszmusz, E., Patthy, A., Trexler, M., Patthy, L., 2001. Localization of Disulfide Bonds in the Frizzled Module of Ror1 Receptor Tyrosine Kinase. J. Biol. Chem. 276, 18485–18490. https://doi.org/10.1074/jbc.M100100200

Rottenberg, S., Jaspers, J.E., Kersbergen, A., Burg, E. van der, Nygren, A.O.H., Zander, S.A.L., Derksen, P.W.B., Bruin, M. de, Zevenhoven, J., Lau, A., Boulter, R.,

Cranston, A., O'Connor, M.J., Martin, N.M.B., Borst, P., Jonkers, J., 2008. High sensitivity of BRCA1-deficient mammary tumors to the PARP inhibitor AZD2281 alone and in combination with platinum drugs. PNAS 105, 17079–17084. https://doi.org/10.1073/pnas.0806092105

Rowinsky, E.K., Donehower, R.C., 1995. Paclitaxel (Taxol). New England Journal of Medicine 332, 1004–1014. https://doi.org/10.1056/NEJM199504133321507

Russell, H., Pranjol, M.Z.I., 2018. Transcription factors controlling E-cadherin down-regulation in ovarian cancer. Bioscience Horizons 11. https://doi.org/10.1093/biohorizons/hzy010

Rustin, G.J., Nelstrop, A.E., McClean, P., Brady, M.F., McGuire, W.P., Hoskins, W.J., Mitchell, H., Lambert, H.E., 1996. Defining response of ovarian carcinoma to initial chemotherapy according to serum CA 125. J. Clin. Oncol. 14, 1545–1551. https://doi.org/10.1200/JCO.1996.14.5.1545

Rustin, G.J., van der Burg, M.E., Griffin, C.L., Guthrie, D., Lamont, A., Jayson, G.C., Kristensen, G., Mediola, C., Coens, C., Qian, W., Parmar, M.K., Swart, A.M., 2010. Early versus delayed treatment of relapsed ovarian cancer (MRC OV05/EORTC 55955): a randomised trial. The Lancet 376, 1155–1163. https://doi.org/10.1016/S0140-6736(10)61268-8

Safaei, R., Larson, B.J., Cheng, T.C., Gibson, M.A., Otani, S., Naerdemann, W., Howell, S.B., 2005. Abnormal lysosomal trafficking and enhanced exosomal export of cisplatin in drug-resistant human ovarian carcinoma cells. Mol Cancer Ther 4, 1595–1604. https://doi.org/10.1158/1535-7163.MCT-05-0102

Sakai, W., Swisher, E.M., Karlan, B.Y., Agarwal, M.K., Higgins, J., Friedman, C., Villegas, E., Jacquemont, C., Farrugia, D.J., Couch, F.J., Urban, N., Taniguchi, T., 2008. Secondary mutations as a mechanism of cisplatin resistance in BRCA2-mutated cancers. Nature 451, 1116–1120. https://doi.org/10.1038/nature06633

Sakata, J., Utsumi, F., Suzuki, S., Niimi, K., Yamamoto, E., Shibata, K., Senga, T., Kikkawa, F., Kajiyama, H., 2017. Inhibition of ZEB1 leads to inversion of metastatic characteristics and restoration of paclitaxel sensitivity of chronic chemoresistant ovarian carcinoma cells. Oncotarget 8, 99482–99494. https://doi.org/10.18632/oncotarget.20107

Samardzija, C., Greening, D.W., Escalona, R., Chen, M., Bilandzic, M., Luwor, R., Kannourakis, G., Findlay, J.K., Ahmed, N., 2017. Knockdown of stem cell regulator Oct4A in ovarian cancer reveals cellular reprogramming associated with key regulators of cytoskeleton-extracellular matrix remodelling. Sci Rep 7, 46312. https://doi.org/10.1038/srep46312

Sapino, A., Marchiò, C., Senetta, R., Castellano, I., Macrì, L., Cassoni, P., Ghisolfi, G., Cerrato, M., D'Ambrosio, E., Bussolati, G., 2006. Routine assessment of prognostic factors in breast cancer using a multicore tissue microarray procedure. Virchows Arch 449, 288–296. https://doi.org/10.1007/s00428-006-0233-2

Sartorius, C.M., Mirza, U., Schötzau, A., Mackay, G., Fink, D., Hacker, N.F., Heinzelmann-Schwarz, V., 2018. Impact of the new FIGO 2013 classification on prognosis of stage I epithelial ovarian cancers. Cancer Manag Res 10, 4709–4718. https://doi.org/10.2147/CMAR.S174777

Schiff, P.B., Fant, J., Horwitz, S.B., 1979. Promotion of microtubule assembly *in vitro* by taxol. Nature 277, 665. https://doi.org/10.1038/277665a0

Schiff, P.B., Horwitz, S.B., 1980. Taxol stabilizes microtubules in mouse fibroblast cells. PNAS 77, 1561–1565.

Scholler, N., Urban, N., 2007. CA125 in Ovarian Cancer. Biomark Med 1, 513–523. https://doi.org/10.2217/17520363.1.4.513

Sedukhina, A.S., Sundaramoorthy, E., Hara, M., Kumai, T., Sato, K., 2015. Beyond resistance to PARP inhibition: Mechanisms and effective treatment options. https://doi.org/10.14800/ccm.821

Seidman, J.D., Horkayne-Szakaly, I., Haiba, M., Boice, C.R., Kurman, R.J., Ronnett, B.M., 2004. The histologic type and stage distribution of ovarian carcinomas of surface epithelial origin. Int. J. Gynecol. Pathol. 23, 41–44. https://doi.org/10.1097/01.pgp.0000101080.35393.16

Seidman, J.D., Kurman, R.J., Ronnett, B.M., 2003. Primary and metastatic mucinous adenocarcinomas in the ovaries: incidence in routine practice with a new approach to improve intraoperative diagnosis. Am. J. Surg. Pathol. 27, 985–993. https://doi.org/10.1097/00000478-200307000-00014

Shaaban, A.M., Rezvani, M., Elsayes, K.M., Baskin, H., Mourad, A., Foster, B.R., Jarboe, E.A., Menias, C.O., 2014. Ovarian Malignant Germ Cell Tumors: Cellular Classification and Clinical and Imaging Features. RadioGraphics 34, 777–801. https://doi.org/10.1148/rg.343130067

Shabani, M., Asgarian-Omran, H., Vossough, P., Sharifian, R.A., Faranoush, M., Ghragozlou, S., Khoshnoodi, J., Roohi, A., Jeddi-Tehrani, M., Mellstedt, H., Rabbani, H., Shokri, F., 2008. Expression profile of orphan receptor tyrosine kinase (ROR1) and Wilms' tumor gene 1 (WT1) in different subsets of B-cell acute lymphoblastic leukemia. Leuk. Lymphoma 49, 1360–1367. https://doi.org/10.1080/10428190802124000

Shahzad, M.M.K., Lopez-Berestein, G., Sood, A.K., 2009. Novel strategies for reversing platinum resistance. Drug Resistance Updates 12, 148–152. https://doi.org/10.1016/j.drup.2009.09.001

Sharma, R., Graham, J., Mitchell, H., Brooks, A., Blagden, S., Gabra, H., 2009. Extended weekly dose-dense paclitaxel/carboplatin is feasible and active in heavily pre-treated platinum-resistant recurrent ovarian cancer. Br. J. Cancer 100, 707–712. https://doi.org/10.1038/sj.bjc.6604914

Shedden, K., Xie, X.T., Chandaroy, P., Chang, Y.T., Rosania, G.R., 2003. Expulsion of small molecules in vesicles shed by cancer cells: association with gene expression and chemosensitivity profiles. Cancer Res 63, 4331–4337.

Sheffer, M., Bacolod, M.D., Zuk, O., Giardina, S.F., Pincas, H., Barany, F., Paty, P.B., Gerald, W.L., Notterman, D.A., Domany, E., 2009. Association of survival and disease progression with chromosomal instability: a genomic exploration of colorectal cancer. Proceedings of the National Academy of Sciences of the United States of America 106, 7131–6. https://doi.org/10.1073/pnas.0902232106

Shen, D.-W., Pouliot, L.M., Hall, M.D., Gottesman, M.M., 2012. Cisplatin resistance: a cellular self-defense mechanism resulting from multiple epigenetic and genetic changes. Pharmacological reviews 64, 706–21. https://doi.org/10.1124/pr.111.005637

Sherman-Baust, C.A., Becker, K.G., Wood III, W.H., Zhang, Y., Morin, P.J., 2011. Gene expression and pathway analysis of ovarian cancer cells selected for resistance to cisplatin, paclitaxel, or doxorubicin. J Ovarian Res 4, 21. https://doi.org/10.1186/1757-2215-4-21

Shibata, D., Schaeffer, J., Li, Z.H., Capella, G., Perucho, M., 1993. Genetic heterogeneity of the c-K-ras locus in colorectal adenomas but not in adenocarcinomas. J. Natl. Cancer Inst. 85, 1058–1063. https://doi.org/10.1093/jnci/85.13.1058

Shih, I.-M., Kurman, R.J., 2004. Ovarian tumorigenesis: a proposed model based on morphological and molecular genetic analysis. Am. J. Pathol. 164, 1511–1518.

Shim, S.-H., Kim, D.-Y., Lee, S.-W., Park, J.-Y., Kim, J.-H., Kim, Y.-M., Kim, Y.-T., Nam, J.-H., 2013. Laparoscopic management of early-stage malignant nonepithelial ovarian tumors: surgical and survival outcomes. Int. J. Gynecol. Cancer 23, 249–255. https://doi.org/10.1097/IGC.0b013e318272e754

Shimokawa, M., Kogawa, T., Shimada, T., Saito, T., Kumagai, H., Ohki, M., Kaku, T., 2018. Overall survival and post-progression survival are potent endpoint in phase III trials of second/third-line chemotherapy for advanced or recurrent epithelial ovarian cancer. J Cancer 9, 872–879. https://doi.org/10.7150/jca.17664

Shu, C.A., Zhou, Q., Jotwani, A.R., Iasonos, A., Leitao, M.M., Konner, J.A., Aghajanian, C.A., 2015. Ovarian Clear Cell Carcinoma, Outcomes by Stage: The MSK Experience. Gynecol Oncol 139, 236–241. https://doi.org/10.1016/j.ygyno.2015.09.016

Shu, C.H., Yang, W.K., Shih, Y.L., Kuo, M.L., Huang, T.S., 1997. Cell cycle G2/M arrest and activation of cyclin-dependent kinases associated with low-dose paclitaxel-induced sub-G1 apoptosis. Apoptosis 2, 463–470. https://doi.org/10.1023/a:1026422111457

Silini, A., Ghilardi, C., Figini, S., Sangalli, F., Fruscio, R., Dahse, R., Pedley, R.B., Giavazzi, R., Bani, M., 2012. Regulator of G-protein signaling 5 (RGS5) protein: a novel marker of cancer vasculature elicited and sustained by the tumor's proangiogenic microenvironment. Cell. Mol. Life Sci. 69, 1167–1178. https://doi.org/10.1007/s00018-011-0862-8

Sims, A.H., Zweemer, A.J.M., Nagumo, Y., Faratian, D., Muir, M., Dodds, M., Um, I., Kay, C., Hasmann, M., Harrison, D.J., Langdon, S.P., 2012. Defining the molecular response to trastuzumab, pertuzumab and combination therapy in ovarian cancer. Br J Cancer 106, 1779–1789. https://doi.org/10.1038/bjc.2012.176

Smith, H.O., Berwick, M., Verschraegen, C.F., Wiggins, C., Lansing, L., Muller, C.Y., Qualls, C.R., 2006. Incidence and survival rates for female malignant germ cell tumors. Obstet Gynecol 107, 1075–1085. https://doi.org/10.1097/01.AOG.0000216004.22588.ce

Sonego, M., Pellizzari, I., Dall'Acqua, A., Pivetta, E., Lorenzon, I., Benevol, S., Bomben, R., Spessotto, P., Sorio, R., Gattei, V., Belletti, B., Schiappacassi, M., Baldassarre, G., 2017. Common biological phenotypes characterize the acquisition of platinum-resistance in epithelial ovarian cancer cells. Scientific Reports 7, 7104. https://doi.org/10.1038/s41598-017-07005-1

Song, Y.S., Kim, H.S., Aoki, D., Dhanasekaran, D.N., Tsang, B.K., 2014. Ovarian Cancer. BioMed Research International 2014, 2. https://doi.org/10.1155/2014/764323

Sousa, D., Lima, R.T., Vasconcelos, M.H., 2015. Intercellular Transfer of Cancer Drug Resistance Traits by Extracellular Vesicles. Trends Mol Med 21, 595–608. https://doi.org/10.1016/j.molmed.2015.08.002

Sousa, G.F. de, Wlodarczyk, S.R., Monteiro, G., 2014a. Carboplatin: molecular mechanisms of action associated with chemoresistance. https://doi.org/10.1590/S1984-82502014000400004

Sousa, G.F. de, Wlodarczyk, S.R., Monteiro, G., Sousa, G.F. de, Wlodarczyk, S.R., Monteiro, G., 2014b. Carboplatin: molecular mechanisms of action associated with chemoresistance. Brazilian Journal of Pharmaceutical Sciences 50, 693–701. https://doi.org/10.1590/S1984-82502014000400004

Spentzos, D., Levine, D.A., Ramoni, M.F., Joseph, M., Gu, X., Boyd, J., Libermann, T.A., Cannistra, S.A., 2004. Gene expression signature with independent prognostic significance in epithelial ovarian cancer. Journal of clinical oncology : official

journal of the American Society of Clinical Oncology 22, 4700–10. https://doi.org/10.1200/JCO.2004.04.070

Stewart, C., Ralyea, C., Lockwood, S., 2019. Ovarian Cancer: An Integrated Review. Seminars in Oncology Nursing, Gynecology Oncology 35, 151–156. https://doi.org/10.1016/j.soncn.2019.02.001

Stewart, D.J., 2007. Mechanisms of resistance to cisplatin and carboplatin. Critical Reviews in Oncology / Hematology 63, 12–31. https://doi.org/10.1016/j.critrevonc.2007.02.001

Stordal, B., Hamon, M., McEneaney, V., Roche, S., Gillet, J.-P., O'Leary, J.J., Gottesman, M., Clynes, M., 2012a. Resistance to paclitaxel in a cisplatin-resistant ovarian cancer cell line is mediated by P-glycoprotein. PLoS ONE 7, e40717. https://doi.org/10.1371/journal.pone.0040717

Stordal, B., Hamon, M., McEneaney, V., Roche, S., Gillet, J.-P., O'Leary, J.J., Gottesman, M., Clynes, M., 2012b. Resistance to Paclitaxel in a Cisplatin-Resistant Ovarian Cancer Cell Line Is Mediated by P-Glycoprotein. PLoS ONE 7, e40717. https://doi.org/10.1371/journal.pone.0040717

Stordal, B., Timms, K., Farrelly, A., Gallagher, D., Busschots, S., Renaud, M., Thery, J., Williams, D., Potter, J., Tran, T., Korpanty, G., Cremona, M., Carey, M., Li, J., Li, Y., Aslan, O., O'Leary, J.J., Mills, G.B., Hennessy, B.T., 2013. BRCA1/2 mutation analysis in 41 ovarian cell lines reveals only one functionally deleterious BRCA1 mutation. Mol Oncol 7, 567–579. https://doi.org/10.1016/j.molonc.2012.12.007

Stronach, E.A., Alfraidi, A., Rama, N., Datler, C., Studd, J.B., Agarwal, R., Guney, T.G., Gourley, C., Hennessy, B.T., Mills, G.B., Mai, A., Brown, R., Dina, R., Gabra, H., 2011. HDAC4-regulated STAT1 activation mediates platinum resistance in ovarian cancer. Cancer Res. 71, 4412–4422. https://doi.org/10.1158/0008-5472.CAN-10-4111

Sui, H., Fan, Z.-Z., Li, Q., 2012. Signal Transduction Pathways and Transcriptional Mechanisms of ABCB1/Pgp-mediated Multiple Drug Resistance in Human Cancer Cells. J Int Med Res 40, 426–435. https://doi.org/10.1177/147323001204000204

Suidan, R.S., Ramirez, P.T., Sarasohn, D.M., Teitcher, J.B., Iyer, R.B., Zhou, Q., Iasonos, A., Denesopolis, J., Zivanovic, O., Long Roche, K.C., Sonoda, Y., Coleman, R.L., Abu-Rustum, N.R., Hricak, H., Chi, D.S., 2017. A multicenter assessment of the ability of preoperative computed tomography scan and CA-125 to predict gross residual disease at primary debulking for advanced epithelial ovarian cancer. Gynecol Oncol 145, 27–31. https://doi.org/10.1016/j.ygyno.2017.02.020

Sun, B., Ye, X., Lin, L., Shen, M., Jiang, T., 2015. Up-regulation of ROR2 is associated with unfavorable prognosis and tumor progression in cervical cancer. Int J Clin Exp Pathol 8, 856–861.

Swart, A.C., 2007. Long-term follow-up of women enrolled in a randomized trial of adjuvant chemotherapy for early stage ovarian cancer (ICON1). JCO 25, 5509–5509. https://doi.org/10.1200/jco.2007.25.18_suppl.5509

Swisher, E.M., Lin, K.K., Oza, A.M., Scott, C.L., Giordano, H., Sun, J., Konecny, G.E., Coleman, R.L., Tinker, A.V., O'Malley, D.M., Kristeleit, R.S., Ma, L., Bell-McGuinn, K.M., Brenton, J.D., Cragun, J.M., Oaknin, A., Ray-Coquard, I., Harrell, M.I., Mann, E., Kaufmann, S.H., Floquet, A., Leary, A., Harding, T.C., Goble, S., Maloney, L., Isaacson, J., Allen, A.R., Rolfe, L., Yelensky, R., Raponi, M., McNeish, I.A., 2017. Rucaparib in relapsed, platinum-sensitive high-grade ovarian carcinoma (ARIEL2 Part 1): an international, multicentre, open-label, phase 2 trial. Lancet Oncol 18, 75–87. https://doi.org/10.1016/S1470-2045(16)30559-9

Swisher, E.M., Sakai, W., Karlan, B.Y., Wurz, K., Urban, N., Taniguchi, T., 2008. Secondary BRCA1 mutations in BRCA1-mutated ovarian carcinomas with platinum resistance. Cancer Res. 68, 2581–2586. https://doi.org/10.1158/0008-5472.CAN-08-0088

Szubert, S., Koper, K., Dutsch-Wicherek, M.M., Jozwicki, W., 2019. High tumor cell vimentin expression indicates prolonged survival in patients with ovarian malignant tumors. Ginekologia Polska 90, 11–19. https://doi.org/10.5603/GP.2019.0003

Takai, M., Terai, Y., Kawaguchi, H., Ashihara, K., Fujiwara, S., Tanaka, T., Tsunetoh, S., Tanaka, Y., Sasaki, H., Kanemura, M., Tanabe, A., Ohmichi, M., 2014. The EMT (epithelial-mesenchymal-transition)-related protein expression indicates the metastatic status and prognosis in patients with ovarian cancer. J Ovarian Res 7, 76. https://doi.org/10.1186/1757-2215-7-76

Tammela, J., Geisler, J.P., Eskew, P.N., Geisler, H.E., 1998. Clear cell carcinoma of the ovary: poor prognosis compared to serous carcinoma. Eur. J. Gynaecol. Oncol. 19, 438–440.

Tan, H., He, Q., Gong, G., Wang, Y., Li, J., Wang, J., Zhu, D., Wu, X., 2016. miR-382 inhibits migration and invasion by targeting ROR1 through regulating EMT in ovarian cancer. International Journal of Oncology 48, 181–190.

Teicher, B.A., Fricker, S.P., 2010. CXCL12 (SDF-1)/CXCR4 pathway in cancer. Clin. Cancer Res. 16, 2927–2931. https://doi.org/10.1158/1078-0432.CCR-09-2329

Thiery, J.P., Acloque, H., Huang, R.Y.J., Nieto, M.A., 2009. Epithelial-mesenchymal transitions in development and disease. Cell 139, 871–890. https://doi.org/10.1016/j.cell.2009.11.007

Thiery, J.P., Sleeman, J.P., 2006. Complex networks orchestrate epithelial–mesenchymal transitions. Nat Rev Mol Cell Biol 7, 131–142. https://doi.org/10.1038/nrm1835

Tolgay Ocal, I., Dolled-Filhart, M., D'Aquila, T.G., Camp, R.L., Rimm, D.L., 2003. Tissue microarray-based studies of patients with lymph node negative breast carcinoma show that met expression is associated with worse outcome but is not correlated with epidermal growth factor family receptors. Cancer 97, 1841–1848. https://doi.org/10.1002/cncr.11335

Tomlins, S.A., Mehra, R., Rhodes, D.R., Cao, X., Wang, L., Dhanasekaran, S.M., Kalyana-Sundaram, S., Wei, J.T., Rubin, M.A., Pienta, K.J., Shah, R.B., Chinnaiyan, A.M., 2007. Integrative molecular concept modeling of prostate cancer progression. Nature Genetics 39, 41–51. https://doi.org/10.1038/ng1935

Toss, A., Cortesi, L., 2013. Molecular mechanisms of PARP inhibitors in BRCA-related ovarian cancer. Journal of Cancer Science & Therapy 5.

Tothill, R.W., Tinker, A.V., George, J., Brown, R., Fox, S.B., Lade, S., Johnson, D.S., Trivett, M.K., Etemadmoghadam, D., Locandro, B., Traficante, N., Fereday, S., Hung, J.A., Chiew, Y.-E., Haviv, I., Australian Ovarian Cancer Study Group, Gertig, D., DeFazio, A., Bowtell, D.D.L., 2008. Novel molecular subtypes of serous and endometrioid ovarian cancer linked to clinical outcome. Clin. Cancer Res. 14, 5198–5208. https://doi.org/10.1158/1078-0432.CCR-08-0196

Trimbos, B., Timmers, P., Pecorelli, S., Coens, C., Ven, K., van der Burg, M., Casado, A., 2010. Surgical Staging and Treatment of Early Ovarian Cancer: Long-term Analysis From a Randomized Trial. J Natl Cancer Inst 102, 982–987. https://doi.org/10.1093/jnci/djq149

Trimbos, J.B., Vergote, I., Bolis, G., Vermorken, J.B., Mangioni, C., Madronal, C., Franchi, M., Tateo, S., Zanetta, G., Scarfone, G., Giurgea, L., Timmers, P., Coens, C., Pecorelli, S., EORTC-ACTION collaborators. European Organisation for Research and Treatment of Cancer-Adjuvant ChemoTherapy in Ovarian Neoplasm,

2003. Impact of adjuvant chemotherapy and surgical staging in early-stage ovarian carcinoma: European Organisation for Research and Treatment of Cancer-Adjuvant ChemoTherapy in Ovarian Neoplasm trial. J. Natl. Cancer Inst. 95, 113–125.

Trudu, F., Amato, F., Vaňhara, P., Pivetta, T., Peña-Méndez, E.M., Havel, J., 2015. Coordination compounds in cancer: Past, present and perspectives. Journal of Applied Biomedicine 13, 79–103. https://doi.org/10.1016/j.jab.2015.03.003

Tsibulak, I., Zeimet, A.G., Marth, C., 2019. Hopes and failures in front-line ovarian cancer therapy. Critical Reviews in Oncology/Hematology 143, 14–19. https://doi.org/10.1016/j.critrevonc.2019.08.002

Tsilidis, K.K., Allen, N.E., Key, T.J., Dossus, L., Lukanova, A., Bakken, K., Lund, E., Fournier, A., Overvad, K., Hansen, L., Tjønneland, A., Fedirko, V., Rinaldi, S., Romieu, I., Clavel-Chapelon, F., Engel, P., Kaaks, R., Schütze, M., Steffen, A., Bamia, C., Trichopoulou, A., Zylis, D., Masala, G., Pala, V., Galasso, R., Tumino, R., Sacerdote, C., Bueno-de-Mesquita, H.B., van Duijnhoven, F.J.B., Braem, M.G.M., Onland-Moret, N.C., Gram, I.T., Rodríguez, L., Travier, N., Sánchez, M.-J., Huerta, J.M., Ardanaz, E., Larrañaga, N., Jirström, K., Manjer, J., Idahl, A., Ohlson, N., Khaw, K.-T., Wareham, N., Mouw, T., Norat, T., Riboli, E., 2011. Oral contraceptive use and reproductive factors and risk of ovarian cancer in the European Prospective Investigation into Cancer and Nutrition. British Journal of Cancer 105, 1436–1442. https://doi.org/10.1038/bjc.2011.371

Tzeng, H.-T., Wang, Y.-C., 2016. Rab-mediated vesicle trafficking in cancer. Journal of Biomedical Science 23, 70. https://doi.org/10.1186/s12929-016-0287-7

van Dalen, A., Favier, J., Burges, A., Hasholzner, U., de Bruijn, H.W.A., Dobler-Girdziunaite, D., Dombi, V.H., Fink, D., Giai, M., McGing, P., Harlozinska, A., Kainz, Ch., Markowska, J., Molina, R., Sturgeon, C., Bowman, A., Einarsson, R., 2000. Prognostic Significance of CA 125 and TPS Levels after 3 Chemotherapy Courses in Ovarian Cancer Patients. Gynecologic Oncology 79, 444–450. https://doi.org/10.1006/gyno.2000.5982

van der Burg, M.E.L., de Wit, R., van Putten, W.L.J., Logmans, A., Kruit, W.H.J., Stoter, G., Verweij, J., 2002. Weekly cisplatin and daily oral etoposide is highly effective in platinum pretreated ovarian cancer. Br. J. Cancer 86, 19–25. https://doi.org/10.1038/sj.bjc.6600002

Van Der Looij, M., Szabo, C., Besznyak, I., Liszka, G., Csokay, B., Pulay, T., Toth, J., Devilee, P., King, M.C., Olah, E., 2000. Prevalence of founder BRCA1 and BRCA2 mutations among breast and ovarian cancer patients in Hungary. Int. J. Cancer 86, 737–740. https://doi.org/10.1002/(sici)1097-0215(20000601)86:5<737::aid-ijc21>3.0.co;2-1

van Staalduinen, J., Baker, D., ten Dijke, P., van Dam, H., 2018. Epithelial–mesenchymal-transition-inducing transcription factors: new targets for tackling chemoresistance in cancer? Oncogene 37, 6195–6211. https://doi.org/10.1038/s41388-018-0378-x

Vargas, A.N., 2014. Natural history of ovarian cancer. Ecancermedicalscience 8. https://doi.org/10.3332/ecancer.2014.465

Varghese, F., Bukhari, A.B., Malhotra, R., De, A., 2014. IHC Profiler: An Open Source Plugin for the Quantitative Evaluation and Automated Scoring of Immunohistochemistry Images of Human Tissue Samples. PLOS ONE 9, e96801. https://doi.org/10.1371/journal.pone.0096801

Vasey, P.A., Jayson, G.C., Gordon, A., Gabra, H., Coleman, R., Atkinson, R., Parkin, D., Paul, J., Hay, A., Kaye, S.B., Scottish Gynaecological Cancer Trials Group, 2004. Phase III randomized trial of docetaxel-carboplatin versus paclitaxel-carboplatin as

first-line chemotherapy for ovarian carcinoma. J. Natl. Cancer Inst. 96, 1682–1691. https://doi.org/10.1093/jnci/djh323

Vega, S., Morales, A.V., Ocaña, O.H., Valdés, F., Fabregat, I., Nieto, M.A., 2004. Snail blocks the cell cycle and confers resistance to cell death. Genes Dev 18, 1131–1143. https://doi.org/10.1101/gad.294104

Venkitaraman, A.R., 2002. Cancer Susceptibility and the Functions of BRCA1 and BRCA2. Cell 108, 171–182. https://doi.org/10.1016/S0092-8674(02)00615-3

Vergara, D., Merlot, B., Lucot, J.-P., Collinet, P., Vinatier, D., Fournier, I., Salzet, M., 2010. Epithelial-mesenchymal transition in ovarian cancer. Cancer Lett 291, 59–66. https://doi.org/10.1016/j.canlet.2009.09.017

Vergote, I., Tropé, C.G., Amant, F., Kristensen, G.B., Ehlen, T., Johnson, N., Verheijen, R.H.M., van der Burg, M.E.L., Lacave, A.J., Panici, P.B., Kenter, G.G., Casado, A., Mendiola, C., Coens, C., Verleye, L., Stuart, G.C.E., Pecorelli, S., Reed, N.S., European Organization for Research and Treatment of Cancer-Gynaecological Cancer Group, NCIC Clinical Trials Group, 2010. Neoadjuvant chemotherapy or primary surgery in stage IIIC or IV ovarian cancer. N Engl J Med 363, 943–953. https://doi.org/10.1056/NEJMoa0908806

Verhaak, R.G.W., Tamayo, P., Yang, J.-Y., Hubbard, D., Zhang, H., Creighton, C.J., Fereday, S., Lawrence, M., Carter, S.L., Mermel, C.H., Kostic, A.D., Etemadmoghadam, D., Saksena, G., Cibulskis, K., Duraisamy, S., Levanon, K., Sougnez, C., Tsherniak, A., Gomez, S., Onofrio, R., Gabriel, S., Chin, L., Zhang, N., Spellman, P.T., Zhang, Y., Akbani, R., Hoadley, K.A., Kahn, A., Köbel, M., Huntsman, D., Soslow, R.A., Defazio, A., Birrer, M.J., Gray, J.W., Weinstein, J.N., Bowtell, D.D., Drapkin, R., Mesirov, J.P., Getz, G., Levine, D.A., Meyerson, M., Cancer Genome Atlas Research Network, 2013. Prognostically relevant gene signatures of high-grade serous ovarian carcinoma. J. Clin. Invest. 123, 517–525. https://doi.org/10.1172/JCI65833

Walsh, V., Goodman, J., 2002. From taxol to taxol®: The changing identities and ownership of an anti-cancer drug. Medical Anthropology 21, 307–336. https://doi.org/10.1080/01459740214074

Wang, D., Lippard, S.J., 2005. Cellular processing of platinum anticancer drugs. Nature Reviews Drug Discovery 4, 307. https://doi.org/10.1038/nrd1691

Wang, J., Wei, Q., Wang, X., Tang, S., Liu, H., Zhang, F., Mohammed, M.K., Huang, J., Guo, D., Lu, M., Liu, F., Liu, J., Ma, C., Hu, X., Haydon, R.C., He, T.-C., Luu, H.H., 2016. Transition to resistance: An unexpected role of the EMT in cancer chemoresistance. Genes Dis 3, 3–6. https://doi.org/10.1016/j.gendis.2016.01.002

Wang, J.-S., Wang, F.-B., Zhang, Q.-G., Shen, Z.-Z., Shao, Z.-M., 2008. Enhanced expression of Rab27A gene by breast cancer cells promoting invasiveness and the metastasis potential by secretion of insulin-like growth factor-II. Mol. Cancer Res. 6, 372–382. https://doi.org/10.1158/1541-7786.MCR-07-0162

Wang, Q., Michalak, K., Wesolowska, O., Deli, J., Molnar, P., Hohmann, J., Molnar, J., Engi, H., 2010. Reversal of Multidrug Resistance by Natural Substances from Plants. Current Topics in Medicinal Chemistry 10, 1757–1768. https://doi.org/10.2174/156802610792928103

Wang, T.-H., Chan, Y.-H., Chen, C.-W., Kung, W.-H., Lee, Y.-S., Wang, S.-T., Chang, T.-C., Wang, H.-S., 2006. Paclitaxel (Taxol) upregulates expression of functional interleukin-6 in human ovarian cancer cells through multiple signaling pathways. Oncogene 25, 4857. https://doi.org/10.1038/sj.onc.1209498

Wang, W., Figg, W.D., 2008. Secondary BRCA1 and BRCA2 alterations and acquired chemoresistance. Cancer Biol. Ther. 7, 1004–1005. https://doi.org/10.4161/cbt.7.7.6409

Wang, W., Wang, L., Mizokami, A., Shi, J., Zou, C., Dai, J., Keller, E.T., Lu, Y., Zhang, J., 2017. Down-regulation of E-cadherin enhances prostate cancer chemoresistance via Notch signaling. Chin J Cancer 36. https://doi.org/10.1186/s40880-017-0203-x

Wang, Yiying, Hong, S., Mu, J., Wang, Yue, Lea, J., Kong, B., Zheng, W., 2019. Tubal Origin of "Ovarian" Low-Grade Serous Carcinoma: A Gene Expression Profile Study [WWW Document]. Journal of Oncology. https://doi.org/10.1155/2019/8659754

WEIDLE, H.U., BIRZELE, F., KOLLMORGEN, G., RÜGER, R., 2016. The Multiple Roles of Exosomes in Metastasis. Cancer Genomics Proteomics 14, 1–16.

Weil, M.K., Chen, A.P., 2011. PARP inhibitor treatment in ovarian and breast cancer. Current problems in cancer 35, 7–50. https://doi.org/10.1016/j.currproblcancer.2010.12.002

Wernyj, R.P., Morin, P.J., 2004. Molecular mechanisms of platinum resistance: still searching for the Achilles' heel. Drug Resistance Updates 7, 227–232. https://doi.org/10.1016/j.drup.2004.08.002

Weterings, E., Chen, D.J., 2008. The endless tale of non-homologous end-joining. Cell Res. 18, 114–124. https://doi.org/10.1038/cr.2008.3

Wheate, N.J., Walker, S., Craig, G.E., Oun, R., 2010. The status of platinum anticancer drugs in the clinic and in clinical trials. Dalton Trans 39, 8113–8127. https://doi.org/10.1039/c0dt00292e

Wheeler, D.B., Zoncu, R., Root, D.E., Sabatini, D.M., Sawyers, C.L., 2015. Identification of an oncogenic RAB protein. Science 350, 211–217. https://doi.org/10.1126/science.aaa4903

Wiechec, E., Overgaard, J., Hansen, L.L., 2008. A fragile site within the HPC1 region at 1q25.3 affecting RGS16, RGSL1, and RGSL2 in human breast carcinomas. Genes Chromosomes Cancer 47, 766–780. https://doi.org/10.1002/gcc.20578

Worst, T.S., Meyer, Y., Gottschalt, M., Weis, C.-A., von Hardenberg, J., Frank, C., Steidler, A., Michel, M.S., Erben, P., 2017. RAB27A, RAB27B and VPS36 are downregulated in advanced prostate cancer and show functional relevance in prostate cancer cells. International Journal of Oncology 50, 920–932. https://doi.org/10.3892/ijo.2017.3872

Wp, T., Mw, S., Jl, W., Aa, S., Aj, B., Jm, S., A, S., L, R., Ks, T., Ca, A., 2018. Randomized phase II trial of bevacizumab plus everolimus versus bevacizumab alone for recurrent or persistent ovarian, fallopian tube or peritoneal carcinoma: An NRG oncology/gynecologic oncology group study. Gynecol Oncol 151, 257–263. https://doi.org/10.1016/j.ygyno.2018.08.027

Wright, A.A., Bohlke, K., Armstrong, D.K., Bookman, M.A., Cliby, W.A., Coleman, R.L., Dizon, D.S., Kash, J.J., Meyer, L.A., Moore, K.N., Olawaiye, A.B., Oldham, J., Salani, R., Sparacio, D., Tew, W.P., Vergote, I., Edelson, M.I., 2016. Neoadjuvant chemotherapy for newly diagnosed, advanced ovarian cancer: Society of Gynecologic Oncology and American Society of Clinical Oncology Clinical Practice Guideline. Gynecol Oncol 143, 3–15. https://doi.org/10.1016/j.ygyno.2016.05.022

Wright, P.K., 2008. Targeting vesicle trafficking: an important approach to cancer chemotherapy. Recent Pat Anticancer Drug Discov 3, 137–147. https://doi.org/10.2174/157489208784638730

Wright, T.M., Brannon, A.R., Gordan, J.D., Mikels, A.J., Mitchell, C., Chen, S., Espinosa, I., Rijn, M. van de, Pruthi, R., Wallen, E., Edwards, L., Nusse, R., Rathmell, W.K., 2009. Ror2, a developmentally regulated kinase, promotes tumor growth potential in renal cell carcinoma. Oncogene 28, 2513. https://doi.org/10.1038/onc.2009.116

Wu, C.-L., Zhao, S.-P., Yu, B.-L., 2013. Microarray analysis provides new insights into the function of apolipoprotein O in HepG2 cell line. Lipids Health Dis 12, 186. https://doi.org/10.1186/1476-511X-12-186

Wu, D., Yu, X., Wang, J., Hui, X., Zhang, Y., Cai, Y., Ren, M., Guo, M., Zhao, F., Dou, J., 2019. Ovarian Cancer Stem Cells with High ROR1 Expression Serve as a New Prophylactic Vaccine for Ovarian Cancer. J Immunol Res 2019, 9394615. https://doi.org/10.1155/2019/9394615

Xu, Y., Ma, Y.-H., Pang, Y.-X., Zhao, Z., Lu, J.-J., Mao, H.-L., Liu, P.-S., 2017. Ectopic repression of receptor tyrosine kinase–like orphan receptor 2 inhibits malignant transformation of ovarian cancer cells by reversing epithelial–mesenchymal transition. Tumour Biol. 39, 1010428317701627. https://doi.org/10.1177/1010428317701627

Yamaguchi, T., Yanagisawa, K., Sugiyama, R., Hosono, Y., Shimada, Y., Arima, C., Kato, S., Tomida, S., Suzuki, M., Osada, H., Takahashi, T., 2012a. NKX2-1/TITF1/TTF-1-Induced ROR1 Is Required to Sustain EGFR Survival Signaling in Lung Adenocarcinoma. Cancer Cell 21, 348–361. https://doi.org/10.1016/j.ccr.2012.02.008

Yamaguchi, T., Yanagisawa, K., Sugiyama, R., Hosono, Y., Shimada, Y., Arima, C., Kato, S., Tomida, S., Suzuki, M., Osada, H., Takahashi, T., 2012b. NKX2-1/TITF1/TTF-1-Induced ROR1 is required to sustain EGFR survival signaling in lung adenocarcinoma. Cancer Cell 21, 348–361. https://doi.org/10.1016/j.ccr.2012.02.008

Yang, A.D., Fan, F., Camp, E.R., van Buren, G., Liu, W., Somcio, R., Gray, M.J., Cheng, H., Hoff, P.M., Ellis, L.M., 2006. Chronic oxaliplatin resistance induces epithelial-to-mesenchymal transition in colorectal cancer cell lines. Clin. Cancer Res. 12, 4147–4153. https://doi.org/10.1158/1078-0432.CCR-06-0038

Yang, H.P., Murphy, K.R., Pfeiffer, R.M., George, N., Garcia-Closas, M., Lissowska, J., Brinton, L.A., Wentzensen, N., 2016. Lifetime Number of Ovulatory Cycles and Risks of Ovarian and Endometrial Cancer Among Postmenopausal Women. Am J Epidemiol 183, 800–814. https://doi.org/10.1093/aje/kwv308

Yang, J., Weinberg, R.A., 2008. Epithelial-mesenchymal transition: at the crossroads of development and tumor metastasis. Dev. Cell 14, 818–829. https://doi.org/10.1016/j.devcel.2008.05.009

Yang, K., Wang, X., Zhang, H., Wang, Z., Nan, G., Li, Y., Zhang, F., Mohammed, M.K., Haydon, R.C., Luu, H.H., Bi, Y., He, T.-C., 2016. The evolving roles of canonical WNT signaling in stem cells and tumorigenesis: implications in targeted cancer therapies. Lab Invest 96, 116–136. https://doi.org/10.1038/labinvest.2015.144

Yasuda, T., Saegusa, C., Kamakura, S., Sumimoto, H., Fukuda, M., 2012. Rab27 effector Slp2-a transports the apical signaling molecule podocalyxin to the apical surface of MDCK II cells and regulates claudin-2 expression. Mol. Biol. Cell 23, 3229–3239. https://doi.org/10.1091/mbc.E12-02-0104

Yi, B.-R., Kim, T.-H., Kim, Y.-S., Choi, K.-C., 2015. Alteration of epithelial-mesenchymal transition markers in human normal ovaries and neoplastic ovarian cancers. Int. J. Oncol. 46, 272–280. https://doi.org/10.3892/ijo.2014.2695

Yin, S., Chen, F.-F., Yang, G.-F., 2018. Vimentin immunohistochemical expression as a prognostic factor in gastric cancer: A meta-analysis. Pathol. Res. Pract. 214, 1376–1380. https://doi.org/10.1016/j.prp.2018.07.014

Yin, Z., Gao, M., Chu, S., Su, Y., Ye, C., Wang, Y., Pan, Z., Wang, Z., Zhang, H., Tong, H., Zhu, J., 2017. Antitumor activity of a newly developed monoclonal antibody against ROR1 in ovarian cancer cells. Oncotarget 8, 94210–94222. https://doi.org/10.18632/oncotarget.21618

Yin, Z., Mao, Y., Zhang, N., Su, Y., Zhu, J., Tong, H., Zhang, H., 2019. A fully chimeric IgG antibody for ROR1 suppresses ovarian cancer growth *in vitro* and *in vivo*. Biomedicine & Pharmacotherapy 119, 109420. https://doi.org/10.1016/j.biopha.2019.109420

Ying, Y., Tao, Q., 2009. Epigenetic disruption of the WNT/ß-catenin signaling pathway in human cancers. Epigenetics 4, 307–312. https://doi.org/10.4161/epi.4.5.9371

Yoon, S.-O., Shin, S., Mercurio, A.M., 2005. Hypoxia Stimulates Carcinoma Invasion by Stabilizing Microtubules and Promoting the Rab11 Trafficking of the α6β4 Integrin. Cancer Res 65, 2761–2769. https://doi.org/10.1158/0008-5472.CAN-04-4122

Yoshioka, S., King, M.L., Ran, S., Okuda, H., MacLean, J.A., McAsey, M.E., Sugino, N., Brard, L., Watabe, K., Hayashi, K., 2012. WNT7A Regulates Tumor Growth and Progression in Ovarian Cancer through the WNT/β-Catenin Pathway. Mol Cancer Res 10, 469–482. https://doi.org/10.1158/1541-7786.MCR-11-0177

Zhang, B., Chen, F., Xu, Q., Han, L., Xu, J., Gao, L., Sun, X., Li, Yiwen, Li, Yan, Qian, M., Sun, Y., 2018. Revisiting ovarian cancer microenvironment: a friend or a foe? Protein Cell 9, 674–692. https://doi.org/10.1007/s13238-017-0466-7

Zhang, D., Yang, R., Wang, S., Dong, Z., 2014. Paclitaxel: new uses for an old drug. Drug Des Devel Ther 8, 279–284. https://doi.org/10.2147/DDDT.S56801

Zhang, H., Qiu, J., Ye, C., Yang, D., Gao, L., Su, Y., Tang, X., Xu, N., Zhang, D., Xiong, L., Mao, Y., Li, F., Zhu, J., 2014a. ROR1 expression correlated with poor clinical outcome in human ovarian cancer. Scientific reports 4, 5811. https://doi.org/10.1038/srep05811

Zhang, H., Qiu, J., Ye, C., Yang, D., Gao, L., Su, Y., Tang, X., Xu, N., Zhang, D., Xiong, L., Mao, Y., Li, F., Zhu, J., 2014b. ROR1 expression correlated with poor clinical outcome in human ovarian cancer. Sci Rep 4, 5811. https://doi.org/10.1038/srep05811

Zhang, J.-X., Huang, X.-X., Cai, M.-B., Tong, Z.-T., Chen, J.-W., Qian, D., Liao, Y.-J., Deng, H.-X., Liao, D.-Z., Huang, M.-Y., Zeng, Y.-X., Xie, D., Mai, S.-J., 2012. Overexpression of the secretory small GTPase Rab27B in human breast cancer correlates closely with lymph node metastasis and predicts poor prognosis. Journal of Translational Medicine 10, 242. https://doi.org/10.1186/1479-5876-10-242

Zhang, S., Chen, L., Cui, B., Chuang, H.-Y., Yu, J., Wang-Rodriguez, J., Tang, L., Chen, G., Basak, G.W., Kipps, T.J., 2012a. ROR1 Is Expressed in Human Breast Cancer and Associated with Enhanced Tumor-Cell Growth. PLoS One 7. https://doi.org/10.1371/journal.pone.0031127

Zhang, S., Chen, L., Wang-Rodriguez, J., Zhang, L., Cui, B., Frankel, W., Wu, R., Kipps, T.J., 2012b. The Onco-Embryonic Antigen ROR1 Is Expressed by a Variety of Human Cancers. Am J Pathol 181, 1903–1910. https://doi.org/10.1016/j.ajpath.2012.08.024

Zhang, S., Cui, B., Lai, H., Liu, G., Ghia, E.M., Widhopf, G.F., Zhang, Z., Wu, C.C.N., Chen, L., Wu, R., Schwab, R., Carson, D.A., Kipps, T.J., 2014. Ovarian cancer stem cells express ROR1, which can be targeted for anti-cancer-stem-cell therapy.

Proc. Natl. Acad. Sci. U.S.A. 111, 17266–17271.
https://doi.org/10.1073/pnas.1419599111

Zhang, S., Zhang, H., Ghia, E.M., Huang, J., Wu, L., Zhang, J., Lam, S., Lei, Y., He, J., Cui, B., Widhopf, G.F., Yu, J., Schwab, R., Messer, K., Jiang, W., Parker, B.A., Carson, D.A., Kipps, T.J., 2019. Inhibition of chemotherapy resistant breast cancer stem cells by a ROR1 specific antibody. PNAS 116, 1370–1377. https://doi.org/10.1073/pnas.1816262116

Zhang, X., Liu, G., Kang, Y., Dong, Z., Qian, Q., Ma, X., 2013. N-Cadherin Expression Is Associated with Acquisition of EMT Phenotype and with Enhanced Invasion in Erlotinib-Resistant Lung Cancer Cell Lines. PLOS ONE 8, e57692. https://doi.org/10.1371/journal.pone.0057692

Zhang, Y., Huang, S., Guo, Y., Li, L., 2018. MiR-1294 confers cisplatin resistance in ovarian Cancer cells by targeting IGF1R. Biomed Pharmacother 106, 1357–1363. https://doi.org/10.1016/j.biopha.2018.07.059

Zhao, H., Wang, Q., Wang, X., Zhu, H., Zhang, S., Wang, W., Wang, Z., Huang, J., 2016. Correlation Between RAB27B and p53 Expression and Overall Survival in Pancreatic Cancer. Pancreas 45, 204–210. https://doi.org/10.1097/MPA.0000000000000453

Zheng, H.X., Cai, Y.D., Wang, Y.D., Cui, X.B., Xie, T.T., Li, W.J., Peng, L., Zhang, Y., Wang, Z.Q., Wang, J., Jiang, B., 2013. Fas signaling promotes motility and metastasis through epithelial-mesenchymal transition in gastrointestinal cancer. Oncogene 32, 1183–1192. https://doi.org/10.1038/onc.2012.126

Zheng, X., Carstens, J.L., Kim, J., Scheible, M., Kaye, J., Sugimoto, H., Wu, C.-C., LeBleu, V.S., Kalluri, R., 2015. Epithelial-to-mesenchymal transition is dispensable for metastasis but induces chemoresistance in pancreatic cancer. Nature 527, 525–530. https://doi.org/10.1038/nature16064

Zheng, Y.-Z., Ma, R., Zhou, J.-K., Guo, C.-L., Wang, Y.-S., Li, Z.-G., Liu, L.-X., Peng, Y., 2016. ROR1 is a novel prognostic biomarker in patients with lung adenocarcinoma. Sci Rep 6. https://doi.org/10.1038/srep36447

Zhu, X., Shen, H., Yin, X., Long, L., Xie, C., Liu, Y., Hui, L., Lin, X., Fang, Y., Cao, Y., Xu, Y., Li, M., Xu, W., Li, Y., 2016. miR-186 regulation of Twist1 and ovarian cancer sensitivity to cisplatin. Oncogene 35, 323–332. https://doi.org/10.1038/onc.2015.84